UNIVERSIDAD NACIONAL AUTÓNOMA DE MÉXICO

DOCTORADO EN CIENCIAS BIOMÉDICAS

FACULTAD DE MEDICINA

"EFECTO DEL ÁCIDO ÚRICO SOBRE LA ACTIVACIÓN DE MONOCITOS-MACRÓFAGOS Y SU RELACIÓN CON ALTERACIONES METABÓLICAS"

TESIS

QUE PARA OPTAR POR EL GRADO DE:

DOCTOR EN CIENCIAS

PRESENTA:

MED. CIR. CAMILO PABLO MARTÍNEZ REYES

DIRECTOR DE TESIS

DR. EUSTACIO GALILEO ESCOBEDO GONZÁLEZ, FACULTAD DE MEDICINA

COMITÉ TUTOR:

DRA. YOLANDA LÓPEZ VIDAL, FACULTAD DE MEDICINA

DR. RAFAEL VILLALOBOS MOLINA, FES IZTACALA

MÉXICO, CDMX, NOVIEMBRE 2023

UNIVERSIDAD NACIONAL AUTÓNOMA DE MÉXICO

DOCTORADO EN CIENCIAS BIOMÉDICAS

FACULTAD DE MEDICINA

"EFECTO DEL ÁCIDO ÚRICO SOBRE LA ACTIVACIÓN DE MONOCITOS-MACRÓFAGOS Y SU RELACIÓN CON ALTERACIONES CARDIOMETABÓLICAS"

TESIS

QUE PARA OPTAR POR EL GRADO DE:

DOCTOR EN CIENCIAS

PRESENTA:

MÉD. CIR. CAMILO PABLO MARTÍNEZ REYES

DIRECTOR DE TESIS

DR. EUSTACIO GALILEO ESCOBEDO GONZÁLEZ, FACULTAD DE MEDICINA

COMITÉ TUTOR:

DRA. YOLANDA LÓPEZ VIDAL, FACULTAD DE MEDICINA

DR. RAFAEL VILLALOBOS MOLINA, FACULTAD DE ESTUDIOS SUPERIORES IZTACALA

MÉXICO, CDMX, NOVIEMBRE 2023

AGRADECIMIENTOS

Agradezco al Programa de Doctorado en Ciencias Biomédicas, Facultad de Medicina, Universidad Nacional Autónoma de México por mi formación académica como Doctor en Ciencias.

Agradezco al Consejo Nacional de Ciencia y Tecnología por el apoyo número 582451, mediante el programa de becas nacionales, con número de becario 414033.

Agradecimientos

Agradezco a mi familia, especialmente a mis padres, por ensenarme el valor del trabajo y del esfuerzo constante. Gracias a mi papa, Camilo, y a mi mama, Margarita, por ser los mejores padres que pude haber tenido. Así mismo agradezco a mis hermanos por sus enseñanzas y por compartir tantos buenos momentos. Espero que sean muchos más.

Agradezco a Bety, mi compañera de vida, por tu apoyo constante, incondicional e ilimitado. Gracias por estar siempre a mi lado y por hacer todo lo posible para que pudiera concluir este trabajo. Además, quiero reconocer tu esfuerzo y dedicación para cuidar de Layla en los momentos en que más lo necesitaba, a pesar de tus múltiples responsabilidades y de tu cansancio. Gracias por todo, gracias por regalarme a Layla, gracias por ser mi amiga y mi amor. Sin ti, este logro no hubiera sido posible.

Agradezco a mi hija, Layla, mi niña linda, mi motor de la vida. Tu sonrisa e inteligencia iluminan y alegran nuestra vida.

Agradezco profundamente a mi hermano Miguel por su invaluable ayuda, por hacer todo lo que estuvo a tu alcance para que yo pudiera dedicar más tiempo a este trabajo, gracias por tu generosidad y apoyo incondicional.

Agradezco a mis amigos y compañeros de laboratorio por su ayuda continua, sus enseñanzas y consejos. Agradezco especialmente al Dr. Israel Torres Castro por haberme enseñado la meticulosidad necesaria para llevar a cabo el trabajo experimental. Así mismo quiero agradecer al Dr. Aaron Manjarrez R. por tu apoyo permanente para llevar a cabo este proyecto, así como por tu invaluable amistad y consejos para concluir este proyecto.

Agradezco a los miembros de mi comité tutoral por el tiempo dedicado para corregir, mejorar y enriquecer este proyecto doctoral.

Agradezco a la Dra. Yolanda López Vidal por haberme abierto las puertas de su laboratorio y por su generosidad al permitirme llevar a cabo una parte significativa de los experimentos de este proyecto. Además, le agradezco por su apoyo moral y sus palabras de aliento cuando

me sentí perdido. Le estaré siempre agradecido por decirme las palabras que necesitaba escuchar.

Gracias al Dr. Galileo Escobedo González, mi tutor principal, por ser un ejemplo de rectitud y superación constante. La confianza depositada en mí, tus consejos y ayuda me han alentado para poder concluir esta etapa con éxito. Gracias por todo, pero especialmente por tu amistad.

Agradezco a la Dra. Beatriz Y. Salazar Vázquez por haberme abierto las puertas de la investigación, por confiar incondicionalmente en mí y por todas las oportunidades que me brindo y los caminos que abrió para que yo pudiera continuar en este camino.

Finalmente quiero agradecer al Dr. Ruy Pérez Tamayo (QEPD) por la oportunidad de ingresar a su laboratorio y por compartir un poco de su vasta experiencia y sabiduría. Sus enseñanzas perdurarán en mi memoria.

ÍNDICE

CONTENIDO

Índice 1
Lista de abreviaturas 2
Resumen 5
Abstract 6
Introducción 7
Antecedentes 9
Planteamiento del problema 27
Hipótesis 28
Objetivos 29
  Objetivo general 29
  Objetivos particulares 29
Materiales y métodos 30
  Sujetos 30
  Aislamiento de monocitos y cultivo de macrófagos 30
  Ensayos de citometría de flujo 32
  Actividad fagocítica de los macrófagos 33
  Expresión del gen URAT1 por qPCR 34
  Estadística 35
Resultados 36
Discusión 47
Conclusión 53
Referencias 55
Anexo i artículos generados durante el doctorado 63

LISTA DE ABREVIATURAS

AMP	Adenosín monofosfato
Arg-1	Arginasa 1
AU	Ácido úrico
CCR2	Receptor de quimiocinas C-C tipo 2, receptor de MCP-1
CD11c	Cluster de diferenciación 11c, subunidad α de la integrina
CD14	Cluster de diferenciación 14, receptor del complejo lipopolisacárido
CD206	Cluster de diferenciación 206, receptor de manosa
CLS	Estructuras similares a coronas
CX3CR1	Receptor 1 de quimiocinas con motivo C-X3C, receptor de fractalcina
DAMP	Patrones moleculares asociados a peligro
DM1	Diabetes Mellitus tipo 1
DM2	Diabetes Mellitus tipo 2
E. coli	*Escherichia coli*
GFP	Proteína verde fluorescente
GLUT-9	Transportador de glucosa 9
GM-CSF	Factor estimulante de colonias de granulocitos-monocitos
GMP	Guanina monofosfato
HU	Hiperuricemia

ICAM-1	Molécula de adhesión intercelular 1
IL-1 β	Interleucina 1 beta, citocina proinflamatoria
IL-10	Interleucina 10
IMP	Inosina monofosfato
iNOs	Óxido nítrico sintasa inducible
iNOS	Óxido nítrico sintasa inducible
IRS	Sustrato del receptor de insulina
LDL	Lipoproteínas de baja densidad
LPS	Lipopolisacárido
MCP-1	Proteína quimioatrayente de monocitos
M-CSF-1	Factor estimulante de colonias de macrófagos
MDM	Macrófagos derivados de monocitos
MSU	Urato monosódico
NF-κB	Factor nuclear Kappa B
NLRP3	NOD-like receptor protein 3
OAT	Transportador de aniones orgánicos
PNP	Purina nucleótido fosforilasa
pro-IL-1β	Pro-interleucina beta
RI	Receptor de insulina

ROS	Especies reactivas de oxígeno
TGF -β	Factor de crecimiento transformante beta
TLR	Receptor tipo toll
TNF-α	Factor de necrosis tumoral alfa
URAT-1	Transportador de aniones de urato 1
VCAM-1	Molécula de adhesión vascular 1
XO	Xantina Oxidasa

RESUMEN

El efecto del ácido úrico sobre los monocitos y los macrófagos todavía no ha sido caracterizado por completo. En esta tesis investigamos el efecto del ácido úrico sobre la capacidad proinflamatoria de los macrófagos humanos y, posteriormente, examinamos el mecanismo molecular posiblemente involucrado. Los monocitos humanos primarios se diferenciaron en macrófagos y se expusieron a 0, 0.23, 0.45 o 0.9 mmol/L de ácido úrico durante 12 horas, en presencia o ausencia de 1 mmol/L de probenecid, un inhibidor competitivo del ácido úrico. La producción de marcadores proinflamatorios se midió por citometría de flujo y la actividad fagocítica de los macrófagos se cuantificó como el número de macrófagos positivos para *Escherichia coli* marcadas con proteína verde fluorescente (*E.coli*+GFP) por 100, entre la suma del número macrófagos positivos y negativos para *E.coli*+GFP. La expresión del transportador de aniones de urato 1 (URAT1) en los macrófagos se midió por qPCR. En comparación con las células control (0 mmol/L), el ácido úrico aumentó significativamente la producción del factor de necrosis tumoral alfa (TNF-α), el receptor tipo toll 4 (TLR4) y el cluster de diferenciación (CD) 11c en los macrófagos. Por el contrario, el tratamiento con ácido úrico redujo de forma gradual la expresión de CD206, el receptor 1 de quimiocinas con motivo CX3C (CX3CR1) y el receptor de quimiocinas C-C tipo 2 (CCR2) en estas células inmunes. De manera adicional, el ácido úrico aumentó progresivamente la actividad fagocítica de los macrófagos y disminuyó la expresión de URAT1. De acuerdo con lo esperado, el probenecid inhibió la producción de citocinas proinflamatorias y la actividad fagocítica en macrófagos expuestos al ácido úrico. Estos resultados sugieren que el ácido úrico tiene un efecto directo de tipo proinflamatorio sobre los macrófagos, posiblemente mediado a través de URAT1.

ABSTRACT

The effect of uric acid on macrophages has not been fully elucidated. We investigated the effect of uric acid on the proinflammatory ability of human macrophages and then examined the possible molecular mechanism involved. Primary human monocytes were differentiated into macrophages for subsequent exposure to 0, 0.23, 0.45, or 0.9 mmol/L uric acid for 12 h in the presence or absence of 1 mmol/L probenecid, a non-specific blocker of uric acid. Flow cytometry was used to measure proinflammatory marker production and phagocytic activity, which was quantified as the percentage of GFP-labeled *Escherichia coli* positive macrophages. qPCR was used to measure the macrophage expression of the urate anion transporter 1 (URAT1). As compared to control cells, the production of tumor necrosis factor-alpha (TNF-alpha), toll-like receptor 4 (TLR4), and cluster of differentiation (CD) 11c was significantly increased by uric acid. In contrast, the number of macrophages expressing CD206, CX3C-motif chemokine receptor 1 (CX3CR1), or C-C chemokine receptor type 2 (CCR2) were significantly reduced. Uric acid progressively increased macrophage phagocytic activity and downregulated URAT1 expression. Probenecid inhibited both proinflammatory cytokine production and phagocytic activity in macrophages that were exposed to uric acid. These results suggest that uric acid has direct proinflammatory effects on macrophages possibly via URAT1.

INTRODUCCIÓN

En los seres humanos y otros primates, el ácido úrico es el producto final del metabolismo de las purinas. Esta molécula se sintetiza principalmente en el hígado, intestinos, endotelio vascular y otros tejidos (Benn et al. 2018; El Ridi and Tallima 2017). Después de su formación, el ácido úrico ingresa al torrente sanguíneo en forma de urato. Al circular por los riñones el ácido úrico se excreta y posteriormente se reabsorbe aproximadamente en un 90%, a través del transportador de aniones de urato (URAT) como el URAT-1 (Enomoto et al. 2002). La concentración sanguínea del ácido úrico depende directamente del balance entre su velocidad de síntesis y excreción (Maiuolo et al. 2016). En condiciones fisiológicas en homeostasis las concentraciones normales de ácido úrico en la sangre en hombres son de 3.4-7 mg/dL y 2.4-6 mg/dL en mujeres (Zhu, Pandya, and Choi 2011). A concentraciones bajas, el ácido úrico es una molécula esencial para la homeostasis, actúa como un potenciador de la respuesta inmune, contribuye en la reparación de los tejidos dañados y es el principal antioxidante del medio extracelular (Ames et al. 1981; Nery et al. 2015; El Ridi and Tallima 2017). Sin embargo, cuando las concentraciones del ácido úrico se encuentran elevadas, una condición conocida como hiperuricemia (HU), el urato se protoniza y se convierte en monourato de sodio, la molécula esencial para la nucleación de los cristales de monourato. Cuando estos cristales se depositan en el tejido articular, se convierten en unos potentes desencadenantes de la respuesta inflamatoria, al inducir el reclutamiento de monocitos y macrófagos hacia estos sitios y estimular la respuesta inflamatoria (Ghaemi-Oskouie and Shi 2011)

El ácido úrico fue aislado por primera vez hace más de dos siglos por Carl Scheele. Desde entonces, se estableció que la hiperuricemia es el factor causal de una patología

inflamatoria conocida como gota (Rosendorff and Jogendra 2013). La gota es una artropatía crónica ocasionada por la deposición de cristales de ácido úrico en diversas articulaciones. Estos cristales desencadenan una intensa respuesta inflamatoria que ocasiona episodios de dolor intenso y causan incapacidad temporal en las personas que la padecen. De manera interesante, evidencia reciente sugiere una posible asociación entre la elevación de los niveles sanguíneos de ácido úrico y una mayor actividad de células del sistema inmunitario, particularmente los macrófagos(Kim et al. 2015a; Li et al. 2023; Liu et al. 2022). Estas células del sistema inmune innato son notables por su plasticidad, pues pueden realizar múltiples tareas tales como la fagocitosis, la producción de citocinas inflamatorias y la reparación tisular, entre otras funciones (Martinez 2011; Murray 2017).

Además de su función en la respuesta inmune, los macrófagos también desempeñan funciones importantes en el desarrollo y perpetuación de diversos trastornos metabólicos como la resistencia a la insulina, la hiperglucemia, la Diabetes Mellitus, la hipertensión arterial sistémica y la hiperuricemia (Jiang et al. 2023; Krishnan et al. 2013). El entendimiento de los mecanismos subyacentes en la relación entre los macrófagos y los trastornos metabólicos, particularmente en el contexto de la hiperuricemia, es fundamental para la investigación básica y clínica.

ANTECEDENTES

Ácido úrico

El ácido úrico ($C_5H_4N_4O_3$) es un ácido orgánico débil con un peso molecular de 165 kDa y dos valores de pKa: pKa_1 5.8 y pKa_2 9.8 (Mandal and Mount 2015). En los humanos, el ácido úrico es el resultado de la degradación de las purinas y su síntesis inicia en el hígado y otros tejidos. La síntesis del ácido úrico implica un proceso complejo que comienza cuando las purinas adenina y guanina, provenientes de fuentes exógenas y endógenas, son metabolizadas a nivel hepático y gastrointestinal. El primer paso ocurre cuando la adenosina monofosfato (AMP) se convierte en inosina por dos vías diferentes. La primera vía consiste en eliminar un grupo amino mediante la enzima desaminasa dando lugar a la inosina monofosfato (IMP), a continuación, el IMP es desfosforilado por la purina nucleotido fosforilasa (PNP) para producir inosina. En el segundo mecanismo una nucleotidasa elimina un grupo fosfato dando lugar a la adenosina, la cual es desaminada y forma la inosina. Por otra parte, la guanina monofosfato (GMP) es desfosforilada por una nucleotidasa, generando guanosina. Los metabolitos intermedios inosina y guanosina también son desfosforilados dando lugar a hipoxantina y guanina, respectivamente. A continuación, la hipoxantina es oxidada por la xantino oxidasa (XO) generando xantina, mientras que también la guanina es desaminada por la guanina desaminasa formando xantina. Posteriormente la XO oxida nuevamente a la xantina para formar al ácido úrico (Figura 1) (Benn et al. 2018).

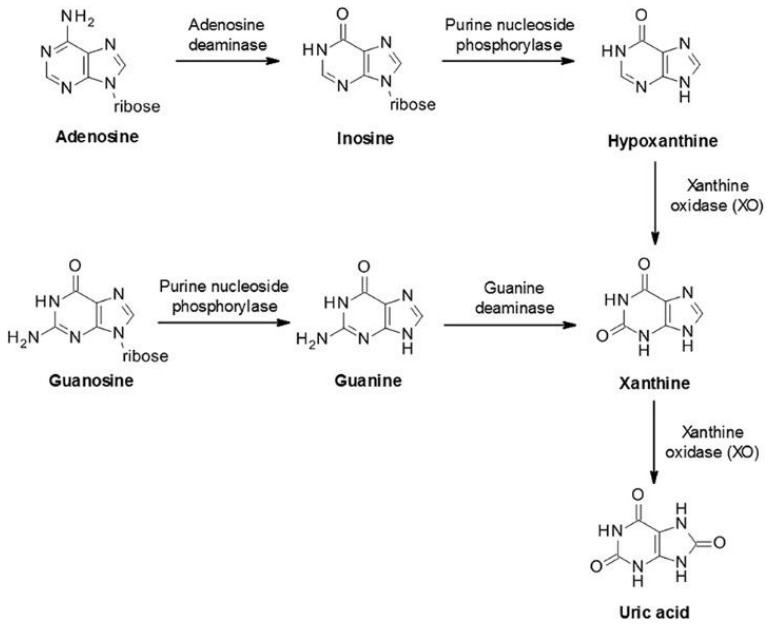

Figura 1. Síntesis del ácido úrico.

En la mayor parte de los mamíferos, el ácido úrico es un producto intermedio que es degradado mediante la enzima uricasa, una enzima peroxisomal que cataliza la oxidación del ácido úrico y da lugar a la producción de alantoína, un compuesto más soluble y de fácil eliminación (Mandal and Mount 2015). Sin embargo, en los seres humanos, una mutación en el gen de la uricasa impide la producción de esta enzima, como consecuencia los seres humanos son incapaces de catabolizar al ácido úrico, lo que conduce a la acumulación y elevación en la concentración de ácido úrico en los seres humanos (Figura 2).

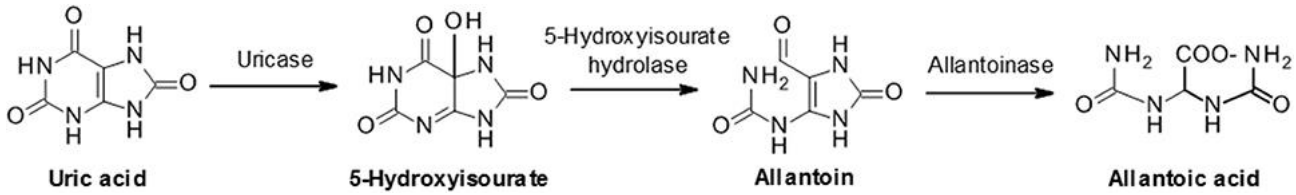

Figura 2. Catabolismo del ácido úrico por la enzima uricasa.

Metabolismo renal del ácido úrico

El metabolismo renal del ácido úrico es un proceso sumamente complejo, en el que la síntesis y el catabolismo se mantienen en niveles relativamente constantes, produciéndose entre 300 y 400 mg diariamente (Maiuolo et al. 2016b). De esta cantidad, los riñones eliminan aproximadamente dos tercios del ácido úrico, mientras que el tercio restante se excreta a través del tracto gastrointestinal (Bobulescu and Moe 2012).

Después de ser transportado por la circulación sanguínea, el ácido úrico ingresa a los riñones y circula a través los capilares, donde es filtrado por los glomérulos. En el túbulo contorneado proximal, se lleva a cabo tanto la secreción como la reabsorción del ácido úrico, aproximadamente el 90% del ácido úrico filtrado es posteriormente reabsorbido. El sitio principal donde esto ocurre es el segmento S1 del túbulo contorneado. En la parte basal de sus células epiteliales se encuentran transportadores que intercambian aniones por ácido úrico, como el transportador de glucosa 9 (GLUT-9) y los transportadores de aniones orgánicos (OAT) 1 y 3. Por otro lado, en la porción apical de las células epiteliales, se encuentran varios transportadores de ácido úrico, siendo el URAT1 el transportador principal de uratos. El URAT1 está codificado por el gen SLC22A12, y mutaciones en este gen están relacionadas con enfermedades relacionadas con el ácido úrico. En el segmento S2 del túbulo proximal, el ácido úrico se secreta en mayor medida que el que se reabsorbe. La reabsorción post-secreción tiene lugar en la porción más distal del túbulo proximal, aproximadamente entre el 5-10% del ácido úrico que se filtra aparece en la orina. Esta alta tasa de reabsorción sugiere que el ácido úrico puede tener funciones biológicas (Bobulescu and Moe 2012; Mandal and Mount 2015).

Funciones biológicas del ácido úrico

Inicialmente se consideró al ácido úrico como una molécula sin funciones biológicas significativas, siendo considerado únicamente como el agente causal de la gota. No obstante, investigaciones posteriores han revelado que el ácido úrico desempeña diversas funciones biológicas, las cuales se detallan a continuación.

Función antioxidante. En los seres humanos, se ha demostrado que más de la mitad de la función antioxidante en el medio extracelular proviene del ácido úrico. El ácido úrico desempeña un papel fundamental al proteger a las células contra el daño oxidativo provocado por los radicales libres y el peroxinitrito (Hooper et al. 1998).

En las células endoteliales se ha demostrado que las concentraciones elevadas de ácido úrico pueden causar disfunción endotelial. Estas células poseen el trasportador URAT1, lo que permite el ingreso del ácido úrico. Esto a su vez, desencadena un proceso inflamatorio y el aumento del estrés oxidativo (Figura 3). Por otra parte, los tratamientos hipouricemiantes han demostrado que mejoran la disfunción endotelial en modelos experimentales y pacientes con enfermedades cardiovasculares (Liang et al. 2015; Maruhashi et al. 2018a).

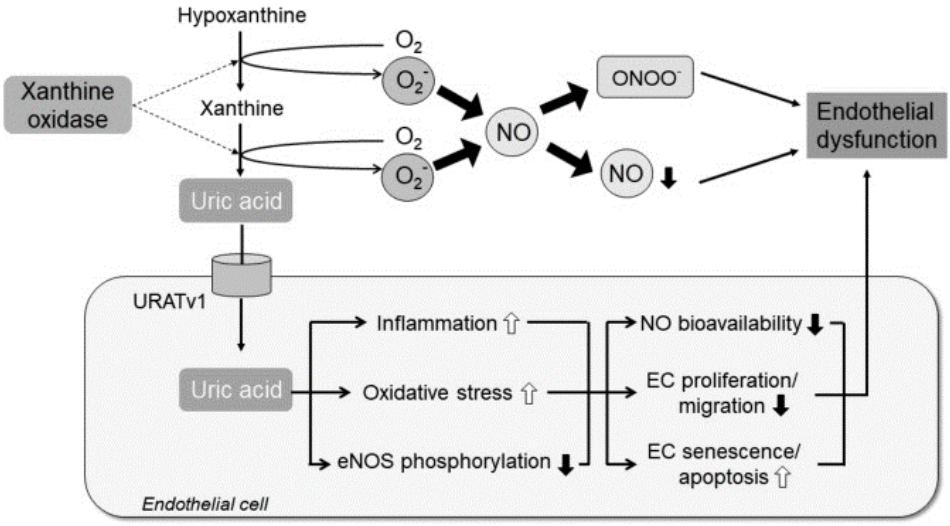

Figura 3. Mecanismos implicados en la disfunción endotelial inducida por la hiperuricemia (Tomado de Maruhashi et al. 2018)

Neuroprotección: existe evidencia que sugiere que el ácido úrico desempeña un papel neuroprotector. Por ejemplo, en personas con enfermedades neurológicas como la esclerosis múltiple, que se caracteriza por el daño en las vainas de mielina que recubren las fibras nerviosas, frecuentemente tienen niveles sanguíneos de ácido úrico más bajos en comparación con las personas sanas. Además, se ha observado que, en personas con gota, la prevalencia de enfermedades neurológicas tiende a ser baja. Estas observaciones sugieren que el ácido úrico podría desempeñar un papel importante en la preservación de la función cognitiva y en la reducción del riesgo para desarrollar enfermedades neurodegenerativas, como la enfermedad de Parkinson (Li et al. 2015; Mijailovic, Vesic, and Borovcanin 2022).

Cicatrización de heridas: En concentraciones fisiológicas, cuando hay un daño en los tejidos, el ácido úrico promueve la cicatrización de las heridas al funcionar como una señal de alarma endógena que estimula el reclutamiento de plaquetas y la producción de colágeno con lo que se estimula la activación plaquetaria (Chung et al. 2004), además estimular la proliferación

de fibroblastos, células que participan en la reparación de tejidos y facilita la adhesión de neutrófilos y monocitos a la matriz extracelular (Nakamura et al. 2001). Por el contrario, se ha observado que en personas con ulceras venosas tienen concentraciones elevadas de ácido úrico en las heridas y que está directamente relacionado con la severidad de la herida (Fernández, Upton, and Shooter 2014).

Respuesta inmune: El ácido úrico está implicado en el desarrollo de la respuesta inmune. Puede actuar como una señal de peligro endógena, que desencadena reacciones inmunes en ciertos contextos, por ejemplo, en modelos animales de inflamación peritoneal, el ácido úrico es esencial y suficiente para inducir respuestas inmunitarias mediadas por anticuerpos y células (Shi, Galusha, and Rock 2006). El ácido úrico liberado en este contexto actua como una señal de peligro que estimula a las células dendríticas derivadas de monocitos inflamatorios (Chen 2006). Además, el ácido úrico liberado en las vías respiratorias de pacientes asmáticos y en ratones expuestos a alérgenos es esencial para desarrollar la inmunidad de tipo 2, eosinofilia y una mayor reactividad bronquial a alergenos inhalados y a los ácaros del polvo doméstico. Por otra parte, cuando se administraron cristales de urato monosódico junto con proteínas inofensivas inhaladas, se desencadenó una respuesta inmunitaria de tipo 2 exacerbadas (Kool et al. 2011). Estos hallazgos sugieren que el ácido úrico actúa como un iniciador y amplificador crucial de la inflamación.

Hiperuricemia y gota

La hiperuricemia, definida como una concentración anormalmente elevada de ácido úrico en sangre, es el agente etiológico clave para el desarrollo de la artritis inflamatoria conocida como gota (Benn et al. 2018). La hiperuricemia es el resultado del incremento de la

producción de ácido úrico, la disminución en la excreción renal de ácido úrico o la combinación de ambos. Aunque los valores que definen a la hiperuricemia en adultos no son iguales en todas las poblaciones, en general se considera tener esta condición cuando la concentración de ácido úrico en sangre es superior a 7,0 mg/dL en hombres y 6,0 mg/dL en mujeres (Zhu et al. 2011). Cuando el ácido úrico, encontrado en la circulación sanguínea en forma de urato, se encuentra en altas concentraciones, se protoniza y da lugar al urato monosódico (MSU), la molécula esencial para la nucleación o formación de su forma cristalizada. Cuando estos cristales se depositan en las articulaciones y en el tejido conectivo periarticular, se convierten en unos potentes desencadenantes de la respuesta inflamatoria, al inducir el reclutamiento de células inmunitarias hacia estos sitios y estimular la respuesta inflamatoria (Ghaemi-Oskouie and Shi 2011), clínicamente interpretada como un ataque agudo de gota. Los cristales de MSU localizados en las articulaciones interactúan con los macrófagos y residentes, así como con neutrófilos y monocitos reclutados, células sinoviales y endoteliales no hematopoyéticas. Todas estas células inmunes pueden fagocitar o endocitar cristales de MSU, lo que provoca la activación, lesión y liberación de enzimas hidrolíticas, especies reactivas de oxígeno y la liberación de patrones moleculares asociados al peligro (DAMP) que pueden ser detectados por las células del sistema inmunológico innato. Una vez en el interior de las células inmunes, los cristales de ácido úrico estimulan la activación del complejo multiproteico conocido como inflamosoma NLRP3 (NOD-like receptor protein 3). Este inflamosoma escinde proteolíticamente a la pro-interleucina 1β (pro IL-1β) y genera a su forma activa, la IL-1β en las articulaciones afectadas (Braga et al. 2017a). Una vez que es liberada esta citocina, se inicia un proceso de reclutamiento de neutrófilos y monocitos al sitio de producción, estas células inmunes producen especies reactivas de oxígeno, enzimas proteolíticas, quimiocinas y citocinas inflamatorias como la proteína quimioatrayente de

monocitos (MCP-1) y la molécula de adhesión intercelular 1 (ICAM-1) seguidas de la activación de los macrófagos y una mayor liberación de moléculas inflamatorias mediadas por el factor nuclear kappa B (NF-κB). Además, hay otras células que también están activas en los ataques agudos de gota, por ejemplo, los fibroblastos reclutados al sitio de inflamación secretan factores de crecimiento fibroblástico y matriz extracelular causante de fibrosis (Zhou et al. 2012).

Hiperuricemia y enfermedades cardiovasculares

Existe evidencia de la fuerte asociación entre la hiperuricemia y el desarrollo de enfermedades cardiovasculares e hipertensión. Estudios recientes sugieren que el ácido úrico ingresa al músculo liso vascular mediante los transportadores URAT-1 y OAT9 desencadenando múltiples vías de señalización que resultan en una mayor expresión de mediadores inflamatorios. Esto a su vez, contribuye al aumento de la presión arterial, la hipertrofia de células del músculo liso vascular e hipertensión (Kanbay et al. 2013; Mazzali et al. 2010). Adicionalmente, el ácido úrico disminuye la producción de la enzima óxido nítrico sintasa generando así una disminución en la producción del óxido nítrico. Asimismo, incrementa la producción del factor de transcripción NF-κB y las citocinas inflamatorias TNF-α y la IL-6 las cuales conducen a la disfunción de las células endoteliales vasculares(Cai et al. 2017). Adicionalmente el ácido úrico también activa el sistema renina-angiotensina aumentando el estrés del retículo endoplásmico, la producción de especies reactivas de oxígeno y nitrógeno, y la disminución en la función antioxidante(Hong et al. 2020).

Hiperuricemia y Diabetes Mellitus

La Diabetes Mellitus tipo 2 (DM2) es una enfermedad metabólica que ha incrementado preocupantemente durante las últimas décadas. Se estima que para el año 2045 habrán cerca de 700 millones de personas con DM2 (Cho et al. 2018; Tancredi et al. 2015). En numerosos estudios clínicos han mostrado que las niños y adultos con hiperuricemia tienen una mayor prevalencia de resistencia a la insulina (Hu et al. 2021). Estos estudios también han mostrado que la hiperuricemia es un factor de riesgo independiente para el desarrollo de hiperglucemia y diabetes, independientemente de otras comorbilidades (Alemayehu et al. 2023; Jiang et al. 2023; Krishnan et al. 2013; Miranda et al. 2015). Adicionalmente, en modelos murinos de hiperuricemia y en células hepáticas HepG2 y cardiomiocitos, se ha demostrado que el ácido úrico incrementa la producción de especies reactivas de oxígeno, inhibe la transducción de la vía de señalización de la insulina a través de la fosforilación de la serina 307 del sustrato del receptor de insulina (IRS), inhibe la fosforilación de la serina 473 del AKT (también conocida como protein cinasa B) e incrementa los niveles de glucosa en sangre (Zhi et al. 2016; Zhu et al. 2014).

Además, en personas con DM2 de larga evolución existe un daño a órganos blanco como los riñones y la retina. El daño a estos órganos es cuantificado mediante la albuminuria, es decir la cantidad de albumina en la orina y a nivel oftálmico por el crecimiento de vasos sanguíneos en la retina o retinopatía diabética. En este sentido, se ha demostrado que los niveles elevados de ácido úrico muestran una asociación positiva y significativa con la gravedad de la albuminuria y la retinopatía diabética en pacientes con DM2 (Pai et al. 2022; Russo et al. 2022).

Macrófagos

Los macrófagos son células del sistema inmune innato encontrados en la mayor parte de los órganos y tejidos del organismo. Estas células fueron descritas por primera vez por Elie Metchnikov quien las nombró macrófagos, del griego "macro" grande y "phagos" comedor, debido a su capacidad fagocítica, es decir, su capacidad para ingerir partículas y microorganismos. Además de la fagocitosis, los macrófagos desempeñan otras funciones, por ejemplo, participan en la formación de los vasos sanguíneos, embriogénesis, reparación y cicatrización de las heridas, además están implicados de forma importante en la obesidad, diabetes y el cáncer (Martinez 2011; Martinez, Helming, and Gordon 2009).

Los macrófagos exhiben una notable plasticidad que les permite modificar su fenotipo y función dependiendo del microambiente en el que se encuentran. Cuando se enfrentan a microorganismos patógenos o señales moleculares de daño, los macrófagos regulan la respuesta inmune en sus diversas etapas; en primera instancia, inician y conducen el proceso inflamatorio con el fin de destruir a los patógenos. Posteriormente, se encargan de eliminar células muertas y restos de patógenos. Finalmente participan en la restauración y restablecimiento de los tejidos dañados, devolviéndolos a su condicional inicial (Kim and Nair 2019; Martinez 2011).

Tipos de macrófagos

Los macrófagos pueden tener 2 orígenes: los macrófagos residentes, que surgen durante la embriogénesis y los macrófagos derivados de monocitos (MDM).

Macrófagos residentes

Los macrófagos residentes se originan de precursores que están presentes en el ser humano desde el desarrollo embrionario y se originan en tres oleadas hematopoyéticas principales, denominadas primitiva, predefinitiva y definitiva. Las dos primeras oleadas tienen lugar en estructuras embrionarias, como el saco vitelino y la alantoides, donde surgen los primeros macrófagos residentes. Estos reciben diferentes denominaciones dependiendo del sitio donde se encuentren. En la piel se les denomina células de Langerhans, en los pulmones células de Kupffer y en el cerebro se les conoce como microglía. En la tercera oleada o fase definitiva, surgen los macrófagos residentes del sistema cardiaco, del musculo esquelético, osteoclastos en el hueso y una cantidad adicional de células de Kupffer. En esta fase, los precursores hematopoyéticos, incluidos los precursores de los monocitos se establecen en la medula ósea (Sreejit et al. 2020) como su sitio de producción definitivo (Figura 4).

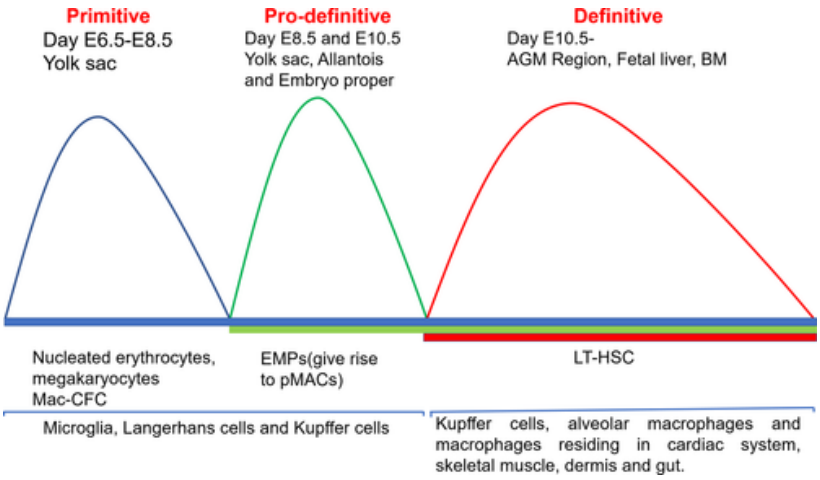

Figura 4. Origen de los macrófagos (Tomado de Sreejit, et al. 2020).

Macrófagos derivados de monocitos

Los macrófagos derivados de monocitos se originan a partir de la diferenciación de sus precursores celulares, los monocitos. Los monocitos son células del sistema inmune que se generan en la medula ósea y constituyen cerca del 10% de los leucocitos en los humanos. En condiciones fisiológicas, los monocitos circulan por los vasos sanguíneos durante uno a tres días, después de lo cual son eliminados por el bazo y son restituidos por la medula ósea para mantener una cantidad constante en el torrente circulatorio (Italiani and Boraschi 2014).

En presencia de microorganismos patógenos o señales de daño tisular, tanto los tejidos lesionados, así como el endotelio vascular secretan citocinas inflamatorias como la IL-6, IL-1β, TNF-α y quimiocinas como la proteína quimioatrayente de macrófagos 1 y 2. Estas citocinas viajan por la circulación sanguínea y se unen a sus receptores localizados en la membrana de los monocitos, con lo cual inicia el redireccionamiento de los monocitos hacia el sitio de inflamación. Adicionalmente las células endoteliales cercanas a la zona de lesión tisular expresan integrinas como la molécula de adhesión intercelular 1 (ICAM-1), la molécula de adhesión vascular 1 (VCAM-1) y las selectinas P y E. Estas moléculas se unen a glucoproteínas y receptores de integrinas presentes en los monocitos, como el antígeno 1 asociado a la función leucocitaria (LFA-1) y el antígeno de liberación tardía (VLA-4), con lo que disminuyen su velocidad de flujo y posteriormente se detienen en el sitio de inflamación. Las células endoteliales adyacentes modifican su citoesqueleto y permiten la extravasación de los monocitos hacia los tejidos lesionados (Gerhardt and Ley 2015).

Diferenciación de monocitos a macrófagos

En condiciones de homeostasis, las células estromales y endoteliales producen una cantidad basal del factor estimulante de colonias de macrófagos 1 (M-CSF-1). Esta proteína es esencial para el desarrollo de los monocitos y la diferenciación de los macrófagos residentes. Sin embargo, en un escenario inflamatorio, el endotelio y las células cercanas al sitio de daño tisular incrementan la producción del M-CSF-1, el factor estimulante de colonias de granulocitos-monocitos (GM-CSF) y la interleucina 34 (IL-34). El incremento en la concentración circulante de las proteínas mencionadas favorece una mayor producción de monocitos en la medula ósea, su salida de la circulación sanguínea y el reclutamiento de estos monocitos, que posteriormente inician su diferenciación hacia macrófagos (Italiani and Boraschi 2014; Martinez 2011).

En condiciones *in vitro* los macrófagos pueden diferenciarse hacia un fenotipo basal conocido como M0. Sin embargo, en condiciones *in vivo* los macrófagos adquieren diversos fenotipos y funciones que dependen del microambiente, mismo que dirige el proceso de diferenciación hacia un perfil pro o antinflamatorio (Italiani and Boraschi 2014; Murray 2017).

Macrófagos M1

Los macrófagos activados clásicamente o también conocidos como M1 son macrófagos proinflamatorios que surgen como resultado de la exposición a moléculas relacionadas con microorganismos infecciosos, como el lipopolisacárido (LPS), el interferón gama (IFN-ɣ) y el factor de necrosis tumoral alfa (TNF-α). Estos macrófagos se caracterizan por su fenotipo y función. Sus marcadores de superficie incluyen al CD80, CD86, CD11c, CCR2 y los

receptores tipo Toll 2 y 4 (TLR-2 y 4). Además, estos macrófagos expresan típicamente a la enzima óxido nítrico sintasa inducible (iNOS), y producen cantidades significativas de especies reactivas de oxígeno (ROS), TNF-α y las interleucinas (IL)1β, 6 y 12. Estas moléculas contribuyen a amplificar la respuesta inflamatoria en el microambiente. Adicionalmente estos macrófagos se pueden caracterizar por los marcadores que reconocen moléculas con capacidad quimioatrayente como CCL20, CXCL10, CXCL11 que inducen el reclutamiento de monocitos y otras células inmunes (Murray 2017).

Macrófagos M2

Los macrófagos activados alternativamente o también conocidos como M2, ejercen funciones antinflamatorias, participan en la reparación y cicatrización de los tejidos, eliminación de restos celulares y células apoptóticas, y son activos frente a parásitos(Italiani and Boraschi 2014; Murray 2017). Existen varios subtipos de macrófagos M2 cuya polarización depende del estímulo con el que son activados. A continuación, se describen los diferentes subtipos de macrófagos:

Macrófagos M2a: Se obtienen este subtipo de macrófagos cuando son estimulados con citocinas tipo Th2 como la IL-4 e IL-13. Los macrófagos M2a se caracterizan por la expresión elevada del receptor de manosa (CD-206) y de galactosa, además de la presencia de la arginasa 1 (Arg-1), una enzima encargada de hidrolizar la L-arginina a L-ornitina, un aminoácido fundamental para la replicación, el crecimiento y la diferenciación celular, además de ser importante en la reparación de lesiones (Italiani and Boraschi 2014; Martinez et al. 2009; Murray 2017).

Macrófagos M2b. Se obtienen con la estimulación con complejos inmunes, agonistas de los receptores tipo toll y el lipopolisacárido. Estos macrófagos producen citocinas antiinflamatorias y proinflamatorias como IL-10, IL-1β y el TNF-α(Gordon 2003; Martinez 2011).

Macrófagos M2c. Son macrófagos activados por glucocorticoides, IL-10 y el factor de crecimiento transformante beta (TGF-β), también son llamados macrófagos desactivados. Actúan eliminando células apoptóticas y secretan IL-10 Y TGF-β (Gordon 2003; Italiani and Boraschi 2014).

Macrófagos y enfermedades metabólicas

Los macrófagos desempeñan un papel fundamental en el inicio, desarrollo y perpetuación de diversas alteraciones y patologías cardiometabólicas. Por ejemplo, en modelos animales y en sujetos con condiciones como hiperglucemia, diabetes, dislipidemias, obesidad e hipertensión arterial se ha observado un incremento en el número de monocitos y macrófagos infiltrados en diversos órganos y tejidos como el endotelio de los vasos sanguíneos, riñones, corazón y el tejido adiposo, en comparación con sujetos sanos (Clozel et al. 1991). Estos macrófagos reclutados adoptan un fenotipo proinflamatorio, en contraste con los sujetos sanos en los que predominan los macrófagos con un fenotipo antinflamatorio.

En este sentido, se ha observado que, en el tejido adiposo de ratones y humanos con obesidad, los adipocitos hipertróficos activan diversas vías de señalización relacionadas con la hipoxia y el estrés celular. Esto conlleva a la liberación de ácidos grasos libres a la circulación sanguínea, al incremento en la producción de especies reactivas de oxígeno y nitrógeno y una producción elevada de quimiocinas como CCL2. Estas moléculas

desempeñan un papel crucial en el direccionamiento de monocitos CCR2+ hacia el tejido adiposo, donde posteriormente se diferencian hacia macrófagos. Se ha reportado un incremento de hasta 4 veces el número de macrófagos infiltrados en el tejido adiposo de individuos con obesidad comparados con sujetos delgados. Estos macrófagos adoptan una disposición característica conocida como "estructuras similares a coronas" (CLS) con la que rodean a los adipocitos disfuncionales (Hotamisligil et al. 1995). En estos conglomerados, los macrófagos expresan cantidades elevadas de marcadores inflamatorios como TLR4 y CD11c+, y producen diferentes citocinas como la IL-1β, IL-6 y TNF-α. El incremento sostenido de estas moléculas inflamatorias resulta perjudicial para los diferentes órganos y tejidos, ya que modifica las vías de señalización metabólicas. Por ejemplo, en los tejidos dependientes de insulina, las citocinas inflamatorias alteran el metabolismo de los carbohidratos al fosforilar la serina del IRS. Esta fosforilación bloquea la vía de señalización de la insulina, con la consecuente inhibición de la función del receptor de insulina (RI). Como resultado de esta fosforilación inadecuada la insulina no puede cumplir su función biológica, una condición conocida como resistencia a la insulina en la que las células son incapaces de captar glucosa, lo que conduce al aumento de la glucosa en la circulación sanguínea. Si esta condición persiste durante un periodo prolongado, puede llevar al desarrollo de la DM2 (Hotamisligil et al. 1995; Li et al. 2022; Russo et al. 2021).

Adicionalmente, se ha reportado que en la hipertensión arterial, las dislipidemias y la ateroesclerosis, se produce un aumento de citocinas inflamatorias tanto a nivel sistémico como local (Fatkhullina, Peshkova, and Koltsova 2016; Hong et al. 2022; Ramji and Davies 2015; Zhang et al. 2023). Además, se ha observado un incremento en el número de monocitos y macrófagos con fenotipo M1 en diferentes tejidos, como los riñones, grasa perivascular,

las placas ateromatosas en las arterias carótidas, el arco aórtico y las arterias coronarias (Caillon, Paradis, and Schiffrin 2019; Rodríguez-Iturbe, Pons, and Johnson 2017). Cuando se utilizan medicamentos antihipertensivos e hipolipemiantes, se observa una disminución en el reclutamiento de los macrófagos en los riñones, grasa perivascular y las placas ateromatosas, así como la actividad de factores de transcripción implicados en la inflamación como el NF-κB. Adicionalmente se ha observado que al utilizar inhibidores específicos de MCP-1, se consigue la disminución en el reclutamiento de macrófagos en diferentes tejidos como el endotelio vascular, así como una reducción moderada en la presión arterial (Elmarakby et al. 2007).

Hiperuricemia y macrófagos

Diversos estudios clínicos han demostrado una asociación significativa entre la hiperuricemia y un estado inflamatorio sistémico. Esta asociación es demostrada particularmente por una mayor producción de citocinas proinflamatorias, como la IL-6, IL-12 y el TNF-α, así como con la proteína C reactiva (Lyngdoh et al. 2011; Ruggiero et al. 2006). Además, se ha observado que los sujetos con hiperuricemia presentan un mayor número leucocitos circulantes, en particular, de monocitos y un mayor número de macrófagos inflamatorios en tejidos como el tejido adiposo y renal(Hotamisligil et al. 1995; Kim et al. 2015a).

Además, se ha reportado que en modelos de hiperuricemia existe un incremento significativo en la producción de MCP-1. Esto a su vez va acompañado del aumento en el número de macrófagos infiltrados (Grainger et al. 2013; Kanellis et al. 2003; Kim et al. 2015b; Wasilewska et al. 2012). Estos macrófagos expuestos a altas concentraciones de ácido úrico tienen la capacidad de inhibir la vía de señalización responsiva a la insulina en tejidos

como el tejido adiposo y el hepático (Baldwin et al. 2011; Yu et al. 2023). Por otro lado, en las placas ateromatosas de ratones ApoE-/- con hiperuricemia se observa un infiltrado activo de macrófagos acompañado de activación de NF-κB así como producción de IL-1β y MCP-1 (Lee et al. 2021). Asimismo, en cultivos de macrófagos derivados de células THP-1 y en MDM, se ha demostrado que el ácido úrico estimula la producción de ROS producidas mitocondrialmente. Estas ROS contribuyen al incremento en la producción de IL-1β vía el inflamosoma NLRP-3 (Braga et al. 2017b; Kim et al. 2015b). De forma similar, en ratones CD-1 y en ratas OLETF que exhiben niveles elevados de ácido úrico, se ha observado un mayor infiltrado de macrófagos en el intersticio tubular del riñón. Adicionalmente, se ha reportado un incremento en la expresión de moléculas quimioatrayentes e inflamatorias como el MCP-1, TGF-β y TNF-α. En contraste, cuando se usa alopurinol, un bloqueador de la reabsorción de ácido úrico en los riñones, disminuye el reclutamiento de macrófagos, la producción de moléculas inflamatorias, una mejora en la función renal y mejora la via de señalización de la insulina (Kim et al. 2015b; Zhou et al. 2012).

PLANTEAMIENTO DEL PROBLEMA

Los antecedentes mencionados sugieren la existencia de una relación entre la elevación de los niveles de ácido úrico y la polarización de los macrófagos hacia un fenotipo inflamatorio, fenómeno que podría estar asociado con el desarrollo de alteraciones metabólicas como la dislipidemia, la hiperglucemia y la resistencia a la insulina. Sin embargo, hasta el momento no se conoce cuál es la naturaleza de la relación entre el ácido úrico y el macrófago, generando así los siguientes cuestionamientos: ¿El ácido úrico promueve de manera directa la activación inflamatoria de los macrófagos? ¿Existe una proteína transportadora de ácido úrico en los macrófagos? ¿Cuáles son las vías de señalización involucradas en mediar el efecto del ácido úrico sobre los macrófagos?

HIPÓTESIS

El ácido úrico promueve directamente la activación M1, y/o disminuye la activación M2, en macrófagos primarios de origen humano *in vitro*, de manera dependiente de la concentración y a través del transportador de aniones de urato como el URAT-1.

OBJETIVOS

Objetivo general

Evaluar el efecto del ácido úrico sobre la activación de macrófagos primarios de origen humano cultivados *in vitro*, estudiando las vías de señalización involucradas en mediar este efecto.

Objetivos particulares

1. Determinar el efecto de concentraciones crecientes de ácido úrico sobre la diferenciación de macrófagos derivados de monocitos en cultivo *in vitro*, evaluando la respuesta de estas células a la exposición a LPS.
2. Evaluar el perfil de activación de macrófagos humanos cultivados en presencia de concentraciones crecientes de ácido úrico a través de la medición de CD14, CD11c, CD206, CCR2, y CX3CR1, TLR-4 en la superficie celular y TNF-α, IL-1β intracelularmente por citometría de flujo.
3. Establecer si el macrófago posee el transportador de ácido úrico URAT 1 y si éste es regulado positiva o negativamente en relación con la exposición a este metabolito.
4. Evaluar el efecto del bloqueador de URAT-1, probenecid, en los macrófagos humanos mediante la expresión de marcadores de superficie celular y citocinas.
5. Determinar la respuesta de los macrófagos expuestos al ácido úrico frente a un reto inmunológico, analizando la actividad fagocítica de los mismos ante la exposición a *Escherichia coli* marcada con proteína verde fluorescente (*E. coli*+GFP).

MATERIALES Y MÉTODOS

Sujetos

Se obtuvieron concentrados leucocitarios de voluntarios varones sanos, con edades entre los 18 a 35 años, sin alteraciones metabólicas, que acudían a donación de sangre del Hospital General de México. Todos los participantes proporcionaron su consentimiento informado por escrito, el cual fue previamente aprobado por el comité de ética institucional del Hospital General de México (con número de registro de aprobación del comité de ética DIC/11/UME/05/029), el cual garantizó la realización adecuada del estudio de acuerdo con los principios descritos en la Declaración de Helsinki(World Medical Association. 2001).

Los donantes de sangre fueron excluidos del estudio si tenían diagnóstico previo de DM1 y DM2, enfermedad cardiovascular aguda o enfermedad hepática crónica, enfermedad renal aguda o crónica, cáncer, trastornos endocrinos, enfermedades infecciosas y enfermedades inflamatorias o autoinmunes. También se excluyeron del estudio a pacientes seropositivos para VIH, hepatitis tipo B y C, así como aquellos sujetos que estaban bajo prescripción de medicamentos antiinflamatorios, antiplaquetarios, antihipertensivos e inmunomoduladores, incluyendo medicamentos antiinflamatorios no esteroideos (AINEs).

Aislamiento de monocitos y cultivo de macrófagos

Los concentrados leucocitarios (n=10) se diluyeron en una proporción 1:2 utilizando PBS1x (Sigma Aldrich, St. Louis, MO, EE. UU.) para llevar a cabo el aislamiento de las células mononucleares de sangre periférica (PBMC) mediante centrifugación por gradiente de densidad para lo cual se utilizó histopaque-1077 (Sigma Aldrich, St. Louis, MO, EE. UU.).

Posteriormente, los monocitos se aislaron de las PBMC mediante selección negativa utilizando columnas magnéticas para CD14 (Miltenyi Biotec, Bergisch Gladbach, Alemania). Los monocitos purificados se cultivaron en medio RPMI-1640 (Sigma Aldrich, St. Louis, MO, EE. UU.) el cual fue suplementado con suero fetal bovino (FBS) al 10 % (GibcoTM, Grand Island, NY, EE. UU.), L-glutamina 2 mM, 50 μg/ mL de gentamicina y 10 ng/mL de factor estimulante de colonias de macrófagos (M-CSF) (GibcoTM, Grand Island, NY, EE. UU.) en placas de cultivo celular de 6 pozos (Costar, Kennebunk, ME, EE. UU.), a una densidad de 3×10^6 monocitos. Los medios de cultivo y el M-CSF se reemplazaron cada dos días durante un periodo de siete días. Tras la diferenciación, los macrófagos derivados de monocitos (MDM) se mantuvieron en medio RPMI-1640 suplementado, como se mencionó anteriormente, y se expusieron a 0,23, 0,45 o 0,9 mmol/l de ácido úrico (Sigma Aldrich, St. Louis, MO, EE. UU.) durante 12 horas. Después de realizar múltiples curvas de tiempo-respuesta a 1, 3, 6 y 12 h, así como 1,3,6 y 9 días, encontramos que los MDM exhibieron la actividad proinflamatoria más significativa a las 12 horas del cultivo *in vitro* en presencia de ácido úrico, por lo que se decidió realizar todos los experimentos en este momento. Antes de la exposición al ácido úrico, se agregó 1 mmol/L de probenecid, un bloqueador del transportador de ácido úrico URAT1 (St. Louis, MO, EE. UU.), y se reemplazó después de 6 h por medios de cultivo que contenían diferentes concentraciones de ácido úrico. Los MDM de control se mantuvieron en medio RPMI-1640 suplementado con FBS en ausencia de ácido úrico durante el mismo tiempo. Inmediatamente después, se recogieron MDM utilizando scrapers estériles (Corning, Reynosa, Tamaulipas, México) y se dividieron en partes iguales en 1 mL de PBS 1x (Sigma Aldrich, St. Louis, MO, EE. UU.) para su análisis mediante citometría de flujo o en 300 μL de reactivo TRIzol (Life

Technologies, Carlsbad, CA, EE. UU.) para ensayos de reacción en cadena de la polimerasa cuantitativa (qPCR).

Ensayos de citometría de flujo

Después de recolectar las células, se resuspendieron 1×10^6 MDM en 50 µL de buffer de tinción celular (BioLegend, Inc., San Diego, CA, EE. UU.). Las células se incubaron a 4ºC en la oscuridad con los anticuerpos anti-CD14 PE/Cy7, anti-CD206 APC/Cy7, anti-TLR4 PE, anti-CX3CR1 BV510, anti-CCR2 AF647 (BioLegend, Inc., San Diego, CA, EE. UU.) y 5 µL True-Stain Monocyte Blocker™ (BioLegend, Inc., San Diego, CA, EE. UU.) durante 20 minutos. Después de lavar con Cell Staining Buffer (BioLegend, Inc., San Diego, CA, EE. UU.), se evaluó la viabilidad celular de los MDM empleando 7-AAD (BD Pharmingen™, San Jose, CA, EE. UU.) durante 10 min. Posteriormente las muestras fueron analizadas en un citómetro de flujo FACSCanto II (BD Biosciences, San Jose, CA, EE. UU.) mediante el software BD FACSDivaTM 6.0, adquiriendo 20.000 eventos por ensayo por triplicado. Los controles de compensación se realizaron utilizando UltraComp eBeads™ (Invitrogen, Carlsbad, CA, EE. UU.) para cada fluorocromo. Los datos de citometría de flujo se analizaron utilizando el software FlowJo 10.0.7 (TreeStar, Inc, Ashland, OR, EE. UU.). Para la tinción de citoquinas intracelulares, los MDM se trataron con Brefeldin A 1:1000 (BioLegend, Inc San Diego, CA, EE. UU.) durante las últimas 2 h de cultivo *in vitro*. Después de recolectar las células, se resuspendieron 1×10^6 MDM en 50 µL de tampón de tinción celular (BioLegend, Inc., San Diego, CA, EE. UU.). Inmediatamente después, los MDM se incubaron simultáneamente con anti-CD14 PE/Cy7, anti-CD11c PE/Cy5, Zombie UV Fixable Viability Kit y 5 µL True-Stain Monocyte Blocker™ (BioLegend, Inc., San Diego, CA, EE. UU.) en la oscuridad durante 20 minutos a 4 °C. Posteriormente, los MDM se

incubaron con 100 µL de medio de fijación A (kit de permeabilización celular FIX & PERM™) (Invitrogen™, Carlsbad, CA, EE. UU.) durante 15 min. a temperatura ambiente. Posteriormente, los MDM se lavaron con Cell Staining Buffer (BioLegend, Inc., San Diego, CA, EE. UU.) para su posterior incubación con 100 µL de medio de permeabilización B (FIX & PERM™ Cell Permeabilization Kit) (Invitrogen™, Carlsbad, CA, EE. UU.) y posteriormente con anti-TNF-α AF488 y anti-IL-1 beta Pacific Blue durante 20 minutos en la oscuridad a temperatura ambiente. Inmediatamente después, los MDM se lavaron con Cell Staining Buffer (BioLegend, Inc., San Diego, CA, EE. UU.) y luego se adquirieron en un citómetro de flujo BD Influx (BD Biosciences, San Jose, CA, EE. UU.) mediante el software BD SortwareTM. 1.2, adquiriendo 20.000 eventos por prueba por triplicado. Los controles de compensación se realizaron utilizando UltraComp eBeads™ (Invitrogen™, Carlsbad, CA, EE. UU.) para cada fluorocromo. Los datos de citometría de flujo se analizaron utilizando el software FlowJo 10.0.7 (TreeStar, Inc, Ashland, OR, EE. UU.).

Actividad fagocítica de los macrófagos

Se transformó *Escherichia coli* de la cepa DH5a con el plásmido pCD353 (E. coli-GFP+) que codifica la proteína verde fluorescente (GFP)-mut2 que está regulada por un promotor lactac. Se indujo el plásmido GFP usando isopropil-b-D-1-tiogalactopiranósido 1 mM (Sigma Aldrich, St. Louis, MO, EE. UU.), como se describió anteriormente(Ikeno and Haruyama 2013). E. *coli*-GFP+ se cultivaron *in vitro* con macrófagos en una proporción de bacterias:células = 30:1 durante 1 hora. Posteriormente, las suspensiones celulares se centrifugaron a 2500 rpm/15 minutos para eliminar las bacterias remanentes y luego se resuspendieron en 50 µL de PBS 1x estéril para su posterior análisis en un citómetro de flujo

FACSCanto II (BD Biosciences, San Jose, CA, EE. UU.) mediante el software BD FACSDivaTM 6.0, adquiriendo 20.000 eventos por prueba por triplicado.

Expresión del gen URAT1 por qPCR

Después de recolectar las células, se resuspendieron 1×10^6 MDM en reactivo TRIzol (Life Technologies, Life Technologies, Carlsbad, CA, EE. UU.) a 4 °C. Inmediatamente después, el ARN total fue aislado por el método de fenol/cloroformo/isotiocianato de guanidina de acuerdo con las instrucciones del fabricante. Las muestras de ARN total se cuantificaron y se sometieron a transcripción inversa utilizando el sistema de retrotranscriptasa M-MLV en presencia del cebador dT (Invitrogen, Carlsbad, CA, EE. UU.). Después de ser incubadas a 37 °C durante 60 min., las muestras de cDNA se obtuvieron y usaron para la amplificación usando la reacción en cadena de la polimerasa en tiempo real (qPCR) en presencia de SYBR Green Master Mix y AmpliTaq® Fast DNA Polymerase (Applied biosystems, Foster City, CA, EE. UU.), según las instrucciones del fabricante. Los cebadores específicos para humanos para URAT1 se diseñaron utilizando el software Primer-BLAST del Centro Nacional de Información Biotecnológica (NCBI), Biblioteca Nacional de Medicina de EE. UU., de la siguiente manera: cebador directo 5′-CGGACCTGTATCTCCACGTT-3′, cebador inverso 5′-TGCCTTCTTTACTGCCTGGT -3′, desnaturalización a 94 °C durante 30 s, recocido a 60 °C durante 45 segundos, elongación a 72 °C durante 45 segundos y 28 ciclos térmicos para una longitud de producto de 570 pares de bases (pb). La secuencia de ARN ribosomal 18S se utilizó como control del gen de mantenimiento de la siguiente manera: cebador directo 5'-CGCGGTTCTATTTTGTTGGT-3', cebador inverso 5'-AGTCGGCATCGTTTATGGTC-3', desnaturalización a 94 °C durante 30 segundos, hibridación a 60 ° C durante 30 segundos, elongación a 72 °C durante 30 s y 40 ciclos

térmicos para una longitud de producto de 570 pb. La expresión del ARNm de URAT1 se normalizó mediante el control del gen de limpieza y se notificó como 2^(ΔΔCt). Los experimentos de qPCR se informan de acuerdo con las pautas de información mínima para la publicación de experimentos de PCR en tiempo real cuantitativos (MIQE) para garantizar la reproducibilidad.

Estadística

La prueba de Shapiro-Wilk estimó la normalidad de la distribución de los datos. Se utilizó ANOVA unidireccional, seguido de una prueba de Tukey post-hoc, para comparar la expresión de CD11c, CD206, TNF-α, IL-1β, TLR4, CX3CR1, CCR2 y URAT1, así como la cantidad intracelular de *E. coli*-GFP+ en macrófagos derivados de monocitos que fueron expuestos a 0, 0,23, 0,45 o 0,9 mmol/L de ácido úrico. Todos los análisis estadísticos se realizaron con el software GraphPad Prism 7. Las diferencias se consideraron significativas cuando el valor de $p < 0,05$.

RESULTADOS

Tras la diferenciación en presencia de M-CSF durante siete días, los macrófagos derivados de monocitos humanos (MDM) mostraron un tamaño celular significativamente mayor que los monocitos (Figura 4A y 4B). Además, mientras que los monocitos exhibieron una apariencia típica que consistía en células redondas, la MDM diferenciada apareció como células de forma fusiforme con numerosos seudópodos que aumentaron su complejidad celular con respecto a los monocitos. Además, la diferenciación a macrófagos también se confirmó mediante la expresión en la superficie celular de CD14. En este sentido, MDM mostró una reducción significativa del 20 % en la expresión de CD14 en comparación con la encontrada en los monocitos (Figura 4C). Para evaluar los singletes se utilizó la dispersión frontal y la dispersión del área (Figura 4D), para evaluar la viabilidad celular se usó la tinción 7-AAD. Luego, los monocitos vivos se seleccionaron en un gráfico de área de dispersión frontal/área de dispersión lateral para evaluar la expresión positiva de CD14 junto con TNF-α, IL-1β, CD11c, CD206 y CX3CR1 y CCR2 (Figura 4D).

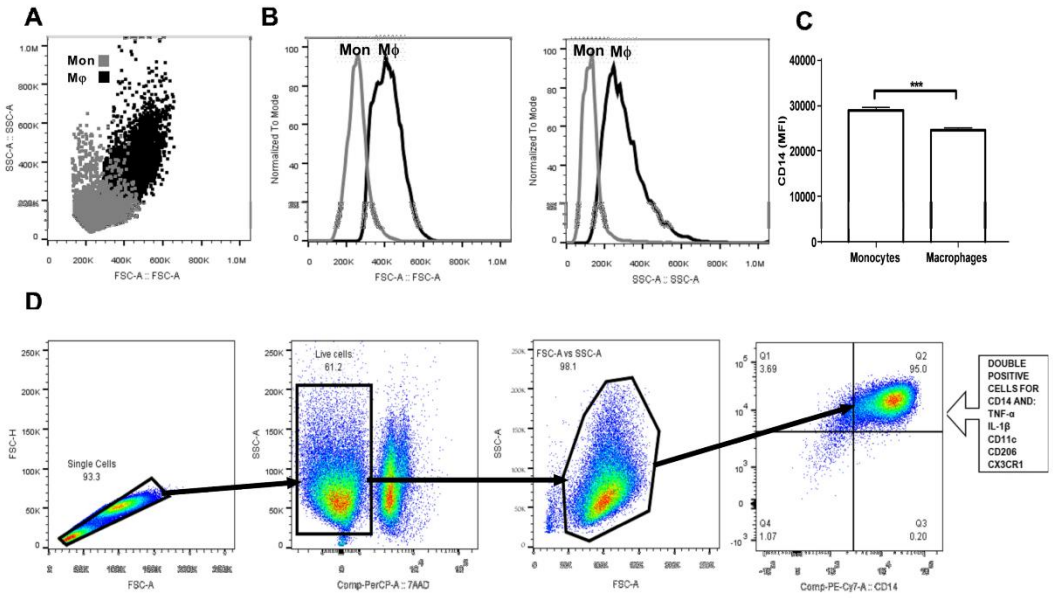

Figura 4. Estrategia para la caracterización primaria de macrófagos derivados de monocitos humanos. Se aislaron monocitos humanos primarios obtenidos de concentrados leucocitarios (n = 10) y se diferenciaron a macrófagos en presencia de M-CSF durante siete días. (A) Diagrama dot plot que muestra una comparación entre monocitos (puntos grises) y macrófagos (puntos negros) en términos de tamaño y complejidad de las células. (B) Los macrófagos son considerablemente más grandes y complejos que los monocitos. (C) Como se informó anteriormente, los macrófagos expresan una cantidad significativamente menor de CD14 en comparación con la que se encuentra en los monocitos. (D) Se seleccionaron a los macrófagos derivados de monocitos (MDM) por singletes en un gráfico de densidad de dispersión frontal del area/dispersión frontal de la altura(FSC-A/FSC-H). Las células resultantes se seleccionaron nuevamente para la detección de macrófagos vivos por medio de las tinciones 7AAD o Zombie UV. Luego, los macrófagos se seleccionaron en un gráfico de densidad por la dispersión FSC-A vs SSC-A. Posteriormente se analizaron las células CD14+ que expresaban simultáneamente uno los marcadores de superficie o citocinas (factor de necrosis tumoral alfa (TNF-α), interleucina (IL-1) beta, CD11c, CD206, CX3CR1 y CCR2). Mon, población de monocitos; Mϕ, población de macrófagos; MFI, intensidad de fluorescencia media; FSC-H, dispersión frontal-altura; FSC-A, dispersión frontal de área; SSC-A, dispersión lateral de area; TNF-α, factor de necrosis tumoral alfa; IL-1β, interleucina 1 beta; CD11c, cluster de diferenciación 11c; CD206, cluster de diferenciación 206 o receptor de manosa; CX3CR1, receptor 1 de quimiocinas con motivo CX3C; CCR2, receptor de quimiocinas C-C tipo 2; M-CSF, factor estimulante de colonias de macrófagos.

En cuanto a la producción de citocinas proinflamatorias, la exposición de MDM a concentraciones crecientes de ácido úrico tendió a elevar el número de células TNF-α positivas (+), aunque no se obtuvieron cambios estadísticamente significativos (Figura 5A). Sin embargo, las MDM cultivadas *in vitro* en presencia de 0,23 mmol/L de ácido úrico

mostraron un aumento significativo del 25% en la producción de TNF-α con respecto a las células control (Figura 5B). No se encontraron diferencias significativas cuando se comparó MDM expuesto a 0,45 o 0,9 mmol/L de ácido úrico con células de control, lo que sugiere que el ácido úrico ejerce sus efectos sobre la producción de TNF-α de forma dependiente de la dosis (Figura 5B). A pesar de que la exposición de MDM a niveles crecientes de ácido úrico tendió a disminuir el número de células IL-1β+ o la producción de IL-1β, no se encontraron diferencias significativas (Figura 5C y D, respectivamente).

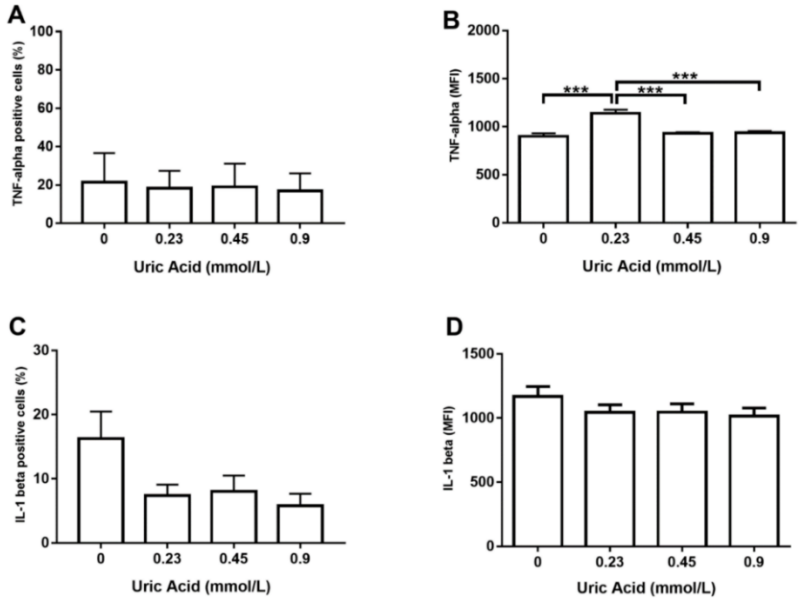

Figura 5. Producción intracelular de TNF-α e IL-1β en macrófagos primarios derivados de monocitos humanos *in vitro* expuestos a ácido úrico (n=10). La exposición *in vitro* a concentraciones crecientes de ácido úrico no alteró el porcentaje de macrófagos primarios derivados de monocitos humanos que expresan TNF-α (A). La exposición *in vitro* a 0,23 mmol/L de ácido úrico aumentó significativamente la producción de TNF-α en macrófagos primarios derivados de monocitos humanos en comparación con las células control (0 mmol/L de ácido úrico) (B). La exposición *in vitro* a concentraciones crecientes de ácido úrico tendió a disminuir el porcentaje de macrófagos primarios derivados de monocitos humanos que expresan IL-1β, aunque no se encontraron diferencias significativas (C). La exposición *in vitro* a concentraciones crecientes de ácido úrico no alteró la producción de IL-1 beta en macrófagos primarios derivados de monocitos humanos (D). Los datos se analizaron mediante ANOVA unidireccional seguido de la prueba post-hoc de Tukey para estimar las diferencias significativas. Los datos se expresan como media ± desviación estándar. Las diferencias se consideraron significativas cuando $p < 0,05$ y se marcan con asteriscos de la siguiente manera: *** = $p < 0,0001$. TNF-α, factor de necrosis tumoral alfa; IL-1β, interleucina 1 beta; MFI, intensidad media de fluorescencia.

Decidimos medir la producción de TLR-4 como un regulador clave de la síntesis de TNF-α ya que la exposición de MDM al ácido úrico aumentó la expresión de TNF-α, pero no la de IL-1β. En este sentido, el ácido úrico indujo la expresión de TLR-4 en MDM de forma dependiente de la dosis, aunque no se alcanzaron diferencias significativas en cuanto al número de células TLR-4+ (Figura 6A). Sin embargo, la exposición de MDM a 0,23 mmol/L de ácido úrico promovió un aumento significativo del 30% en la producción de TLR-4 de forma muy similar a la observada para el caso de TNF-α (Figura 6B). También se ha demostrado que los macrófagos positivos para TNF-α expresan CD11c, una integrina que se expresa en gran medida en los monocitos proinflamatorios reclutados hacia las placas ateroscleróticas. El ácido úrico no afectó el número de MDM que expresan CD11c (Figura 6C); sin embargo, el ácido úrico aumentó la expresión de CD11c en MDM de forma dependiente de la dosis, alcanzando la mayor producción de esta integrina a 0,23 y 0,45 mmol/L de ácido úrico (Figura 6D).

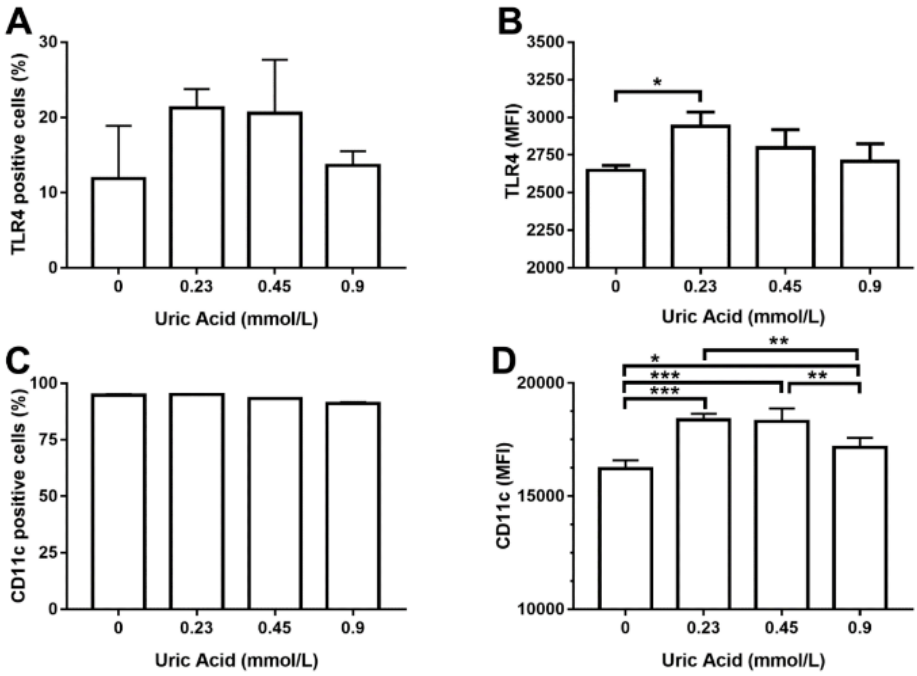

Figura 6. Expresión en la superficie celular de TLR-4 y CD11c en macrófagos primarios derivados de monocitos humanos *in vitro* expuestos a ácido úrico (n=10). La exposición *in vitro* a concentraciones crecientes de ácido úrico no alteró el porcentaje de macrófagos primarios derivados de monocitos humanos que expresan TLR-4 (A). La exposición *in vitro* a 0,23 mmol/L de ácido úrico aumentó significativamente la producción de TLR-4 en macrófagos primarios derivados de monocitos humanos en comparación con las células control (0 mmol/L de ácido úrico) (B). La exposición *in vitro* a concentraciones crecientes de ácido úrico no alteró el porcentaje de macrófagos primarios derivados de monocitos humanos que expresan CD11c (C). La exposición *in vitro* a 0,23, 0,45 y 0,9 mmol/L de ácido úrico alteró significativamente la producción de CD11c en macrófagos primarios derivados de monocitos humanos en una forma de respuesta a la dosis en comparación con las células de control (0 mmol/L de ácido úrico) (D). Los datos se analizaron mediante ANOVA unidireccional, seguido de la prueba post-hoc de Tukey para estimar las diferencias significativas. Los datos se expresan como media ± desviación estándar. Las diferencias se consideraron significativas cuando $p < 0,05$ y están marcadas con asteriscos de la siguiente manera: * = $p < 0,01$; ** = $p < 0,001$; *** = $p < 0,0001$. TLR4, receptor tipo toll 4; CD11c, grupo de diferenciación 11c; MFI, intensidad de fluorescencia media.

Existen reportes que indican que los macrófagos ganan capacidad proinflamatoria mientras pierden la capacidad antiinflamatoria. Por esta razón, queríamos medir la producción de CD206, un marcador expresado por macrófagos humanos y murinos con propiedades antiinflamatorias. La exposición de MDM a niveles crecientes de ácido úrico redujo progresivamente el número de células que expresaban CD206 con respecto a las células

control (Figura 7A). En general, el ácido úrico no afectó la expresión de CD206 en MDM, a excepción de 0,45 mmol/L de ácido úrico que indujo un ligero aumento en la expresión de este marcador antiinflamatorio característico de los macrófagos M2 (Figura 7B).

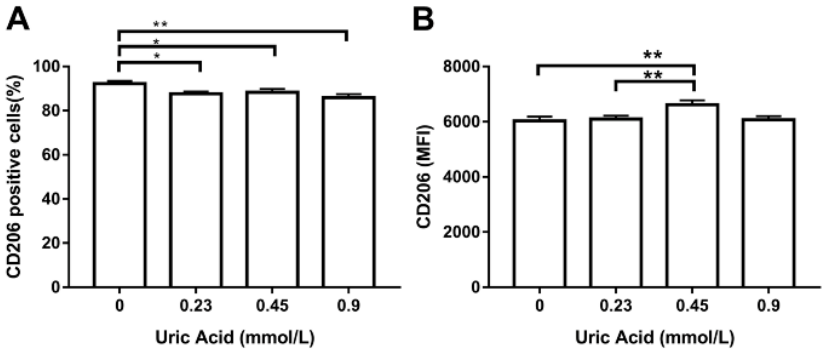

Figura 7. Expresión en la superficie celular de CD206 en macrófagos primarios derivados de monocitos humanos *in vitro* expuestos a ácido úrico (n=10). La exposición *in vitro* a 0,23, 0,45 y 0,9 mmol/L de ácido úrico disminuyó significativamente el porcentaje de macrófagos primarios derivados de monocitos humanos que expresan CD206 en comparación con las células control (0 mmol/L de ácido úrico) (A). La exposición *in vitro* a 0,45 mmol/L de ácido úrico aumentó significativamente la producción de CD206 en macrófagos primarios derivados de monocitos humanos en comparación con las células control (0 mmol/L de ácido úrico) (B). Los datos se analizaron mediante ANOVA unidireccional seguido de la prueba post-hoc de Tukey para estimar las diferencias significativas. Los datos se expresan como media ± desviación estándar. Las diferencias se consideraron significativas cuando $p < 0,05$ y se marcan con asteriscos de la siguiente manera: * = $p < 0,01$; ** = $p < 0,001$. CD206, grupo de diferenciación 206 o receptor de manosa; MFI, intensidad media de fluorescencia.

A continuación, decidimos examinar el efecto de este metabolito en la expresión de CX3CR1 y CCR2, dos receptores de quimiocinas que disminuyen en los macrófagos proinflamatorios. La exposición de MDM al ácido úrico disminuyó progresivamente el número de macrófagos CX3CR1+, alcanzando la máxima respuesta cuando las células se incubaron en presencia de 0,9 mmol/L de ácido úrico (Figura 8A). Asimismo, el ácido úrico redujo gradualmente la expresión de CX3CR1 en MDM en comparación con la encontrada en las células control (Figura 8B). Paralelamente, la exposición de MDM al ácido úrico disminuyó gradualmente

el número de células que expresaban CCR2, alcanzando el nivel más bajo de este receptor de quimiocinas cuando se usaba 0,9 mmol/L de ácido úrico (Figura 8C). Como era de esperar, el ácido úrico también disminuyó la expresión de CCR2 en MDM a 0,45 y 0,9 mmol/l y proporcionó pruebas experimentales sólidas de que la producción de CX3CR1 y CCR2 se comporta de manera similar en macrófagos expuestos a LPS o ácido úrico.

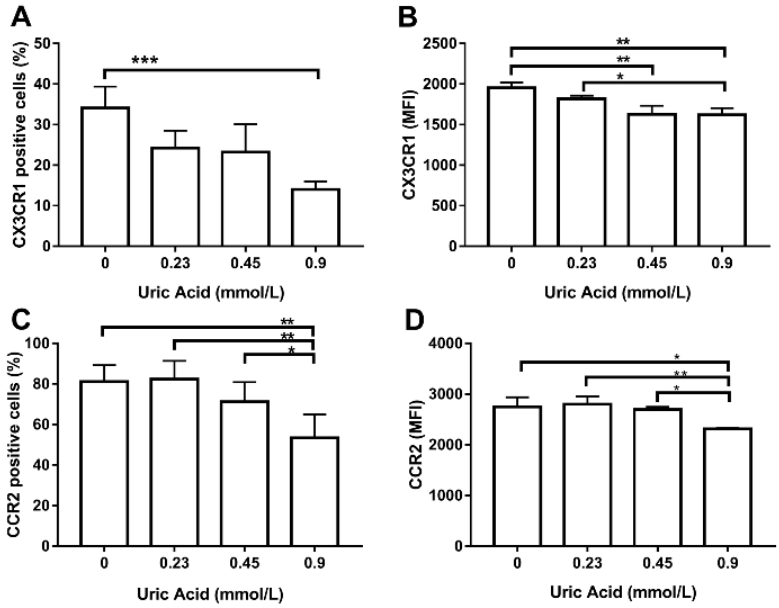

Figura 8. Expresión en la superficie celular de CX3CR1 y CCR2 en macrófagos primarios derivados de monocitos humanos *in vitro* expuestos a ácido úrico (n=10). La exposición *in vitro* a 0,9 mmol/L de ácido úrico disminuyó significativamente el porcentaje de macrófagos primarios derivados de monocitos humanos que expresan CX3CR1 en comparación con las células\control (0 mmol/L de ácido úrico) (A). La exposición *in vitro* a 0,45 y 0,9 mmol/L de ácido úrico disminuyó significativamente la producción de CX3CR1 en los macrófagos, en comparación con las células control (0 mmol/L de ácido úrico) (B). La exposición *in vitro* a 0,9 mmol/L de ácido úrico disminuyó significativamente el porcentaje de macrófagos que expresan CCR2 en comparación con las células de control (0 mmol/L de ácido úrico (C). La exposición *in vitro* a 0,9 mmol/L de ácido úrico disminuyó significativamente disminución de la producción de CCR2 en macrófagos, en comparación con las células control (0 mmol/ácido úrico) (D). Los datos se analizaron mediante ANOVA unidireccional seguido de la prueba post-hoc de Tukey para estimar las diferencias significativas. Los datos son expresados como media ± desviación estándar. Las diferencias se consideraron significativas cuando $p < 0,05$ y se marcan con asteriscos de la siguiente manera: * = $p < 0,01$ ** = $p < 0,001$ *** = $p < 0,0001$ CX3CR1, CX3C- receptor de quimiocinas motivo 1, CCR2, receptor de quimiocinas C-C tipo 2, MFI, intensidad media de fluorescencia.

La activación proinflamatoria de los macrófagos humanos también se asocia con una mayor capacidad para fagocitar bacterias. Por lo tanto, evaluamos el efecto de aumentar las concentraciones de ácido úrico en la actividad fagocítica de MDM mientras usamos *E. coli*-GFP+. En ausencia de ácido úrico, el 15% de los MDM fueron *E. coli*-GFP+ (Figura 9). Tras la exposición de los MDM a 0,23 mmol/L de ácido úrico se observó que el 26% de los MDM eran *E. coli*-GFP+. Además, los MDM expuestos a 0,45 y 0,9 mmol/L de ácido úrico tuvieron un aumento del 40% y 120%, respectivamente, en comparación con las células control, lo que confirmó que el ácido úrico aumenta la capacidad fagocítica de los macrófagos humanos cultivados *in vitro*.

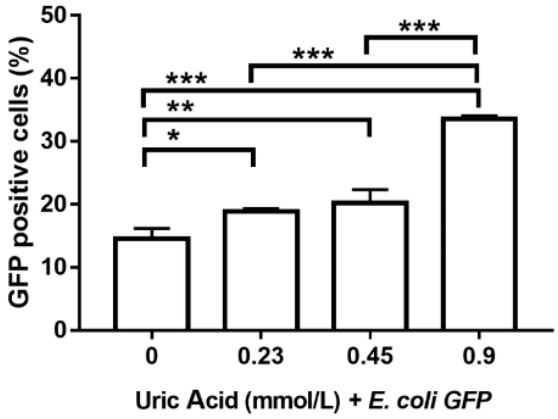

Figura 9. Actividad fagocítica bacteriana de macrófagos primarios derivados de monocitos humanos *in vitro* expuestos a ácido úrico. La exposición *in vitro* a 0,23, 0,45 y 0,9 mmol/l de ácido úrico mejoró significativamente la actividad fagocítica de los macrófagos al aumentar progresivamente el porcentaje de células positivas para la proteína fluorescente verde (GFP) de *Escherichia coli* en comparación con los controles (0 mmol/ácido lúrico). Los datos se analizaron mediante ANOVA unidireccional seguido de la prueba post-hoc de Tukey para estimar las diferencias significativas. Los datos se expresan como media ± desviación estándar. Las diferencias se consideraron significativas cuando $p < 0,05$ y se marcan con asteriscos de la siguiente manera: * = $p < 0,01$; ** = $p < 0,001$; *** = $p < 0,0001$. GFP, proteína fluorescente verde; *E. coli*, *Escherichia coli*.

Un objetivo adicional de este trabajo fue explorar el posible mecanismo molecular por el cual el ácido úrico ejerce sus efectos sobre los macrófagos derivados de monocitos humanos. Por esta razón, decidimos evaluar la expresión de URAT1, un mediador clave del transporte de ácido úrico dentro de la célula. En particular, la exposición de MDM a 0,23 mmol/L de ácido úrico indujo una reducción significativa del 90 % en la expresión de URAT1 en comparación con la encontrada en células de control cultivadas en ausencia de este metabolito (Figura 10). De manera similar, los MDM expuestos a 0,45 mmol/L de ácido úrico mostraron una disminución significativa del 95% en los niveles de ARNm de URAT1 con respecto al encontrado en las células de control. Vale la pena mencionar que la exposición de MDM a 0.9 mmol/L de ácido úrico abolió totalmente la expresión de URAT1, lo que sugiere que URAT1 es sensible a las concentraciones de ácido úrico y puede participar en la mediación de los efectos de este metabolito en los macrófagos.

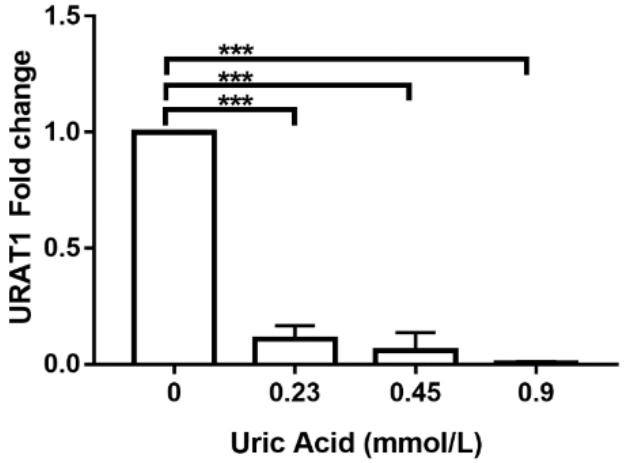

Figura 10. Expresión de URAT1 en macrófagos primarios derivados de monocitos humanos *in vitro* expuestos a ácido úrico (n=10). La exposición *in vitro* a 0,23, 0,45 y 0,9 mmol/L de ácido úrico eliminó progresivamente la expresión de URAT1 en macrófagos primarios derivados de monocitos humanos en comparación con los controles (0 mmol/L de ácido úrico). La expresión de URAT1 se normalizó utilizando el gen del ARN ribosomal 18S como gen de control de mantenimiento y se notificó como un cambio de 2^(ΔΔCt) veces mediante la reacción en cadena de la polimerasa en tiempo real (qPCR) utilizando SYBR Green Master Mix y AmpliTaq® Fast DNA Polimerasa. Los datos se analizaron mediante ANOVA unidireccional seguido de la prueba post-hoc de Tukey para estimar las diferencias significativas. Los datos se expresan como media ± desviación estándar. Las diferencias se consideraron significativas cuando $p < 0,05$ y se marcan con asteriscos de la siguiente manera: *** = $p < 0,0001$. URAT1, transportador de anión urato 1.

Decidimos usar probenecid que es capaz de inhibir el transporte de ácido úrico dependiente de URAT1 y también examinar su efecto sobre la producción de TNF-α y la actividad fagocítica para confirmar la aparente participación de URAT1 en los macrófagos. Como era de esperar, el uso de probenecid eliminó por completo la producción de TNF-α en los macrófagos que también estuvieron expuestos a diferentes concentraciones de ácido úrico (Figura 11A). Asimismo, el probenecid también indujo una disminución del 11% en el número intracelular de macrófagos *E. coli-GFP+* que se trataron con 0,23 mmol/L de ácido úrico (Figura 11B). Además, los MDM tratados con probenecid mostraron reducciones significativas del 78 y el 61 % de *E. coli-GFP+*, incluso en presencia de 0,45 y 0,9 mmol/l de ácido úrico, respectivamente. Estos resultados sugieren funcionalmente que el ácido úrico podría transportarse dentro del macrófago a través de URAT1 que, a su vez, podría mediar sus efectos proinflamatorios en estas células inmunitaria.

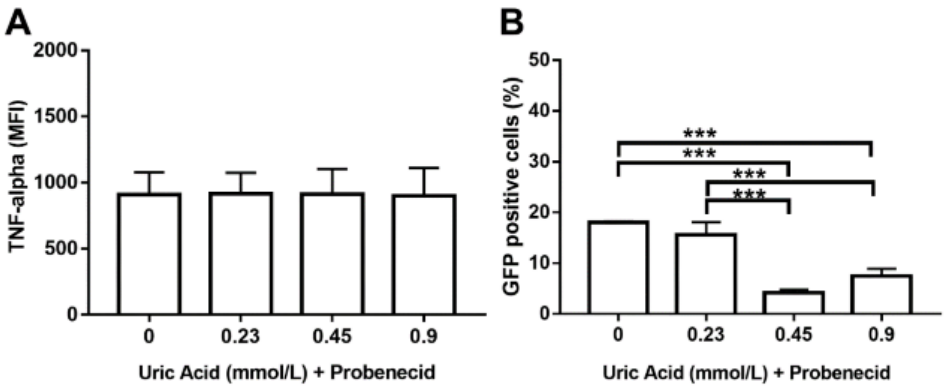

Figura 11. El probenecid parece abolir los efectos proinflamatorios del ácido úrico dependientes de URAT-1 en macrófagos derivados de monocitos humanos primarios (n=10). La exposición *in vitro* a 1 mmol/L de probenecid eliminó el efecto estimulador del ácido úrico sobre la producción de TNF-α en macrófagos derivados de monocitos humanos primarios en comparación con las células expuestas al ácido úrico en ausencia de probenecid (A). La exposición *in vitro* a 1 mmol/L de probenecid disminuyó significativamente el efecto estimulante del ácido úrico sobre la actividad fagocítica de los macrófagos primarios derivados de monocitos humanos al disminuir el porcentaje de células positivas para *Escherichia coli*-GFP en comparación con los macrófagos expuestos al ácido úrico en ausencia de probenecid (B). Los datos se analizaron mediante ANOVA unidireccional seguido de la prueba post-hoc de Tukey para estimar las diferencias significativas. Los datos se expresan como media ± desviación estándar. Las diferencias se consideraron significativas cuando $p < 0,05$ y están marcadas con asteriscos, así: *** = $p < 0,0001$. TNF-a, factor de necrosis tumoral alfa; MFI, intensidad de fluorescencia media; GFP, proteína fluorescente verde.

DISCUSIÓN

La asociación de la hiperuricemia con el riesgo de desarrollar anomalías metabólicas y enfermedades cardiovasculares se ha relacionado con una mayor actividad proinflamatoria de los macrófagos. Sin embargo, aún se desconoce si la hiperuricemia simplemente coincide con cambios en la actividad de los macrófagos o si el ácido úrico puede inducir directamente la activación proinflamatoria de los macrófagos humanos. Por esta razón, decidimos probar el efecto *in vitro* del aumento de las concentraciones de ácido úrico en el perfil proinflamatorio de los macrófagos humanos primarios derivados de monocitos.

Después de confirmar que los monocitos humanos se diferenciaron correctamente en macrófagos utilizando una estrategia que combinaba el tamaño y la complejidad de las células, así como la expresión de CD14, descubrimos que el ácido úrico estimula la producción de TNF-α, pero no la de IL-1β, de manera dependiente de la dosis. El TNF-α y la IL-1β son citocinas proinflamatorias que desempeñan funciones clave en procesos como la fiebre, la caquexia, la inhibición de la tumorigénesis, la muerte celular relacionada con la piroptosis y el reclutamiento de células inmunitarias. Sin embargo, el TNF-α, pero no la IL-1β, se ha asociado consistentemente con niveles séricos elevados de ácido úrico en varios escenarios patológicos. Por ejemplo, los niveles séricos de ácido úrico aumentan a medida que los monocitos productores de TNF-α también aumentan en mujeres con preeclampsia. De manera similar, se ha demostrado que el ácido úrico estimula la expresión de TNF-α en las células del músculo liso vascular de ratas Sprague-Dawley. Por otro lado, la IL-1β plasmática mostró una asociación muy pobre con el aumento de los niveles séricos de ácido úrico en 1684 mujeres y hombres, mientras que los valores séricos de TNF-α aumentaron en la misma proporción que el ácido úrico plasmático. Junto con la información previa, nuestros

resultados proporcionan una evidencia experimental de que el ácido úrico podría favorecer un estado proinflamatorio al estimular principalmente la producción de TNF-α en los macrófagos humanos. Es bien sabido que la síntesis de TNF-α depende de la vía de señalización dependiente de TLR4, mientras que la producción de IL-1β depende de la actividad del inflamasoma. Por esta razón, decidimos evaluar TLR4 en los mismos macrófagos diferenciados *in vitro*.

TLR4 es una proteína transmembrana capaz de reconocer numerosos patrones moleculares asociados a daños (DAMP) y patrones moleculares asociados a patógenos (PAMP), incluidos los ácidos grasos libres y LPS. Cuando se activa, TLR4 es capaz de inducir la activación del factor nuclear kappa B (NF-kB), lo que finalmente conduce a la producción de TNF-α. De acuerdo con esta información, nuestros resultados demuestran que TLR4 se produce en respuesta al ácido úrico de la misma manera que lo hace el TNF-α en los macrófagos humanos. En este sentido, un trabajo previo informó que el riesgo de gota, una patología conocida por el depósito de cristales de urato monosódico en las articulaciones está directamente asociado con el polimorfismo rs2149356 relacionado con la producción alta de TLR4. Asimismo, un estudio muy reciente demostró que el ácido úrico promueve la expresión de ARNm de TLR4 en adipocitos de rata *in vitro*. Por lo tanto, especulamos que el ácido úrico puede inducir la producción de TNF-α a través de la mayor expresión de TLR4, un fenómeno que proporciona características proinflamatorias a los macrófagos humanos. Sin embargo, la idea de que el ácido úrico puede inducir la expresión de TLR4 debe tomarse con precaución, ya que solo evaluamos TLR4 a nivel de proteína sin evaluar su capacidad como transductor de señal celular.

Hasta aquí, nuestros resultados parecían indicar que el ácido úrico ejerce la capacidad de polarizar los macrófagos humanos hacia un estado proinflamatorio. Así, decidimos confirmar la capacidad aparentemente proinflamatoria de los macrófagos analizando CD11c y CD206. CD11c es una integrina beta-2 que se expresa en gran medida en monocitos y macrófagos con importantes funciones proinflamatorias, mientras que CD206, también conocido como receptor de manosa, es una lectina de tipo C que se expresa predominantemente en macrófagos murinos y humanos que ejercen funciones antiinflamatorias. Curiosamente, descubrimos que el ácido úrico puede aumentar la expresión de CD11c al mismo tiempo que reduce la cantidad de macrófagos que expresan CD206. En este sentido, se ha informado previamente que el bloqueo de la síntesis de ácido úrico por el tratamiento con uricasa disminuye el número de monocitos CD11c+ en ratones, lo que sugiere, por primera vez, una relación entre el ácido úrico y la producción de CD11c. Paralelamente, un informe anterior mostró que los macrófagos localizados en líquido sinovial de pacientes con gota tienden a mostrar una expresión reducida de CD206 en comparación con la que se encuentra en los macrófagos de pacientes con artritis reumatoide. En conjunto, esta información concuerda con la idea de que los macrófagos adoptan funciones proinflamatorias mientras pierden capacidades antiinflamatorias en presencia de niveles elevados de ácido úrico.

La idea de que el ácido úrico podría actuar como un estímulo proinflamatorio directo para los macrófagos humanos también está respaldada por dos hechos adicionales: (a) el patrón de expresión de CX3CR1 y CCR2 y (b) la actividad fagocítica de los macrófagos. CX3CR1 y CCR2 participan en la mediación del reclutamiento de monocitos en los sitios de inflamación, donde estas células se diferenciarán en macrófagos y orquestarán respuestas

inflamatorias o reparación de tejidos. Curiosamente, numerosos estudios han informado consistentemente la regulación a la baja de CX3CR1 y CCR2 en presencia de estímulos inflamatorios prototípicos, como LPS. En este sentido, un trabajo seminal informó que los monocitos circulantes de pacientes sépticos o incubados con LPS muestran una expresión dramáticamente disminuida de CX3CR1. De manera similar, la exposición *in vitro* e in vivo de células sanguíneas periféricas murinas a LPS puede regular a la baja la expresión de CCR2 con consecuencias directas para la capacidad migratoria de los macrófagos. Por lo tanto, la expresión de CX3CR1 y CCR2 parece comportarse de manera similar en los macrófagos que están expuestos a LPS o ácido úrico, lo que proporciona una sólida evidencia experimental sobre el posible papel inflamatorio de este metabolito en los macrófagos. Además, es bien sabido que los macrófagos con funciones proinflamatorias muestran una mayor capacidad para fagocitar bacterias que la descrita en los macrófagos antiinflamatorios. Curiosamente, la exposición de los macrófagos a concentraciones crecientes de ácido úrico mejoró progresivamente su actividad fagocítica, lo que una vez más respalda la noción de que el ácido úrico actúa como un estímulo proinflamatorio directo para estas células inmunitarias.

Además de estudiar el efecto aparentemente proinflamatorio del ácido úrico sobre los macrófagos, también queríamos explorar el mecanismo molecular potencialmente involucrado. En nuestro estudio, la producción de TNF-α, TLR4 y CD11c en respuesta al ácido úrico mostró una típica relación dosis-respuesta, donde se encuentra un efecto máximo y, más allá de este punto, se puede ver una meseta, lo que indica saturación y la supresión del efecto observado. La relación dosis-respuesta se ha atribuido a la interacción entre el ligando y su receptor, lo que nos sugirió la posible implicación de una molécula capaz de transportar ácido úrico al interior del macrófago, como es el caso de URAT1. De esta forma,

describimos por primera vez que los macrófagos humanos expresan URAT1, una proteína transmembrana que solo había sido reportada en células endoteliales, adipocitos y condrocitos de cartílago. En particular, encontramos que la expresión de URAT1 en los macrófagos disminuyó a medida que aumentaba la concentración de ácido úrico, lo que podría explicar parcialmente el hecho de que la expresión de TNF-α, TLR4 y CD11c alcanzara un punto de saturación, lo que a su vez condujo a una disminución de sus niveles de proteína. Teniendo en cuenta que el ácido úrico puede aumentar la actividad transcripcional de NF-kB en la línea celular beta pancreática Min6, especulamos que la producción de TNF-α en los macrófagos podría depender de la interacción entre el ácido úrico, URAT1 y posiblemente NF-kB.

Realizamos ensayos funcionales destinados a bloquear farmacológicamente este transportador de urato usando probenecid para confirmar la posible participación de URAT1 en la mediación de los efectos del ácido úrico en los macrófagos. El probenecid actúa como un inhibidor competitivo de URAT1, evitando así la recaptación y el transporte de ácido úrico por las células del tubo proximal renal. Curiosamente, el bloqueo de URAT1 eliminó la producción de TNF-α y la actividad fagocítica que se había visto anteriormente con el ácido úrico, lo que sugiere que el efecto proinflamatorio del ácido úrico depende por completo de su entrada a los macrófagos. En este sentido, se ha propuesto previamente que la entrada de urato monosódico a las células THP-1 puede inducir la fosforilación de IkB a través de las tirosina-quinasas de la familia Src, lo que lleva a la activación de NF-kB y, finalmente, a la producción de citoquinas proinflamatorias. De esta forma, nuestros resultados confirman que (1) la entrada de ácido úrico a los macrófagos tiene efectos proinflamatorios por un mecanismo aún desconocido, y (2) la entrada de ácido úrico a los macrófagos parece implicar

a URAT1, cuya expresión es, a su vez, sensible a diferentes concentraciones de ácido úrico. Sin embargo, URAT1 no es el único transportador de urato y el probenecid no es un inhibidor específico de URAT1, por lo que la medición en macrófagos de otros transportadores de urato, incluido el transportador de aniones orgánicos (OAT) 1, OAT3 y el miembro 2 de la subfamilia G del casete de unión a ATP (ABCG2), y queda por hacer la prueba de otros inhibidores de la captación de urato, como la benzbromarona, el dotinurad y losartán.

CONCLUSIÓN

El ácido úrico actúa como un estímulo proinflamatorio para los macrófagos humanos primarios cultivados *in vitro* mediante (a) el aumento de la producción de TNF-α, TLR4 y CD11c, (b) el incremento en de la actividad fagocítica de los macrófagos y (c) la disminución en la expresión de CD206, CX3CR1 y CCR2. El posible mecanismo por el cual el ácido úrico ejerce sus efectos proinflamatorios sobre los macrófagos humanos parece involucrar a URAT1 en una forma de respuesta a la dosis. URAT1 podría, a su vez, mejorar la activación de NF-kB y conducir a la producción de citocinas proinflamatorias por vías que aún no se han dilucidado (Fig. 12). El uso de probenecid demostró funcionalmente que la entrada de ácido úrico al macrófago tiene acciones proinflamatorias y depende parcialmente de URAT1 (Fig. 12). Estos resultados proporcionan una sólida evidencia experimental que respalda la idea de que los niveles elevados de ácido úrico pueden promover directamente el estado inflamatorio sistémico mediado por macrófagos que, a su vez, está asociado con un alto riesgo cardiovascular en pacientes con enfermedades crónicas. La noción de que el ácido úrico podría actuar como un ligando metabólico con efectos proinflamatorios en los macrófagos humanos debe examinarse más a fondo.

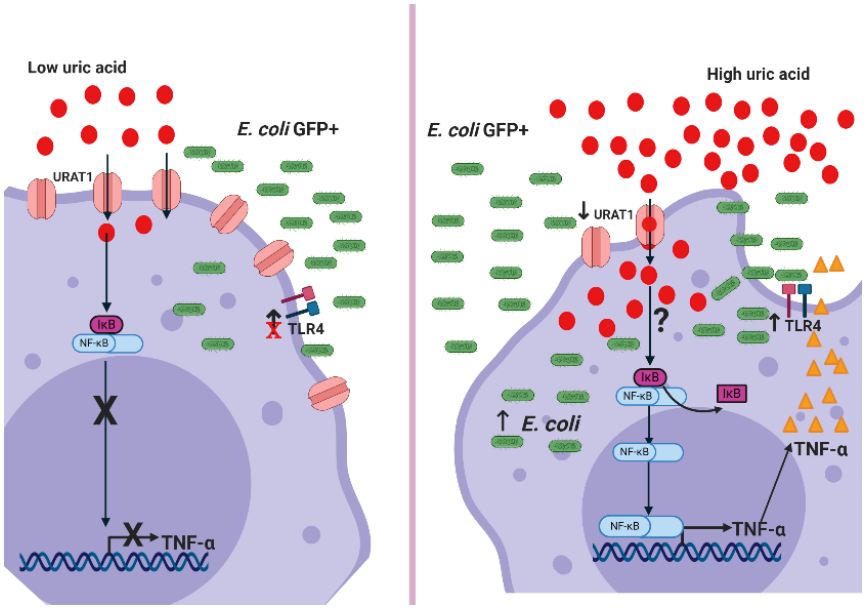

Figura 12. Mecanismo propuesto mediante el cual el ácido úrico ejerce efectos proinflamatorios sobre los macrófagos a través de URAT-1.

REFERENCIAS

Alemayehu, Ermiyas, Temesgen Fiseha, Getachew Mesfin Bambo, Samuel Sahile Kebede, Habtye Bisetegn, Mihret Tilahun, Habtu Debash, Hussen Ebrahim, Ousman Mohammed, Melaku Ashagrie Belete, and Alemu Gedefie. 2023. 'Prevalence of Hyperuricemia among Type 2 Diabetes Mellitus Patients in Africa: A Systematic Review and Meta-Analysis'. *BMC Endocrine Disorders* 23(1):153. doi: 10.1186/s12902-023-01408-0.

Ames, B. N., R. Cathcart, E. Schwiers, and P. Hochstein. 1981. 'Uric Acid Provides an Antioxidant Defense in Humans against Oxidant- and Radical-Caused Aging and Cancer: A Hypothesis.' *Proceedings of the National Academy of Sciences* 78(11):6858–62. doi: 10.1073/pnas.78.11.6858.

Baldwin, William, Steven McRae, George Marek, David Wymer, Varinderpal Pannu, Chris Baylis, Richard J. Johnson, and Yuri Y. Sautin. 2011. 'Hyperuricemia as a Mediator of the Proinflammatory Endocrine Imbalance in the Adipose Tissue in a Murine Model of the Metabolic Syndrome'. *Diabetes* 60(4):1258–69. doi: 10.2337/db10-0916.

Benn, Caroline L., Pinky Dua, Rachel Gurrell, Peter Loudon, Andrew Pike, R. Ian Storer, and Ciara Vangjeli. 2018. 'Physiology of Hyperuricemia and Urate-Lowering Treatments'. *Frontiers in Medicine* 5. doi: 10.3389/fmed.2018.00160.

Bobulescu, Ion Alexandru, and Orson W. Moe. 2012. 'Renal Transport of Uric Acid: Evolving Concepts and Uncertainties'. *Advances in Chronic Kidney Disease* 19(6):358–71. doi: 10.1053/j.ackd.2012.07.009.

Braga, Tarcio Teodoro, Maria Fernanda Forni, Matheus Correa-Costa, Rodrigo Nalio Ramos, Jose Alexandre Barbuto, Paola Branco, Angela Castoldi, Meire Ioshie Hiyane, Mariana Rodrigues Davanso, Eicke Latz, Bernardo S. Franklin, Alicia J. Kowaltowski, and Niels Olsen Saraiva Camara. 2017a. 'Soluble Uric Acid Activates the NLRP3 Inflammasome'. *Scientific Reports* 7(1):39884. doi: 10.1038/srep39884.

Braga, Tarcio Teodoro, Maria Fernanda Forni, Matheus Correa-Costa, Rodrigo Nalio Ramos, Jose Alexandre Barbuto, Paola Branco, Angela Castoldi, Meire Ioshie Hiyane, Mariana Rodrigues Davanso, Eicke Latz, Bernardo S. Franklin, Alicia J. Kowaltowski, and Niels Olsen Saraiva Camara. 2017b. 'Soluble Uric Acid Activates the NLRP3 Inflammasome'. *Scientific Reports* 7(1):39884. doi: 10.1038/srep39884.

Cai, Wei, Xi-Mei Duan, Ying Liu, Jiao Yu, Yun-Liang Tang, Ze-Lin Liu, Shan Jiang, Chun-Ping Zhang, Jian-Ying Liu, and Ji-Xiong Xu. 2017. 'Uric Acid Induces Endothelial Dysfunction by Activating the HMGB1/RAGE Signaling Pathway'. *BioMed Research International* 2017:1–11. doi: 10.1155/2017/4391920.

Caillon, Antoine, Pierre Paradis, and Ernesto L. Schiffrin. 2019. 'Role of Immune Cells in Hypertension'. *British Journal of Pharmacology* 176(12):1818–28. doi: 10.1111/bph.14427.

Chen, C. J. 2006. 'MyD88-Dependent IL-1 Receptor Signaling Is Essential for Gouty Inflammation Stimulated by Monosodium Urate Crystals'. *Journal of Clinical Investigation* 116(8):2262–71. doi: 10.1172/JCI28075.

Cho, N. H., J. E. Shaw, S. Karuranga, Y. Huang, J. D. da Rocha Fernandes, A. W. Ohlrogge, and B. Malanda. 2018. 'IDF Diabetes Atlas: Global Estimates of Diabetes Prevalence for 2017 and Projections for 2045'. *Diabetes Research and Clinical Practice* 138:271–81. doi: 10.1016/j.diabres.2018.02.023.

Chung, Ada W. Y., Anna Radomski, David Alonso-Escolano, Paul Jurasz, Michael W. Stewart, Tadeusz Malinski, and Marek W. Radomski. 2004. 'Platelet-Leukocyte Aggregation Induced by PAR Agonists: Regulation by Nitric Oxide and Matrix Metalloproteinases'. *British Journal of Pharmacology* 143(7):845–55. doi: 10.1038/sj.bjp.0705997.

Clozel, M., H. Kuhn, F. Hefti, and H. R. Baumgartner. 1991. 'Endothelial Dysfunction and Subendothelial Monocyte Macrophages in Hypertension. Effect of Angiotensin Converting Enzyme Inhibition.' *Hypertension* 18(2):132–41. doi: 10.1161/01.HYP.18.2.132.

Elmarakby, Ahmed A., Jeffrey E. Quigley, Jeffrey J. Olearczyk, Aarthi Sridhar, Anthony K. Cook, Edward W. Inscho, David M. Pollock, and John D. Imig. 2007. 'Chemokine Receptor 2b Inhibition Provides Renal Protection in Angiotensin II–Salt Hypertension'. *Hypertension* 50(6):1069–76. doi: 10.1161/HYPERTENSIONAHA.107.098806.

Enomoto, Atsushi, Hiroaki Kimura, Arthit Chairoungdua, Yasuhiro Shigeta, Promsuk Jutabha, Seok Ho Cha, Makoto Hosoyamada, Michio Takeda, Takashi Sekine, Takashi Igarashi, Hirotaka Matsuo, Yuichi Kikuchi, Takashi Oda, Kimiyoshi Ichida, Tatsuo Hosoya, Kaoru Shimokata, Toshimitsu Niwa, Yoshikatsu Kanai, and Hitoshi Endou. 2002. 'Molecular Identification of a Renal Urate–Anion Exchanger That Regulates Blood Urate Levels'. *Nature* 417(6887):447–52. doi: 10.1038/nature742.

Fatkhullina, A. R., I. O. Peshkova, and E. K. Koltsova. 2016. 'The Role of Cytokines in the Development of Atherosclerosis'. *Biochemistry (Moscow)* 81(11):1358–70. doi: 10.1134/S0006297916110134.

Fernandez, Melissa L., Zee Upton, and Gary K. Shooter. 2014. 'Uric Acid and Xanthine Oxidoreductase in Wound Healing'. *Current Rheumatology Reports* 16(2):396. doi: 10.1007/s11926-013-0396-1.

Gerhardt, Teresa, and Klaus Ley. 2015. 'Monocyte Trafficking across the Vessel Wall'. *Cardiovascular Research* 107(3):321–30. doi: 10.1093/cvr/cvv147.

Ghaemi-Oskouie, Faranak, and Yan Shi. 2011. 'The Role of Uric Acid as an Endogenous Danger Signal in Immunity and Inflammation'. *Current Rheumatology Reports* 13(2):160–66. doi: 10.1007/s11926-011-0162-1.

Gordon, Siamon. 2003. 'Alternative Activation of Macrophages'. *Nature Reviews Immunology* 3(1):23–35. doi: 10.1038/nri978.

Grainger, R., R. J. McLaughlin, A. A. Harrison, and J. L. Harper. 2013. 'Hyperuricaemia Elevates Circulating CCL2 Levels and Primes Monocyte Trafficking in Subjects with Inter-Critical Gout'. *Rheumatology* 52(6):1018–21. doi: 10.1093/rheumatology/kes326.

Hong, Najiao, Yongjun Lin, Zhirong Ye, Chunbaixue Yang, Yulong Huang, Qi Duan, and Sixin Xie. 2022. 'The Relationship between Dyslipidemia and Inflammation among Adults in East Coast China: A Cross-Sectional Study'. *Frontiers in Immunology* 13. doi: 10.3389/fimmu.2022.937201.

Hong, Quan, Liyuan Wang, Zhiyong Huang, Zhe Feng, Shaoyuan Cui, Bo Fu, Guangyan Cai, Xiangmei Chen, and Di Wu. 2020. 'High Concentrations of Uric Acid and Angiotensin II Act Additively to Produce Endothelial Injury'. *Mediators of Inflammation* 2020:1–11. doi: 10.1155/2020/8387654.

Hooper, D. C., S. Spitsin, R. B. Kean, J. M. Champion, G. M. Dickson, I. Chaudhry, and H. Koprowski. 1998. 'Uric Acid, a Natural Scavenger of Peroxynitrite, in Experimental Allergic Encephalomyelitis and Multiple Sclerosis'. *Proceedings of the National Academy of Sciences* 95(2):675–80. doi: 10.1073/pnas.95.2.675.

Hotamisligil, G. S., P. Arner, J. F. Caro, R. L. Atkinson, and B. M. Spiegelman. 1995. 'Increased Adipose Tissue Expression of Tumor Necrosis Factor-Alpha in Human Obesity and Insulin Resistance.' *Journal of Clinical Investigation* 95(5):2409–15. doi: 10.1172/JCI117936.

Hu, Xueting, Shuang Rong, Qiang Wang, Taoping Sun, Wei Bao, Liangkai Chen, and Liegang Liu. 2021. 'Association between Plasma Uric Acid and Insulin Resistance in Type 2 Diabetes: A Mendelian Randomization Analysis'. *Diabetes Research and Clinical Practice* 171:108542. doi: 10.1016/j.diabres.2020.108542.

Ikeno, Shinya, and Tetsuya Haruyama. 2013. 'Boost Protein Expression through Co-Expression of LEA-Like Peptide in Escherichia Coli'. *PLoS ONE* 8(12):e82824. doi: 10.1371/journal.pone.0082824.

Italiani, Paola, and Diana Boraschi. 2014. 'From Monocytes to M1/M2 Macrophages: Phenotypical vs. Functional Differentiation'. *Frontiers in Immunology* 5. doi: 10.3389/fimmu.2014.00514.

Jiang, Jinguo, Tingjing Zhang, Yashu Liu, Qing Chang, Yuhong Zhao, Chuanji Guo, and Yang Xia. 2023. 'Prevalence of Diabetes in Patients with Hyperuricemia and Gout: A Systematic Review and Meta-Analysis'. *Current Diabetes Reports* 23(6):103–17. doi: 10.1007/s11892-023-01506-2.

Kanbay, Mehmet, Mark Segal, Baris Afsar, Duk-Hee Kang, Bernardo Rodriguez-Iturbe, and Richard J. Johnson. 2013. 'The Role of Uric Acid in the Pathogenesis of Human Cardiovascular Disease'. *Heart* 99(11):759–66. doi: 10.1136/heartjnl-2012-302535.

Kanellis, John, Susumu Watanabe, Jin H. Li, Duk Hee Kang, Ping Li, Takahiko Nakagawa, Ann Wamsley, David Sheikh-Hamad, Hui Y. Lan, Lili Feng, and Richard J. Johnson. 2003. 'Uric Acid Stimulates Monocyte Chemoattractant Protein-1 Production in Vascular Smooth Muscle Cells Via Mitogen-Activated Protein Kinase and Cyclooxygenase-2'. *Hypertension* 41(6):1287–93. doi: 10.1161/01.HYP.0000072820.07472.3B.

Kim, Sang Yong, and Meera G. Nair. 2019. 'Macrophages in Wound Healing: Activation and Plasticity'. *Immunology & Cell Biology* 97(3):258–67. doi: 10.1111/imcb.12236.

Kim, Su-Mi, Sang-Ho Lee, Yang-Gyun Kim, Se-Yun Kim, Jung-Woo Seo, Young-Wook Choi, Dong-Jin Kim, Kyung-Hwan Jeong, Tae-Won Lee, Chun-Gyoo Ihm, Kyu-Yeoun Won, and Ju-Young Moon. 2015a. 'Hyperuricemia-Induced NLRP3 Activation of Macrophages Contributes to the Progression of Diabetic Nephropathy'. *American Journal of Physiology-Renal Physiology* 308(9):F993–1003. doi: 10.1152/ajprenal.00637.2014.

Kim, Su-Mi, Sang-Ho Lee, Yang-Gyun Kim, Se-Yun Kim, Jung-Woo Seo, Young-Wook Choi, Dong-Jin Kim, Kyung-Hwan Jeong, Tae-Won Lee, Chun-Gyoo Ihm, Kyu-Yeoun Won, and Ju-Young Moon. 2015b. 'Hyperuricemia-Induced NLRP3 Activation of Macrophages Contributes to the Progression of Diabetic Nephropathy'. *American Journal of Physiology-Renal Physiology* 308(9):F993–1003. doi: 10.1152/ajprenal.00637.2014.

Kool, Mirjam, Monique A. M. Willart, Menno van Nimwegen, Ingrid Bergen, Philippe Pouliot, J. Christian Virchow, Neil Rogers, Fabiola Osorio, Caetano Reis e Sousa, Hamida Hammad, and Bart N. Lambrecht. 2011. 'An Unexpected Role for Uric Acid as an Inducer of T Helper 2 Cell Immunity to Inhaled Antigens and Inflammatory Mediator of Allergic Asthma'. *Immunity* 34(4):527–40. doi: 10.1016/j.immuni.2011.03.015.

Krishnan, E., K. S. Akhras, H. Sharma, M. Marynchenko, E. Q. Wu, R. Tawk, J. Liu, and L. Shi. 2013. 'Relative and Attributable Diabetes Risk Associated with Hyperuricemia in US Veterans with Gout'. *QJM* 106(8):721–29. doi: 10.1093/qjmed/hct093.

Lee, Tzong-Shyuan, Tse-Min Lu, Chia-Hui Chen, Bei-Chia Guo, and Chiao-Po Hsu. 2021. 'Hyperuricemia Induces Endothelial Dysfunction and Accelerates Atherosclerosis by Disturbing the Asymmetric Dimethylarginine/Dimethylarginine Dimethylaminotransferase 2 Pathway'. *Redox Biology* 46:102108. doi: 10.1016/j.redox.2021.102108.

Li, Delun, Siyu Yuan, Yiyao Deng, Xiaowan Wang, Shouhai Wu, Xuesheng Chen, Yimeng Li, Jianting Ouyang, Danyao Lin, Haohao Quan, Xinwen Fu, Chuang Li, and Wei Mao. 2023. 'The Dysregulation of Immune Cells Induced by Uric Acid: Mechanisms of Inflammation Associated with Hyperuricemia and Its Complications'. *Frontiers in Immunology* 14. doi: 10.3389/fimmu.2023.1282890.

Li, He, Ya Meng, Shuwang He, Xiaochuan Tan, Yujia Zhang, Xiuli Zhang, Lulu Wang, and Wensheng Zheng. 2022. 'Macrophages, Chronic Inflammation, and Insulin Resistance'. *Cells* 11(19):3001. doi: 10.3390/cells11193001.

Li, Rong, Chen Huang, Jian Chen, Yang Guo, and Sheng Tan. 2015. 'The Role of Uric Acid as a Potential Neuroprotectant in Acute Ischemic Stroke: A Review of Literature'. *Neurological Sciences* 36(7):1097–1103. doi: 10.1007/s10072-015-2151-z.

Liang, W. Y., X. Y. Zhu, J. W. Zhang, X. R. Feng, Y. C. Wang, and M. L. Liu. 2015. 'Uric Acid Promotes Chemokine and Adhesion Molecule Production in Vascular Endothelium via Nuclear Factor-Kappa B Signaling'. *Nutrition, Metabolism and Cardiovascular Diseases* 25(2):187–94. doi: 10.1016/j.numecd.2014.08.006.

Liu, Lei, Lingjiang Zhu, Mengdan Liu, Li Zhao, Yiyun Yu, Yu Xue, and Lizhen Shan. 2022. 'Recent Insights Into the Role of Macrophages in Acute Gout'. *Frontiers in Immunology* 13. doi: 10.3389/fimmu.2022.955806.

Lyngdoh, Tanica, Pedro Marques-Vidal, Fred Paccaud, Martin Preisig, Gérard Waeber, Murielle Bochud, and Peter Vollenweider. 2011. 'Elevated Serum Uric Acid Is Associated with High Circulating Inflammatory Cytokines in the Population-Based Colaus Study'. *PLoS ONE* 6(5):e19901. doi: 10.1371/journal.pone.0019901.

Maiuolo, Jessica, Francesca Oppedisano, Santo Gratteri, Carolina Muscoli, and Vincenzo Mollace. 2016a. 'Regulation of Uric Acid Metabolism and Excretion'. *International Journal of Cardiology* 213:8–14. doi: 10.1016/j.ijcard.2015.08.109.

Maiuolo, Jessica, Francesca Oppedisano, Santo Gratteri, Carolina Muscoli, and Vincenzo Mollace. 2016b. 'Regulation of Uric Acid Metabolism and Excretion'. *International Journal of Cardiology* 213:8–14. doi: 10.1016/j.ijcard.2015.08.109.

Mandal, Asim K., and David B. Mount. 2015. 'The Molecular Physiology of Uric Acid Homeostasis'. *Annual Review of Physiology* 77(1):323–45. doi: 10.1146/annurev-physiol-021113-170343.

Martinez, Fernando O. 2011. 'Regulators of Macrophage Activation'. *European Journal of Immunology* 41(6):1531–34. doi: 10.1002/eji.201141670.

Martinez, Fernando O., Laura Helming, and Siamon Gordon. 2009. 'Alternative Activation of Macrophages: An Immunologic Functional Perspective'. *Annual Review of Immunology* 27(1):451–83. doi: 10.1146/annurev.immunol.021908.132532.

Maruhashi, Tatsuya, Ichiro Hisatome, Yasuki Kihara, and Yukihito Higashi. 2018a. 'Hyperuricemia and Endothelial Function: From Molecular Background to Clinical Perspectives'. *Atherosclerosis* 278:226–31. doi: 10.1016/j.atherosclerosis.2018.10.007.

Maruhashi, Tatsuya, Ichiro Hisatome, Yasuki Kihara, and Yukihito Higashi. 2018b. 'Hyperuricemia and Endothelial Function: From Molecular Background to Clinical Perspectives'. *Atherosclerosis* 278:226–31. doi: 10.1016/j.atherosclerosis.2018.10.007.

Mazzali, Marilda, Mehmet Kanbay, Mark S. Segal, Mohamed Shafiu, Diana Jalal, Daniel I. Feig, and Richard J. Johnson. 2010. 'Uric Acid and Hypertension: Cause or Effect?' *Current Rheumatology Reports* 12(2):108–17. doi: 10.1007/s11926-010-0094-1.

Mijailovic, Natasa R., Katarina Vesic, and Milica M. Borovcanin. 2022. 'The Influence of Serum Uric Acid on the Brain and Cognitive Dysfunction'. *Frontiers in Psychiatry* 13. doi: 10.3389/fpsyt.2022.828476.

Miranda, Josiane Aparecida de, Guilherme Gomide Almeida, Raissa Isabelle Leão Martins, Mariana Botrel Cunha, Vanessa Almeida Belo, José Eduardo Tanus dos Santos, Carlos Alberto Mourão-Júnior, and Carla Márcia Moreira Lanna. 2015. 'O Papel Do Ácido Úrico Na Resistência Insulínica Em Crianças e Adolescentes Com Obesidade'. *Revista Paulista de Pediatria* 33(4):431–36. doi: 10.1016/j.rpped.2015.03.009.

Murray, Peter J. 2017. 'Macrophage Polarization'. *Annual Review of Physiology* 79(1):541–66. doi: 10.1146/annurev-physiol-022516-034339.

Nakamura, Hajime, Leonore A. Herzenberg, Jie Bai, Shinichi Araya, Norihiko Kondo, Yumiko Nishinaka, Leonard A. Herzenberg, and Junji Yodoi. 2001. 'Circulating Thioredoxin Suppresses Lipopolysaccharide-Induced Neutrophil Chemotaxis'. *Proceedings of the National Academy of Sciences* 98(26):15143–48. doi: 10.1073/pnas.191498798.

NERY, Rodrigo Araldi, Barbara Stadler KAHLOW, Thelma L. SKARE, Fernando Issamu TABUSHI, and Adham do Amaral e CASTRO. 2015. 'URIC ACID AND TISSUE REPAIR'. *ABCD. Arquivos Brasileiros de Cirurgia Digestiva (São Paulo)* 28(4):290–92. doi: 10.1590/s0102-6720201500040018.

Pai, Hung-Liang, Sophie Meng-Tien Hsieh, Yu-Shan Su, Xin-Yuan Sue, Han-Hsin Chang, and David Pei-Cheng Lin. 2022. 'Short-Term Hyperuricemia Leads to Structural Retinal Changes That Can Be Reversed by Serum Uric Acid Lowering Agents in Mice'. *Investigative Opthalmology & Visual Science* 63(10):8. doi: 10.1167/iovs.63.10.8.

Ramji, Dipak P., and Thomas S. Davies. 2015. 'Cytokines in Atherosclerosis: Key Players in All Stages of Disease and Promising Therapeutic Targets'. *Cytokine & Growth Factor Reviews* 26(6):673–85. doi: 10.1016/j.cytogfr.2015.04.003.

El Ridi, Rashika, and Hatem Tallima. 2017a. 'Physiological Functions and Pathogenic Potential of Uric Acid: A Review'. *Journal of Advanced Research* 8(5):487–93. doi: 10.1016/j.jare.2017.03.003.

El Ridi, Rashika, and Hatem Tallima. 2017b. 'Physiological Functions and Pathogenic Potential of Uric Acid: A Review'. *Journal of Advanced Research* 8(5):487–93. doi: 10.1016/j.jare.2017.03.003.

Rodriguez-Iturbe, Bernardo, Hector Pons, and Richard J. Johnson. 2017. 'Role of the Immune System in Hypertension'. *Physiological Reviews* 97(3):1127–64. doi: 10.1152/physrev.00031.2016.

Rosendorff, Clive, and Mather R. D. Jogendra. 2013. 'Uric Acid: Where Are We?' *The Journal of Clinical Hypertension* 15(1):5–6. doi: 10.1111/jch.12034.

Ruggiero, Carmelinda, Antonio Cherubini, Alessandro Ble, Angelo J. G. Bos, Marcello Maggio, Vishwa D. Dixit, Fulvio Lauretani, Stefania Bandinelli, Umberto Senin, and Luigi Ferrucci. 2006. 'Uric Acid and Inflammatory Markers'. *European Heart Journal* 27(10):1174–81. doi: 10.1093/eurheartj/ehi879.

Russo, Elisa, Francesca Viazzi, Roberto Pontremoli, Carlo Maria Barbagallo, Michele Bombelli, Edoardo Casiglia, Arrigo Francesco Giuseppe Cicero, Massimo Cirillo, Pietro Cirillo, Giovambattista Desideri, Lanfranco D'Elia, Claudio Ferri, Ferruccio Galletti, Loreto Gesualdo, Cristina Giannattasio, Guido Iaccarino, Giovanna Leoncini, Francesca Mallamaci, Alessandro Maloberti, Stefano Masi, Alessandro Mengozzi, Alberto Mazza, Maria Lorenza Muiesan, Pietro Nazzaro, Paolo Palatini, Gianfranco Parati, Marcello Rattazzi, Giulia Rivasi, Massimo Salvetti, Valérie Tikhonoff, Giuliano Tocci, Andrea Ungar, Paolo Verdecchia, Agostino Virdis,

Massimo Volpe, Guido Grassi, and Claudio Borghi. 2022. 'Association of Uric Acid with Kidney Function and Albuminuria: The Uric Acid Right for HeArt Health (URRAH) Project'. *Journal of Nephrology* 35(1):211–21. doi: 10.1007/s40620-021-00985-4.

Russo, Sara, Marcel Kwiatkowski, Natalia Govorukhina, Rainer Bischoff, and Barbro N. Melgert. 2021. 'Meta-Inflammation and Metabolic Reprogramming of Macrophages in Diabetes and Obesity: The Importance of Metabolites'. *Frontiers in Immunology* 12. doi: 10.3389/fimmu.2021.746151.

Shi, Yan, Shelly A. Galusha, and Kenneth L. Rock. 2006. 'Cutting Edge: Elimination of an Endogenous Adjuvant Reduces the Activation of CD8 T Lymphocytes to Transplanted Cells and in an Autoimmune Diabetes Model'. *The Journal of Immunology* 176(7):3905–8. doi: 10.4049/jimmunol.176.7.3905.

Sreejit, Gopalkrishna, Andrew J. Fleetwood, Andrew J. Murphy, and Prabhakara R. Nagareddy. 2020. 'Origins and Diversity of Macrophages in Health and Disease'. *Clinical & Translational Immunology* 9(12). doi: 10.1002/cti2.1222.

Tancredi, Mauro, Annika Rosengren, Ann-Marie Svensson, Mikhail Kosiborod, Aldina Pivodic, Soffia Gudbjörnsdottir, Hans Wedel, Mark Clements, Sofia Dahlqvist, and Marcus Lind. 2015. 'Excess Mortality among Persons with Type 2 Diabetes'. *New England Journal of Medicine* 373(18):1720–32. doi: 10.1056/NEJMoa1504347.

Wasilewska, Anna, Edyta Tenderenda, Katarzyna Taranta-Janusz, Jolanta Tobolczyk, and Justyna Stypułkowska. 2012. 'Markers of Systemic Inflammation in Children with Hyperuricemia'. *Acta Paediatrica* 101(5):497–500. doi: 10.1111/j.1651-2227.2011.02582.x.

World Medical Association. 2001. 'World Medical Association Declaration of Helsinki. Ethical Principles for Medical Research Involving Human Subjects.' *Bulletin of the World Health Organization* 79(4):373–74.

Yu, Wei, De Xie, Tetsuya Yamamoto, Hidenori Koyama, and Jidong Cheng. 2023. 'Mechanistic Insights of Soluble Uric Acid-Induced Insulin Resistance: Insulin Signaling and Beyond'. *Reviews in Endocrine and Metabolic Disorders* 24(2):327–43. doi: 10.1007/s11154-023-09787-4.

Zhang, Zenglei, Lin Zhao, Xingyu Zhou, Xu Meng, and Xianliang Zhou. 2023. 'Role of Inflammation, Immunity, and Oxidative Stress in Hypertension: New Insights and Potential Therapeutic Targets'. *Frontiers in Immunology* 13. doi: 10.3389/fimmu.2022.1098725.

Zhi, Li, Zhu Yuzhang, Huang Tianliang, Ichiro Hisatome, Tetsuya Yamamoto, and Cheng Jidong. 2016. 'High Uric Acid Induces Insulin Resistance in Cardiomyocytes In Vitro and In Vivo'. *PLOS ONE* 11(2):e0147737. doi: 10.1371/journal.pone.0147737.

Zhou, Yang, Li Fang, Lei Jiang, Ping Wen, Hongdi Cao, Weichun He, Chunsun Dai, and Junwei Yang. 2012. 'Uric Acid Induces Renal Inflammation via Activating Tubular NF-KB Signaling Pathway'. *PLoS ONE* 7(6):e39738. doi: 10.1371/journal.pone.0039738.

Zhu, Yanyan, Bhavik J. Pandya, and Hyon K. Choi. 2011. 'Prevalence of Gout and Hyperuricemia in the US General Population: The National Health and Nutrition Examination Survey 2007-2008'. *Arthritis & Rheumatism* 63(10):3136–41. doi: 10.1002/art.30520.

Zhu, Yuzhang, Yaqiu Hu, Tianliang Huang, Yongneng Zhang, Zhi Li, Chaohuan Luo, Yinfeng Luo, Huier Yuan, Ichiro Hisatome, Tetsuya Yamamoto, and Jidong Cheng. 2014. 'High Uric Acid Directly Inhibits Insulin Signalling and Induces Insulin Resistance'. *Biochemical and Biophysical Research Communications* 447(4):707–14. doi: 10.1016/j.bbrc.2014.04.080.

ANEXO I ARTÍCULOS GENERADOS DURANTE EL DOCTORADO

biomolecules

MDPI

Article

Uric Acid Has Direct Proinflammatory Effects on Human Macrophages by Increasing Proinflammatory Mediators and Bacterial Phagocytosis Probably via URAT1

Camilo P. Martínez-Reyes [1], Aarón N. Manjarrez-Reyna [1], Lucia A. Méndez-García [1], José A. Aguayo-Guerrero [1], Beatriz Aguirre-Sierra [1], Rafael Villalobos-Molina [2], Yolanda López-Vidal [3], Karen Bobadilla [4] and Galileo Escobedo [1,*]

1 Laboratory for Proteomics and Metabolomics, Research Division, General Hospital of Mexico "Dr. Eduardo Liceaga", 06726 Mexico City, Mexico; nava111222@hotmail.com (C.P.M.-R.); aaron.manjarrez@gmail.com (A.N.M.-R.); angelica.mendez.86@hotmail.com (L.A.M.-G.); jose.aguayo01@iest.edu.mx (J.A.A.-G.); bety_agsi@hotmail.com (B.A.-S.)

2 Unidad de Biomedicina, Facultad de Estudios Superiores Iztacala, Universidad Nacional Autónoma de México, 54090 Mexico City, Mexico; villalobos@campus.iztacala.unam.mx

3 Programa de Inmunología Molecular Microbiana, Facultad de Medicina, Universidad Nacional Autónoma de México, 04510 Mexico City, Mexico; lvidal@unam.mx

4 Department of Immunology, Instituto Nacional de Enfermedades Respiratorias Ismael Cosío Villegas, 14080 Mexico City, Mexico; karenbolo@hushmail.com

* Correspondence: gescobedog@msn.com or gescobedo@unam.mx; Tel.: +52-(55)-2789-2000 (ext. 5646)

Received: 10 March 2020; Accepted: 5 April 2020; Published: 9 April 2020

Abstract: The relationship of uric acid with macrophages has not been fully elucidated. We investigated the effect of uric acid on the proinflammatory ability of human macrophages and then examined the possible molecular mechanism involved. Primary human monocytes were differentiated into macrophages for subsequent exposure to 0, 0.23, 0.45, or 0.9 mmol/L uric acid for 12 h, in the presence or absence of 1 mmol/L probenecid. Flow cytometry was used to measure proinflammatory marker production and phagocytic activity that was quantified as a percentage of GFP-labeled *Escherichia coli* positive macrophages. qPCR was used to measure the macrophage expression of the urate anion transporter 1 (URAT1). As compared to control cells, the production of tumor necrosis factor-alpha (TNF-alpha), toll-like receptor 4 (TLR4), and cluster of differentiation (CD) 11c was significantly increased by uric acid. In contrast, macrophages expressing CD206, CX3C-motif chemokine receptor 1 (CX3CR1), and C-C chemokine receptor type 2 (CCR2) were significantly reduced. Uric acid progressively increased macrophage phagocytic activity and downregulated URAT1 expression. Probenecid—a non-specific blocker of URAT1-dependent uric acid transport—inhibited both proinflammatory cytokine production and phagocytic activity in macrophages that were exposed to uric acid. These results suggest that uric acid has direct proinflammatory effects on macrophages possibly via URAT1.

Keywords: macrophage; uric acid; TNF-alpha; TLR4; phagocytosis; probenecid; URAT1

1. Introduction

In humans, monosodium urate—also referred to as uric acid—is the end-product of purine metabolism [1]. Uric acid is mainly excreted in urine and then reabsorbed in epithelial cells of the proximal convoluted tubule by urate transporters, such as the urate anion transporter 1 (URAT1), a transmembrane protein highly expressed in endothelial cells, adipocytes, and cartilage chondrocytes [2–5].

Normal blood levels of uric acid are 2.4–6.0 mg/dL for women and 3.4–7.0 mg/dL for men [6,7]. However, hyperuricemia is a pathological entity that is characterized by blood uric acid values beyond upper limits that has been largely associated with metabolic syndrome and increased cardiovascular risk [8–10]. In this sense, a recent study conducted in 22,983 Chinese adults demonstrated that subjects with hyperuricemia had higher prevalence of cardiovascular risk factors, such as dyslipidemia, hypertension, and type 2 diabetes (T2D), than individuals with normal uric acid values [11]. It is also worth mentioning that uric acid concentration associated directly with the number of cardiovascular risk factors; in other words, the cardiovascular risk increases as the uric acid elevates in blood.

The association of hyperuricemia with cardiovascular diseases is accompanied by a low-grade inflammation state that is characterized by increased proinflammatory activation of macrophages [11,12]. In this regard, the exposure of ApoE$^{-/-}$ mice to allopurinol (an inhibitor of uric acid production) does not only reduce atherosclerotic plaque size, but also macrophage infiltration and the expression of tumor necrosis factor-alpha (TNF-alpha) and interleukin (IL-) 1 beta, both typical proinflammatory cytokines [12]. Thus, such a seminal work proposed, for the first time, a relationship between uric acid and macrophages in the scenario of cardiovascular disease.

Macrophages are innate immune cells that differentiate from monocytes and play prominent roles in phagocytosis, inflammation, and wound healing [13]. Macrophages exhibit extremely high plasticity by exerting the ability of orchestrating either proinflammatory responses or anti-inflammatory actions, depending on the extracellular milieu [14]. In the presence of prototypical molecules, such as lipopolysaccharide (LPS) and/or interferon gamma (IFN-gamma), human macrophages show proinflammatory functions by producing TNF-alpha, IL-1 beta, CD11c, and toll-like receptor 4 (TLR4) [15,16]. On the contrary, the exposure of macrophages to dexamethasone or cytokines, such as interleukin IL-4 and IL-13, leads these cells to adopt an anti-inflammatory profile that is characterized by the production of IL-10 and/or CD206 [15]. Furthermore, the exposure of macrophages to pro- or anti-inflammatory stimuli also affects the expression of molecules that are involved in leukocyte trafficking, such as CX3C-motif chemokine receptor 1 (CX3CR1) and C-C chemokine receptor type 2 (CCR2) [17,18]. More importantly, the inflammatory activation enhances the ability of macrophages to ingest bacteria with respect to that described in macrophages with anti-inflammatory functions [19,20].

Although previous evidence suggests that high uric acid levels associate with increased proinflammatory activity of human macrophages, there is not yet conclusive data in this respect. For this reason, we investigated the effect of increasing uric acid concentrations on the proinflammatory or anti-inflammatory ability of primary human macrophages in vitro, and then examined the possible molecular mechanism involved.

2. Materials and Methods

2.1. Subjects

Human monocytes were isolated from buffy coat suspensions of ten healthy male volunteers aged 18–35 years with no metabolic alterations, attending the Blood Bank of the General Hospital of Mexico. All of the participants provided written informed consent, being previously approved by the institutional ethical committee of the General Hospital of Mexico (registration number of the ethical code approval: DIC/11/UME/05/029), which guaranteed that the study was conducted in rigorous adherence to the principles that were described in the 1964 Declaration of Helsinki and its posterior amendment in 2013. Blood donors were excluded of the study if they had previous diagnosis of type 1 *Diabetes Mellitus* (T1D), T2D, cardiovascular disease, acute or chronic liver disease, acute or chronic renal disease, cancer, endocrine disorders, infectious diseases, and inflammatory or autoimmune disease. We also excluded of the study to HIV, HCV, and HBV-seropositive patients, and subjects with anti-inflammatory, antiplatelet drugs, anti-hypertensive, and immunomodulatory medication, including non-steroidal anti-inflammatory drugs.

2.2. Monocyte Isolation and Macrophage Culture

Buffy coat suspensions ($n = 10$) were separately diluted 1:2 with PBS1X (Sigma Aldrich, St. Louis, MO, USA) for the subsequent isolation of peripheral blood mononuclear cells (PBMCs) by density gradient centrifugation while using histopaque-1077 (Sigma Aldrich, St. Louis, MO, USA). The monocytes were then isolated from PBMCs by CD14-negative selection using magnetic columns (Miltenyi Biotec, Bergisch Gladbach, Germany). Purified monocytes were placed in RPMI-1640 medium (Sigma Aldrich, St. Louis, MO, USA) containing 10% fetal bovine serum (FBS) (Gibco™, Grand Island, NY, USA), 2 mM L-glutamine, 50 µg/mL gentamicin, and 10 ng/mL macrophage-colony stimulating factor (M-CSF) (Gibco™, Grand Island, NY, USA) in six-well cell-culture plates (Costar, Kennebunk, ME, USA), at a density of 3×10^6 monocytes per well. Culture media and M-CSF were replaced every other day for seven days. Upon differentiation, the monocyte-derived macrophages (MDM) were cultured in RPMI-1640 medium supplemented, as mentioned above and exposed to 0.23, 0.45, or 0.9 mmol/L uric acid (Sigma Aldrich, St. Louis, MO, USA) for 12 h. After performing several time-response curves at 1, 3, 6, and 12 h, and one, three, six, and nine days, we found that MDM exhibited the most significant proinflammatory activity at 12 h of in vitro culture in the presence of uric acid, and we decided to perform all experiments at this time. Prior uric acid exposure, 1 mmol/L probenecid—a non-specific blocker of URAT1-dependent uric acid transport (St. Louis, MO, USA)—was added and replaced after 6 h by culture media that contained different uric acid concentrations. Control MDM were placed in supplemented RPMI-1640 medium in the absence of uric acid for the same time. Immediately after, MDM were collected while using sterile cell scrapers (Corning, Reynosa, Tamaulipas, Mexico) and equally divided into 1 mL PBS1X (Sigma Aldrich, St. Louis, MO, USA) for flow cytometry analysis or 300 µL TRIzol Reagent (Life Technologies, Carlsbad, CA, USA) for quantitative polymerase chain reaction (qPCR) assays.

2.3. Flow Cytometry Assays

After collecting the cells, 1×10^6 MDM were resuspended in 50 µL Cell Staining Buffer (BioLegend, Inc., San Diego, CA, USA). Subsequently, the cells were incubated with anti-CD14 PE/Cy7, anti-CD206 APC/Cy7, anti-TLR4 PE, anti-CX3CR1 BV510, anti-CCR2 AF647 (BioLegend, Inc., San Diego, CA, USA), and 5 µL True-Stain Monocyte Blocker™ (BioLegend, Inc., San Diego, CA, USA) for 20 min. in darkness at 4 °C. After being rinsed with Cell Staining Buffer (BioLegend, Inc., San Diego, CA, USA), MDM were incubated with 7-AAD (BD Pharmingen™, San Jose, CA, USA) for 10 min. for subsequent analysis on a FACSCanto II flow cytometer (BD Biosciences, San Jose, CA, USA) by means of BD FACSDiva™ software 6.0, acquiring 20,000 events per test in triplicate. The compensation controls were performed using UltraComp eBeads™ (Invitrogen, Carlsbad, CA, USA) for each fluorochrome. Flow cytometry data were analyzed using the FlowJo 10.0.7 software (TreeStar, Inc, Ashland, OR, USA). For intracellular cytokine stain, MDM were treated with 1:1000 Brefeldin A (BioLegend, Inc., San Diego, CA, USA) for the last 2 h of in vitro culture. After collecting cells, 1×10^6 MDM were resuspended in 50 µL Cell Staining Buffer (BioLegend, Inc., San Diego, CA, USA). Immediately after, the MDM were simultaneously incubated with anti-CD14 PE/Cy7, anti-CD11c PE/Cy5, Zombie UV Fixable Viability Kit, and 5 µL True-Stain Monocyte Blocker™ (BioLegend, Inc., San Diego, CA, USA) for 20 min. in darkness at 4 °C. Afterwards, MDM were incubated with 100 µL Fixation Medium A (FIX & PERM™ Cell Permeabilization Kit) (Invitrogen™, Carlsbad, CA, USA) for 15 min. at room temperature. Afterwards, MDM were rinsed with Cell Staining Buffer (BioLegend, Inc., San Diego, CA, USA) for subsequent incubation with 100 µL Permeabilization Medium B (FIX & PERM™ Cell Permeabilization Kit) (Invitrogen™, Carlsbad, CA, USA), and anti-TNF-alpha AF488 and anti-IL-1 beta Pacific Blue for 20 min. in darkness at room temperature. Immediately after, the MDM were rinsed with Cell Staining Buffer (BioLegend, Inc., San Diego, CA, USA) and then acquired on a BD Influx flow cytometer (BD Biosciences, San Jose, CA, USA) by means of BD Sortware™ software 1.2, acquiring 20,000 events per test in triplicate. Compensation controls were performed using UltraComp eBeads™

(Invitrogen™, Carlsbad, CA, USA) for each fluorochrome. Flow cytometry data were analyzed while using the FlowJo 10.0.7 software (TreeStar, Inc, Ashland, OR, USA).

2.4. Macrophage Phagocytic Activity

Escherichia coli of the strain DH5a were transformed while using the green fluorescent protein (GFP)-mut2 encoding plasmid pCD353 (*E. coli*-GFP+) that is regulated by a lactac promoter. GFP was induced using 1mM isopropyl-b-D-1-thiogalactopyranoside (Sigma Aldrich, St. Louis, MO, USA), as previously described [21]. *E. coli*-GFP+ were in vitro cultured with macrophages in a ratio of bacteria:cells = 30:1 for 1 h. Afterwards, cell suspensions were centrifuged at 2500 rpm/15 min. to remove remnant bacteria and then resuspended in 50 µL of sterile PBS 1X for posterior analysis on a FACSCanto II flow cytometer (BD Biosciences, San Jose, CA, USA) by means of BD FACSDiva™ software 6.0, acquiring 20,000 events per test in triplicate.

2.5. URAT1 Gene Expression by qPCR

After collecting cells, 1×10^6 MDM were resuspended in TRIzol Reagent (Life Technologies, Life Technologies, Carlsbad, CA, USA) at 4 °C. Immediately after, the total RNA was isolated by the phenol/chloroform/guanidine isothiocyanate method according to the manufacturer's instructions. Total RNA samples were quantified and subjected to reverse transcription using the M-MLV Retrotranscriptase system in the presence of dT primer (Invitrogen, Carlsbad, CA, USA). After being incubated at 37 °C for 60 min., cDNA samples were obtained and used for amplification while using the real-time polymerase chain reaction (qPCR) in the presence of SYBR Green Master Mix and AmpliTaq® Fast DNA Polymerase (Applied biosystems, Foster City, CA, USA), according to the manufacturer's instructions. Human-specific primers for URAT1 were designed using the Primer-BLAST software from the National Center for Biotechnology Information (NCBI), U.S. National Library of Medicine, as follows: forward primer 5′-CGGACCTGTATCTCCACGTT-3′, reverse primer 5′-TGCCTTCTTTACTGCCTGGT-3′, denaturation at 94 °C for 30 s, annealing at 60 °C for 45 s, elongation at 72 °C for 45 s, and 28 thermal cycles for a 570 base pair (bp) product length. The 18S-ribosomal RNA sequence was used as house-keeping gene control as follows: forward primer 5′-CGCGGTTCTATTTTGTTGGT-3′, reverse primer 5′-AGTCGGCATCGTTTATGGTC-3′, denaturation at 94 °C for 30 s, annealing at 60 °C for 30 s, elongation at 72 °C for 30 s, and 40 thermal cycles for a 570 bp product length. URAT1 mRNA expression was normalized using the house-keeping gene control and reported as 2^(ΔΔCt). The qPCR experiments are reported according to the Minimum Information for Publication of Quantitative Real-Time PCR Experiments (MIQE) guidelines to guarantee reproducibility.

2.6. Statistics

The Shapiro–Wilk test estimated the normality of data distribution. One-way ANOVA, followed by a post-hoc Tukey test, was used to compare the expression of CD11c, CD206, TNF-alpha, IL-1 beta, TLR4, CX3CR1, CCR2, and URAT1, as well as the intracellular amount of *E. coli*-GFP+ in monocyte-derived macrophages that were exposed to 0, 0.23, 0.45, or 0.9 mmol/L uric acid. All of the statistical analyses were performed using the GraphPad Prism 7 software. Differences were considered to be significant when $p < 0.05$.

3. Results

Upon differentiation in the presence of M-CSF for seven days, human monocyte-derived macrophages (MDM) showed significantly higher cell size than monocytes (Figure 1A,B). Furthermore, while monocytes exhibited a typical appearance that consisted of round cells, differentiated MDM appeared as fusiform-shaped cells with numerous pseudopodia that increased their cell complexity with respect to monocytes (Figure 1A,B). Additionally, macrophage differentiation was also confirmed by means of CD14 cell surface expression. In this sense, MDM showed a significant 20% reduction in CD14 expression when compared to that found in monocytes (Figure 1C). Once gated for singlets

on a forward scatter height/forward scatter area density plot (Figure 1D), the living cells were gated while using the 7-AAD staining for dead cells. The living monocytes were then gated on a forward scatter area/side scatter area plot to assess CD14 positive expression together with TNF-alpha, IL-1 beta, CD11c, CD206, and CX3CR1, and CCR2 (Figure 1D).

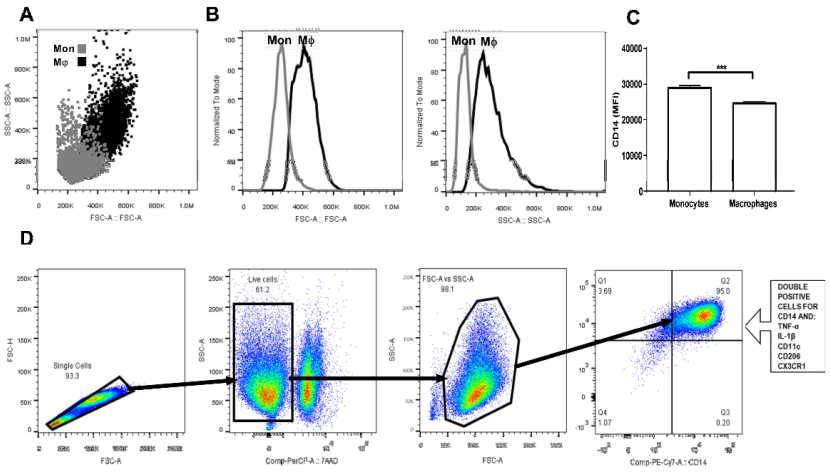

Figure 1. Gating strategy for primary human monocyte-derived macrophage characterization. Primary human monocytes were isolated from buffy coat suspensions (n = 10) and differentiated into macrophages in the presence of M-CSF for seven days. (**A**) Dot plot showing a comparison between monocytes (grey dots) and macrophages (black dots) in terms of cell size and complexity. (**B**) Macrophages are considerably larger and more complex than monocytes. (**C**) As previously reported, macrophages exhibit significantly decreased CD14 cell surface expression as compared to that found in monocytes. (**D**) Monocyte-derived macrophages (MDM) were gated for singlets on a forward scatter height/forward scatter area density plot. Resulting cells were gated again for detection of living macrophages by means of the 7AAD or Zombie UV stains. Macrophages were then gated on a side scatter area/forward scatter area density plot for detection of CD14+ cells that simultaneously expressed tumor necrosis factor-alpha (TNF-alpha), interleukin (IL-1) beta, CD11c, CD206, CX3CR1, and CCR2. Mon, monocyte population; Mϕ, macrophage population; MFI, mean fluorescence intensity; FSC-H, forward scatter height density plot; FSC-A, forward scatter area density plot; SSC-A, side scatter area density plot; TNF-a, tumor necrosis factor alpha; IL-1b, interleukin 1 beta; CD11c, cluster of differentiation 11c; CD206, cluster of differentiation 206 or mannose receptor; CX3CR1, CX3C-motif chemokine receptor 1; CCR2, C-C chemokine receptor type 2; M-CSF, macrophage-colony stimulating factor.

Regarding the production of proinflammatory cytokines, the exposure of MDM to increasing uric acid concentrations tended to raise the number of TNF-alpha+ cells, although no significant changes were reached (Figure 2A). However, MDM in vitro cultured in the presence of 0.23 mmol/L uric acid showed a significant 25% increase in TNF-alpha production with respect to that found in the control cells (Figure 2B). No significant differences were found when compared MDM exposed to 0.45 or 0.9 mmol/L uric acid with control cells, thus suggesting that uric acid exerts its effects on TNF-alpha production in a dose-dependent fashion (Figure 2B). Despite exposure of MDM to increasing uric acid levels tended to diminish either the number of IL-1 beta+ cells or IL-1 beta production, no significant differences were found (Figure 2C,D, respectively).

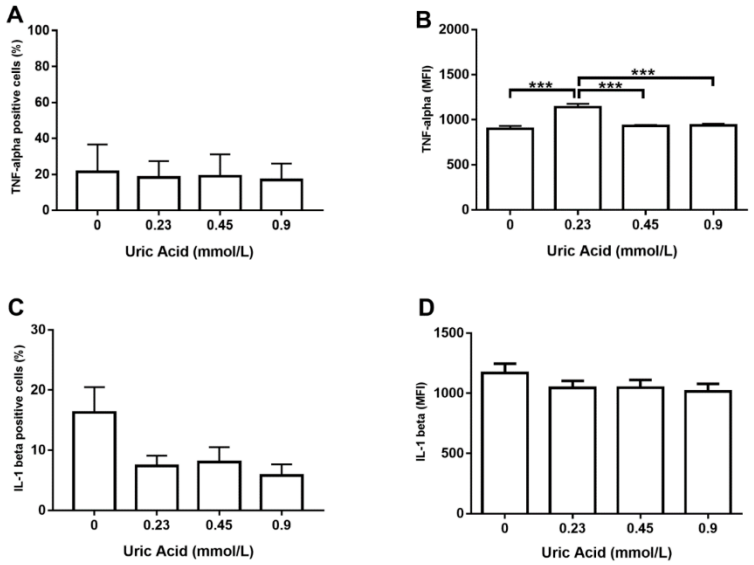

Figure 2. Intracellular production of TNF-alpha and IL-1 beta in primary human monocyte-derived macrophages in vitro exposed to uric acid. In vitro exposure to increasing concentrations of uric acid did not alter the percentage of primary human monocyte-derived macrophages expressing TNF-alpha (**A**). In vitro exposure to 0.23 mmol/L uric acid significantly increased TNF-alpha production in primary human monocyte-derived macrophages as compared to control cells (0 mmol/L uric acid) (**B**). In vitro exposure to increasing concentrations of uric acid tended to decrease the percentage of primary human monocyte-derived macrophages expressing IL-1 beta, although no significant differences were found (**C**). In vitro exposure to increasing concentrations of uric acid did not alter IL-1 beta production in primary human monocyte-derived macrophages (**D**). Data were analyzed using one-way ANOVA followed by the post-hoc Tukey test to estimate significant differences. Data are expressed as mean ± standard deviation. Differences were considered significant when $p < 0.05$ and are marked with asterisks as follows: *** = $p < 0.0001$. TNF-alpha, tumor necrosis factor alpha; IL-1 beta, interleukin 1 beta; MFI, mean fluorescence intensity.

We decided to measure TLR4 production as a key regulator of TNF-alpha synthesis since exposure of MDM to uric acid increased the expression of TNF-alpha, but not IL-1 beta. In this sense, uric acid induced TLR4 expression on MDM in a dose-dependent fashion, even though no significant differences were reached in terms of the number of TLR4+ cells (Figure 3A). However, exposure of MDM to 0.23 mmol/L uric acid promoted a significant 30% increase in TLR4 production in a very similar way than that observed for the case of TNF-alpha (Figure 3B). TNF-alpha positive macrophages have been also shown to produce CD11c, an integrin that is highly expressed in proinflammatory monocytes recruited toward atherosclerotic plaques. Uric acid did not affect the number of MDM expressing CD11c (Figure 3C); however, uric acid increased CD11c expression on MDM in a dose-dependent fashion, reaching the highest production of this integrin at 0.23 and 0.45 mmol/L uric acid (Figure 3D).

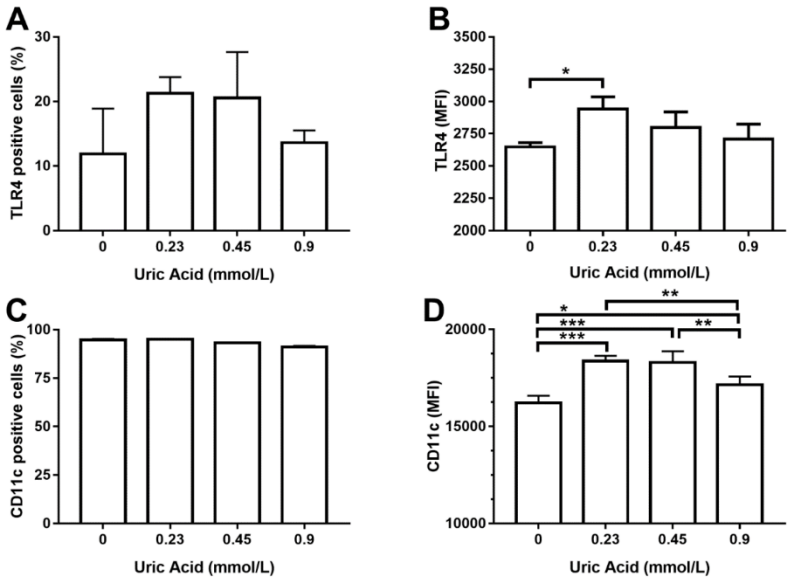

Figure 3. Cell surface expression of TLR4 and CD11c in primary human monocyte-derived macrophages in vitro exposed to uric acid. In vitro exposure to increasing concentrations of uric acid did not alter the percentage of primary human monocyte-derived macrophages expressing TLR4 (**A**). In vitro exposure to 0.23 mmol/L uric acid significantly increased TLR4 production in primary human monocyte-derived macrophages as compared to control cells (0 mmol/L uric acid) (**B**). In vitro exposure to increasing concentrations of uric acid did not alter the percentage of primary human monocyte-derived macrophages expressing CD11c (**C**). In vitro exposure to 0.23, 0.45, and 0.9 mmol/L uric acid significantly altered CD11c production in primary human monocyte-derived macrophages in a dose-response manner as compared to control cells (0 mmol/L uric acid) (**D**). Data were analyzed using one-way ANOVA, followed by the post-hoc Tukey test to estimate significant differences. Data are expressed as mean ± standard deviation. Differences were considered to be significant when $p < 0.05$ and are marked with asterisks as follows: * = $p < 0.01$; ** = $p < 0.001$; *** = $p < 0.0001$. TLR4, toll-like receptor 4; CD11c, cluster of differentiation 11c; MFI, mean fluorescence intensity.

It is well known that macrophages gain proinflammatory ability while losing the anti-inflammatory capacity. For this reason, we wanted to measure CD206 production, a typical anti-inflammatory marker of human and murine macrophages. As expected, the exposure of MDM to increasing levels of uric acid progressively reduced the number of cells expressing CD206 with respect to control cells (Figure 4A). Overall, uric acid did not affect CD206 expression in MDM, except for 0.45 mmol/L uric acid that induced a slight increase in the expression of this anti-inflammatory marker (Figure 4B).

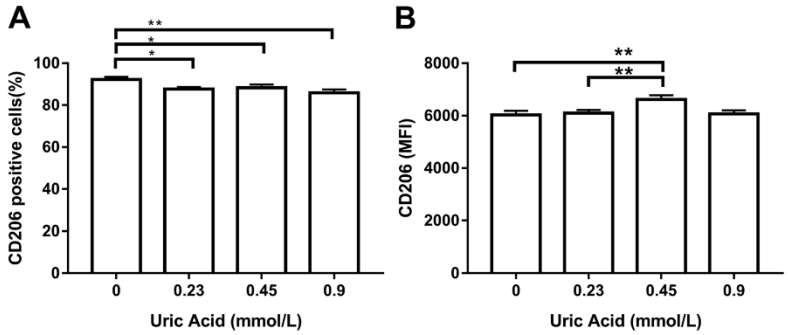

Figure 4. Cell surface expression of CD206 in primary human monocyte-derived macrophages in vitro exposed to uric acid. In vitro exposure to 0.23, 0.45, and 0.9 mmol/L uric acid significantly decreased the percentage of primary human monocyte-derived macrophages expressing CD206 as compared to control cells (0 mmol/L uric acid) (**A**). In vitro exposure to 0.45 mmol/L uric acid significantly increased CD206 production in primary human monocyte-derived macrophages as compared to control cells (0 mmol/L uric acid) (**B**). Data were analyzed using one-way ANOVA followed by the post-hoc Tukey test to estimate significant differences. Data are expressed as mean ± standard deviation. Differences were considered significant when $p < 0.05$ and are marked with asterisks as follows: * = $p < 0.01$; ** = $p < 0.001$. CD206, cluster of differentiation 206 or mannose receptor; MFI, mean fluorescence intensity.

We decided to examine the effect of this metabolite on the expression of CX3CR1 and CCR2, two chemokine receptors that decreases in proinflammatory macrophages. The exposure of MDM to uric acid progressively diminished the number of CX3CR1+ macrophages, reaching the maximum response when cells were incubated in the presence of 0.9 mmol/L uric acid (Figure 5A). Likewise, uric acid gradually reduced CX3CR1 expression in MDM as compared to that found in the control cells (Figure 5B). In parallel, the exposure of MDM to uric acid gradually decreased the number of cells expressing CCR2, reaching the lowest level of this chemokine receptor when using 0.9 mmol/L uric acid (Figure 5C). As expected, uric acid also diminished CCR2 expression in MDM at 0.45 and 0.9 mmol/L and provided solid experimental evidence that CX3CR1 and CCR2 production behaves similarly in macrophages that were exposed either to LPS or uric acid.

Proinflammatory activation of human macrophages is also associated with an increased ability to phagocytose bacteria. Thus, we evaluated the effect of increasing uric acid concentrations on the phagocytic activity of MDM while using *E. coli*-GFP+. In the absence of uric acid, MDM were able to ingest around 15% of *E. coli*-GFP+ (Figure 6). Notably, the exposure of MDM to 0.23 mmol/L uric acid induced a significant 26% increase in the intracellular number of *E. coli*-GFP+ as compared to control cells (Figure 6). Accordingly, MDM exposed to 0.45 and 0.9 mmol/L uric acid showed significant 40 and 120% increases, respectively, in the intracellular amount of *E. coli*-GFP+ as compared to control cells (Figure 6), which confirmed that uric acid acts as a proinflammatory stimulus for in vitro cultured human macrophages.

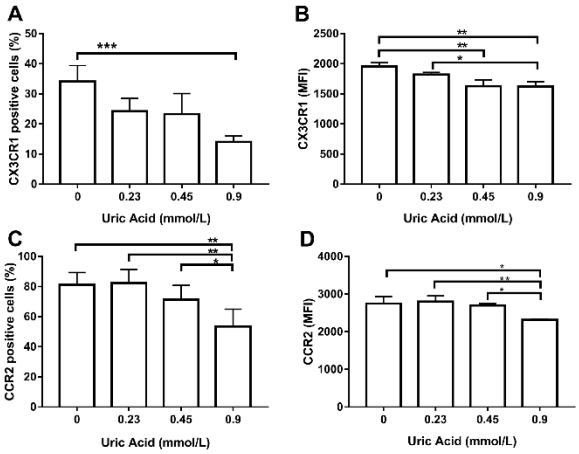

Figure 5. Cell surface expression of CX3CR1 and CCR2 in primary human monocyte-derived macrophages in vitro exposed to uric acid. In vitro exposure to 0.9 mmol/L uric acid significantly decreased the percentage of primary human monocyte-derived macrophages expressing CX3CR1 as compared to control cells (0 mmol/L uric acid) (**A**). In vitro exposure to 0.45 and 0.9 mmol/L uric acid significantly decreased CX3CR1 production in primary human monocyte-derived macrophages as compared to control cells (0 mmol/L uric acid) (**B**). In vitro exposure to 0.9 mmol/L uric acid significantly decreased the percentage of primary human monocyte-derived macrophages expressing CCR2 as compared to control cells (0 mmol/L uric acid (**C**). In vitro exposure to 0.9 mmol/L uric acid significantly decreased CCR2 production in primary human monocyte-derived macrophages as compared to control cells (0 mmol/L uric acid) (**D**). Data were analyzed using one-way ANOVA followed by the post-hoc Tukey test to estimate significant differences. Data are expressed as mean ± standard deviation. Differences were considered to be significant when $p < 0.05$ and are marked with asterisks as follows: * = $p < 0.01$; ** = $p < 0.001$; *** = $p < 0.0001$. CX3CR1, CX3C-motif chemokine receptor 1; CCR2, C-C chemokine receptor type 2; MFI, mean fluorescence intensity.

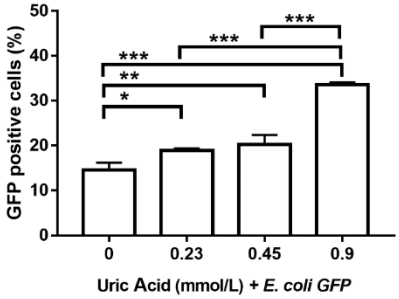

Figure 6. Bacterial phagocytic activity of primary human monocyte-derived macrophages in vitro exposed to uric acid. In vitro exposure to 0.23, 0.45, and 0.9 mmol/L uric acid significantly enhanced the phagocytic activity of primary human monocyte-derived macrophages by progressively increasing the percentage of *Escherichia coli*-green fluorescent protein (GFP) positive cells as compared to controls (0 mmol/L uric acid). Data were analyzed using one-way ANOVA followed by the post-hoc Tukey test to estimate significant differences. Data are expressed as mean ± standard deviation. Differences were considered significant when $p < 0.05$ and are marked with asterisks as follows: * = $p < 0.01$; ** = $p < 0.001$; *** = $p < 0.0001$. GFP, green fluorescent protein; *E. coli*, *Escherichia coli*.

An additional goal of this work was to explore the possible molecular mechanism by which uric acid exerts its effects on human monocyte-derived macrophages. For this reason, we decided to evaluate URAT1 expression, a key mediator of uric acid transport inside the cell. Notably, the exposure of MDM to 0.23 mmol/L uric acid induced a significant 90% reduction in URAT1 expression when compared to that found in control cells cultured in the absence of this metabolite (Figure 7). Similarly, MDM exposed to 0.45 mmol/L uric acid showed a significant 95% decrease in the mRNA levels of URAT1 with respect to that found in control cells (Figure 7). It is worth mentioning that exposure of MDM to 0.9 mmol/L uric acid totally abolished URAT1 expression (Figure 7), thus suggesting that URAT1 is sensitive to uric acid concentrations and it may take part in mediating the effects of this metabolite on macrophages.

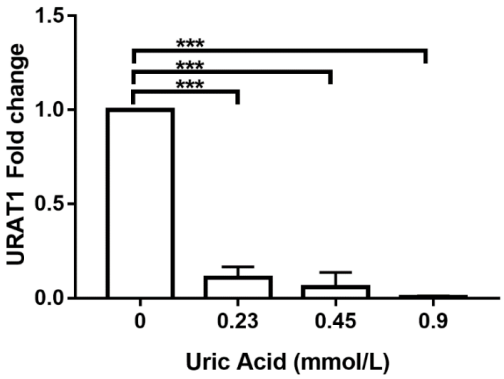

Figure 7. URAT1 expression in primary human monocyte-derived macrophages in vitro exposed to uric acid. In vitro exposure to 0.23, 0.45, and 0.9 mmol/L uric acid progressively abolished URAT1 expression in primary human monocyte-derived macrophages as compared to controls (0 mmol/L uric acid). URAT1 expression was normalized using the 18S-ribosomal RNA gene as house-keeping control gene and reported as 2^(ΔΔCt)-fold change by real-time polymerase chain reaction (qPCR) using SYBR Green Master Mix and AmpliTaq® Fast DNA Polymerase. Data were analyzed using one-way ANOVA followed by the post-hoc Tukey test to estimate significant differences. Data are expressed as mean ± standard deviation. Differences were considered significant when $p < 0.05$ and are marked with asterisks as follows: *** = $p < 0.0001$. URAT1, urate anion transporter 1.

We decided to use probenecid that is able to inhibit URAT1-dependent uric acid transport also examining its effect on TNF-alpha production and phagocytic activity to confirm the apparent involvement of URAT1 in macrophages. As expected, the use of probenecid totally abolished TNF-alpha production in macrophages that were also exposed to different concentrations of uric acid (Figure 8A). Likewise, probenecid also induced an 11% decrease in the intracellular number of *E. coli*-GFP+ macrophages that were treated with 0.23 mmol/L uric acid (Figure 8B). Furthermore, MDM treated with probenecid showed significant 78 and 61% reductions in the percentage of *E. coli*-GFP+, even in the presence of 0.45 and 0.9 mmol/L uric acid, respectively (Figure 8B). These results functionally suggest that uric acid might be transported inside the macrophage via URAT1 that, in turn, could mediate its proinflammatory effects on these immune cells.

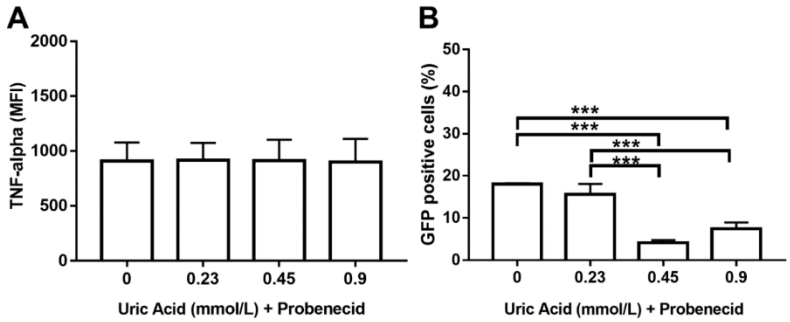

Figure 8. Probenecid seems to abolish URAT1-dependent proinflammatory effects of uric acid on primary human monocyte-derived macrophages. In vitro exposure to 1 mmol/L probenecid abolished the stimulatory effect of uric acid on TNF-alpha production in primary human monocyte-derived macrophages as compared to cells exposed to uric acid in the absence of probenecid (**A**). In vitro exposure to 1 mmol/L probenecid significantly decreased the stimulatory effect of uric acid on the phagocytic activity of primary human monocyte-derived macrophages by decreasing the percentage of Escherichia coli-GFP positive cells as compared to macrophages exposed to uric acid in the absence of probenecid (**B**). Data were analyzed using one-way ANOVA followed by the post-hoc Tukey test to estimate significant differences. Data are expressed as mean ± standard deviation. Differences were considered significant when $p < 0.05$ and are marked with asterisks, as follows: *** = $p < 0.0001$. TNF-a, tumor necrosis factor alpha; MFI, mean fluorescence intensity; GFP, green fluorescent protein.

4. Discussion

The association of hyperuricemia with the risk of developing metabolic abnormalities and cardiovascular diseases has been linked to an increased proinflammatory activity of macrophages [22,23]. However, it remains unknown whether hyperuricemia merely concurs with changes in macrophage activity or if uric acid is able to directly induce proinflammatory activation of human macrophages. For this reason, we decided to test the in vitro effect of increasing the uric acid concentrations on the proinflammatory profile of primary human macrophages differentiated from circulating monocytes.

We found that uric acid stimulates TNF-alpha production, but not IL-1 beta, in a dose-dependent fashion after confirming that human monocytes were properly differentiated into macrophages using a strategy that combined cell size and complexity as well CD14 expression. TNF-alpha and IL-1 beta are proinflammatory cytokines that play key roles in fever, cachexia, tumorigenesis inhibition, pyroptosis-related cell death, and immune cell recruitment [24–26]. However, TNF-alpha, but not IL-1 beta, has been consistently associated with increased serum levels of uric acid in several pathologic scenarios. For instance, the serum uric acid levels rise as TNF-alpha-producing monocytes also increase in women with preeclampsia [27]. Similarly, uric acid has been shown to stimulate TNF-alpha expression in vascular smooth muscle cells of Sprague–Dawley rats [28]. On the other hand, plasma IL-1 beta showed very poor association with increasing serum levels of uric acid in 1684 women and men, whereas TNF-alpha serum values rose in the same proportion than plasma uric acid [10]. Together with previous information, our results provide strong experimental evidence that uric acid might favor a proinflammatory state by predominantly stimulating TNF-alpha production in human macrophages. It is well known that TNF-alpha synthesis depends on the TLR4-dependent signaling pathway, whereas IL-1 beta production depends on the activity of the NLRP3 (NOD-LRR-and pyrin domain-containing protein 3) inflammasome [29–31]. For this reason, we decided to assess TLR4 in the same in vitro differentiated macrophages.

TLR4 is a transmembrane protein that is able to recognize numerous damage-associated molecular patterns (DAMP) and pathogen-associated molecular patterns (PAMPs), including free-fatty acids and

LPS [32,33]. Upon activation, TLR4 is capable of inducing downstream nuclear factor-kappa B (NF-kB) activation, finally leading to TNF-alpha production [34]. Concurring with this information, our results demonstrate that TLR4 is produced in response to uric acid in the same way that TNF-alpha does in human macrophages. In this regard, a previous work reported that the risk of gout—a pathology known by deposition of monosodium urate crystals in joints—is directly associated with the polymorphism rs2149356 related to high TLR4 production [35]. Likewise, a very recent study demonstrated that uric acid promotes the mRNA expression of TLR4 in rat adipocytes in vitro [36]. Thus, we speculate that uric acid is able to induce TNF-alpha production via TLR4 activation, a phenomenon that provides proinflammatory features to human macrophages. However, the idea that uric acid can activate TLR4 should be taken with caution, since we only evaluated TLR4 at the protein level without assessing its ability as a cell signal transducer.

Until here, our results appeared to indicate that uric acid exerts the ability to polarize human macrophages towards a proinflammatory state. Thus, we decided to confirm the apparently proinflammatory capacity of macrophages by analyzing CD11c and CD206. CD11c is a beta-2 integrin that is highly expressed in monocytes and macrophages with prominent proinflammatory functions, whereas CD206—also referred to as the mannose receptor—is a C-type lectin that is predominantly expressed in murine and human macrophages exerting anti-inflammatory actions [37–39]. Interestingly, we found that uric acid is able to increase CD11c production at the same time, which reduces the number of macrophages expressing CD206. In this sense, it has been previously reported that blockage of uric acid synthesis by uricase treatment decreases the number of CD11c+ monocytes in mice [40], which suggested, for the first time, a relationship between uric acid and CD11c production. In parallel, a previous report showed that macrophages from synovial fluid of patients with gout tend to show reduced CD206 expression as compared to that found in the macrophages of patients with rheumatoid arthritis [41]. Altogether, this information concurs with the idea that macrophages adopt proinflammatory functions while losing anti-inflammatory capacities in the presence of elevated levels of uric acid.

The idea that uric acid might act as a direct proinflammatory stimulus for human macrophages is also supported by two additional facts: (a) the expression pattern of CX3CR1 and CCR2 and (b) the phagocytic activity of macrophages. CX3CR1 and CCR2 are both involved in mediating monocyte recruitment to the inflammation sites, where these cells will differentiate into macrophages and orchestrate inflammatory responses or tissue repair [42,43]. Interestingly, numerous studies have consistently reported the downregulation of CX3CR1 and CCR2 in the presence of prototypical inflammatory stimuli, such as LPS. In this sense, a seminal work reported that circulating monocytes either of septic patients or incubated with LPS show dramatically decreased CX3CR1 expression [44]. Similarly, in vitro and in vivo exposure of murine peripheral blood cells to LPS can downregulate CCR2 expression with direct consequences for macrophage migratory ability [45,46]. Therefore, CX3CR1 and CCR2 expression appears to behave similarly in macrophages that are exposed either to LPS or uric acid, which provides solid experimental evidence regarding the possible inflammatory role of this metabolite in macrophages. Additionally, it is well known that macrophages with proinflammatory functions show greater ability to phagocytose bacteria than that described in anti-inflammatory macrophages [19,20]. Interestingly, the exposure of macrophages to increasing uric acid concentrations progressively improved their phagocytic activity, which once again supports the notion that uric acid acts as a direct proinflammatory stimulus for these immune cells.

Besides studying the apparently proinflammatory effect of uric acid on macrophages, we also wanted to explore the molecular mechanism that is potentially involved. In our study, the production of TNF-alpha, TLR4, and CD11c in response to uric acid exhibited a typical dose-response relationship, where a maximum effect is found and, beyond this point, a plateau can be seen, which indicates saturation and the abolishment of the observed effect [47]. The dose-response relationship has been attributed to the interaction between ligand and its receptor [47,48], which suggested to us the possible involvement of a molecule able to transport uric acid inside the macrophage, as is the case of URAT1.

In this way, we describe for, the first time, that human macrophages express URAT1, a transmembrane protein that had been only reported in endothelial cells, adipocytes, and cartilage chondrocytes [5]. Notably, we found that URAT1 expression in macrophages decreased as uric acid concentration increased, which might partially explain the fact that TNF-alpha, TLR4, and CD11c expression reached a saturation point, which in turn led to a decrease their protein levels. Taking into consideration that uric acid can increase NF-kB transcriptional activity in the pancreatic beta cell line Min6 [49], we thus speculate that TNF-alpha production in macrophages might depend on the interaction among uric acid, URAT1, and possibly NF-kB.

We performed functional assays aimed to pharmacologically block this urate transporter using probenecid to confirm the possible involvement of URAT1 in mediating the effects of uric acid on macrophages. Probenecid acts as a competitive inhibitor of URAT1 thus preventing reuptake and transport of uric acid by cells of the renal proximal tube [50]. Interestingly, the blockage of URAT1 abolished TNF-alpha production and phagocytic activity previously seen with uric acid, which suggests that the proinflammatory effect of uric acid entirely depends on its entry to macrophages. In this regard, it has been previously proposed that the entry of monosodium urate to THP-1 cells can induce IkB phosphorylation via Src family tyrosine kinases, thus leading to NF-kB activation and, finally, proinflammatory cytokine production [51]. In this way, our results confirm that (1) the entry of uric acid to macrophages has proinflammatry effects by a mechanism that is still unknown, and (2) entry of uric acid to macrophages seems to involve URAT1, whose expression is, in turn, sensitive to different concentrations of uric acid. However, URAT1 is not the only urate transporter and probenecid is not a URAT1 specific inhibitor, so measuring in macrophages other urate transporters, including organic anion transporter (OAT) 1, OAT3, and ATP-binding cassette subfamily G member 2 (ABCG2), and testing other urate uptake inhibitors, such as benzbromarone, dotinurad, and losartan, remains to be done.

5. Conclusions

Uric acid acts as a proinflammatory stimulus for in vitro cultured primary human macrophages through (a) increasing the production of TNF-alpha, TLR4, and CD11c, (b) improving the macrophage phagocytic activity, and (c) decreasing CD206, CX3CR1, and CCR2 expression. The possible mechanism by which uric acid exerts its proinflammatory effects on human macrophages appears to involve URAT1 in a dose-response fashion. URAT1 might, in turn, enhance NF-kB activation and lead to the production of proinflammatory cytokines by ways that remain to be elucidated. The use of probenecid functionally demonstrated that the entry of uric acid to the macrophage (d) has proinflammatory actions and (e) partially depends on URAT1. These results provide solid experimental evidence supporting the idea that elevated levels of uric acid can directly promote the macrophage-mediated systemic inflammatory state that is, in turn, associated with high cardiovascular risk in patients with chronic diseases. The idea that uric acid might act as a metabolic ligand with proinflammatory effects on human macrophages should be further examined.

Author Contributions: Conceptualization, C.P.M.-R. and G.E.; methodology, C.P.M.-R., A.N.M.-R., J.A.A.-G., L.A.M.-G. and B.A.-S.; formal analysis, C.P.M.-R., A.N.M.-R., K.B. and G.E.; data curation, C.P.M.-R., A.N.M.-R., R.V.-M., Y.L.-V., K.B. and G.E.; writing—original draft preparation, C.P.M.-R. and G.E.; writing—review and editing, R.V.-M., Y.L.-V., K.B. and G.E.; funding acquisition, G.E. All authors have read and agreed to the published version of the manuscript.

Funding: This work was supported by grant no. CB-2016-01-286209 from the Fondo Sectorial de Investigación para la Educación-CONACYT-México and grant no. SALUD-2017-02-290345 from the Fondo Sectorial de Investigación y Desarrollo en Salud y Seguridad Social SS/IMSS/ISSSTE/CONACYT-México to GE.

Acknowledgments: Camilo Pablo Martinez Reyes is a doctoral student from the Programa de Doctorado en Ciencias Biomédicas, Universidad Nacional Autónoma de México (UNAM) and has received CONACyT fellowship 582451. Authors thank to the Flow Cytometry core facility of "Coordinación de Investigación en Salud" at "Centro Médico Nacional Siglo XXI" of IMSS, Mexico for instrumentation and technical support, especially to Jessica L. Prieto-Chávez.

Conflicts of Interest: The authors declare that there is no conflict of interest regarding the publication of this article.

References

1. Enomoto, A.; Kimura, H.; Chairoungdua, A.; Shigeta, Y.; Jutabha, P.; Cha, S.H.; Hosoyamada, M.; Takeda, M.; Sekine, T.; Igarashi, T.; et al. Molecular identification of a renal urate anion exchanger that regulates blood urate levels. *Nature* **2002**, *417*, 447–452. [CrossRef] [PubMed]
2. Price, K.L.; Sautin, Y.Y.; Long, D.A.; Zhang, L.; Miyazaki, H.; Mu, W.; Endou, H.; Johnson, R.J. Human vascular smooth muscle cells express a urate transporter. *J. Am. Soc. Nephrol.* **2006**, *17*, 1791–1795. [CrossRef] [PubMed]
3. Sautin, Y.Y.; Nakagawa, T.; Zharikov, S.; Johnson, R.J. Adverse effects of the classic antioxidant uric acid in adipocytes: NADPH oxidase-mediated oxidative/nitrosative stress. *Am. J. Physiol. Cell Physiol.* **2007**, *293*, C584–C596. [CrossRef] [PubMed]
4. Sugihara, S.; Hisatome, I.; Kuwabara, M.; Niwa, K.; Maharani, N.; Kato, M.; Ogino, K.; Hamada, T.; Ninomiya, H.; Higashi, Y.; et al. Depletion of Uric Acid Due to SLC22A12 (URAT1) Loss-of-Function Mutation Causes Endothelial Dysfunction in Hypouricemia. *Circ. J.* **2015**, *79*, 1125–1132. [CrossRef]
5. Zhang, B.; Duan, M.; Long, B.; Zhang, B.; Wang, D.; Zhang, Y.; Chen, J.; Huang, X.; Jiao, Y.; Zhu, L.; et al. Urate transport capacity of glucose transporter 9 and urate transporter 1 in cartilage chondrocytes. *Mol. Med. Rep.* **2019**, *20*, 1645–1654. [CrossRef]
6. Bardin, T.; Richette, P. Definition of hyperuricemia and gouty conditions. *Curr. Opin. Rheumatol.* **2014**, *26*, 186–191. [CrossRef]
7. Chen-Xu, M.; Yokose, C.; Rai, S.K.; Pillinger, M.H.; Choi, H.K. Contemporary Prevalence of Gout and Hyperuricemia in the United States and Decadal Trends: The National Health and Nutrition Examination Survey, 2007–2016. *Arthritis Rheumatol.* **2019**, *71*, 991–999. [CrossRef]
8. Liu, Z.; Que, S.; Zhou, L.; Zheng, S. Dose-response Relationship of Serum Uric Acid with Metabolic Syndrome and Non-alcoholic Fatty Liver Disease Incidence: A Meta-analysis of Prospective Studies. *Sci. Rep.* **2015**, *5*, 14325. [CrossRef]
9. Yu, T.Y.; Jee, J.H.; Bae, J.C.; Jin, S.M.; Baek, J.H.; Lee, M.K.; Kim, J.H. Serum uric acid: A strong and independent predictor of metabolic syndrome after adjusting for body composition. *Metabolism* **2016**, *65*, 432–440. [CrossRef]
10. Lyngdoh, T.; Marques-Vidal, P.; Paccaud, F.; Preisig, M.; Waeber, G.; Bochud, M.; Vollenweider, P. Elevated serum uric acid is associated with high circulating inflammatory cytokines in the population-based Colaus study. *PLoS ONE* **2011**, *6*, e19901. [CrossRef]
11. Wu, J.; Qiu, L.; Cheng, X.Q.; Xu, T.; Wu, W.; Zeng, X.J.; Ye, Y.C.; Guo, X.Z.; Cheng, Q.; Liu, Q.; et al. Hyperuricemia and clustering of cardiovascular risk factors in the Chinese adult population. *Sci. Rep.* **2017**, *7*, 5456. [CrossRef] [PubMed]
12. Kushiyama, A.; Okubo, H.; Sakoda, H.; Kikuchi, T.; Fujishiro, M.; Sato, H.; Kushiyama, S.; Iwashita, M.; Nishimura, F.; Fukushima, T.; et al. Xanthine oxidoreductase is involved in macrophage foam cell formation and atherosclerosis development. *Arterioscler. Thromb. Vasc. Biol.* **2012**, *32*, 291–298. [CrossRef] [PubMed]
13. Wynn, T.A.; Chawla, A.; Pollard, J.W. Macrophage biology in development, homeostasis and disease. *Nature* **2013**, *496*, 445–455. [CrossRef]
14. Murray, P.J. Macrophage Polarization. *Annu. Rev. Physiol* **2017**, *79*, 541–566. [CrossRef]
15. Martinez, F.O.; Gordon, S.; Locati, M.; Mantovani, A. Transcriptional profiling of the human monocyte-to-macrophage differentiation and polarization: New molecules and patterns of gene expression. *J. Immunol.* **2006**, *177*, 7303–7311. [CrossRef]
16. Li, G.; Qiao, W.; Zhang, W.; Li, F.; Shi, J.; Dong, N. The shift of macrophages toward M1 phenotype promotes aortic valvular calcification. *J. Thorac. Cardiovasc. Surg.* **2017**, *153*, 1318–1327.e1. [CrossRef]
17. Amsellem, V.; Abid, S.; Poupel, L.; Parpaleix, A.; Rodero, M.; Gary-Bobo, G.; Latiri, M.; Dubois-Rande, J.L.; Lipskaia, L.; Combadiere, C.; et al. Roles for the CX3CL1/CX3CR1 and CCL2/CCR2 Chemokine Systems in Hypoxic Pulmonary Hypertension. *Am. J. Respir. Cell. Mol. Biol.* **2017**, *56*, 597–608. [CrossRef]
18. Deci, M.B.; Ferguson, S.W.; Scatigno, S.L.; Nguyen, J. Modulating Macrophage Polarization through CCR2 Inhibition and Multivalent Engagement. *Mol. Pharm.* **2018**, *15*, 2721–2731. [CrossRef]

19. Zhang, M.; Hutter, G.; Kahn, S.A.; Azad, T.D.; Gholamin, S.; Xu, C.Y.; Liu, J.; Achrol, A.S.; Richard, C.; Sommerkamp, P.; et al. Anti-CD47 Treatment Stimulates Phagocytosis of Glioblastoma by M1 and M2 Polarized Macrophages and Promotes M1 Polarized Macrophages In Vivo. *PLoS ONE* **2016**, *11*, e0153550. [CrossRef]
20. Lam, R.S.; O'Brien-Simpson, N.M.; Holden, J.A.; Lenzo, J.C.; Fong, S.B.; Reynolds, E.C. Unprimed, M1 and M2 Macrophages Differentially Interact with Porphyromonas gingivalis. *PLoS ONE* **2016**, *11*, e0158629. [CrossRef]
21. Gille, C.; Spring, B.; Tewes, L.; Poets, C.F.; Orlikowsky, T. A new method to quantify phagocytosis and intracellular degradation using green fluorescent protein-labeled Escherichia coli: Comparison of cord blood macrophages and peripheral blood macrophages of healthy adults. *Cytom. A* **2006**, *69*, 152–154. [CrossRef] [PubMed]
22. Haryono, A.; Nugrahaningsih, D.A.A.; Sari, D.C.R.; Romi, M.M.; Arfian, N. Reduction of Serum Uric Acid Associated with Attenuation of Renal Injury, Inflammation and Macrophages M1/M2 Ratio in Hyperuricemic Mice Model. *Kobe. J. Med. Sci.* **2018**, *64*, E107–E114. [PubMed]
23. Lu, W.; Xu, Y.; Shao, X.; Gao, F.; Li, Y.; Hu, J.; Zuo, Z.; Shao, X.; Zhou, L.; Zhao, Y.; et al. Uric Acid Produces an Inflammatory Response through Activation of NF-kappaB in the Hypothalamus: Implications for the Pathogenesis of Metabolic Disorders. *Sci. Rep.* **2015**, *5*, 12144. [CrossRef] [PubMed]
24. McGeough, M.D.; Wree, A.; Inzaugarat, M.E.; Haimovich, A.; Johnson, C.D.; Pena, C.A.; Goldbach-Mansky, R.; Broderick, L.; Feldstein, A.E.; Hoffman, H.M. TNF regulates transcription of NLRP3 inflammasome components and inflammatory molecules in cryopyrinopathies. *J. Clin. Investig.* **2017**, *127*, 4488–4497. [CrossRef]
25. Patel, H.J.; Patel, B.M. TNF-alpha and cancer cachexia: Molecular insights and clinical implications. *Life Sci.* **2017**, *170*, 56–63. [CrossRef]
26. Kaplanov, I.; Carmi, Y.; Kornetsky, R.; Shemesh, A.; Shurin, G.V.; Shurin, M.R.; Dinarello, C.A.; Voronov, E.; Apte, R.N. Blocking IL-1beta reverses the immunosuppression in mouse breast cancer and synergizes with anti-PD-1 for tumor abrogation. *Proc. Natl. Acad. Sci. USA* **2019**, *116*, 1361–1369. [CrossRef]
27. Peracoli, M.T.; Bannwart, C.F.; Cristofalo, R.; Borges, V.T.; Costa, R.A.; Witkin, S.S.; Peracoli, J.C. Increased reactive oxygen species and tumor necrosis factor-alpha production by monocytes are associated with elevated levels of uric acid in pre-eclamptic women. *Am. J. Reprod. Immunol.* **2011**, *66*, 460–467. [CrossRef]
28. Tang, L.; Xu, Y.; Wei, Y.; He, X. Uric acid induces the expression of TNFalpha via the ROSMAPKNFkappaB signaling pathway in rat vascular smooth muscle cells. *Mol. Med. Rep.* **2017**, *16*, 6928–6933. [CrossRef]
29. Lin, X.; Kong, J.; Wu, Q.; Yang, Y.; Ji, P. Effect of TLR4/MyD88 signaling pathway on expression of IL-1beta and TNF-alpha in synovial fibroblasts from temporomandibular joint exposed to lipopolysaccharide. *Mediat. Inflamm.* **2015**, *2015*, 329405. [CrossRef]
30. Grebe, A.; Hoss, F.; Latz, E. NLRP3 Inflammasome and the IL-1 Pathway in Atherosclerosis. *Circ. Res.* **2018**, *122*, 1722–1740. [CrossRef]
31. He, Y.; Franchi, L.; Nunez, G. TLR agonists stimulate Nlrp3-dependent IL-1beta production independently of the purinergic P2X7 receptor in dendritic cells and in vivo. *J. Immunol.* **2013**, *190*, 334–339. [CrossRef] [PubMed]
32. Rocha, D.M.; Caldas, A.P.; Oliveira, L.L.; Bressan, J.; Hermsdorff, H.H. Saturated fatty acids trigger TLR4-mediated inflammatory response. *Atherosclerosis* **2016**, *244*, 211–215. [CrossRef] [PubMed]
33. Park, B.S.; Lee, J.O. Recognition of lipopolysaccharide pattern by TLR4 complexes. *Exp. Mol. Med.* **2013**, *45*, e66. [CrossRef] [PubMed]
34. Harada, K.; Ohira, S.; Isse, K.; Ozaki, S.; Zen, Y.; Sato, Y.; Nakanuma, Y. Lipopolysaccharide activates nuclear factor-kappaB through toll-like receptors and related molecules in cultured biliary epithelial cells. *Lab. Investig.* **2003**, *83*, 1657–1667. [CrossRef]
35. Rasheed, H.; McKinney, C.; Stamp, L.K.; Dalbeth, N.; Topless, R.K.; Day, R.; Kannangara, D.; Williams, K.; Smith, M.; Janssen, M.; et al. The Toll-Like Receptor 4 (TLR4) Variant rs2149356 and Risk of Gout in European and Polynesian Sample Sets. *PLoS ONE* **2016**, *11*, e0147939. [CrossRef]
36. Zhang, J.; Diao, B.; Lin, X.; Xu, J.; Tang, F. TLR2 and TLR4 mediate an activation of adipose tissue renin-angiotensin system induced by uric acid. *Biochimie* **2019**, *162*, 125–133. [CrossRef]

37. Arnold, I.C.; Mathisen, S.; Schulthess, J.; Danne, C.; Hegazy, A.N.; Powrie, F. CD11c(+) monocyte/macrophages promote chronic Helicobacter hepaticus-induced intestinal inflammation through the production of IL-23. *Mucosal Immunol.* **2016**, *9*, 352–363. [CrossRef]
38. Torres-Castro, I.; Arroyo-Camarena, U.D.; Martinez-Reyes, C.P.; Gomez-Arauz, A.Y.; Duenas-Andrade, Y.; Hernandez-Ruiz, J.; Bejar, Y.L.; Zaga-Clavellina, V.; Morales-Montor, J.; Terrazas, L.I.; et al. Human monocytes and macrophages undergo M1-type inflammatory polarization in response to high levels of glucose. *Immunol. Lett.* **2016**, *176*, 81–89. [CrossRef]
39. Nawaz, A.; Aminuddin, A.; Kado, T.; Takikawa, A.; Yamamoto, S.; Tsuneyama, K.; Igarashi, Y.; Ikutani, M.; Nishida, Y.; Nagai, Y.; et al. CD206(+) M2-like macrophages regulate systemic glucose metabolism by inhibiting proliferation of adipocyte progenitors. *Nat. Commun.* **2017**, *8*, 286. [CrossRef]
40. Kool, M.; Soullie, T.; van Nimwegen, M.; Willart, M.A.; Muskens, F.; Jung, S.; Hoogsteden, H.C.; Hammad, H.; Lambrecht, B.N. Alum adjuvant boosts adaptive immunity by inducing uric acid and activating inflammatory dendritic cells. *J. Exp. Med.* **2008**, *205*, 869–882. [CrossRef]
41. Jeong, J.H.; Jung, J.H.; Lee, J.S.; Oh, J.S.; Kim, Y.G.; Lee, C.K.; Yoo, B.; Hong, S. Prominent Inflammatory Features of Monocytes/Macrophages in Acute Calcium Pyrophosphate Crystal Arthritis: A Comparison with Acute Gouty Arthritis. *Immune Netw.* **2019**, *19*, e21. [CrossRef] [PubMed]
42. Bjorkander, S.; Heidari-Hamedani, G.; Bremme, K.; Gunnarsson, I.; Holmlund, U. Peripheral monocyte expression of the chemokine receptors CCR2, CCR5 and CXCR3 is altered at parturition in healthy women and in women with systemic lupus erythematosus. *Scand. J. Immunol.* **2013**, *77*, 200–212. [CrossRef]
43. Lee, M.; Lee, Y.; Song, J.; Lee, J.; Chang, S.Y. Tissue-specific Role of CX3CR1 Expressing Immune Cells and Their Relationships with Human Disease. *Immune Netw.* **2018**, *18*, e5. [CrossRef]
44. Pachot, A.; Cazalis, M.A.; Venet, F.; Turrel, F.; Faudot, C.; Voirin, N.; Diasparra, J.; Bourgoin, N.; Poitevin, F.; Mougin, B.; et al. Decreased expression of the fractalkine receptor CX3CR1 on circulating monocytes as new feature of sepsis-induced immunosuppression. *J. Immunol.* **2008**, *180*, 6421–6429. [CrossRef] [PubMed]
45. Zhou, Y.; Yang, Y.; Warr, G.; Bravo, R. LPS down-regulates the expression of chemokine receptor CCR2 in mice and abolishes macrophage infiltration in acute inflammation. *J. Leukoc. Biol.* **1999**, *65*, 265–269. [CrossRef] [PubMed]
46. Heesen, M.; Renckens, R.; de Vos, A.F.; Kunz, D.; van der Poll, T. Human endotoxemia induces down-regulation of monocyte CC chemokine receptor 2. *Clin. Vaccine. Immunol.* **2006**, *13*, 156–159. [CrossRef]
47. Salahudeen, M.S.; Nishtala, P.S. An overview of pharmacodynamic modelling, ligand-binding approach and its application in clinical practice. *Saudi. Pharm. J.* **2017**, *25*, 165–175. [CrossRef]
48. Auerbach, A. Dose-Response Analysis When There Is a Correlation between Affinity and Efficacy. *Mol. Pharmacol.* **2016**, *89*, 297–302. [CrossRef]
49. Jia, L.; Xing, J.; Ding, Y.; Shen, Y.; Shi, X.; Ren, W.; Wan, M.; Guo, J.; Zheng, S.; Liu, Y.; et al. Hyperuricemia causes pancreatic beta-cell death and dysfunction through NF-kappaB signaling pathway. *PLoS ONE* **2013**, *8*, e78284. [CrossRef]
50. Tan, P.K.; Ostertag, T.M.; Miner, J.N. Mechanism of high affinity inhibition of the human urate transporter URAT1. *Sci. Rep.* **2016**, *6*, 34995. [CrossRef]
51. Liu-Bryan, R.; Lioté, F. Monosodium urate and calcium pyrophosphate dihydrate (CPPD) crystals, inflammation, and cellular signaling. *Jt. Bone Spine* **2005**, *72*, 295–302. [CrossRef]

47. Nielsen, M.H.; Irvine, H.; Vedel, S.; Raungaard, B.; Beck-Nielsen, H.; Handberg, A. Elevated Atherosclerosis-Related Gene Expression, Monocyte Activation and Microparticle-Release Are Related to Increased Lipoprotein-Associated Oxidative Stress in Familial Hypercholesterolemia. *PLoS ONE* **2015**, *10*, e0121516. [CrossRef]
48. Geng, S.; Chen, K.; Yuan, R.; Peng, L.; Maitra, U.; Diao, N.; Chen, C.; Zhang, Y.; Hu, Y.; Qi, C.-F.; et al. The persistence of low-grade inflammatory monocytes contributes to aggravated atherosclerosis. *Nat. Commun.* **2016**, *7*, 13436. [CrossRef]
49. Poznyak, A.V.; Nikiforov, N.G.; Markin, A.M.; Kashirskikh, D.A.; Myasoedova, V.A.; Gerasimova, E.V.; Orekhov, A.N. Overview of OxLDL and Its Impact on Cardiovascular Health: Focus on Atherosclerosis. *Front. Pharmacol.* **2021**, *11*, 613780. [CrossRef]
50. Bowman, J.D.; Surani, S.; Horseman, M. Endotoxin, Toll-like Receptor-4, and Atherosclerotic Heart Disease. *Curr. Cardiol. Rev.* **2017**, *13*, 86–93. [CrossRef]
51. Grin, P.; Dwivedi, D.J.; Chathely, K.M.; Trigatti, B.; Dino, L.; Prat, A.; Seidah, N.; Liaw, P.C.; Fox-Robichaud, A.E. Low-density lipoprotein (LDL)-dependent uptake of Gram-positive lipoteichoic acid and Gram-negative lipopolysaccharide occurs through LDL receptor. *Sci. Rep.* **2018**, *8*, 10496. [CrossRef] [PubMed]
52. Vreugdenhil, A.C.; Snoek, A.P.; van 't Veer, C.; Greve, J.W.; Buurman, W.A. LPS-binding protein circulates in association with apoB-containing lipoproteins and enhances endotoxin-LDL/VLDL interaction. *J. Clin. Investig.* **2001**, *107*, 225–234. [CrossRef] [PubMed]

Hindawi
Journal of Diabetes Research
Volume 2018, Article ID 7209872, 11 pages
https://doi.org/10.1155/2018/7209872

Clinical Study

Serum Levels of Interleukin-13 Increase in Subjects with Insulin Resistance but Do Not Correlate with Markers of Low-Grade Systemic Inflammation

Camilo P. Martínez-Reyes,[1] Angélica Y. Gómez-Arauz,[1] Israel Torres-Castro,[1] Aarón N. Manjarrez-Reyna,[1] León F. Palomera,[1] Alfonso Olivos-García,[2] Edith Mendoza-Tenorio,[2] Gabriela A. Sánchez-Medina,[3] Sergio Islas-Andrade,[3] Guillermo Melendez-Mier,[3] and Galileo Escobedo[1]

[1]*Unit of Experimental Medicine, School of Medicine, National University of Mexico, General Hospital of Mexico "Dr. Eduardo Liceaga", 06726 Mexico City, Mexico*
[2]*Departamento de Medicina Experimental, Facultad de Medicina, Universidad Nacional Autónoma de México, 04510 México, DF, Mexico*
[3]*Research Division, General Hospital of Mexico "Dr. Eduardo Liceaga", 06726 Mexico City, Mexico*

Correspondence should be addressed to Galileo Escobedo; gescobedog@msn.com

Received 1 September 2017; Revised 7 December 2017; Accepted 18 December 2017; Published 21 February 2018

Academic Editor: Bernard Portha

Experimental evidence in mice suggests a role for interleukin- (IL-) 13 in insulin resistance and low-grade systemic inflammation. However, IL-13 serum levels have not been assessed in subjects with insulin resistance, and associations of IL-13 with parameters of low-grade systemic inflammation are still unknown. Our main goal was to examine the systemic levels of IL-13 in patients with insulin resistance, while also studying the relationship of IL-13 with anthropometric, metabolic, and low-grade systemic inflammatory markers. Ninety-two participants were included in the study and divided into insulin-resistant patients and noninsulin-resistant controls. Blood levels of IL-13, glucose, insulin, triglycerides, cholesterol, tumor necrosis factor-alpha (TNF-α), IL-10, proinflammatory (Mon-CD11c$^+$CD206$^-$), and anti-inflammatory (Mon-CD11c$^-$CD206$^+$) monocytes, as well as anthropometric parameters, were measured in all volunteers. Insulin-resistant patients showed 2.5-fold higher serum levels of IL-13 than controls ($P < 0.0001$) and significantly increased values of TNF-α and Mon-CD11c$^+$CD206$^-$, with concomitant reductions in IL-10 and Mon-CD11c$^-$CD206$^+$. Increased IL-13 was extraordinarily well associated with hyperglycemia ($r = 0.7362$) and hypertriglyceridemia ($r = 0.7632$) but unexpectedly exhibited no significant correlations with TNF-α ($r = 0.2907$), IL-10 ($r = -0.3882$), Mon-CD11c$^+$CD206$^-$ ($r = 0.2745$) or Mon-CD11c$^-$CD206$^+$ ($r = -0.3237$). This study demonstrates that IL-13 serum levels are elevated in patients with insulin resistance without showing correlation with parameters of low-grade systemic inflammation.

1. Introduction

Insulin resistance is a key pathophysiological event in the development of type 2 diabetes (T2D), a serious public health problem of global proportions, with alarmingly high morbidity and mortality rates in several countries including USA and Mexico [1, 2]. A growing body of clinical and experimental evidence has consistently shown that insulin resistance is linked to obesity and low-grade systemic inflammation [3, 4]. Specifically, increased body mass index (BMI) and visceral fat accumulation have been shown to augment the risk to develop dyslipidemia, hyperglycemia, and insulin resistance [5]. Low-grade systemic inflammation is characterized by abnormally high serum levels of proinflammatory cytokines (i.e., tumor necrosis factor alpha [TNF-α]) and increased percentage of proinflammatory monocytes such

as monocytes that exhibit high expression of CD11c and no expression of CD206 (Mon-CD11c$^+$CD206$^-$) [6, 7]. Low-grade systemic inflammation is also associated with decreased serum concentrations of anti-inflammatory cytokines such as interleukin- (IL-) 10 and low percentages of monocytes exerting anti-inflammatory abilities as is the case of monocytes that show high expression of CD206 and no expression of CD11c (Mon-CD11c$^-$CD206$^+$) [7, 8]. High amounts of TNF-α have been reported to concur with increased adiposity [9], hypertriglyceridemia [8], and impaired insulin sensitivity in adipose and hepatic tissue [10]. Moreover, Saghizadeh and coworkers have previously demonstrated that TNF-α is actively expressed in skeletal muscle tissue of insulin-resistant patients as compared to subjects with normal insulin sensitivity [11]. In the same sense, TNF-α infusion in healthy individuals is able to induce muscle insulin resistance by increasing phosphorylation of p70 S6 kinase, extracellular signal-regulated kinase −1/2 (ERK-1/2), and c-Jun NH2 terminal kinase (JNK) [12]. Interestingly, phosphorylation of p70 S6 kinase, ERK-1/2, and JNK is associated with decreased activation of the insulin receptor substrate-1 (IRS-1) and Akt substrate 160 [12], which supports the notion that TNF-α is a major contributor of insulin resistance in skeletal muscle. On the other side, decreased IL-10 has been related to elevated serum concentrations of TNF-α, increased proportion of Mon-CD11c$^+$CD206$^-$ over the Mon-CD11c$^-$CD206$^+$ subpopulation, hyperglycemia, and higher levels of insulin resistance in obese subjects [7, 13]. Therefore, low-grade systemic inflammation has now gained increasing attention since it appears to play a causative role in the development of insulin resistance in liver, adipose tissue, and skeletal muscle of obese patients [14].

IL-13 is a cytokine belonging to the alpha-helix protein family that is mainly produced by activated Th2 cells, mast cells, and basophils and has been widely studied in the scenario of helminth parasite infections and allergic asthma [15, 16]. Nevertheless, recent experimental evidence in mice has now found that IL-13 may also participate in low-grade systemic inflammation and insulin resistance [17, 18]. In this sense, it has been reported that exogenous administration of IL-13 improves insulin sensitivity while also decreasing TNF-α expression and macrophage infiltration in epididymal adipose tissue of C57BL/6J mice fed a high-fat diet (HFD) [17]. Likewise, a further study demonstrated that IL-13 gene transfer plays a protective role during experimental obesity by diminishing adipocyte hypertrophy, glucose intolerance, insulin resistance, and macrophage infiltration into adipose tissue of HFD-fed C57BL/6J mice [18]. Interestingly, IL-13 has been also associated with improved insulin secretion. In this sense, Darkhal and colleagues previously showed that IL-13 gene overexpression concurs with increased insulin serum levels in mice [18]. Additionally, a recent study demonstrated that IL-13 *in vitro* increases insulin secretion in beta-cells of humans and rats [19], supporting the fact that IL-13 also has an impact on insulin production and release. In parallel, IL-13 has been also shown to play a role in the development of insulin resistance in human beings. In this regard, a previous study demonstrated that IL-13 serum levels are reduced in T2D patients that exhibit increased insulin resistance [20]. However, the role of IL-13 in the pathogenesis of insulin resistance in humans is still unclear, and potential associations of this cytokine with parameters of low-grade systemic inflammation and metabolic dysfunction remain obscure.

The main goal of this work was to examine the systemic levels of IL-13 in patients with insulin resistance, while also studying the relationship of IL-13 with parameters of low-grade systemic inflammation such as TNF-α, IL-10, Mon-CD11c$^+$CD206$^-$ percentage, and Mon-CD11c$^-$CD206$^+$ percentage, and other insulin resistance-related metabolic markers including fasting blood glucose and insulin, BMI, central obesity, body fat percentage, waist-to-hip ratio, triglycerides, and cholesterol.

2. Materials and Methods

2.1. Subjects. Ninety-two Mexican adult women and men from the south-central region of Mexico were included in the study. All of the volunteers provided written informed consent, previously approved by the institutional review board of the General Hospital of Mexico, which guaranteed that the study was conducted in accordance with the principles described at the Helsinki Declaration. Volunteers were excluded from the study if they had previous or recent diagnosis of *Diabetes Mellitus*, cardiovascular diseases, chronic renal disease, chronic or acute hepatic disease, blood pressure higher than 135/85 mm Hg, inflammatory or autoimmune disorders, acute or chronic infectious diseases, cancer, and endocrine disorders including hypothyroidism. We also excluded pregnant or lactating women, patients with cardiovascular drug therapy including anti-inflammatory, antiaggregant, and antihypertensive drugs, and subjects without having an overnight fasting of 8–10 hours. All participants enrolled into the study received full medical evaluation, including achievement of clinical history and physical examination by expert physicians.

2.2. Insulin Resistance Assessment. The insulin resistance level was estimated by means of calculating the homeostatic model assessment of insulin resistance (HOMA-IR) in each participant. The HOMA-IR value resulted from multiplying fasting insulin concentration (mU/l) by fasting glucose concentration (mmol/l) and then divided by 22.5. Cut-off points for insulin resistance were given according to previous studies validated in the Mexican population [21], as follows: subjects showing HOMA-IR < 3.8 were considered as the control group by having a normal level of insulin resistance. On the contrary, subjects showing HOMA-IR ≥ 3.8 were considered as the insulin-resistant group by having a significant level of insulin resistance.

2.3. Anthropometric Measurements. BMI resulted from dividing corporal weight (kg) by height squared (m^2) and was recorded in all participants, as follows: BMI 18.5–24.9 kg/m^2, normal weight subjects; BMI 25–29.9 kg/m^2, overweight subjects; and BMI ≥ 30 kg/m^2, obese subjects. Central obesity was estimated in each participant by measuring the midpoint

between the lower rib margin and iliac crest with a conventional tape in centimeters (cm). Cut-off point values for central obesity were given as follows: women showing 80 cm waist circumference or higher were considered to have central obesity, while men showing 90 cm waist circumference or higher were considered to have central obesity. Body fat percentage was individually estimated by means of using a body composition analyzer (TANITA®, Body Composition Analyzer, Model TBF-300A, Tokyo, Japan).

2.4. Metabolic Measurements. Blood samples were collected after overnight fasting and placed into pyrogen-free tubes (Vacutainer™, BD Diagnostics, NJ, USA) at room temperature. Afterwards, collection tubes were centrifuged at 1000g/4°C for 25 min and serum samples obtained and stored at −80°C until use. Serum levels of insulin were individually measured in triplicate by means of the Enzyme-Linked ImmunoSorbent Assay (ELISA), following the manufacturer's instructions (Abnova Corporation, Taiwan). Serum levels of glucose were individually measured in triplicate by the glucose oxidase assay, following the manufacturer's instructions (Megazyme International, Ireland). Total cholesterol and triglyceride levels were individually measured in triplicate by enzymatic assays according to the manufacturer's instructions (Roche Diagnostics, Mannheim, Germany). All biochemical parameters were measured at the same time to avoid procedural variations.

2.5. Assessment of the Serum Levels of IL-13, TNF-α, and IL-10 by ELISA. Blood samples were collected after overnight fasting and placed into pyrogen-free tubes (Vacutainer, BD Diagnostics, NJ, USA) at room temperature. Afterwards, collection tubes were centrifuged at 1000g/4°C for 25 min and serum samples obtained and stored at −80°C until use. Serum levels of IL-13, TNF-α, and IL-10 were determined in triplicate by ELISA, following the manufacturer's instructions (Peprotech, Mexico). All cytokines were measured at the same time to avoid procedural variations.

2.6. Characterization of Monocyte Surface Markers by Flow Cytometry. Blood samples were collected after overnight fasting and placed into pyrogen-free tubes containing EDTA (Vacutainer, BD Diagnostics, NJ, USA). Afterwards, collection tubes were centrifuged at 1800g/8°C for 10 min and white blood cells (WBCs) separated using a micropipette. WBCs were separately placed into 1.6 ml pyrogen-free eppendorf tubes containing 1 ml of ACK Lysing Buffer (Life Technologies, USA) and incubated at 4°C for 5 min. Immediately after, cell suspensions were centrifuged at 1800g/8°C for 5 minutes and resulting cell pellets washed twice using PBS 1X (Sigma-Aldrich, Mexico). After an extra centrifugation step, supernatants were discarded and resulting cell pellets resuspended in 50 μl of PBS 1X (Sigma-Aldrich, Mexico) for posterior cell counting using trypan blue staining with Neubauer chamber. In each case, 3 μl of Human TruStrain Reagent (BioLegend Inc., USA) was added to 1×10^6 WBCs and then incubated for 7 minutes on ice. Afterwards, each WBC sample was simultaneously incubated with human anti-CD14 PE/Cy7, anti-CD11c PE/Cy5, and anti-CD206/Cy7 APC at 8°C for 20 min in the absence of light. Analysis of the cell surface markers CD11c and CD206 was exclusively performed on CD14-positive cells that correspond to monocytes, using a FACSCanto II flow cytometer (BD Biosciences, Mexico) by means of BD FACSDiva™ software 6.0, acquiring 50,000 events per test in triplicate. PE/Cy7 mouse IgG2, APC/Cy7 mouse IgG1, and PE/Cy5 mouse IgG1 (BioLegend Inc., USA) were used as isotype control antibodies.

2.7. Statistical Analysis. Student's t-test was used to compare noninsulin-resistant (NIR) and insulin-resistant (IR) subjects in terms of age, HOMA-IR, BMI, waist circumference, body fat percentage, waist-to-hip ratio, fasting blood glucose, serum insulin, systolic blood pressure, total cholesterol, triglycerides, TNF-α, IL-10, Mon-CD11c$^+$CD206$^-$ percentage, and Mon-CD11c$^-$CD206$^+$ percentage. Student's t-test results are expressed as mean ± standard deviation. Pearson's correlation coefficient was calculated for examining the association of IL-13 with anthropometric, metabolic, and systemic inflammation parameters. Pearson's correlation coefficient results are expressed as coefficients (r) and P values. Differences were considered significant when $P < 0.05$. All statistical analyses were performed using the GraphPad Prism 6.01 software.

3. Results

Ninety-two participants of both sexes were included in the study (47 noninsulin-resistant and 45 insulin-resistant subjects). No significant differences were found in age (for noninsulin-resistant controls mean age 31.02 ± 10.41 years, whereas for insulin-resistant subjects mean age 36.75 ± 11.18 years), woman/man proportion (23 women and 24 men in the noninsulin-resistant group, whereas 22 women and 23 men in the insulin-resistant group), and systolic blood pressure (SBP) (for noninsulin-resistant controls mean systolic pressure 128.40 ± 3.57 mmHg, whereas for insulin-resistant subjects mean systolic pressure 127.9 ± 4.28 mmHg) (Table 1). On the other hand, BMI, waist circumference, and body fat percentage exhibited a significant increase in insulin-resistant subjects as compared to noninsulin-resistant controls (Table 1). Similarly, fasting blood glucose, serum insulin, and HOMA-IR were also higher in the insulin-resistant group than in the noninsulin-resistant group (Table 1). When dyslipidemia was evaluated, triglyceride values showed a clear elevation in insulin-resistant subjects with respect to noninsulin-resistant controls; however, cholesterol levels did not significantly differ between groups (Table 1). In terms of systemic inflammatory parameters, serum levels of TNF-α were significantly increased in the insulin-resistant group as compared to noninsulin-resistant individuals, whereas IL-10 was clearly reduced in insulin-resistant subjects with respect to controls (Table 1). At the same time, insulin-resistant subjects showed a significant increase in the proinflammatory monocyte percentage (Mon-CD11c$^+$CD206$^-$) accompanied by decreasing numbers of monocytes with anti-inflammatory profile (Mon-CD11c$^-$CD206$^+$) as compared to controls. Figure 1 shows representative flow cytometry dot plots illustrating the

Table 1: Demographic, anthropometric, metabolic, and immunological characteristics of the study subjects.

Parameters	NIR	IR	P
Gender (W/M)	23/24	22/23	n.s.
Age (years)	31.02 ± 10.41	36.75 ± 11.18	n.s.
BMI (kg/m^2)	26.82 ± 4.89	32.92 ± 2.34	<0.001
Waist circumference (cm)	86.87 ± 13.00	105.00 ± 6.21	<0.001
Body fat (%)	26.61 ± 8.15	36.99 ± 7.42	<0.001
Waist-to-hip ratio	0.92 ± 0.12	0.97 ± 0.04	n.s.
SBP (mmHg)	128.4 ± 3.57	127.9 ± 4.28	n.s.
Blood glucose (mg/dl)	84.17 ± 9.79	104.9 ± 5.58	<0.0001
Serum insulin (mU/l)	11.16 ± 2.38	21.56 ± 1.89	<0.0001
HOMA-IR	2.28 ± 0.39	5.59 ± 0.64	<0.0001
Total cholesterol (mg/dl)	193.7 ± 10.28	198.0 ± 10.18	n.s.
Triglycerides (mg/dl)	159.40 ± 37.93	256.6 ± 13.19	<0.0001
TNF-α (pg/ml)	8.26 ± 3.45	30.29 ± 3.93	<0.0001
IL-10 (pg/ml)	100.8 ± 26.41	37.04 ± 10.36	<0.0001
Mon-CD11c$^+$CD206$^-$ (%)	28.30 ± 17.18	60.93 ± 20.68	<0.001
Mon-CD11c$^-$CD206$^+$ (%)	24.23 ± 9.46	6.05 ± 5.71	<0.0001

Data are expressed as mean ± standard deviation. Significant differences were estimated by means of performing two-way Student's t-test. Differences were considered significant when $P < 0.05$. W: women; M: men; BMI: body mass index; SBP: systolic blood pressure; HOMA-IR: homeostatic model assessment of insulin resistance; TNF-α: tumor necrosis factor alpha; IL: interleukin; Mon CD11c$^+$CD206$^-$: proinflammatory monocytes; Mon CD11c$^-$CD206$^+$: anti-inflammatory monocytes; n.s.: nonsignificant differences.

amount of Mon-CD11c$^+$CD206$^-$ in (A) noninsulin-resistant controls and (B) patients with insulin resistance, as well as the amount of Mon-CD11c$^-$CD206$^+$ in (C) noninsulin-resistant controls and (D) patients with insulin resistance.

When IL-13 was examined, we found a significant 2.5-fold increase in the serum levels of IL-13 in insulin-resistant subjects as compared to noninsulin-resistant controls (37.69 ± 17.82 versus 15.88 ± 6.71 pg/ml, resp.) (Figure 2).

IL-13 was significantly elevated in the insulin-resistant group. Therefore, our next step was to identify anthropometric, metabolic, and inflammatory parameters that were clearly related to the elevation in the serum concentrations of this cytokine. IL-13 exhibited a strong positive correlation with BMI ($r = 0.6727$, $P < 0.0001$) and waist circumference ($r = 0.6394$, $P < 0.0001$) (Figures 3(a) and 3(b), resp.). Moreover, serum levels of IL-13 were moderately associated with body fat percentage ($r = 0.4310$, $P < 0.001$) and waist-to-hip ratio ($r = 0.2410$, $P = 0.026$) (Figures 3(c) and 3(d), resp.).

In the specific case of metabolic parameters, serum IL-13 showed a strong positive relationship with fasting blood glucose ($r = 0.7362$, $P < 0.0001$) and HOMA-IR ($r = 0.6673$, $P < 0.0001$) (Figures 4(a) and 4(c), resp.). Despite being significant, statistical correlation between IL-13 and serum insulin was positive but tended to be moderate ($r = 0.5468$, $P < 0.0001$) (Figure 4(b)). Furthermore, IL-13 was strongly related to the amount of triglycerides ($r = 0.7632$, $P < 0.0001$) but showed no significant correlation with total cholesterol ($r = 0.2104$, $P = 0.055$) (Figures 5(a) and 5(b), resp.).

In terms of systemic inflammatory markers, circulating levels of IL-13 exhibited no significant correlations with serum TNF-α ($r = 0.2907$, $P = 0.066$) or Mon-CD11c$^+$CD206$^-$ monocyte percentage ($r = 0.2745$, $P = 0.062$), both of them typical proinflammatory parameters (Figures 6(a) and 6(b), resp.). On the contrary, IL-13 was barely correlated with IL-10 serum levels ($r = -0.3882$, $P = 0.0471$) but showed no significant association with Mon-CD11c$^-$CD206$^+$ monocyte percentage ($r = -0.3237$, $P = 0.0544$), which have been shown to exert anti-inflammatory actions (Figures 6(c) and 6(d), resp.).

4. Discussion

IL-13 is a cytokine that belongs to the alpha-helix protein family and is mainly produced by Th2-activated T lymphocytes, mast cells, and basophils [22]. Besides having been shown to play a critical role in helminth parasite infections and allergic asthma [13, 14], IL-13 has been now suggested to exert additional functions in the development of metabolic alterations such as insulin resistance and hyperglycemia [17, 18]. However, clinical findings in humans regarding the role of IL-13 in metabolic disease are still controversial.

In this sense, it has been previously shown that serum levels of IL-13 are significantly reduced in type 2 diabetic patients with coronary artery disease as compared to healthy controls [23]. Similarly, a recent study demonstrated that type 2 diabetic patients show decreased serum levels of IL-13 with respect to normal-glucose tolerant individuals [20]. On the contrary, it has been also reported that morbidly obese patients with insulin resistance exhibit higher values of serum IL-13 than normal weight controls, and bariatric surgery was able to reduce IL-13 serum concentrations after 1-year of the surgical procedure [24]. Likewise, expression of interleukin-13 receptor subunit alpha-2 (IL-13RA2) has been demonstrated to increase in peripheral blood mononuclear cells (PBMC) of obese children with abnormal insulin sensitivity as compared to normal weight boys [25]. This apparent contradiction could be attributed to the possible role of IL-13 in the insulin resistance pathogenesis that involves the liver, adipose tissue, skeletal muscle, and pancreatic beta-cells. In this regard, a previous study in mice showed that IL-13 gene deficiency concurs with reduced phosphorylation of IRS-1 and AKT in liver, adipose tissue, and skeletal muscle, which was directly related to decreased insulin sensitivity in the aforementioned tissues [26]. Interestingly, IRS-1 and AKT phosphorylation was found to depend on the activation of the signal transducer and activator of transcription (STAT) 3 and STAT6 [26], a well-known family of transcription factors with the ability to elicit anti-inflammatory signaling pathways in response to IL-13. Also, IL-13 has been shown to promote insulin secretion in pancreatic beta-cells [19], which is associated with compensatory hyperinsulinemia aimed to counteract hyperglycemia and insulin resistance. Then, it is reasonable to speculate that IL-13 plays a protective role in insulin resistance by promoting IRS-1 and AKT phosphorylation in insulin-dependent tissues via STAT3 and STAT6 activation as well as improvement of the beta-cell function. However, together with other

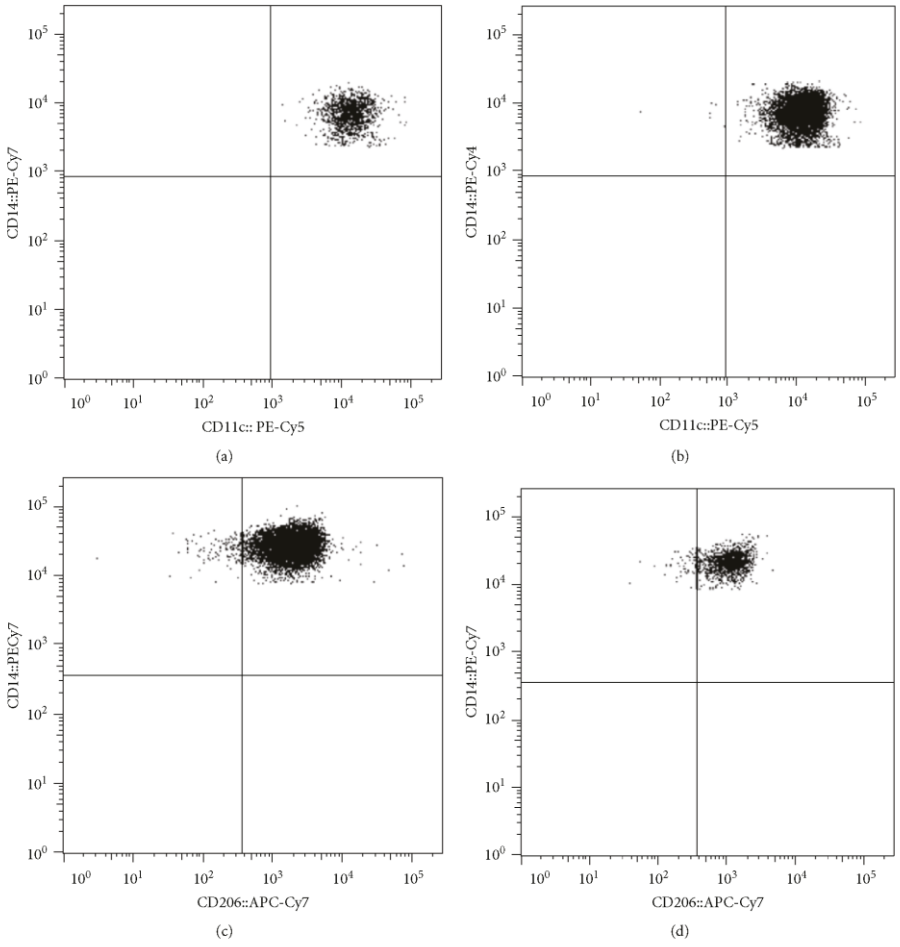

FIGURE 1: Representative dot plots showing percentages of proinflammatory and anti-inflammatory monocytes in patients with insulin resistance and noninsulin-resistant controls. (a) and (b) illustrate representative flow cytometry dot plots showing percentages of proinflammatory monocytes that express CD11c but do not express CD206 (Mon-CD11c$^+$CD206$^-$) in controls and insulin-resistant patients, respectively. (c) and (d) illustrate representative dot plots showing percentages of anti-inflammatory monocytes that express CD206 but do not express CD11c (Mon-CD11c$^-$CD206$^+$) in controls and insulin-resistant patients, respectively. Dot plot quantification can be seen in Table 1.

studies [17, 24, 25], our work shows a significant increase in the serum levels of IL-13 in insulin-resistant patients, which appears to disagree with previous evidence. In this sense, a previous work showed that IL-13 serum levels significantly increase as the severity of T2D-related chronic heart failure also increases [27]. Similarly, a very recent study demonstrated that IL-13 gene expression tended to increase in the left ventricular free wall of T2D patients with heart failure as compared to healthy donors [28]. Interestingly, despite IL-13 gene tended to be upregulated, the IL-13 receptor subunit alpha 1 (IL-13Rα1) production was significantly decreased in the same cardiac muscle specimens of T2D patients with heart failure, who are by definition insulin-resistant [28]. In some extent, this information is consistent with our findings and suggests a progressive loss of the cellular capacity to respond to IL-13 in the scenario of insulin resistance. Such a state of "IL-13 action resistance" may partially explain the increment of the IL-13 serum levels in

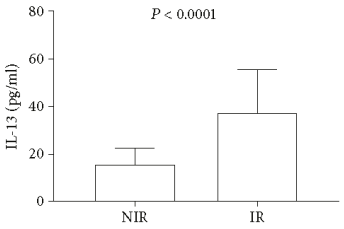

FIGURE 2: Serum levels of IL-13 in patients with insulin resistance and controls. Systemic levels of IL-13 showed a 2.5-fold significant increase in patients with insulin resistance as compared to noninsulin resistance controls. NIR: noninsulin resistance controls; IR: patients with insulin resistance. A 3.8 cut-off point was used for defining insulin resistance in the study population. Data are expressed as mean ± standard deviation. Differences were considered significant when $P < 0.05$ and calculated using Student's t-test.

several cohorts of patients with insulin resistance, including our own study population. To the best of our knowledge, this is one of the first studies suggesting a state of IL-13 action resistance, characterized by high levels of IL-13, reduced activation of the IL-13-dependent signaling pathway in insulin-dependent tissue, and consequently increased insulin resistance. Nevertheless, we have drawn a speculative hypothesis to explain the apparently contradictory results regarding the role of IL-13 in the development of insulin resistance, and the discussion of this information makes no attempt to conjecture beyond that. For this reason, it is still of enormous importance to study the role of IL-13 in the pathogenesis of insulin resistance, also evaluating the possible existence of a state of IL-13 action resistance in patients with altered insulin sensitivity.

In our study, serum concentrations of IL-13 exhibited a strong correlation with obesity-related anthropometrical parameters including BMI and central obesity. As it has been previously reported, increased BMI and central obesity are key contributing factors to the development of insulin resistance, metabolic syndrome, and type 2 diabetes [29]. Central obesity directly results from the expansion of white adipose cells that accumulate around the viscera of the abdominal cavity [30]. Interestingly, it has been recently shown that increased central obesity and body weight are associated with elevation in the circulating levels of IL-13 [31]. Furthermore, Kwon and coworkers demonstrated that IL-13 is overproduced in the white adipose tissue of HFD-fed mice and obese humans while also reported that adipocytes were the main cellular source of this cytokine [17]. These findings may explain the extremely strong association observed in our study between serum IL-13 levels and obesity-related anthropometrical parameters such as central obesity and, in some extent, BMI. In other words, our data confirm a direct link between fat mass expansion and IL-13 overproduction, which could be supported by the fact that hypertrophic and hyperplasic adipocytes increase their ability to synthesize IL-13. However, we only studied the relationship of obesity-related anthropometrical parameters with IL-13 serum concentrations by means of statistical correlation models and the discussion of these results makes no attempt to conjecture beyond that. Further research is needed to draw conclusions regarding the capacity of white adipose cells to release IL-13 into the bloodstream and the potential role of this cytokine in the development of insulin resistance in obese patients.

Another phenomenon captured in our study is that IL-13 serum levels appear to be extraordinarily correlated with elevated blood values of glucose in the study population, and especially in subjects with insulin resistance. Consistent with our results, Nehete and coworkers previously demonstrated that obese chimpanzees show increased serum levels of IL-13, glucose, and glucagon, a peptide hormone in charge of raising glucose concentration in the bloodstream [32]. This finding suggests a direct link among IL-13, glucagon, and elevated glucose levels. In this sense, glucagon-like peptide-1 (GLP-1) is a peptide hormone able to reduce glucose levels by restricting the secretion of glucagon [33]. Recently, GLP-1 has been also shown to decrease IL-13 production in LPS-treated human eosinophils [34], which supports the idea that increased serum IL-13 could be directly associated with elevated blood glucose levels via glucagon-dependent mechanisms. Nevertheless, it is important to note that IL-13 has been also demonstrated to downregulate the hepatic production of glucose in mice [26] and increase glucose uptake in skeletal muscle cells *in vitro* [20], which seems to disagree with our results. We want to speculate that such a discrepancy could be explained by the fact that protective effects of IL-13 depend on reaching a critical concentration, in which high IL-13 levels are able to counteract the elevation of blood glucose and insulin resistance. In this hypothetical scenario, it is expected to find a positive correlation between IL-13 and insulin, a hormone widely known to counteract the effects of glucagon and decrease glucose levels. Interestingly, our results show a positive correlation between increased IL-13 and elevated values of serum insulin. Consistent with this hypothesis, it has been recently demonstrated that IL-13 promotes beta-cell survival and insulin secretion in human pancreatic beta-cell *in vitro* cultures [19]. However, it is still of great importance to examine the possible effect of IL-13 in regulating glucagon, GLP-1, insulin, and blood glucose levels with the aim of merging apparently controversial data regarding the role of this cytokine in glucose metabolism.

Numerous studies have suggested a direct relationship between IL-13 and lipid metabolism, especially in the scenario of metabolic dysfunction. For instance, a recent work demonstrated that PBMC show increased IL-13 expression in type 2 diabetic nephropathy patients that also exhibit hypertriglyceridemia [35]. Similarly, overweight and obese pregnant women with gestational hypertension show increased IL-13 concentration, which in turn is associated with elevated triglyceride levels [36]. Moreover, metabolic syndrome subjects exhibit increased serum IL-13 that is also correlated with rising concentration of blood sugar and triglycerides [37]. Our data expand on this body of work by revealing that circulating levels of IL-13 are strongly correlated with triglyceride values in insulin-resistant individuals.

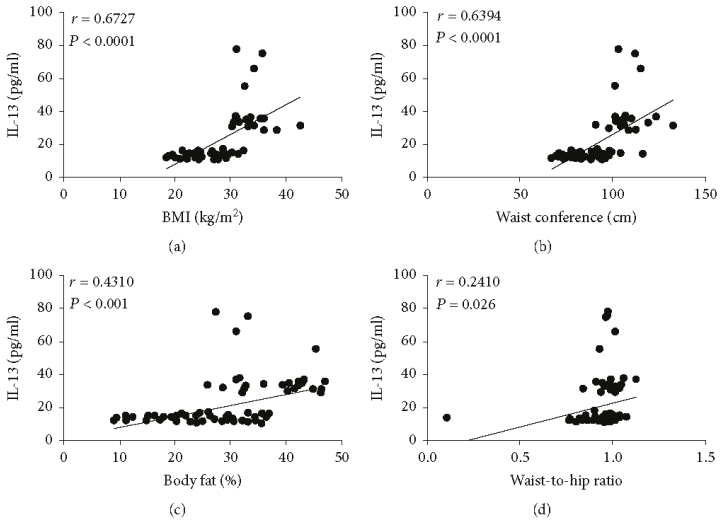

Figure 3: Correlation analysis between IL-13 serum levels and anthropometric parameters in the study population. (a) Correlation analysis between IL-13 serum levels and BMI. (b) Correlation analysis between IL-13 serum levels and waist circumference. (c) Correlation analysis between IL-13 serum levels and body fat percentage. (d) Correlation analysis between IL-13 serum levels and waist-to-hip ratio. Serum levels of IL-13 were moderately associated with BMI and waist circumference and showed to be barely related to body fat percentage and waist-to-hip ratio. BMI: body mass index. Coefficients (r) and P values were calculated by Pearson's correlation model. The correlation level was considered significant when $P < 0.05$.

Interestingly, Tsao and coworkers previously demonstrated that IL-4, another Th2 cytokine with a similar structure and function to IL-13, is able to induce lipolysis in 3T3L1 adipocytes, thus increasing glycerol release and secretion into the culture supernatant [38]. This work concurs with our findings and reveals a novel function of Th2 cytokines in the regulation of triglyceride metabolism; however, there is no evidence yet exploring whether IL-13 may have a similar effect to IL-4. Further research is needed to evaluate the possible role of IL-13 in lipid metabolism and identify novel molecular targets with the aim of reducing triglyceride levels and cardiovascular risk in patients with insulin resistance.

Besides examining its association with insulin resistance-related metabolic markers, IL-13 was also studied in terms of low-grade systemic inflammation. As described above, low-grade systemic inflammation is hallmarked by increased levels of proinflammatory cells and cytokines whereby immune cells and cytokines with anti-inflammatory actions are decreased [39]. Consistent with this notion, we saw a clear elevation in the circulating levels of TNF-α and proinflammatory monocytes Mon-CD11c$^+$CD206$^-$ in insulin-resistant patients with respect to noninsulin-resistant controls. Simultaneously, circulating levels of IL-10 and anti-inflammatory monocytes Mon-CD11c$^-$CD206$^+$ were also significantly diminished in patients with insulin resistance. However, this state of low-grade systemic inflammation did not relate to serum IL-13, although several reports suggest an association of IL-13 with proinflammatory and anti-inflammatory immune responses [17, 18, 40, 41]. In this sense, it has been previously reported that IL-13 does not always correlate with low-grade systemic inflammation parameters. In fact, a recent study conducted in morbidly obese men with metabolic syndrome showed a significant increase in the serum levels of IL-6 and IL-12, both cytokines with proinflammatory actions, without reporting any difference in IL-13 [42]. Similarly, TNF-α soluble receptor levels were shown to raise in plasma of burn-induced systemic inflammatory response syndrome children whereas IL-13 serum levels remained unchanged [43]. Furthermore, Matia-García and coworkers recently reported that young obese subjects with hypertriglyceridemia exhibit low-grade systemic inflammation characterized by increasing levels of C-reactive protein (CRP) and IL-6, accompanied by reduced IL-10 serum concentration [44]. Interestingly, IL-13 showed neither statistical changes between obese and normal weight subjects nor significant correlation coefficients with CRP, IL-6, and IL-10 [44]. Therefore, our results reveal that serum levels of IL-13 elevate in insulin resistance without showing correlation with markers of low-grade systemic inflammation in humans.

Finally, it is important to note that serum IL-13 levels appear to be grouped in two main clusters, characterized by high and low production of this cytokine. Notably, ninety-five percent of low-IL-13 producers showed a HOMA-IR value below 3, whereas an inverse tendency was seen in high-IL-13 producers that exhibited increasing levels of

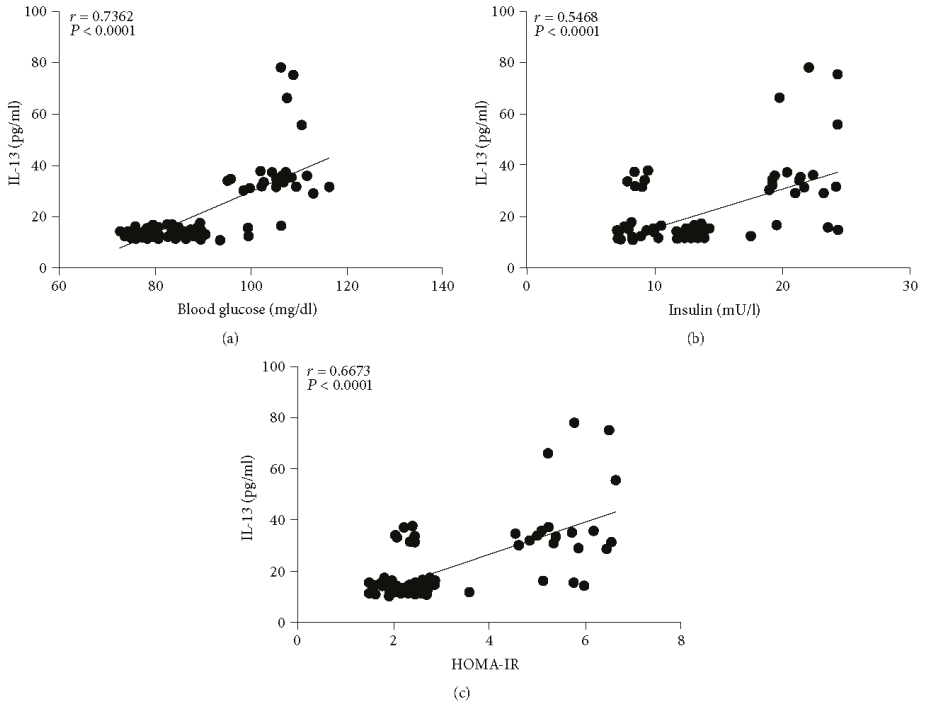

Figure 4: Correlation analysis between IL-13 serum levels and parameters of glucose metabolism in the study population. (a) Correlation analysis between IL-13 serum levels and blood glucose. (b) Correlation analysis between IL-13 serum levels and insulin. (c) Correlation analysis between IL-13 serum levels and HOMA-IR value. Serum levels of IL-13 were strongly associated with blood glucose and showed to be moderately related to insulin and HOMA-IR value. HOMA-IR, homeostatic model assessment of insulin resistance. Coefficients (r) and P values were calculated by Pearson's correlation model. The correlation level was considered significant when $P < 0.05$.

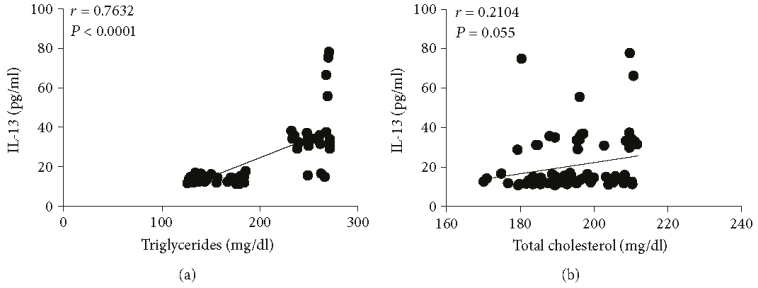

Figure 5: Correlation analysis between IL-13 serum levels and parameters of lipid metabolism in the study population. (a) Correlation analysis between IL-13 serum levels and triglycerides. (b) Correlation analysis between IL-13 serum levels and total cholesterol. Serum levels of IL-13 were strongly associated with blood triglycerides but showed no significant correlation with cholesterol. Coefficients (r) and P values were calculated by Pearson's correlation model. The correlation level was considered significant when $P < 0.05$.

insulin resistance (HOMA-IR > 4.5). Moreover, ninety percent of high-IL-13 producers had central obesity and hyperglycemia, while a similar amount also showed triglyceride levels higher than 200 mg/dl (data not shown), which suggests that increased IL-13 could concur with the development of metabolic syndrome. However, we did not categorize the

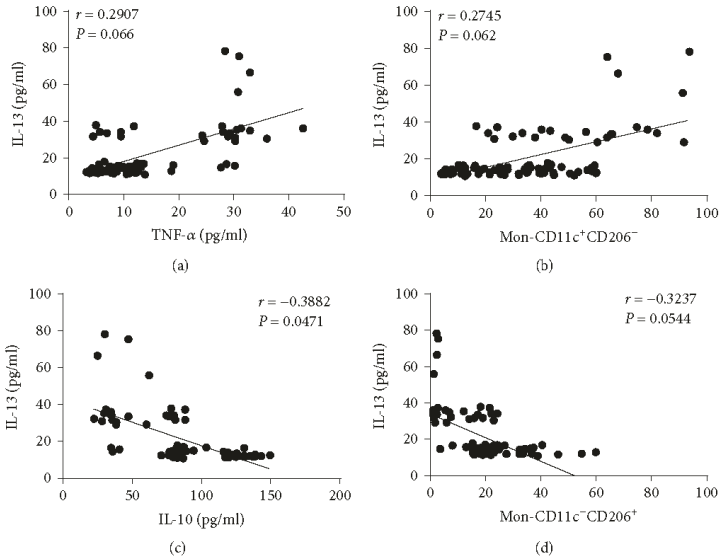

Figure 6: Correlation analysis between IL-13 serum levels and parameters of low-grade systemic inflammation in the study population. (a) Correlation analysis between IL-13 serum levels and circulating concentration of TNF-α. (b) Correlation analysis between IL-13 serum levels and the percentage of proinflammatory monocytes Mon-CD11c$^+$CD206$^-$. (c) Correlation analysis between IL-13 serum levels and circulating concentration of IL-10. (d) Correlation analysis between IL-13 serum levels and the percentage of anti-inflammatory monocytes Mon-CD11c$^-$CD206$^+$. Serum levels of IL-13 were barely associated with IL-10 but showed no significant correlations with TNF-α, Mon-CD11c$^+$CD206$^-$, and Mon-CD11c$^-$CD206$^+$. Mon-CD11c$^+$CD206$^-$, proinflammatory monocytes that express CD11c but do not express CD206; Mon-CD11c$^-$CD206$^+$, anti-inflammatory monocytes that express CD206 but do not express CD11c. Coefficients (r) and P values were calculated by Pearson's correlation model. The correlation level was considered significant when $P < 0.05$.

study subjects according to the number of metabolic syndrome risk factors and the discussion of these results makes no attempt to conjecture beyond that. Further clinical research is needed to understand whether low and high-IL-13 producers have different risks for developing metabolic syndrome and its cardiovascular comorbidities.

5. Conclusions

This study demonstrates that serum levels of IL-13 are significantly elevated in insulin-resistant patients without showing correlation with parameters of low-grade systemic inflammation such as TNF-α, IL-10, and monocytes that show expression of CD11c and CD206. Hyperglycemia and hypertriglyceridemia appear to be strongly linked to the increase in IL-13, which suggest a novel role of this cytokine in the regulation of glucagon-dependent pathways and lipolysis that should be addressed in patients at higher cardiovascular risk such as the vast majority of individuals living with insulin resistance, metabolic syndrome, and T2D. Current results also allow us to speculate regarding the existence of a state of IL-13 action resistance that could be associated with increased serum IL-13 levels in insulin-resistant patients, a notion that needs to be elucidated in basic and clinical research studies. The study of IL-13 in the development of insulin resistance may provide novel insights regarding the role of cytokines in the pathogenesis of metabolic disease and immune hyperactivation. We also remark the urgency of performing clinical studies evaluating whether IL-13 may represent a novel risk marker of insulin resistance in human beings.

Conflicts of Interest

The authors declare that there is no conflict of interest regarding the publication of this article.

Acknowledgments

This work was supported by Grants (no. 261575) from the Fondo Sectorial de Investigación y Desarrollo en Salud y Seguridad Social SS/IMSS/ISSSTE/CONACYT-México and CONACYT 247430 and is a component of the Ph.D. requirements of Camilo P. Martínez-Reyes in the Programa de Doctorado en Ciencias Biomédicas de la Universidad Nacional Autónoma de México. Camilo P. Martínez-Reyes thanks financial support from CONACYT by granting the Scholarship no. 414033.

References

[1] R. Meza, T. Barrientos-Gutierrez, R. Rojas-Martinez et al., "Burden of type 2 diabetes in Mexico: past, current and future prevalence and incidence rates," *Preventive Medicine*, vol. 81, pp. 445–450, 2015.

[2] E. K. Spanakis and S. H. Golden, "Race/ethnic difference in diabetes and diabetic complications," *Current Diabetes Reports*, vol. 13, no. 6, pp. 814–823, 2013.

[3] N. Esser, S. Legrand-Poels, J. Piette, A. J. Scheen, and N. Paquot, "Inflammation as a link between obesity, metabolic syndrome and type 2 diabetes," *Diabetes Research and Clinical Practice*, vol. 105, no. 2, pp. 141–150, 2014.

[4] N. Mahalle, M. V. Kulkarni, S. S. Naik, and M. K. Garg, "Association of dietary factors with insulin resistance and inflammatory markers in subjects with diabetes mellitus and coronary artery disease in Indian population," *Journal of Diabetes and its Complications*, vol. 28, no. 4, pp. 536–541, 2014.

[5] R. V. Shah, V. L. Murthy, S. A. Abbasi et al., "Visceral adiposity and the risk of metabolic syndrome across body mass index: the MESA study," *JACC: Cardiovascular Imaging*, vol. 7, no. 12, pp. 1221–1235, 2014.

[6] S. U. Amano, J. L. Cohen, P. Vangala et al., "Local proliferation of macrophages contributes to obesity-associated adipose tissue inflammation," *Cell Metabolism*, vol. 19, no. 1, pp. 162–171, 2014.

[7] I. Torres-Castro, U. D. Arroyo-Camarena, C. P. Martinez-Reyes et al., "Human monocytes and macrophages undergo M1-type inflammatory polarization in response to high levels of glucose," *Immunology Letters*, vol. 176, pp. 81–89, 2016.

[8] S. Leon-Cabrera, Y. Arana-Lechuga, E. Esqueda-Leon et al., "Reduced systemic levels of IL-10 are associated with the severity of obstructive sleep apnea and insulin resistance in morbidly obese humans," *Mediators of Inflammation*, vol. 2015, Article ID 493409, 9 pages, 2015.

[9] T. Tzanavari, P. Giannogonas, and K. P. Karalis, "TNF-α and obesity," *Current Directions in Autoimmunity*, vol. 11, pp. 145–156, 2010.

[10] H. Kwon and J. E. Pessin, "Adipokines mediate inflammation and insulin resistance," *Frontiers in Endocrinology*, vol. 4, p. 71, 2013.

[11] M. Saghizadeh, J. M. Ong, W. T. Garvey, R. R. Henry, and P. A. Kern, "The expression of TNF alpha by human muscle. Relationship to insulin resistance," *The Journal of Clinical Investigation*, vol. 97, no. 4, pp. 1111–1116, 1996.

[12] P. Plomgaard, K. Bouzakri, R. Krogh-Madsen, B. Mittendorfer, J. R. Zierath, and B. K. Pedersen, "Tumor necrosis factor-α induces skeletal muscle insulin resistance in healthy human subjects via inhibition of Akt substrate 160 phosphorylation," *Diabetes*, vol. 54, no. 10, pp. 2939–2945, 2005.

[13] C. N. Lumeng, J. L. Bodzin, and A. R. Saltiel, "Obesity induces a phenotypic switch in adipose tissue macrophage polarization," *The Journal of Clinical Investigation*, vol. 117, no. 1, pp. 175–184, 2007.

[14] L. Chen, R. Chen, H. Wang, and F. Liang, "Mechanisms linking inflammation to insulin resistance," *International Journal of Endocrinology*, vol. 2015, Article ID 508409, 9 pages, 2015.

[15] K. Oeser, C. Schwartz, and D. Voehringer, "Conditional IL-4/IL-13-deficient mice reveal a critical role of innate immune cells for protective immunity against gastrointestinal helminths," *Mucosal Immunology*, vol. 8, no. 3, pp. 672–682, 2015.

[16] S. Agrawal and R. G. Townley, "Role of periostin, FENO, IL-13, lebrikzumab, other IL-13 antagonist and dual IL-4/IL-13 antagonist in asthma," *Expert Opinion on Biological Therapy*, vol. 14, no. 2, pp. 165–181, 2014.

[17] H. Kwon, S. Laurent, Y. Tang, H. Zong, P. Vemulapalli, and J. E. Pessin, "Adipocyte-specific IKKβ signaling suppresses adipose tissue inflammation through an IL-13-dependent paracrine feedback pathway," *Cell Reports*, vol. 9, no. 5, pp. 1574–1583, 2014.

[18] P. Darkhal, M. Gao, Y. Ma, and D. Liu, "Blocking high-fat diet-induced obesity, insulin resistance and fatty liver by overexpression of Il-13 gene in mice," *International Journal of Obesity*, vol. 39, no. 8, pp. 1292–1299, 2015.

[19] S. Rutti, C. Howald, C. Arous, E. Dermitzakis, P. A. Halban, and K. Bouzakri, "IL-13 improves beta-cell survival and protects against IL-1beta-induced beta-cell death," *Molecular Metabolism*, vol. 5, no. 2, pp. 122–131, 2016.

[20] L. Q. Jiang, N. Franck, B. Egan et al., "Autocrine role of interleukin-13 on skeletal muscle glucose metabolism in type 2 diabetic patients involves microRNA let-7," *American Journal of Physiology Endocrinology and Metabolism*, vol. 305, no. 11, pp. E1359–E1366, 2013.

[21] H. Q. Qu, Q. Li, A. R. Rentfro, S. P. Fisher-Hoch, and J. B. McCormick, "The definition of insulin resistance using HOMA-IR for Americans of Mexican descent using machine learning," *PLoS One*, vol. 6, no. 6, article e21041, 2011.

[22] J. Zhu, "T helper 2 (Th2) cell differentiation, type 2 innate lymphoid cell (ILC2) development and regulation of interleukin-4 (IL-4) and IL-13 production," *Cytokine*, vol. 75, no. 1, pp. 14–24, 2015.

[23] H. Madhumitha, V. Mohan, M. Deepa, S. Babu, and V. Aravindhan, "Increased Th1 and suppressed Th2 serum cytokine levels in subjects with diabetic coronary artery disease," *Cardiovascular Diabetology*, vol. 13, no. 1, p. 1, 2014.

[24] T. K. Nestvold, E. W. Nielsen, J. K. Ludviksen, H. Fure, A. Landsem, and K. T. Lappegard, "Lifestyle changes followed by bariatric surgery lower inflammatory markers and the cardiovascular risk factors C3 and C4," *Metabolic Syndrome and Related Disorders*, vol. 13, no. 1, pp. 29–35, 2015.

[25] D. O. Minchenko, V. V. Davydov, O. A. Budreiko et al., "The expression of *CCN2, IQSEC, RSPO1, DNAJC15, RIPK2, IL13RA2, IRS1,* and *IRS2* genes in blood of obese boys with insulin resistance," *Fiziologicheskiĭ Zhurnal*, vol. 61, no. 1, pp. 10–18, 2015.

[26] K. J. Stanya, D. Jacobi, S. Liu et al., "Direct control of hepatic glucose production by interleukin-13 in mice," *The Journal of Clinical Investigation*, vol. 123, no. 1, pp. 261–271, 2013.

[27] Y. Nishimura, T. Inoue, T. Nitto, T. Morooka, and K. Node, "Increased interleukin-13 levels in patients with chronic heart failure," *International Journal of Cardiology*, vol. 131, no. 3, pp. 421–423, 2009.

[28] U. Amit, D. Kain, A. Wagner et al., "New role for interleukin-13 receptor α1 in myocardial homeostasis and heart failure," *Journal of the American Heart Association*, vol. 6, no. 5, article e005108, 2017.

[29] S. A. Westphal, "Obesity, abdominal obesity, and insulin resistance," *Clinical Cornerstone*, vol. 9, no. 1, pp. 23–31, 2008.

[30] D. C. Berry, D. Stenesen, D. Zeve, and J. M. Graff, "The developmental origins of adipose tissue," *Development*, vol. 140, no. 19, pp. 3939–3949, 2013.

[31] F. M. Schmidt, J. Weschenfelder, C. Sander et al., "Inflammatory cytokines in general and central obesity and modulating effects of physical activity," *PLoS One*, vol. 10, no. 3, article e0121971, 2015.

[32] P. Nehete, E. R. Magden, B. Nehete, P. W. Hanley, and C. R. Abee, "Obesity related alterations in plasma cytokines and metabolic hormones in chimpanzees," *International Journal of Inflammation*, vol. 2014, Article ID 856749, 11 pages, 2014.

[33] V. Marks, "Temporary removal: rebirth of the incretin concept; its conception and early development," *Peptides*, 2017, In press.

[34] P. D. Mitchell, B. M. Salter, J. P. Oliveria et al., "Glucagon-like peptide-1 receptor expression on human eosinophils and its regulation of eosinophil activation," *Clinical & Experimental Allergy*, vol. 47, no. 3, pp. 331–338, 2017.

[35] P. Lu, Y. Xu, Z. Su, and H. Xu, "Enhanced ILC2 activity contributes to metabolic syndrome multicomponent aggregation state in patients with type 2 diabetic nephropathy," *Xi Bao Yu Fen Zi Mian Yi Xue Za Zhi*, vol. 33, no. 6, pp. 820–825, 2017.

[36] L. H. Tangeras, M. Austdal, R. B. Skrastad et al., "Distinct first trimester cytokine profiles for gestational hypertension and preeclampsia," *Arteriosclerosis, Thrombosis, and Vascular Biology*, vol. 35, no. 11, pp. 2478–2485, 2015.

[37] J. Surendar, V. Mohan, M. M. Rao, S. Babu, and V. Aravindhan, "Increased levels of both Th1 and Th2 cytokines in subjects with metabolic syndrome (CURES-103)," *Diabetes Technology & Therapeutics*, vol. 13, no. 4, pp. 477–482, 2011.

[38] C. H. Tsao, M. Y. Shiau, P. H. Chuang, Y. H. Chang, and J. Hwang, "Interleukin-4 regulates lipid metabolism by inhibiting adipogenesis and promoting lipolysis," *Journal of Lipid Research*, vol. 55, no. 3, pp. 385–397, 2014.

[39] M. M. van Greevenbroek, C. G. Schalkwijk, and C. D. Stehouwer, "Obesity-associated low-grade inflammation in type 2 diabetes mellitus: causes and consequences," *The Netherlands Journal of Medicine*, vol. 71, no. 4, pp. 174–187, 2013.

[40] M. Chalubinski, E. Luczak, K. Wojdan, P. Gorzelak-Pabis, and M. Broncel, "Innate lymphoid cells type 2 - emerging immune regulators of obesity and atherosclerosis," *Immunology Letters*, vol. 179, pp. 43–46, 2016.

[41] S. K. Chang, A. C. Kohlgruber, F. Mizoguchi et al., "Stromal cell cadherin-11 regulates adipose tissue inflammation and diabetes," *The Journal of Clinical Investigation*, vol. 127, no. 9, pp. 3300–3312, 2017.

[42] A. Pilatz, C. Hudemann, J. Wolf et al., "Metabolic syndrome and the seminal cytokine network in morbidly obese males," *Andrology*, vol. 5, no. 1, pp. 23–30, 2017.

[43] J. P. Sikora, W. Kuzanski, and E. Andrzejewska, "Soluble cytokine receptors sTNFR I and sTNFR II, receptor antagonist IL-1ra, and anti-inflammatory cytokines IL-10 and IL-13 in the pathogenesis of systemic inflammatory response syndrome in the course of burns in children," *Medical Science Monitor*, vol. 15, no. 1, pp. CR26–CR31, 2009.

[44] I. Matia-García, J. Muñoz-Valle, Z. Reyes-Castillo et al., "Correlation between cytokine profile and metabolic abnormalities in young subjects," *International Journal of Clinical and Experimental Medicine*, vol. 9, no. 8, pp. 16596–16604, 2016.

biomolecules

MDPI

Article

Native Low-Density Lipoproteins Act in Synergy with Lipopolysaccharide to Alter the Balance of Human Monocyte Subsets and Their Ability to Produce IL-1 Beta, CCR2, and CX3CR1 In Vitro and In Vivo: Implications in Atherogenesis

Aarón N. Manjarrez-Reyna [1], Camilo P. Martínez-Reyes [1], José A. Aguayo-Guerrero [1], Lucia A. Méndez-García [1], Marcela Esquivel-Velázquez [1], Sonia León-Cabrera [2,3], Gilberto Vargas-Alarcón [4], José M. Fragoso [4], Elizabeth Carreón-Torres [4], Oscar Pérez-Méndez [4,5], Jessica L. Prieto-Chávez [6] and Galileo Escobedo [1,*]

1 Laboratory of Immunometabolism, Research Division, General Hospital of Mexico "Dr. Eduardo Liceaga", Mexico City 06720, Mexico; aaron.manjarrez@gmail.com (A.N.M.-R.); nava111222@hotmail.com (C.P.M.-R.); jose.aguayo01@iest.edu.mx (J.A.A.-G.); angelica.mendez.86@hotmail.com (L.A.M.-G.); esquivel.marcela@gmail.com (M.E.-V.)

2 Unidad de Biomedicina, Facultad de Estudios Superiores-Iztacala, Universidad Nacional Autónoma de México, Tlalnepantla, Edo. De Mexico 54090, Mexico; soleon81@gmail.com

3 Carrera de Médico Cirujano, Facultad de Estudios Superiores-Iztacala, Universidad Nacional Autónoma de México, Tlalnepantla, Edo. De Mexico 54090, Mexico

4 Department of Molecular Biology, Instituto Nacional de Cardiología "Ignacio Chávez", Juan Badiano 1, Sección XVI, Tlalpan, Mexico City 14080, Mexico; gvargas63@yahoo.com (G.V.-A.); mfragoso1275@yahoo.com.mx (J.M.F.); qfbelizabethcm@yahoo.es (E.C.-T.); opmendez@yahoo.com (O.P.-M.)

5 School of Engineering and Sciences Campus CDMX, Tecnológico de Monterrey, Calle Puente 222, Tlalpan, Mexico City 14380, Mexico

6 Laboratorio de Citometría de Flujo, Centro de Instrumentos, Coordinación de Investigación en Salud, Hospital de Especialidades del Centro Médico Siglo XXI, Instituto Mexicano del Seguro Social, Mexico City 06720, Mexico; lakshmi.litmus@hotmail.com

* Correspondence: gescobedog@msn.com or gescobedo@unam.mx; Tel.: +52-(55)-2789-2000 (ext. 5646)

Citation: Manjarrez-Reyna, A.N.; Martínez-Reyes, C.P.; Aguayo-Guerrero, J.A.; Méndez-García, L.A.; Esquivel-Velázquez, M.; León-Cabrera, S.; Vargas-Alarcón, G.; Fragoso, J.M.; Carreón-Torres, E.; Pérez-Méndez, O.; et al. Native Low-Density Lipoproteins Act in Synergy with Lipopolysaccharide to Alter the Balance of Human Monocyte Subsets and Their Ability to Produce IL-1 Beta, CCR2, and CX3CR1 In Vitro and In Vivo: Implications in Atherogenesis. *Biomolecules* **2021**, *11*, 1169. https://doi.org/10.3390/biom11081169

Academic Editors: Alessandro Mattina, Giuseppe Mandraffino and Roberto Scicali

Received: 11 June 2021
Accepted: 4 August 2021
Published: 7 August 2021

Abstract: Increasing evidence has demonstrated that oxidized low-density lipoproteins (oxLDL) and lipopolysaccharide (LPS) enhance accumulation of interleukin (IL)-1 beta-producing macrophages in atherosclerotic lesions. However, the potential synergistic effect of native LDL (nLDL) and LPS on the inflammatory ability and migration pattern of monocyte subpopulations remains elusive and is examined here. In vitro, whole blood cells from healthy donors (n = 20) were incubated with 100 µg/mL nLDL, 10 ng/mL LPS, or nLDL + LPS for 9 h. Flow cytometry assays revealed that nLDL significantly decreases the classical monocyte (CM) percentage and increases the non-classical monocyte (NCM) subset. While nLDL + LPS significantly increased the number of NCMs expressing IL-1 beta and the C-C chemokine receptor type 2 (CCR2), the amount of NCMs expressing the CX3C chemokine receptor 1 (CX3CR1) decreased. In vivo, patients (n = 85) with serum LDL-cholesterol (LDL-C) >100 mg/dL showed an increase in NCM, IL-1 beta, LPS-binding protein (LBP), and Castelli's atherogenic risk index as compared to controls (n = 65) with optimal LDL-C concentrations (≤100 mg/dL). This work demonstrates for the first time that nLDL acts in synergy with LPS to alter the balance of human monocyte subsets and their ability to produce inflammatory cytokines and chemokine receptors with prominent roles in atherogenesis.

Keywords: atherogenesis; monocyte subpopulations; native LDL; LPS; IL-1 beta; CCR2; CX3CR1; LBP

1. Introduction

Atherosclerosis is a chronic inflammatory disease of the arteries and a leading cause of death worldwide [1]. Atherogenesis is the pathological process through which atheromatous plaque is formed in the inner layer of the arteries, leading to vessel thickening, arterial remodeling, and potential obstruction of blood flow at the site of the lesion [2].

Atherosclerotic plaque formation is a highly dynamic process involving the adhesion of circulating monocytes to the tunica intima, wherein these cells differentiate into macrophages [3]. Then, monocyte-derived macrophages can migrate to the subendothelial space and turn into foam cells after ingesting oxidized low-density lipoproteins (oxLDL), triggering an inflammatory response that injures endothelial cells and promotes arterial remodeling [4]. In this scenario, the role of macrophages and oxLDL in atherogenesis appears to be clear [5]; however, monocytes and native LDL (nLDL) might also contribute to atherosclerosis by mechanisms that are not yet fully understood.

In the blood stream, human monocytes are sorted into three subsets based on the cell surface expression of CD14 and CD16 [6]. Classical monocytes (CMs) express high CD14 levels but do not express CD16 (CD14++CD16−). Intermediate monocytes (IMs) exhibit CD16 expression and high CD14 levels (CD14++CD16+), while non-classical monocytes (NCMs) also express CD16 but show low CD14 levels (CD14+CD16+) [7]. Upon lipopolysaccharide (LPS) stimulation, human monocyte subpopulations differentially respond to produce interleukin (IL)-1 beta, a proinflammatory cytokine with key roles in atherosclerosis [8]. Monocyte subsets also differentially express the C-C chemokine receptor type 2 (CCR2) and the CX3C chemokine receptor 1 (CX3CR1), each of which are chemokine receptors with prominent functions in cell migration and endothelial adhesion during atherosclerosis [9,10].

The immune function of monocyte subpopulations is regulated by prototypical factors such as LPS, double-stranded ribonucleic acid (dsRNA), and tumor necrosis factor alpha (TNF-alpha) [11,12]. However, emerging evidence suggests that non-prototypical immunometabolic ligands can also influence the cytokine and chemokine expression profile in these cells. In this sense, excess glucose increases TNF-alpha expression in in vitro cultured primary human monocytes [13]. Free-fatty acids induce IL-1 beta secretion in in vitro cultured THP-1 cells and primary human monocytes [14]. Furthermore, immunometabolic agents can also act in synergy with prototypical immune factors to regulate the activity of monocyte subsets. In this regard, low concentration of high-density lipoproteins (HDL) increases IL-1 beta expression in NCMs stimulated with LPS and in subjects with high serum levels of LPS-binding protein (LBP) [15–17]. On the contrary, the study of the action of LDL in monocytes has been restricted to its role as oxLDL [4,5], even though accumulating evidence also suggests that monocytes and nLDL could interact in circulation, thus contributing to atherosclerotic plaque formation [18,19]. In this sense, elevated circulating nLDL levels are associated with an increment in the percentage of CMs that can migrate into endothelial tissue by mainly expressing CX3CR1 and CCR2 in *ApoE*$^{-/-}$ mice, an animal model of atherosclerosis [20]. In parallel, LPS directly increases lipid deposition in primary human adventitial fibroblasts, inducing secretion of molecules with prominent roles in atherosclerosis such as monocyte chemoattractant protein 1 (MCP-1), the main ligand for CCR2 [21]. Interestingly, consumption of Western-style high-fat diets is associated with increased serum LPS levels in humans [22,23]. However, the potential contribution of nLDL and LPS to the inflammatory activity of human monocyte subsets during atherogenesis remains unclear.

The main goal of this study was to examine the effect of nLDL on the immune function of human monocyte subpopulations in in vitro LPS-stimulated primary monocytes and in patients with high LDL-cholesterol (LDL-C) and LBP serum levels.

2. Materials and Methods

2.1. In Vitro Culture of Primary Human Monocytes

Twenty healthy blood donors with LDL-C serum levels less than 100 mg/dL and high-sensitive C-reactive protein (hs-CRP) serum values of 1.35 ± 0.26 mg/L, on average, were enrolled in the study. Each participant agreed to donate 8 mL of blood, which was collected into a tube containing heparin (Vacutainer^{TM}, BD Diagnostics, Franklin Lakes, NJ, USA). Subsequently, whole blood samples were individually divided and placed in 6-well cell-culture plates (Costar, Kennebunk, ME, USA), adding 2 mL of blood plus 1 mL of

RPMI-1640 (Sigma-Aldrich, St. Louis, MO, USA) supplemented with 5% fetal bovine serum (FBS), 2 mM L-glutamine, 10 nM HEPES buffer, and 50 µg/mL gentamicin (Gibco™, Grand Island, NY, USA) per well. The blood sample contained in the first well was designated as the control and received 300 µL of RPMI-1640 for 9 h. The second well was incubated in the presence of 100 µg nLDL (Sigma-Aldrich, St. Louis, MO, USA) dissolved in 300 µL of RPMI-1640 for 9 h. The third well was incubated in the presence of 10 ng/mL LPS (Sigma-Aldrich, St. Louis, MO, USA) dissolved in 300 µL of RPMI-1640 for 9 h. The sample contained in the fourth well was incubated in the presence of 100 µg nLDL plus 10 ng/mL LPS dissolved in 300 µL of RPMI-1640 for 9 h. Exposure time of in vitro cultures was selected based on time-response curves at 3, 6, and 9 h, finding that monocytes show the most significant changes at 9 h. The cell-culture plates were incubated at 37 °C in humidified 5% CO_2 atmosphere. For intracellular cytokine stain, white blood cells (WBCs) were treated with 1:1000 Brefeldin A (BioLegend, Inc., San Diego, CA, USA) for the last 2 h of in vitro culture. All of the participants provided written informed consent, previously approved by the institutional ethical committee of the General Hospital of Mexico (registration number of ethical approval code: DI/20/501/03/17), which guaranteed that the study was conducted in rigorous adherence to the principles described in the 1964 Declaration of Helsinki and its posterior amendment in 2013.

2.2. *Flow Cytometry*

After incubation, whole blood samples were collected and centrifuged at 500× *g* for 10 min. Immediately afterwards, WBCs were separated using a micropipette and resuspended in 1 mL PBS1X (Sigma-Aldrich, St. Louis, MO, USA). After an additional centrifugation step and removal of the supernatant, each cell pellet was resuspended in 50 µL cell staining buffer (BioLegend, Inc., San Diego, CA, USA). WBCs were incubated with 5 µL True-Stain Monocyte Blocker™ (BioLegend, Inc., San Diego, CA, USA) for 10 min on ice. Then, WBCs were incubated with anti-CD14 PE/Cy7, anti-CD16 PE/Cy5, anti-CCR2 AF647, anti-CX3CR1 BV510, Zombie ultraviolet (UV) Fixable Viability Kit (BioLegend, Inc., San Diego, CA, USA), and anti-human leukocyte antigen-DR (HLA-DR) BUV661 (BD Biosciences, San Jose, CA, USA) for 20 min in darkness at 4 °C. Afterwards, WBCs were incubated with 100 µL Fixation Medium A (FIX & PERM™ Cell Permeabilization Kit) (Invitrogen™, Carlsbad, CA, USA) for 20 min at room temperature. After being rinsed using Cell Staining Buffer (BioLegend, Inc., San Diego, CA, USA), peripheral blood mononuclear cells (PBMCs) were incubated with 100 µL Permeabilization Medium B (FIX & PERM™ Cell Permeabilization Kit, Invitrogen™, Carlsbad, CA, USA) and anti-IL-1 beta Pacific Blue (BioLegend, Inc., San Diego, CA, USA) for 20 min in darkness at room temperature. After being rinsed using Cell Staining Buffer (BioLegend, Inc., San Diego, CA, USA), PBMCs were acquired on a BD Influx flow cytometer (BD Biosciences, San Jose, CA, USA) using the BD Sortware™ software 1.2, acquiring 20,000 events per test in triplicate. For the gating strategy, WBCs were first gated on a time/side scatter density plot, and then gated on the Zombie UV negative cell population for detection of living cells. Afterwards, living cells were gated for singlets on a forward scatter (FS)/Trigger Pulse Width density plot. Monocytes were recognized on the HLA-DR gating. Then, monocytes were selected using the rectangular gating strategy on the CD14+/CD16+ population for identification of CMs (CD14++CD16−), IMs (CD14++CD16+), and NCMs (CD14+CD16+), as previously reported [24]. The median fluorescence intensity (MFI) for IL-1 beta, CCR2, and CX3CR1 was obtained by considering both positive and negative cell populations for each marker. The percentage of positive cells for each marker was obtained using proper fluorescence minus one (FMO) controls. Compensation controls were performed by means of UltraComp eBeads™ (Invitrogen™, Carlsbad, CA, USA) for each fluorochrome. Data were analyzed by means of the FlowJo 10.0.7 software (TreeStar, Inc., Ashland, OR, USA).

2.3. Subjects for In Vivo Assays

One hundred fifty volunteers from both sexes, aged 18 years or older, with 8 h fasting who attended the Blood Bank and the Department of Internal Medicine of the General Hospital of Mexico were included in the study. A group of three trained physicians registered gender, age, body mass index (BMI), waist circumference, body fat percentage, and the serum levels of glucose, insulin, C-reactive protein (CRP), total cholesterol, triglycerides, HDL-C, and LDL-C in all participants. BMI resulted from dividing weight by height squared. Waist circumference was measured at the midpoint between the lower rib margin and the iliac crest using a tape. Body fat percentage was obtained by means of a body composition analyzer (TANITA® Body Composition Analyzer, Model TBF-300A, Tokyo, Japan). CRP was measured in triplicate by immunoturbidimetry (Randox Laboratories, Meenmore, Ireland). Serum glucose, total cholesterol, triglycerides, HDL-C, and LDL-C were measured in triplicate by enzymatic assays (Roche Diagnostics, Mannheim, Germany). Serum insulin was measured in triplicate by the Enzyme-Linked Immunosorbent Assay (ELISA) (Abnova, Corporation, Taipei City, Taiwan). The estimate of insulin resistance was individually calculated using the homeostatic model assessment of insulin resistance (HOMA-IR) by multiplying glucose concentration (mM) by insulin concentration (mU/L) and then dividing by 22.5. All of the participants received full medical evaluation and provided written informed consent, previously approved by the institutional ethical committee of the General Hospital of Mexico (registration number of ethical approval code: DIC/11/UME/05/029), which guaranteed that the study was conducted in rigorous adherence to the principles described in the 1964 Declaration of Helsinki and its posterior amendment in 2013. Volunteers were excluded from the study if they had a previous diagnosis of type 1 diabetes (T1D), T2D, coronary disease, acute or chronic liver or renal disease, cancer, endocrine disorders, infectious diseases, chronic inflammatory disease, and/or autoimmune disorders. We also excluded from the study human immunodeficiency virus (HIV), hepatitis C virus (HCV), and hepatitis B virus (HBV)-seropositive patients, pregnant or lactating woman, and subjects with anti-inflammatory or immunomodulatory medication, including non-steroidal anti-inflammatory drugs (NSAIDs).

2.4. Effects of LDL and LBP on Monocyte Subpopulations and IL-1 Beta In Vivo

According to clinical guidelines of the National Cholesterol Education Program (NCEP) Expert Panel on Detection, Evaluation and Treatment of High Blood Cholesterol in Adults (Adult Treatment Panel III), the study participants were divided in two groups of LDL-C concentration, as follows: subjects with optimal concentration of LDL-C $\leq$ 100 mg/dL, and individuals with high concentration of LDL-C > 100 mg/dL [25]. Then, BMI, waist circumference, body fat percentage, glucose metabolism, HOMA-IR, and lipid profile were registered and compared between both groups. Blood samples (6 mL) were obtained from all volunteers for posterior isolation of WBCs. WBCs were incubated with anti-CD14 PE/Cy7 and anti-CD16 FITC, acquiring 20,000 events per test in triplicate on a BD Influx flow cytometer (BD Biosciences, San Jose, CA, USA) using the BD Sortware™ software 1.2 and the FlowJo 10.0.7 software (TreeStar, Inc., Ashland, OR, USA), as described above. In all participants, serum IL-1 beta (Peprotech, Mexico City, Mexico) and LBP (Invitrogen™, Carlsbad, CA, USA) were measured in triplicate by ELISA and analyzed according to LDL-C levels.

2.5. Statistics

Normality of data distribution was estimated by the Shapiro–Wilk test. For in vitro assays, one-way ANOVA, followed by a post-hoc Tukey test, was used to compare percentages of CMs, IMs, and NCMs, and expression of IL-1 beta, CCR2, and CX3CR1 in the cell groups designated as control, nLDL, LPS, and nLDL + LPS. For in vivo assays, the unpaired Student's *t*-test was used to compare subjects with serum LDL-C $\leq$ 100 mg/dL and individuals with serum LDL-C > 100 mg/dL in terms of gender, age, BMI, waist circumference, body fat percentage, fasting glucose, insulin, HOMA-IR, CRP, total cholesterol,

triglycerides, HDL, percentages of CMs, IMs, and NCMs, serum IL-1 beta, and circulating LBP levels. Differences were considered significant when $p < 0.05$. All of the statistical analyses were performed by means of the GraphPad Prism 7 software (GraphPad Software, La Jolla, CA 92037, USA).

3. Results

For the gating strategy, WBCs were first gated on a time/side scatter (SS) density plot, and then gated on the Zombie UV negative cell population for detection of living WBCs (Figure 1, top panel). Afterwards, WBCs were gated for singlets on a forward scatter (FS)/Trigger Pulse Width density plot, and after that gated on the HLA-DR+ population for monocyte recognition. Monocytes were then gated on the CD14+/CD16+ population for identification of CMs (CD14++CD16−), IMs (CD14++CD16+), and NCMs (CD14+CD16+). Monocyte subsets were then gated on the IL-1 beta+, CCR2+, and CX3CR1+ populations for assessing the effects of nLDL and LPS on the immune activity of these cells (Figure 1, bottom panel).

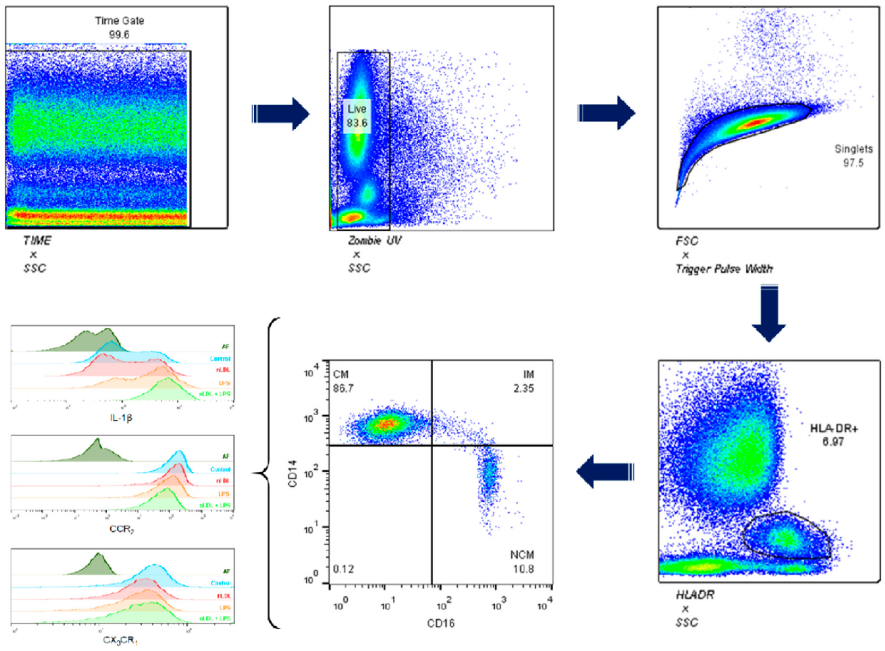

Figure 1. Gating strategy for characterizing human monocyte subsets. White blood cells were first gated on a time/side scatter (SS) density plot, and then gated on the Zombie UV negative cell population for detection of living cells. Afterwards, living cells were gated for singlets on a forward scatter (FS)/Trigger Pulse Width density plot. Monocytes were recognized on the HLA-DR gating. Then, monocytes were gated on the CD14+/CD16+ population for identification of CMs (CD14++CD16−), IMs (CD14++CD16+), and NCMs (CD14+CD16+). Expression of IL-1 beta, CCR2, and CX3CR1 was measured in all monocyte subsets. SSC, side scatter; FSC, forward scatter; HLA-DR, human leukocyte antigen-DR isotype; CM, classical monocytes; IM, intermediate monocytes; NCM, non-classical monocytes; IL-1 beta, interleukin 1 beta; CCR2, C-C chemokine receptor type 2; CX3CR1, CX3C chemokine receptor 1.

Figure 2 illustrates representative plots showing the percentages of CMs, IMs, and NCMs treated with nLDL and/or LPS (Figure 2A–D). As compared to control cells, the percentage of CMs was significantly reduced when treated with 100 µg/mL nLDL (Figure 2E). While the percentage of IMs did not change (Figure 2F), the percentage of NCMs exhibited

a significant 20% increase when exposed to 100 µg/mL nLDL with respect to that found in untreated cells (Figure 2G). Monocyte subpopulations also differentially responded to LPS. LPS, alone or in combination with nLDL, induced a significant 10% increase in CMs (Figure 2E). Conversely, IMs and NCMs showed significant reductions when treated with LPS or nLDL + LPS with respect to that found in control cells (Figure 2F,G, respectively). The percentages of CMs, IMs, and NCMs showed similar behavior in response to LPS or nLDL + LPS, suggesting that this effect was mainly mediated by LPS (Figure 2E–G, respectively).

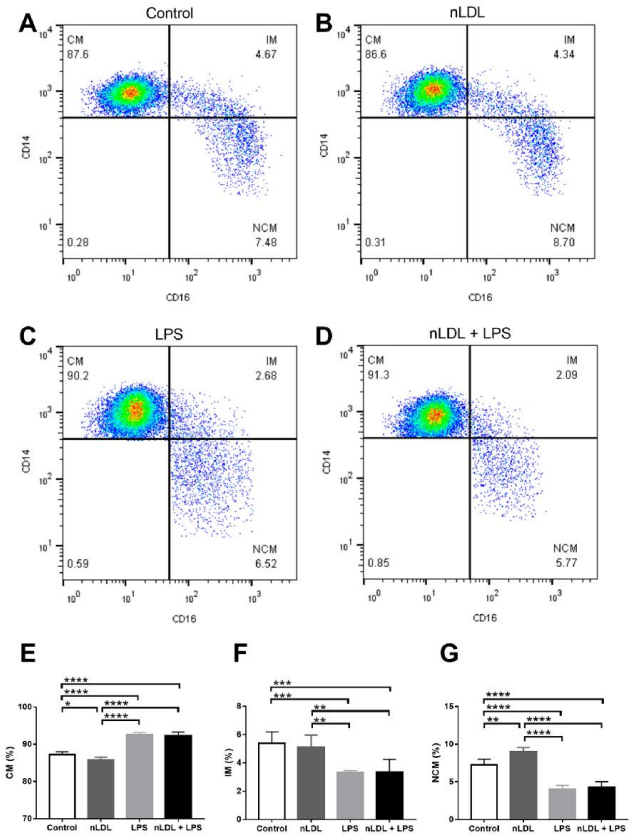

Figure 2. Effects of nLDL and LPS on the dynamics of human monocyte subpopulations. Representative plots showing the percentages of CMs, IMs, and NCMs in response to control conditions (**A**), nLDL (**B**), LPS (**C**), or a combination of nLDL + LPS (**D**). nLDL significantly decreased the CM percentage and increased the amount of NCMs as compared to control cells (**E**,**G**, respectively). LPS, alone or in combination with nLDL, significantly increased the CM percentage and decreased the amount of IMs and NCMs (**E**–**G**, respectively). Cells were incubated in the presence or absence of 100 µg/mL nLDL and/or 10 ng/mL LPS for 9 h. Data are expressed as mean ± standard deviation. Data were compared using one-way ANOVA followed by the post-hoc Tukey test. Differences were considered significant when $p < 0.05$. * = $p < 0.05$; ** = $p < 0.01$; *** = $p < 0.001$; **** = $p < 0.0001$. CM, classical monocytes; IM, intermediate monocytes; NCM, non-classical monocytes; nLDL, native low-density lipoproteins; LPS, lipopolysaccharide.

Exposure of cells to nLDL and LPS not only affected the balance among monocyte subpopulations but also their ability to produce IL-1 beta, a cytokine with key proinflammatory actions. Exposure of monocytes to 100 μg/mL nLDL had no significant effects on IL-1 beta production in all monocyte subpopulations (Figure 3A). LPS significantly increased IL-1 beta production in CMs, IMs, and NCMs, and this increase was even more evident when cells were exposed to LPS in combination with nLDL (Figure 3A). In parallel, the percentages of CMs, IMs, and NCMs that expressed IL-1 beta also tended to decrease in response to nLDL (Figure 3B). LPS, alone or in combination with nLDL, significantly increased the number of IL-1 beta+ cells in all monocyte subpopulations with respect to untreated cells (Figure 3B).

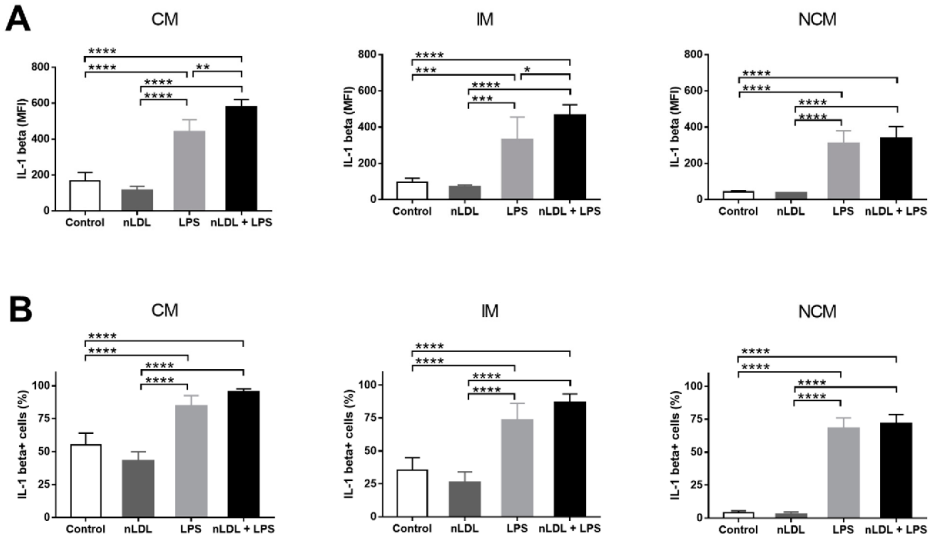

Figure 3. Effects of nLDL and LPS on IL-1 beta production in human monocyte subpopulations. Although no significant differences were found, nLDL tended to decrease IL-1 beta production in CMs, IMs, and NCMs (**A**, left, middle, and right panels, respectively). LPS, alone or in combination with nLDL, significantly increased IL-1 beta expression in CMs, IMs, and NCMs (**A**, left, middle, and right panels, respectively). Although no significant differences were found, nLDL tended to decrease the percentages of IL-1 beta+ cells in all monocyte subsets (**B**, left, middle, and right panels, respectively). LPS, alone or in combination with nLDL, significantly increased the amount of IL-1 beta+ cells in all monocyte subpopulations (**B**, left, middle, and right panels, respectively). Cells were incubated in the presence or absence of 100 μg/mL nLDL and/or 10 ng/mL LPS for 9 h. Data are expressed as mean ± standard deviation. Data were compared using one-way ANOVA followed by the post-hoc Tukey test. Differences were considered significant when $p < 0.05$. * = $p < 0.05$; ** = $p < 0.01$; *** = $p < 0.001$; **** = $p < 0.0001$. CM, classical monocytes; IM, intermediate monocytes; NCM, non-classical monocytes; nLDL, native low-density lipoproteins; LPS, lipopolysaccharide; IL-1 beta, interleukin 1 beta; MFI, median fluorescence intensity.

Besides IL-1 beta expression, monocyte subsets have also been shown to differentially express chemokine receptors. In this sense, CCR2 expression was clearly higher in CMs than IMs and NCMs; however, CMs did not differentially express CCR2 in response to nLDL, alone or in combination with LPS (Figure 4A). Overall, the percentage of CMs and IMs expressing CCR2 did not change in response to nLDL or LPS (Figure 4B, left and middle panels, respectively). Conversely, nLDL + LPS significantly increased the amount of NCMs expressing CCR2 as compared to that found when cells were only exposed to nLDL (Figure 4B, right panel). Expression of CX3CR1 was significantly higher in IMs and NCMs

than CMs (Figure 4C). Furthermore, nLDL induced a decrease in CX3CR1 expression that was even more evident in NCMs than CMs and IMs (Figure 4C, right panel). The exposure of cells to LPS, alone or in combination with nLDL, decreased the expression of CX3CR1 in all monocyte subpopulations (Figure 4C). Interestingly, the number of CX3CR1+ NCMs significantly decreased in response to nLDL (Figure 4D, right panel), while LPS together with nLDL had the same effect upon IMs and NCMs (Figure 4D, middle and right panels, respectively).

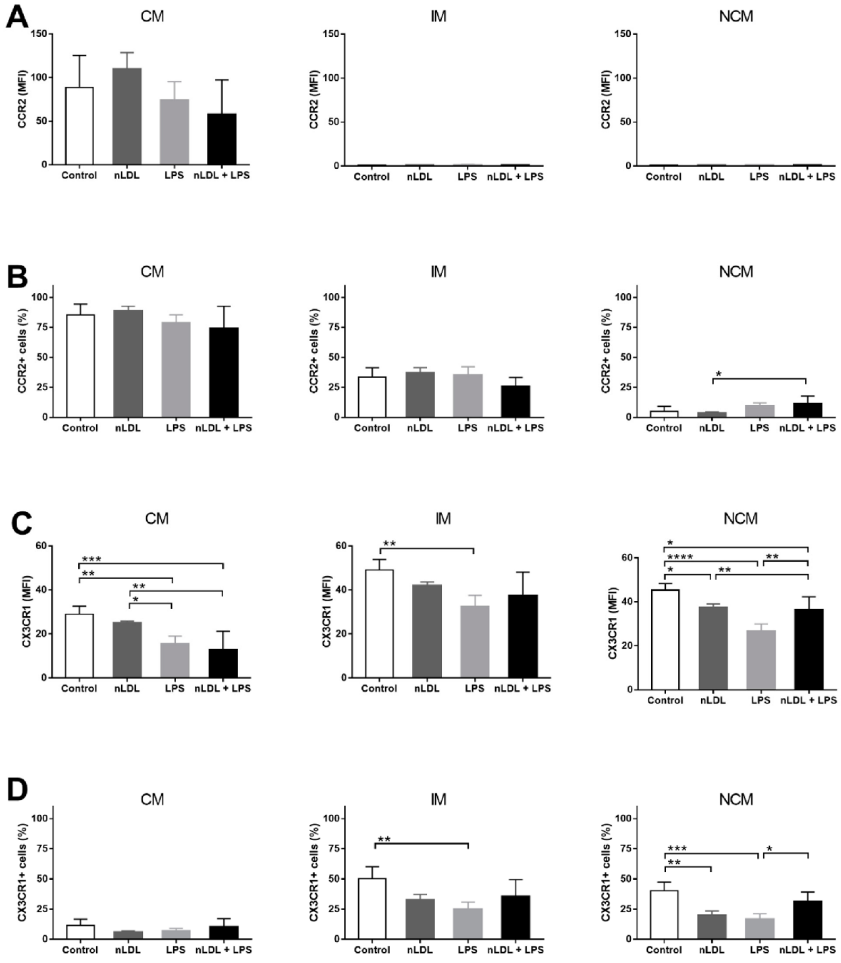

Figure 4. Effects of nLDL and LPS on CCR2 and CX3CR1 expression in human monocyte subpopulations. Although no significant differences were found, CCR2 expression was clearly higher in CMs than in IMs and NCMs (**A**, left, middle, and right panels, respectively). The number of CCR2+ cells increased in the CM subset as compared to IM and NCM subpopulations (**B**, left, middle, and right panels, respectively). In the NCM subset, LPS acted in synergy with nLDL to increase the amount of CCR2+ cells as compared to that found in cells only treated with nLDL (**B**, right panel). Expression

of CX3CR1 increased in IMs and NCMs as compared to CMs (**C**, left, middle, and right panels, respectively). In NCMs, nLDL significantly decreased CX3CR1 expression as compared to control cells (**C**, right panel). LPS, alone or in combination with nLDL, decreased CX3CR1 expression in CMs, IMs, and NCMs (**C**, left, middle, and right panels, respectively). In IMs, LPS decreased the percentage of CX3CR1+ cells as compared to control cells (**D**, middle panel). In NCMs, nLDL significantly decreased the amount of CX3CR1+ cells as compared to control cells (**D**, right panel). Cells were incubated in the presence or absence of 100 μg/mL nLDL and/or 10 ng/mL LPS for 9 h. Data are expressed as mean ± standard deviation. Data were compared using one-way ANOVA followed by the post-hoc Tukey test. Differences were considered significant when $p < 0.05$. * = $p < 0.05$; ** = $p < 0.01$; *** = $p < 0.001$; **** = $p < 0.0001$. CM, classical monocytes; IM, intermediate monocytes; NCM, non-classical monocytes; nLDL, native low-density lipoproteins; LPS, lipopolysaccharide; CCR2, C-C chemokine receptor type 2; CX3CR1, CX3C chemokine receptor 1; MFI, median fluorescence intensity.

In vitro, nLDL and LPS not only changed the balance of monocyte subsets but also the expression pattern of molecules that have been previously associated with the inflammatory response in atherogenesis. Thus, we decided to confirm these results by conducting similar experiments but now with an in vivo approach in patients with elevated LDL-C serum levels. Table 1 summarizes the differences in metabolic syndrome-related risk factors between subjects with normal and elevated LDL-C serum levels (76.53 ± 4.1 vs. 128.7 ± 3.6, respectively). There were no significant differences between subjects with LDL-C values below and above 100 mg/dL with respect to sex proportion, age, BMI, waist circumference, body fat percentage, triglycerides, HDL-C, fasting insulin and glucose, HOMA-IR, and CRP (Table 1). On the contrary, total cholesterol and Castelli's cardiovascular risk index II significantly increased in subjects with LDL-C greater than 100 mg/dL (Table 1).

Table 1. Anthropometric and biochemical parameters of the study subjects. The study participants were divided into two groups of LDL-C concentration, as follows: subjects with optimal concentration of LDL-C ≤ 100 mg/dL, and individuals with high concentration of LDL-C > 100 mg/dL. Total cholesterol and Castelli's atherogenic risk index significantly increased in patients with LDL-C greater than 100 mg/dL. Abbreviations: F, female; M, male; BMI, body mass index; LDL-C, low-density lipoproteins; HDL-C, high-density lipoproteins; HOMA-IR, homeostatic model assessment of insulin resistance; CRP, C-reactive protein; a.u., arbitrary units. Data are presented as mean ± standard deviation. Differences were considered significant when $p < 0.05$.

	LDL-C		
	<100 mg/dL	**>100 mg/dL**	***p*-Value**
Sex (F/M)	28/37	41/44	0.2650
Age (years)	47.2 ± 1.056	49.49 ± 1.031	0.1913
BMI (kg/m^2)	28.22 ± 1.172	28.05 ± 0.9035	0.9155
Waist circumference (cm)	91.58 ± 2.94	96.73 ± 2.002	0.1696
Body fat (%)	31.87 ± 1.696	31.91 ± 2.614	0.9909
Cholesterol (mg/dL)	166.7 ± 7.079	220.7 ± 4.723	<0.0001
Triglycerides (mg/dL)	242.6 ± 41.08	186.4 ± 11.14	0.0769
LDL-C (mg/dL)	76.53 ± 4.156	128.7 ± 3.653	<0.0001
HDL-C (mg/dL)	42.13 ± 3.44	47.06 ± 2.226	0.2332
Insulin (μU/L)	14.43 ± 1.057	13.52 ± 0.8046	0.5208
Glucose (mmol/L)	5.104 ± 0.2653	5.346 ± 0.2502	0.5675
HOMA-IR (a.u.)	3.299 ± 0.3261	3.126 ± 0.1866	0.6290
CRP (mg/L)	5.095 ± 0.4755	5.012 ± 0.6004	0.6328
Castelli's risk index II	1.966 ± 0.1827	2.892 ± 0.1294	0.0002

Confirming our in vitro results, the CM percentage significantly decreased in subjects with LDL-C > 100 mg/dL (Figure 5A). Although the IM percentage showed no differences (Figure 5B), the NCM percentage exhibited a significant 1.5-fold increase in individuals with LDL-C greater than 100 mg/dL (Figure 5C). The serum levels of IL-1 beta also significantly increased in subjects with LDL-C values above 100 mg/dL (Figure 5D). Moreover, LBP levels clearly raised in subjects with LDL-C > 100 mg/dL, suggesting the presence of abnormally high LPS serum values in these individuals (Figure 5E).

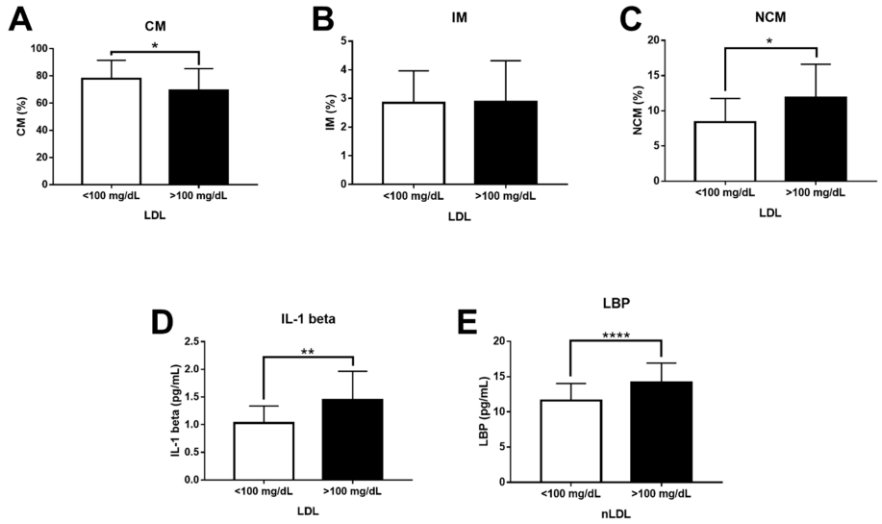

Figure 5. Levels of CMs, IMs, NCMs, IL-1 beta, and LBP in subjects with optimal and high serum levels of LDL-C. (**A**) The CM percentage significantly decreased in patients with serum LDL-C > 100 mg/dL (n = 85) as compared to controls (n = 65). (**B**) There were no significant changes between subjects with optimal and high LDL-C concentration for the IM percentage. (**C**) The NCM percentage significantly increased in patients with serum LDL-C > 100 mg/dL as compared to controls. (**D**) IL-1 beta serum levels significantly increased in patients with serum LDL-C > 100 mg/dL as compared to controls. (**E**) LBP serum levels significantly increased in patients with serum LDL-C > 100 mg/dL as compared to controls. Data are expressed as mean ± standard deviation. Data were compared using the unpaired Student's *t*-test. Differences were considered significant when $p < 0.05$. * = $p < 0.05$; ** = $p < 0.01$; **** = $p < 0.0001$. CM, classical monocytes; IM, intermediate monocytes; NCM, non-classical monocytes; IL-1 beta, interleukin 1 beta; LBP, LPS-binding protein; LDL-C, low-density lipoproteins.

4. Discussion

Macrophages and oxLDL are considered to be the main contributors to foam cell formation and inflammatory cell infiltration in atherosclerotic lesions [18]. However, the fact that monocytes and nLDL are able to interact in the blood stream has raised the question as to whether these precursors might also play a pivotal role in atherogenesis [19]. In this sense, intraperitoneal administration of triglyceride-rich lipoproteins decreases the number of non-classical Ly6C/Gr1low monocytes in mice [26]. Similarly, dyslipidemia with elevated levels of either LDL or very low-density lipoproteins (VLDL) increases both classical Ly6C/Gr1high and non-classical Ly6C/Gr1low monocyte subsets in mice fed a high-fat diet [19]. In line with this evidence, our results demonstrate that nLDL can alter the balance of human monocyte subpopulations by directly decreasing CMs and increasing NCMs in vitro and in vivo.

The mechanism through which nLDL induce imbalance of monocyte subsets remains unclear, and it probably involves CD14 and CD16 expression. As mentioned, CD14 and CD16 expression is the primary feature that defines monocyte subpopulations in humans [27]. CD14 is a transmembrane protein that forms the LPS receptor complex together with Toll-like receptor 4 (TLR4) and the myeloid differentiation factor 2 (MD-2) [28]. The trimeric CD14/TLR4/MD-2 complex triggers the nuclear factor kappa B (NFκB)-dependent signaling pathway in charge of regulating the expression of inflammatory cytokines such as IL-6, TNF-alpha, and IL-1 beta [29]. CD14 expression is regulated by specificity protein 1 (Sp1), a transcription factor that is activated via LDL receptor (LDLr)

promoter [30,31]. This body of evidence supports the idea that nLDL could decrease the CM proportion and increase the NCM percentage by regulating CD14 expression, probably via LDLr-Sp1. CD16 is an Fc-gamma receptor that recognizes IgG-coated microorganisms and immune complexes [32]. Recent evidence has demonstrated that CD16 expression is under the post-transcriptional control of microRNA (miR)-218 in human natural killer (NK) cells [33]. In vitro, oxLDL are able to decrease miR-218 expression in cardiac microvascular endothelial cells from rats. In vivo, miR-218 expression is inversely correlated with oxLDL levels in patients with coronary artery disease (CAD) [34]. In this sense, the increase in CD14+CD16+ non-classical monocytes and the decrease in CD14+CD16− classical monocytes that we found may be potentially related to the miR-218 suppression that in turn favors CD16 expression, promoting conversion of classical monocytes into non-classical monocytes in response to nLDL. Thus, circulating nLDL may induce imbalance of human monocyte subpopulations by mechanisms able to regulate CD14 and CD16 expression such as those orchestrated by LDLr, Sp1, and miR-218; however, this hypothesis remains to be elucidated in further studies.

A solid body of evidence has demonstrated that human monocyte subsets display important inflammatory actions by preferably expressing IL-1 beta in response to LPS [8,35]. LPS is a component of the outer membrane of Gram-negative bacteria that can translocate across the intestinal wall to the hepatic portal circulation, wherein it binds to LBP [36]. The LPS/LBP complex is considered a key inflammatory trigger for monocytes and macrophages and has been found to be increased in obese subjects with atherosclerotic heart disease, among whom nLDL is also increased [37,38]. Upon recognition, LPS induces the NFκB-dependent synthesis of pro-IL-1 beta, which in turn is proteolytically excised by the NOD-, LRR-, and pyrin domain-containing protein 3 (NLRP3) inflammasome to form mature IL-1 beta [39]. IL-1 beta has multiple functions in atherogenesis. In human microvascular endothelial cells, IL-1 beta stimulates the expression of the intracellular adhesion molecule-1 (ICAM-1) and the vascular cell adhesion molecule-1 (VCAM-1), which have the ability to recruit leukocytes into the inner layer of arteries [40]. In human aorta smooth muscle cells, IL-1 beta induces the expression of the monocyte chemoattractant protein-1 (MCP-1), which in turn contributes to mononuclear cell migration toward the vascular endothelium [41]. IL-1 beta also directly promotes atherosclerotic lesion formation by stimulating production of platelet-derived growth factor, a molecule with the ability to induce proliferation of vascular smooth muscle cells in the atheroma [42]. Interestingly, the exposure of endothelial cells and vascular smooth muscle cells to LPS increases release of IL-1 beta in atherosclerotic plaques of patients with suboptimally controlled hyperlipidemia LDL [43]. Our data expand on this body of evidence by demonstrating for the first time that LPS acts in synergy with nLDL to increase IL-1 beta synthesis in in vitro cultured human monocytes, especially CMs and IMs. In vivo, our results confirm this finding by revealing that subjects with elevated LDL-C serum levels also display higher LBP, IL-1 beta, and atherogenic index than those found in individuals with optimal LDL-C concentrations. However, it is worth mentioning that we still need to assess the potential effect of LDL particle number and size on the dynamics of human monocyte subpopulations and their ability to produce IL-1 beta, which may expand on the knowledge regarding the multiple actions of LDL in the inflammatory response associated with atherosclerosis.

nLDL and LPS not only displayed synergistic effects on the distribution of human monocyte subsets and their ability to produce IL-1 beta, but also affected the expression pattern of chemokine receptors such as CCR2 and CX3CR1. CCR2 is a C-C chemokine receptor mainly expressed in mononuclear cells that mediates migration of monocytes to inflamed tissues in response to MCP-1 [44]. CX3CR1 is the cell receptor for fractalkine, a chemokine with the ability to induce retention of monocytes in circulation, preferably those expressing CD16 such as IMs and NCMs [45]. In our study, the number of CCR2+ NCMs increased in response to nLDL and LPS, which may act in favor of promoting recruitment of these cells to the vascular endothelium. In line with these findings, a seminal work conducted by Han et al. informed that CCR2 expression increases in primary monocytes

from patients with elevated LDL-C serum values with respect to normocholesterolemic controls [46]. Additionally, exposure of THP-1 monocytes to nLDL induces a significant increase in both CCR2 expression and in vitro chemotactic response to MCP-1, suggesting that nLDL can directly enhance monocyte recruitment to the atherosclerotic lesion [46]. Concurring with the idea of increased cell recruitment, our data show that nLDL and LPS also decreased the amount of CX3CR1+ NCMs. In this sense, Nielsen et al. found altered expression of TNF-alpha and CX3CR1 in primary monocytes from patients with familial hypercholesterolemia as compared to subjects with normal LDL-C levels [47]. Interestingly, TNF-alpha and CX3CR1 expression positively correlated with increased intima-media thickness and hs-CRP, both of which are markers of atherosclerosis and cardiovascular risk [47]. In parallel, Geng et al. demonstrated that LPS administration to $ApoE^{-/-}$ mice enhances monocyte recruitment and macrophage accumulation in aortic atherosclerotic plaques, which concurs with increased lipid deposition in the atheroma [48]. Altogether, these findings support the idea that nLDL and LPS may directly contribute to atherogenesis by altering the expression pattern of inflammatory cytokines and chemokine receptors in monocytes, which may promote recruitment of these cells to atherosclerotic plaques. However, this notion should be still tested in in vivo experimental approaches focused on characterizing how nLDL and LPS affect the recruiting pattern of IL-1 beta-, CCR2-, and CX3CR1-producing monocytes to atherosclerotic lesions.

As we have outlined here, nLDL appear to have additional proinflammatory roles in atherogenesis that differed from those classically described for oxLDL [49]. Moreover, the effects of nLDL on the inflammatory ability of human monocyte subpopulations are enhanced by LPS, confirming previous evidence suggesting that nLDL and LBP form a negative loop that contributes to atherosclerosis [50–52].

5. Conclusions

In conclusion, using in vitro and in vivo complementary assays, this work demonstrates for the first time that nLDL act in synergy with LPS to alter the balance of human monocyte subsets and their ability to produce inflammatory cytokines and chemokine receptors with prominent roles in atherogenesis.

Author Contributions: Conceptualization, A.N.M.-R. and G.E.; methodology, A.N.M.-R., C.P.M.-R., J.A.A.-G., L.A.M.-G., M.E.-V., E.C.-T. and J.L.P.-C.; software data acquisition, J.L.P.-C. and A.N.M.-R.; formal analysis, A.N.M.-R., C.P.M.-R., S.L.-C., G.V.-A., J.M.F., O.P.-M. and G.E.; data curation, A.N.M.-R., S.L.-C., G.V.-A., O.P.-M., J.M.F. and G.E.; writing—original draft preparation, A.N.M.-R. and G.E.; writing—review and editing, S.L.-C., G.V.-A., J.M.F., O.P.-M. and G.E.; funding acquisition, G.E. All authors have read and agreed to the published version of the manuscript.

Funding: This work was supported by grant no. CB-2016-01-286209 from the Fondo Sectorial de Investigación para la Educación-CONACYT-México and grant no. SALUD-2017-02-290345 from the Fondo Sectorial de Investigación y Desarrollo en Salud y Seguridad Social SS/IMSS/ISSSTE/CONACYT-México to G.E.

Institutional Review Board Statement: The study was conducted in rigorous adherence to the principles described in the 1964 Declaration of Helsinki and its posterior amendment in 2013, and approved by the Ethics Committee of the General Hospital of Mexico with registration numbers of ethical approval code DI/20/501/03/17 and DIC/11/UME/05/029.

Informed Consent Statement: Informed consent was obtained from all subjects involved in the study.

Data Availability Statement: The data presented in this study are available upon request.

Acknowledgments: Aarón N. Manjarrez-Reyna is a doctoral student from the Programa de Doctorado en Ciencias Biomédicas, Universidad Nacional Autónoma de México (UNAM) and has received CONACyT fellowship 626423. The authors thank the Flow Cytometry core facility of "Coordinación de Investigación en Salud" at "Centro Médico Nacional Siglo XXI" of IMSS, Mexico for instrumentation and technical support.

Conflicts of Interest: The authors declare no conflict of interest regarding the publication of this article.

References

1. Song, P.; Fang, Z.; Wang, H.; Cai, Y.; Rahimi, K.; Zhu, Y.; Fowkes, F.G.R.; Fowkes, F.J.I.; Rudan, I. Global and regional prevalence, burden, and risk factors for carotid atherosclerosis: A systematic review, meta-analysis, and modelling study. *Lancet Glob. Health* **2020**, *8*, e721–e729. [CrossRef]
2. Markin, A.; Sobenin, I.A.; Grechko, A.V.; Zhang, D.; Orekhov, A.N. Cellular Mechanisms of Human Atherogenesis: Focus on Chronification of Inflammation and Mitochondrial Mutations. *Front. Pharmacol.* **2020**, *11*, 642. [CrossRef] [PubMed]
3. Kloc, M.; Uosef, A.; Villagran, M.; Zdanowski, R.; Kubiak, J.; Wosik, J.; Ghobrial, R. RhoA- and Actin-Dependent Functions of Macrophages from the Rodent Cardiac Transplantation Model Perspective—Timing Is the Essence. *Biology* **2021**, *10*, 70. [CrossRef]
4. Ganesan, R.; Henkels, K.M.; Wrenshall, L.E.; Kanaho, Y.; Di Paolo, G.; Frohman, M.A.; Gomez-Cambronero, J. Oxidized LDL phagocytosis during foam cell formation in atherosclerotic plaques relies on a PLD2-CD36 functional interdependence. *J. Leukoc. Biol.* **2018**, *103*, 867–883. [CrossRef]
5. Chen, C.; Khismatullin, D.B. Oxidized Low-Density Lipoprotein Contributes to Atherogenesis via Co-activation of Macrophages and Mast Cells. *PLoS ONE* **2015**, *10*, e0123088. [CrossRef] [PubMed]
6. Marimuthu, R.; Francis, H.; Dervish, S.; Li, S.C.; Medbury, H.; Williams, H. Characterization of Human Monocyte Subsets by Whole Blood Flow Cytometry Analysis. *J. Vis. Exp.* **2018**, e57941. [CrossRef] [PubMed]
7. Appleby, L.J.; Nausch, N.; Midzi, N.; Mduluza, T.; Allen, J.; Mutapi, F. Sources of heterogeneity in human monocyte subsets. *Immunol. Lett.* **2013**, *152*, 32–41. [CrossRef]
8. Mukherjee, R.; Barman, P.K.; Thatoi, P.K.; Tripathy, R.; Das, B.K.; Ravindran, B. Non-Classical monocytes display inflammatory features: Validation in Sepsis and Systemic Lupus Erythematous. *Sci. Rep.* **2015**, *5*, 13886. [CrossRef] [PubMed]
9. Tacke, F.; Alvarez, D.; Kaplan, T.J.; Jakubzick, C.; Spanbroek, R.; Llodra, J.; Garin, A.; Liu, J.; Mack, M.; Van Rooijen, N.; et al. Monocyte subsets differentially employ CCR2, CCR5, and CX3CR1 to accumulate within atherosclerotic plaques. *J. Clin. Investig.* **2007**, *117*, 185–194. [CrossRef]
10. Idzkowska, E.; Eljaszewicz, A.; Miklasz, P.; Musial, W.J.; Tycinska, A.M.; Moniuszko, M. The Role of Different Monocyte Subsets in the Pathogenesis of Atherosclerosis and Acute Coronary Syndromes. *Scand. J. Immunol.* **2015**, *82*, 163–173. [CrossRef]
11. Dimitrov, S.; Shaikh, F.; Pruitt, C.; Green, M.; Wilson, K.; Beg, N.; Hong, S. Differential TNF production by monocyte subsets under physical stress: Blunted mobilization of proinflammatory monocytes in prehypertensive individuals. *Brain Behav. Immun.* **2013**, *27*, 101–108. [CrossRef]
12. Cockx, M.; Gouwy, M.; Ruytinx, P.; Lodewijckx, I.; Van Hout, A.; Knoops, S.; Pörtner, N.; Ronsse, I.; Vanbrabant, L.; Godding, V.; et al. Monocytes from patients with Primary Ciliary Dyskinesia show enhanced inflammatory properties and produce higher levels of pro-inflammatory cytokines. *Sci. Rep.* **2017**, *7*, 14657. [CrossRef] [PubMed]
13. González, Y.; Herrera, M.T.; Soldevila, G.; Garcia-Garcia, L.; Fabián, G.; Pérez-Armendariz, E.M.; Bobadilla, K.; Guzman-Beltran, S.; Sada, E.; Torres, M. High glucose concentrations induce TNF-α production through the down-regulation of CD33 in primary human monocytes. *BMC Immunol.* **2012**, *13*, 19. [CrossRef] [PubMed]
14. Dasu, M.R.; Jialal, I. Free fatty acids in the presence of high glucose amplify monocyte inflammation via Toll-like receptors. *Am. J. Physiol. Endocrinol. Metab.* **2011**, *300*, E145–E154. [CrossRef]
15. Grün, J.L.; Manjarrez-Reyna, A.N.; Gómez-Arauz, A.Y.; Leon-Cabrera, S.; Rückert, F.; Fragoso, J.M.; Bueno-Hernández, N.; Islas-Andrade, S.; Meléndez-Mier, G.; Escobedo, G. High-Density Lipoprotein Reduction Differentially Modulates to Classical and Nonclassical Monocyte Subpopulations in Metabolic Syndrome Patients and in LPS-Stimulated Primary Human Monocytes In Vitro. *J. Immunol. Res.* **2018**, *2018*, 2737040. [CrossRef]
16. Kopp, F.; Kupsch, S.; Schromm, A.B. Lipopolysaccharide-binding protein is bound and internalized by host cells and colocalizes with LPS in the cytoplasm: Implications for a role of LBP in intracellular LPS-signaling. *Biochim. Biophys. Acta Bioenerg.* **2016**, *1863*, 660–672. [CrossRef]
17. Aw, N.H.; Canetti, E.; Suzuki, K.; Goh, J. Monocyte Subsets in Atherosclerosis and Modification with Exercise in Humans. *Antioxidants* **2018**, *7*, 196. [CrossRef]
18. Orekhov, A.N.; Oishi, Y.; Nikiforov, N.G.; Zhelankin, A.V.; Dubrovsky, L.; Sobenin, I.A.; Kel, A.; Stelmashenko, D.; Makeev, V.J.; Foxx, K.; et al. Modified LDL Particles Activate Inflammatory Pathways in Monocyte-derived Macrophages: Transcriptome Analysis. *Curr. Pharm. Des.* **2018**, *24*, 3143–3151. [CrossRef] [PubMed]
19. Jackson, W.; Weinrich, T.W.; Woollard, K.J. Very-low and low-density lipoproteins induce neutral lipid accumulation and impair migration in monocyte subsets. *Sci. Rep.* **2016**, *6*, 20038. [CrossRef]
20. Combadiere, C.; Potteaux, S.; Rodero, M.; Simon, T.; Pezard, A.; Esposito, B.; Merval, R.; Proudfoot, A.; Tedgui, A.; Mallat, Z. Combined Inhibition of CCL2, CX3CR1, and CCR5 Abrogates Ly6C hi and Ly6C lo Monocytosis and Almost Abolishes Atherosclerosis in Hypercholesterolemic Mice. *Circulation* **2008**, *117*, 1649–1657. [CrossRef] [PubMed]
21. Wang, J.; Si, Y.; Wu, C.; Sun, L.; Ma, Y.; Ge, A.; Li, B. Lipopolysaccharide promotes lipid accumulation in human adventitial fibroblasts via TLR4-NF-κB pathway. *Lipids Health Dis.* **2012**, *11*, 139. [CrossRef] [PubMed]
22. Ahola, A.J.; Lassenius, M.I.; Forsblom, C.; Harjutsalo, V.; Lehto, M.; Groop, P.-H. Dietary patterns reflecting healthy food choices are associated with lower serum LPS activity. *Sci. Rep.* **2017**, *7*, 6511. [CrossRef] [PubMed]
23. Pendyala, S.; Walker, J.M.; Holt, P.R. A High-Fat Diet Is Associated With Endotoxemia That Originates From the Gut. *Gastroenterol.* **2012**, *142*, 1100–1101.e2. [CrossRef] [PubMed]

24. Zawada, A.M.; Fell, L.H.; Untersteller, K.; Seiler, S.; Rogacev, K.S.; Fliser, D.; Ziegler-Heitbrock, L.; Heine, G.H. Comparison of two different strategies for human monocyte subsets gating within the large-scale prospective CARE FOR HOMe Study. *Cytom. Part A* **2015**, *87*, 750–758. [CrossRef] [PubMed]
25. Expert Panel on Detection, Evaluation, and Treatment of High Blood Cholesterol in Adults. Executive Summary of the Third Report of the National Cholesterol Education Program (NCEP) Expert Panel on Detection, Evaluation, and Treatment of High Blood Cholesterol in Adults (Adult Treatment Panel III). *JAMA* **2001**, *285*, 2486–2497. [CrossRef] [PubMed]
26. Saja, M.F.; Baudino, L.; Jackson, W.; Cook, H.T.; Malik, T.H.; Fossati-Jimack, L.; Ruseva, M.; Pickering, M.C.; Woollard, K.J.; Botto, M. Triglyceride-Rich Lipoproteins Modulate the Distribution and Extravasation of Ly6C/Gr1low Monocytes. *Cell Rep.* **2015**, *12*, 1802–1815. [CrossRef] [PubMed]
27. Merah-Mourah, F.; Cohen, S.O.; Charron, D.; Mooney, N.; Haziot, A. Identification of Novel Human Monocyte Subsets and Evidence for Phenotypic Groups Defined by Interindividual Variations of Expression of Adhesion Molecules. *Sci. Rep.* **2020**, *10*, 4397. [CrossRef] [PubMed]
28. Calvano, J.E.; Agnese, D.; Um, J.Y.; Goshima, M.; Singhal, R.; Coyle, S.M.; Reddell, M.T.; Kumar, A.; Calvano, S.E.; Lowry, S.F. Modulation of the Lipopolysaccharide Receptor Complex (CD14, TLR4, MD-2) and Toll-Like Receptor 2 in Systemic Inflammatory Response Syndrome-Positive Patients With and Without Infection: Relationship to Tolerance. *Shock.* **2003**, *20*, 415–419. [CrossRef]
29. Ott, L.W.; Resing, K.A.; Sizemore, A.W.; Heyen, J.W.; Cocklin, R.R.; Pedrick, N.M.; Woods, H.C.; Chen, J.Y.; Goebl, M.G.; Witzmann, F.A.; et al. Tumor Necrosis Factor-alpha- and interleukin-1-induced cellular responses: Coupling proteomic and genomic information. *J. Proteome. Res.* **2007**, *6*, 2176–2185. [CrossRef]
30. E Zhang, D.; Hetherington, C.J.; Gonzalez, D.A.; Chen, H.M.; Tenen, D. Regulation of CD14 expression during monocytic differentiation induced with 1 alpha,25-dihydroxyvitamin D. *J. Immunol.* **1994**, *153*, 3276–3284.
31. Yieh, L.; Sanchez, H.B.; Osborne, T.F. Domains of transcription factor Sp1 required for synergistic activation with sterol regulatory element binding protein 1 of low density lipoprotein receptor promoter. *Proc. Natl. Acad. Sci. USA* **1995**, *92*, 6102–6106. [CrossRef]
32. Junker, F.; Gordon, J.; Qureshi, O. Fc Gamma Receptors and Their Role in Antigen Uptake, Presentation, and T Cell Activation. *Front. Immunol.* **2020**, *11*, 1393. [CrossRef] [PubMed]
33. Victor, A.R.; Weigel, C.; Scoville, S.D.; Chan, W.K.; Chatman, K.; Nemer, M.M.; Mao, C.; Young, K.A.; Zhang, J.; Yu, J.; et al. Epigenetic and Posttranscriptional Regulation of CD16 Expression during Human NK Cell Development. *J. Immunol.* **2017**, *200*, 565–572. [CrossRef] [PubMed]
34. Gao, W.; Cui, H.; Li, Q.; Zhong, H.; Yu, J.; Li, P.; He, X. Upregulation of microRNA-218 reduces cardiac microvascular endothelial cells injury induced by coronary artery disease through the inhibition of HMGB. *J. Cell. Physiol.* **2020**, *235*, 3079–3095. [CrossRef] [PubMed]
35. Devêvre, E.F.; Renovato-Martins, M.; Clément, K.; Sautes-Fridman, C.; Cremer, I.; Poitou, C. Profiling of the Three Circulating Monocyte Subpopulations in Human Obesity. *J. Immunol.* **2015**, *194*, 3917–3923. [CrossRef]
36. Guerville, M.; Boudry, G. Gastrointestinal and hepatic mechanisms limiting entry and dissemination of lipopolysaccharide into the systemic circulation. *Am. J. Physiol. Liver Physiol.* **2016**, *311*, G1–G15. [CrossRef]
37. Hersoug, L.; Møller, P.; Loft, S. Gut microbiota-derived lipopolysaccharide uptake and trafficking to adipose tissue: Implications for inflammation and obesity. *Obes. Rev.* **2016**, *17*, 297–312. [CrossRef]
38. Lepper, P.M.; Schumann, C.; Triantafilou, K.; Rasche, F.M.; Schuster, T.; Frank, H.; Schneider, E.M.; Triantafilou, M.; von Eynatten, M. Association of Lipopolysaccharide-Binding Protein and Coronary Artery Disease in Men. *J. Am. Coll. Cardiol.* **2007**, *50*, 25–31. [CrossRef]
39. Zasłona, Z.; Pålsson-McDermott, E.M.; Menon, D.; Haneklaus, M.; Flis, E.; Prendeville, H.; Corcoran, S.E.; Peters-Golden, M.; O'Neill, L.A.J. The Induction of Pro–IL-1β by Lipopolysaccharide Requires Endogenous Prostaglandin E2Production. *J. Immunol.* **2017**, *198*, 3558–3564. [CrossRef]
40. Haraldsen, G.; Kvale, D.; Lien, B.; Farstad, I.N.; Brandtzaeg, P. Cytokine-regulated expression of E-selectin, intercellular adhesion molecule-1 (ICAM-1), and vascular cell adhesion molecule-1 (VCAM-1) in human microvascular endothelial cells. *J. Immunol.* **1996**, *156*, 2558–2565. [PubMed]
41. Lim, J.H.; Um, H.J.; Park, J.-W.; Lee, I.-K.; Kwon, T.K. Interleukin-1β promotes the expression of monocyte chemoattractant protein-1 in human aorta smooth muscle cells via multiple signaling pathways. *Exp. Mol. Med.* **2009**, *41*, 757–764. [CrossRef]
42. Libby, P. Interleukin-1 Beta as a Target for Atherosclerosis Therapy. *J. Am. Coll. Cardiol.* **2017**, *70*, 2278–2289. [CrossRef] [PubMed]
43. Jiang, X.; Wang, F.; Wang, Y.; Gisterå, A.; Roy, J.; Paulsson-Berne, G.; Hedin, U.; Lerman, A.; Hansson, G.K.; Herrmann, J.; et al. Inflammasome-Driven Interleukin-1α and Interleukin-1β Production in Atherosclerotic Plaques Relates to Hyperlipidemia and Plaque Complexity. *JACC Basic Transl. Sci.* **2019**, *4*, 304–317. [CrossRef] [PubMed]
44. Teh, Y.C.; Ding, J.L.; Ng, L.G.; Chong, S.Z. Capturing the Fantastic Voyage of Monocytes Through Time and Space. *Front. Immunol.* **2019**, *10*, 834. [CrossRef] [PubMed]
45. Ancuta, P.; Rao, R.; Moses, A.; Mehle, A.; Shaw, S.K.; Luscinskas, F.W.; Gabuzda, D. Fractalkine Preferentially Mediates Arrest and Migration of CD16+ Monocytes. *J. Exp. Med.* **2003**, *197*, 1701–1707. [CrossRef]
46. Han, K.H.; Tangirala, R.K.; Green, S.R.; Quehenberger, O. Chemokine receptor CCR2 expression and monocyte chemoattractant protein-1-mediated chemotaxis in human monocytes. A regulatory role for plasma LDL. *Arterioscler. Thromb. Vasc. Biol.* **1998**, *18*, 1983–1991. [CrossRef] [PubMed]

47. Nielsen, M.H.; Irvine, H.; Vedel, S.; Raungaard, B.; Beck-Nielsen, H.; Handberg, A. Elevated Atherosclerosis-Related Gene Expression, Monocyte Activation and Microparticle-Release Are Related to Increased Lipoprotein-Associated Oxidative Stress in Familial Hypercholesterolemia. *PLoS ONE* **2015**, *10*, e0121516. [CrossRef]
48. Geng, S.; Chen, K.; Yuan, R.; Peng, L.; Maitra, U.; Diao, N.; Chen, C.; Zhang, Y.; Hu, Y.; Qi, C.-F.; et al. The persistence of low-grade inflammatory monocytes contributes to aggravated atherosclerosis. *Nat. Commun.* **2016**, *7*, 13436. [CrossRef]
49. Poznyak, A.V.; Nikiforov, N.G.; Markin, A.M.; Kashirskikh, D.A.; Myasoedova, V.A.; Gerasimova, E.V.; Orekhov, A.N. Overview of OxLDL and Its Impact on Cardiovascular Health: Focus on Atherosclerosis. *Front. Pharmacol.* **2021**, *11*, 613780. [CrossRef]
50. Bowman, J.D.; Surani, S.; Horseman, M. Endotoxin, Toll-like Receptor-4, and Atherosclerotic Heart Disease. *Curr. Cardiol. Rev.* **2017**, *13*, 86–93. [CrossRef]
51. Grin, P.; Dwivedi, D.J.; Chathely, K.M.; Trigatti, B.; Dino, L.; Prat, A.; Seidah, N.; Liaw, P.C.; Fox-Robichaud, A.E. Low-density lipoprotein (LDL)-dependent uptake of Gram-positive lipoteichoic acid and Gram-negative lipopolysaccharide occurs through LDL receptor. *Sci. Rep.* **2018**, *8*, 10496. [CrossRef] [PubMed]
52. Vreugdenhil, A.C.; Snoek, A.P.; van 't Veer, C.; Greve, J.W.; Buurman, W.A. LPS-binding protein circulates in association with apoB-containing lipoproteins and enhances endotoxin-LDL/VLDL interaction. *J. Clin. Investig.* **2001**, *107*, 225–234. [CrossRef] [PubMed]

Hindawi
Journal of Immunology Research
Volume 2019, Article ID 6105059, 10 pages
https://doi.org/10.1155/2019/6105059

Clinical Study

A Single 48 mg Sucralose Sip Unbalances Monocyte Subpopulations and Stimulates Insulin Secretion in Healthy Young Adults

Angélica Y. Gómez-Arauz,[1] Nallely Bueno-Hernández,[1] Leon F. Palomera,[1] Raúl Alcántara-Suárez,[1] Karen L. De León,[1] Lucía A. Méndez-García,[1] Miguel Carrero-Aguirre,[1] Aaron N. Manjarrez-Reyna,[1] Camilo P. Martínez-Reyes,[1] Marcela Esquivel-Velázquez,[1] Alejandra Ruiz-Barranco,[2] Neyla Baltazar-López,[3] Sergio Islas-Andrade,[1] Galileo Escobedo,[1] and Guillermo Meléndez[1]

[1]*Laboratory for Proteomics and Metabolomics, Research Division, General Hospital of Mexico "Dr. Eduardo Liceaga", 06720 Mexico City, Mexico*
[2]*Clinical Nutrition Division, General Hospital of Mexico "Dr. Eduardo Liceaga", 06720 Mexico City, Mexico*
[3]*Research Coordination at Central Laboratories, General Hospital of Mexico "Dr. Eduardo Liceaga", 06720 Mexico City, Mexico*

Correspondence should be addressed to Galileo Escobedo; gescobedog@msn.com
and Guillermo Meléndez; melendez651@gmail.com

Received 12 December 2018; Revised 25 February 2019; Accepted 14 March 2019; Published 28 April 2019

Guest Editor: Daniel Ortuño-Sahagún

Sucralose is a noncaloric artificial sweetener that is widely consumed worldwide and has been associated with alteration in glucose and insulin homeostasis. Unbalance in monocyte subpopulations expressing CD11c and CD206 hallmarks metabolic dysfunction but has not yet been studied in response to sucralose. Our goal was to examine the effect of a single sucralose sip on serum insulin and blood glucose and the percentages of classical, intermediate, and nonclassical monocytes in healthy young adults subjected to an oral glucose tolerance test (OGTT). This study was a randomized, placebo-controlled clinical trial. Volunteers randomly received 60 mL water as placebo ($n = 20$) or 48 mg sucralose dissolved in 60 mL water ($n = 25$), fifteen minutes prior to an OGTT. Blood samples were individually drawn every 15 minutes for 180 minutes for quantifying glucose and insulin concentrations. Monocyte subsets expressing CD11c and CD206 were measured at -15 and 180 minutes by flow cytometry. As compared to controls, volunteers receiving sucralose exhibited significant increases in serum insulin at 30, 45, and 180 minutes, whereas blood glucose values showed no significant differences. Sucralose consumption caused a significant 7% increase in classical monocytes and 63% decrease in nonclassical monocytes with respect to placebo controls. Pearson's correlation models revealed a strong association of insulin with sucralose-induced monocyte subpopulation unbalance whereas glucose values did not show significant correlations. Sucralose ingestion decreased CD11c expression in all monocyte subsets and reduced CD206 expression in nonclassical monocytes suggesting that sucralose does not only unbalance monocyte subpopulations but also alter their expression pattern of cell surface molecules. This work demonstrates for the first time that a 48 mg sucralose sip increases serum insulin and unbalances monocyte subpopulations expressing CD11c and CD206 in noninsulin-resistant healthy young adults subjected to an OGTT. The apparently innocuous consumption of sucralose should be reexamined in light of these results.

1. Introduction

Noncaloric artificial sweeteners, including aspartame, acesulfame k, and sucralose, are food additives that preserve the taste of sweetness without increasing the calories of food and beverages [1]. For this reason, consumption of noncaloric artificial sweeteners is now widely spread among people from all ages and socioeconomic status worldwide [2, 3].

Nevertheless, a growing number of clinical and experimental studies have now suggested that noncaloric artificial sweeteners are linked to the development of metabolic abnormalities including insulin resistance and glucose intolerance, especially sucralose [4–8]. A seminal study demonstrated that ingestion of 48 mg sucralose significantly increases the serum values of glucose and insulin in morbidly obese subjects of both sexes subjected to a 75 g oral glucose tolerance test (OGTT) [9]. Similarly, overweight subjects that consumed sucralose prior to an OGTT exhibited a 1.2-fold elevation in the insulin peak as compared to placebo controls [10]. Therefore, the apparently innocuous effect of sucralose and others noncaloric artificial sweeteners on glucose and insulin homeostasis should be reexamined in light of this evidence.

It is now well accepted that low-grade systemic inflammation is a central player in obesity and contributes to the pathogenesis of metabolic disease, especially alteration of glucose and insulin homeostasis [11–13]. Besides being characterized by abnormally high levels of cytokines such as tumor necrosis factor alpha (TNF-alpha) and interleukin-1 beta (IL-1beta), low-grade systemic inflammation is accompanied by alteration in monocyte subpopulations [14]. In humans, circulating monocytes are sorted in three different subpopulations according to the cell surface expression of CD14 and CD16 [15]. Classical monocytes exhibit high CD14 levels and show no expression of CD16 ($CD14^{++}$ $CD16^{-}$). The intermediate monocyte subpopulation shows high CD14 expression and also exhibit CD16 expression ($CD14^{++}CD16^{+}$) whereas nonclassical monocytes produce low CD14 levels and show expression of CD16 ($CD14^{+}$ $CD16^{+}$) [15, 16]. Interestingly, the percentage of nonclassical monocytes has been shown to elevate in obese subjects that exhibit increased insulin resistance and metabolic syndrome [17, 18]. In the same sense, the classical monocyte subpopulation has been shown to increase in obese individuals and correlates with higher proportion of $CD11c^{+}$ macrophages in the visceral adipose tissue (VAT) [19]. CD11c is a beta-2 integrin with prominent functions in cell adherence of monocytes and macrophages to vascular endothelial tissue and VAT [19, 20]. Furthermore, monocytes have been shown to express CD206 [21], a cell surface marker highly expressed in anti-inflammatory macrophages that is also associated with improved insulin sensitivity in both humans and mice [22, 23]. In this way, modulation of CD11c and CD206 expression in monocyte-macrophage lineage cells is crucial not only in typical immune functions such as cell migration and inflammation but also in obesity and insulin resistance [24]. Thus, imbalance in monocyte subpopulations expressing CD11c and CD206 hallmarks metabolic dysfunction but has not yet been studied in response to noncaloric artificial sweetener consumption such as sucralose.

The main goal of this study was to examine the effect of a single sucralose sip on the percentages of classical, intermediate, and nonclassical monocytes expressing CD11c and CD206 in healthy young adults subjected to an OGTT, while also exploring the possible relationship of monocyte subpopulations with changes in glucose and insulin homeostasis.

2. Materials and Methods

2.1. Subjects and Study Design. Forty-five healthy adult volunteers of both sexes with homeostasis model assessment (HOMA) values ≤3.8, aging between 18 and 35 years, who attended to the Department of Internal Medicine and the Laboratory for Proteomics and Metabolomics of the General Hospital of Mexico from September 2016 to April 2018 were included in the randomized, parallel-group, placebo-controlled clinical trial. All of the study participants provided written informed consent, previously approved by the Institutional Ethical Committee of the General Hospital of Mexico, which guaranteed that the study was conducted in rigorous adherence to the principles described in the 1964 Declaration of Helsinki and its posterior amendment in 2013. Subjects were excluded of the study if they had previous diagnosis of type 1 diabetes mellitus (T1D), type 2 diabetes mellitus (T2D), cardiovascular disease, acute or chronic liver disease, acute or chronic renal disease, cancer, endocrine disorders, infectious diseases, and inflammatory or autoimmune disease. We also excluded of the study to HIV-, HCV-, and HBV-seropositive patients, pregnant or lactating women, and individuals with anti-inflammatory, antiaggregant, antihypertensive, and immunomodulatory medication including nonsteroidal anti-inflammatory drugs. All participants included in the study had 8-10 hr overnight fasting before being subjected to the OGTT.

2.2. Oral Glucose Tolerance Test. The present study was a randomized, parallel-group, placebo-controlled clinical trial, where volunteers randomly drank 60 mL water as placebo ($n = 20$) or 48 mg sucralose dissolved in 60 mL water ($n = 25$), fifteen minutes prior to an OGTT. A regular "light" beverage available in the market approximately contains 48 mg sucralose. For this reason, we decided to use 48 mg sucralose dissolved in 60 mL water, as previously reported [9]. Each participant had up to three minutes to finish the sip of water or sucralose. Starting with oral glucose load at min zero, venous blood samples were drawn from all study subjects every 15 min for 180 min for quantifying the blood levels of glucose and insulin. Additional blood samples were also collected at -15 and 180 min for white blood cell isolation and characterization of monocyte subpopulations by flow cytometry.

2.3. Anthropometric and Biochemical Measurements. Body mass index (BMI), waist circumference, and blood pressure were measured in all study volunteers. Serum levels of insulin were measured in triplicate by the enzyme-linked immunosorbent assay (ELISA) following the manufacturer's instructions (Abnova Corporation, Taiwan). Serum levels of glucose were measured in triplicate by the glucose oxidase assay, following the manufacturer's instructions (Megazyme International, Ireland). The HOMA index was individually calculated by multiplying glucose concentration (mmol/L) by insulin concentration (mU/L) and then divided by 22.5. The cut-off point for HOMA index was established according to studies previously validated in a Mexican population [25]. Total cholesterol, low-density lipoproteins (LDL), high-

density lipoproteins (HDL), and triglyceride levels were measured in triplicate by enzymatic assays following the manufacturer's instructions (Roche Diagnostics, Mannheim, Germany). Glycated hemoglobin (HbA1c), blood urea nitrogen (BUN), serum creatinine, and hematic biometry were determined by standard laboratory assays.

2.4. Flow Cytometry. Isolation of white blood cells was performed by centrifuging blood samples previously collected in tubes containing EDTA (Vacutainer™, BD Diagnostics, NJ, USA) at 1800 g for 10 min. Then, white blood cells were placed in 1.6 mL pyrogen-free Eppendorf tubes containing 1 mL ACK Lysing Buffer (Life Technologies, USA) and incubated at 4°C for 5 min. Afterward, cell suspension was centrifuged at 1800 g/4°C for 10 min and cell pellets washed twice with PBS 1x (Sigma-Aldrich, Mexico). After an additional centrifugation step and removal of the supernatant, cell pellets were resuspended in 50 μL PBS 1x (Sigma-Aldrich, Mexico). Immediately after, 3 μL Human TruStrain Reagent (BioLegend Inc., USA) was added to 2×10^5 white blood cells and then incubated for 10 min at 4°C. Then, each cell suspension was incubated with anti-CD14 PE/Cy7, anti-CD16 FITC, anti-CD11c APC, and anti-CD206 PE (BioLegend Inc., USA) for 30 min at 4°C. Flow cytometry analysis was performed on a FACSCanto II flow cytometer by using the BD FACSDiva™ software 6.0 (BD Biosciences, Mexico), acquiring 1×10^5 monocyte events per test in duplicate.

2.5. Gating Strategy for Flow Cytometry. White blood cells were gated for singlets on a forward scatter height/forward scatter area density plot. Afterward, areas corresponding to lymphocyte, polymorphonuclear leukocyte, and monocyte cell populations were clearly revealed and gated on a FSC-A/side scatter area plot. The monocyte gate was then selected for detection of living monocytes by using the Live/Dead Aqua Stain (Thermo Fisher Scientific Inc., USA) and posterior measurement of CD14, CD16, CD11c, and CD206 exclusively on this immune cell population. In this way, we deliberately excluded any other CD14-CD16-CD11c-CD206 signal coming from a different cellular source than monocytes. Monocyte subpopulations were then characterized according to the cell surface expression of CD14 and CD16 as follows: $CD14^{++}CD16^{-}$, classical monocytes; $CD14^{++}CD16^{+}$, intermediate monocytes; and $CD14^{+}CD16^{+}$, nonclassical monocytes.

2.6. Statistics. Normality of data distribution was estimated by the Shapiro-Wilk test. The Student T-test was used to compare the placebo and sucralose groups regarding age, BMI, waist circumference, systolic and diastolic blood pressure, blood glucose, glycated hemoglobin percentage, serum insulin, HOMA-IR, total cholesterol, LDL, HDL, triglycerides, blood urea nitrogen, serum creatinine, and hematic biometry, and data were expressed as mean ± standard deviation. The mean fluorescence intensity (MFI) of CD11c and CD206 as well as the percentages of classical, intermediate, and nonclassical monocytes at -15 and 180 min of the OGTT were analyzed using two-tailed 2-way ANOVA with correction for multiple comparisons by means of the Bonferroni multiple comparison test, and data were expressed as media ± standard deviation. Differences in the mean values of glucose and insulin at -15, 0, 15, 30, 45, 60, 75, 90, 105, 120, and 180 min of the OGTT, between volunteers enrolled in placebo or sucralose groups, were estimated by means of two-tailed 2-way ANOVA with correction for multiple comparisons using the Bonferroni multiple comparison test. Furthermore, the women/men proportion in placebo and sucralose groups was analyzed by means of the chi-squared test and data expressed as absolute values. Pearson's correlation coefficients were estimated for examining the statistical correlation of classical, intermediate, and nonclassical monocytes with glucose and insulin and expressed as coefficients (r) and P values. Differences were considered significant when $P < 0.05$. Statistical analyses were performed by means of the GraphPad Prism 6.01 software (GraphPad Software, La Jolla, CA 92037 USA).

3. Results

There were no differences between subjects receiving placebo ($n = 20$) or sucralose ($n = 25$) in terms of demographic, metabolic, and hematic characteristics, including gender, age, BMI, HOMA-IR, lipid profile, renal function, and monocytes per microliter of blood (Table 1).

Blood glucose values showed no significant differences in subjects receiving placebo or sucralose all along the oral glucose tolerance test (Figure 1(a)). On the contrary, volunteers that received 48 mg sucralose prior glucose load showed a significant 1.3-fold increase in the serum levels of insulin at 30 min as compared to subjects drinking water as placebo ($P = 0.041$) (Figure 1(b)). At 45 min, subjects receiving sucralose exhibited a significant 1.4-fold elevation in serum insulin with respect to placebo controls ($P = 0.046$) (Figure 1(b)). At 180 min, subjects that received sucralose showed a significant 2-fold increase in the serum levels of insulin as compared to placebo controls ($P = 0.048$) (Figure 1(b)).

Representative dot plots illustrating monocyte subpopulations in subjects that received placebo or sucralose are shown in Figure 2. At the beginning of the oral glucose tolerance test (-15 min), no differences were seen in the percentages of classical, intermediate, and nonclassical monocytes in subjects receiving placebo or sucralose (Figure 2(a) versus 2c, respectively). At the end of the experiment (180 min), the percentage of classical monocytes increased in subjects that received 48 mg sucralose as compared to placebo controls (Figure 2(d) versus 2b, respectively). In contrast, the nonclassical monocyte percentage was reduced in subjects exposed to sucralose with respect to placebo controls (Figure 2(d) versus 2b, respectively). Quantification of monocyte subpopulation percentages confirmed a significant 7% increase in the number of classical monocytes from subjects that received sucralose in comparison to controls receiving placebo ($P = 0.0028$) (Figure 2(e)). On the other side, the nonclassical monocyte percentage exhibited a significant 63% reduction in subjects exposed to sucralose with respect to placebo controls ($P < 0.0001$) (Figure 2(e)). No significant differences were found in the percentage of intermediate monocytes in subjects that received placebo or sucralose.

Table 1: Demographic, metabolic, and hematic characteristics of the study population.

Parameters	Placebo	Sucralose	P value
Gender (W/M)	8/12	8/17	0.288
Age (years)	21.55 ± 2.18	22.36 ± 2.99	0.158
BMI (kg/m^2)	24.58 ± 3.63	23.67 ± 2.88	0.177
Waist circumference (cm)	82.27 ± 8.44	78.57 ± 8.37	0.074
SBP (mmHg)	111.10 ± 8.16	113.70 ± 13.91	0.225
DBP (mmHg)	70.75 ± 5.77	71.16 ± 7.33	0.419
Blood glucose (mg/dL)	88.20 ± 6.65	89.96 ± 5.68	0.172
HbA1c (%)	5.26 ± 0.24	5.23 ± 0.19	0.497
Serum insulin (μU/L)	7.94 ± 2.91	8.31 ± 2.82	0.335
HOMA-IR (a.u.)	1.75 ± 0.70	1.85 ± 0.65	0.298
Total cholesterol (mg/dL)	166.70 ± 31.21	168.60 ± 32.53	0.418
LDL (mg/dL)	102.10 ± 28.92	99.80 ± 26.60	0.393
HDL (mg/dL)	43.05 ± 10.60	44.40 ± 12.20	0.349
Triglycerides (mg/dL)	111.20 ± 58.10	118.20 ± 102.70	0.392
BUN (mg/dL)	22.40 ± 6.98	23.71 ± 5.95	0.249
Serum creatinine (mg/dL)	0.82 ± 0.13	0.78 ± 0.13	0.165
Hematocrit (%)	45.63 ± 3.53	44.04 ± 4.37	0.097
Total leukocytes ($10^3/\mu$L)	6.38 ± 1.49	6.05 ± 0.96	0.187
Monocytes ($10^3/\mu$L)	0.43 ± 0.11	0.39 ± 0.10	0.109
Monocytes (%)	6.94 ± 1.77	6.42 ± 1.33	0.134

Data are expressed as media ± standard deviation. The Shapiro-Wilk test was used to estimate normality in data distribution. Significant differences were estimated by means of performing the Student T-test with the exception of women/men proportion that was estimated by means of the chi-squared test. Differences were considered significant when $P < 0.05$. Abbreviations: W: women; M: men; BMI: body mass index; SBP: systolic blood pressure; DBP: diastolic blood pressure; HbA1c: glycated hemoglobin; HOMA-IR: homeostatic model assessment of insulin resistance; LDL: low-density lipoprotein; HDL: high-density lipoprotein; BUN: blood urea nitrogen; a.u.: arbitrary units.

Analysis of Pearson's correlation coefficients showed no significant associations of monocyte subpopulations with blood glucose (Table 2). On the contrary, serum insulin showed a positive relationship with classical monocytes ($r = 0.41$, $P = 0.02$), whereas it also exhibited a strong inverse association with nonclassical monocytes ($r = -0.42$, $P = 0.01$) (Table 2).

At the beginning of the OGTT, CD11c expression in classical, intermediate, and nonclassical monocytes showed no significant differences in subjects receiving placebo or sucralose (Figure 3(a)). At 180 min, CD11c expression was significantly reduced in intermediate and nonclassical monocytes of subjects receiving sucralose as compared to placebo controls ($P = 0.0012$ and $P = 0.0064$, respectively) (Figure 3(a)). CD11c expression also exhibited a significant reduction in intermediate and nonclassical monocytes of subjects exposed to sucralose at the beginning (-15 min) and at the end (180 min) of the OGTT ($P = 0.0004$ and $P = 0.0001$, respectively) (Figure 3(a)). In classical monocytes, CD11c expression significantly diminished in the sucralose group at the beginning (-15 min) and at the end (180 min) of the OGTT ($P = 0.0008$) (Figure 3(a)).

At the beginning of the OGTT, CD206 expression in classical, intermediate, and nonclassical monocytes showed no significant differences in subjects that received placebo or sucralose (Figure 3(b)). At 180 min, CD206 expression was significantly reduced in nonclassical monocytes of volunteers that received sucralose as compared to placebo controls ($P = 0.0098$) (Figure 3(b)).

4. Discussion

Noncaloric artificial sweeteners are now consumed by millions of people from all ages, gender, and socioeconomic status around the globe [26]. However, sucralose and other noncaloric artificial sweeteners have been now linked to disturbances in glucose and insulin homeostasis in both animal models and humans [5–9]. For this reason, it is still of great relevance to keep characterizing the possible deleterious effects of sucralose on human metabolism in randomized, parallel-group, placebo-controlled clinical trials.

In this study, we found that one single 48 mg sip of sucralose, a sucralose amount that is contained in numerous "light" beverages available in the market, increases serum insulin but not glucose in age- and sex-matched healthy young adults subjected to an OGTT. These data appear contrary to previous information showing that a similar amount of sucralose is able to elevate both insulin and glucose in morbidly obese individuals receiving a glucose load [9]. Nevertheless, this apparently contradictory evidence should

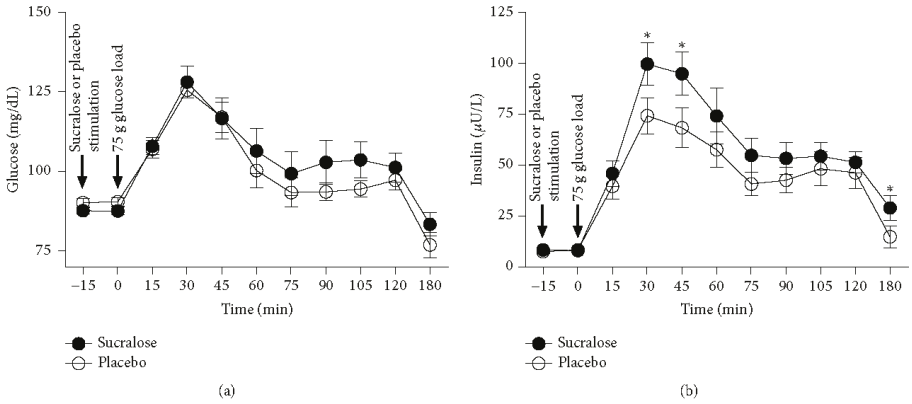

Figure 1: Blood levels of glucose and insulin in healthy young adults that received sucralose or placebo during an oral glucose tolerance test. Volunteers randomly received 60 mL water as placebo ($n = 20$) or 48 mg sucralose dissolved in 60 mL water ($n = 25$) 15 min prior to a 75 g oral glucose tolerance test (OGTT). Starting with glucose load at minute zero, venous blood samples were drawn from all study subjects every 15 min for 180 min for quantifying the blood levels of glucose and insulin. (a) Blood glucose did not show significant changes in subjects receiving placebo or sucralose all along the OGTT. (b) Serum insulin significantly increased at 30, 45, and 180 min in volunteers that received sucralose as compared to placebo controls. Timing of stimulation with sucralose, placebo, or glucose is shown on the graphic by black arrows. The placebo group is shown in open circles, whereas the sucralose group can be seen in closed circles. Data are expressed as media ± standard error. Significant differences between subjects receiving placebo or sucralose were estimated on each point of the OGTT by performing two-tailed 2-way ANOVA with correction for multiple comparisons by means of the Bonferroni multiple comparisons test. Significant differences are indicated by asterisks. Differences were considered significant when $P < 0.05$.

be examined in light of previous information showing that healthy young adults with no insulin resistance have the ability to increase insulin secretion and thus effectively decrease the excess of blood glucose [27, 28]. In contrast, numerous studies have consistently shown that nondiabetic morbidly obese subjects exposed to a glucose load can clearly increase insulin secretion without achieving blood glucose clearance due to a marked insulin resistance [29–32]. In this scenario, it is feasible to suppose that sucralose consumption may have differential effects on healthy young adults and morbidly obese subjects due to the presence of insulin resistance. In other words, sucralose ingestion may stimulate insulin secretion and, in this way, reduce glucose levels in healthy young adults but not morbidly obese subjects that show higher levels of insulin resistance and thus glucose intolerance. The fact that sucralose is able to stimulate directly insulin secretion has been previously reported in pancreatic beta cell lines and mouse islets [33], but remains elusive in humans. However, present results support the role of sucralose in promoting pancreatic insulin secretion in healthy young women and men that show normal insulin sensitivity, a probable phenomenon that needs to be confirmed in other human populations with different genetic background.

As mentioned before, low-grade activation of monocytes and macrophages has been shown to associate with the development of hyperinsulinemia, glucose intolerance, and insulin resistance [17–19, 34]. In this sense, it is well known that nutritive sweeteners such as sucrose or glucose exert the ability to increase TNF-alpha and IL-1beta expression and downregulate interleukin-10 (IL-10) production in human monocyte-derived macrophages *in vitro* [35, 36]. However, the effect of noncaloric artificial sweeteners on immune cells remains elusive. A previous study showed that exposure of human whole blood leukocytes to sucralose is able to suppress interleukin-6 (IL-6) and IL-10 secretion *in vitro*, even in the presence of phytohemagglutinin (PHA) or lipopolysaccharide (LPS) [37]. Likewise, the $CD3^+$ T cell percentage has been shown to increase in Peyer's patches and lamina propria of mice receiving sucralose in drinking water [5]. Moreover, $CD3^+$ T cells in Peyer's patches also showed elevation in TNF-alpha and interferon-gamma (IFN-gamma) production, accompanied by reduced expression of IL-10, which supports the role of sucralose in modulating immune cell activation [5]. Concurring with previous information, our findings show for the first time that a single sip of sucralose significantly increases the percentage of classical monocytes and reduces the nonclassical monocyte subpopulation in healthy young adults receiving a 75 g glucose load.

Another phenomenon captured in our study involves the possible mechanism by which sucralose exerts its effects on classical and nonclassical monocytes in healthy young adults. Sweet taste of sucralose and other caloric and noncaloric sweeteners is mediated by G protein-coupled receptors (GPCR) T1R1, T1R2, and T1R3 [38]. Sweet taste receptors were firstly described in the gut [39], enteroendocrine cells, and pancreas [40]. Nevertheless, T1R3 has been also indentified in mouse peritoneal macrophages [41]. Notably, *in vitro* exposure of T1R3 to trehalose (a disaccharide consisting of two molecules of glucose) has been shown to associate with suppression of TNF-alpha and IL-1beta

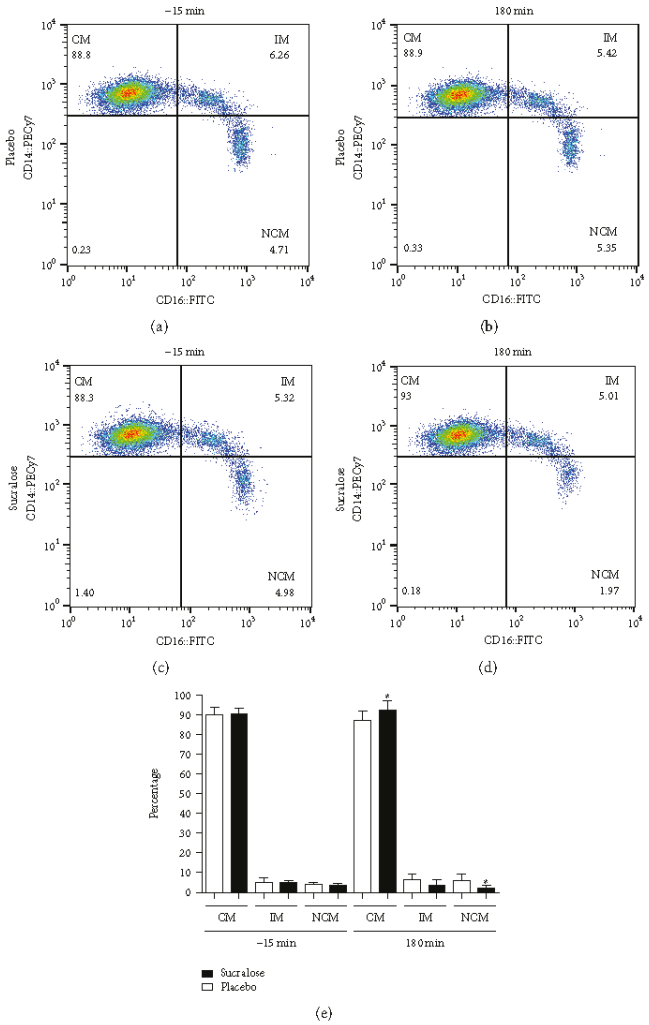

Figure 2: Percentages of classical, intermediate, and nonclassical monocytes in healthy young adults that received sucralose or placebo at the beginning and at the end of an oral glucose tolerance test. Representative flow cytometry dot plots showing the percentages of classical (CM), intermediate (IM), and nonclassical monocytes (NCM) in the placebo group at the beginning (a) and at the end (b) of the oral glucose tolerance test (OGTT). Representative dot plots showing the percentages of CM, IM, and NCM in the sucralose group at the beginning and at the end of the OGTT can be seen in (c) and (d), respectively. (e) As expected, quantification of monocyte subpopulation percentages showed no differences between placebo and sucralose groups at the beginning of the OGTT (-15 min). At 180 min, the CM percentage significantly increased whereas the NCM percentage decreased in volunteers that received 48 mg sucralose as compared to subjects that received water as placebo. No significant differences were seen in the IM percentage. The placebo group is shown in open bars, whereas the sucralose group can be seen in closed bars. Monocytes were gated on a $CD14^+CD16^+$ dot plot to identify monocyte subpopulations as follows: $CD14^{++}CD16^-$, classical monocytes; $CD14^{++}CD16^+$, intermediate monocytes; and $CD14^+CD16^+$, nonclassical monocytes. Data are expressed as media ± standard deviation. Significant differences between placebo and sucralose groups were estimated by performing two-tailed, 2-way ANOVA followed by the Bonferroni multiple comparisons test. Significant differences are indicated by asterisks. Differences were considered significant when $P < 0.05$.

Table 2: Statistical correlations of monocyte subpopulations with blood levels of glucose and insulin in placebo and sucralose groups.

	Placebo				Sucralose				
	-15		180		-15		180		
	r	*P*	*r*	*P*	*r*	*P*	*r*	*P*	
Classical monocyte (%)	0.24	0.12	0.35	0.06	0.19	0.18	0.14	0.25	
Intermediate monocyte (%)	-0.15	0.28	-0.25	0.13	-0.20	0.16	0.06	0.38	Glucose
Nonclassical monocyte (%)	-0.20	0.18	-0.24	0.14	-0.37	0.06	0.12	0.27	
Classical monocyte (%)	0.01	0.46	0.10	0.33	0.06	0.37	*0.41*	*0.02*	
Intermediate monocyte (%)	0.31	0.08	-0.21	0.17	0.24	0.12	-0.27	0.09	Insulin
Nonclassical monocyte (%)	-0.36	0.06	0.04	0.42	-0.29	0.07	*-0.42*	*0.01*	

Coefficients (r) and P values were calculated by the Pearson correlation model. The correlation level was considered significant when $P < 0.05$. Significant associations are marked in italic.

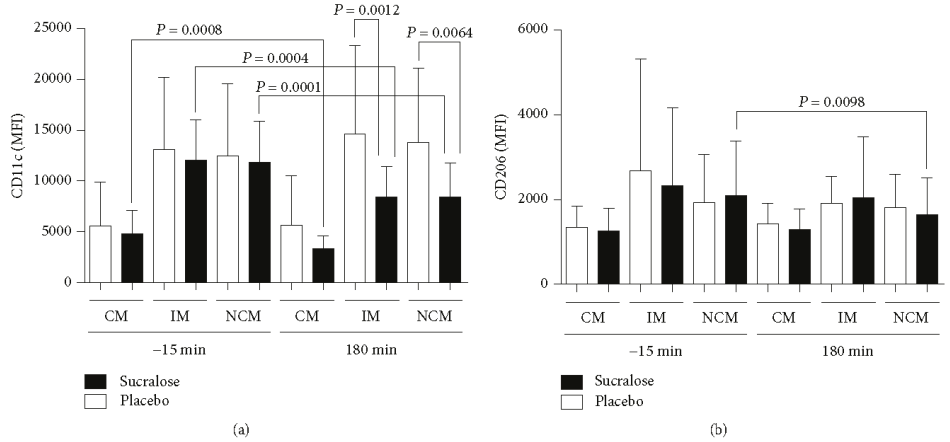

Figure 3: Cell surface expression of CD11c and CD206 in classical, intermediate, and nonclassical monocytes of healthy young adults that received sucralose or placebo at the beginning and at the end of an oral glucose tolerance test. (a) As expected, CD11c expression showed no differences between placebo and sucralose groups at the beginning (-15 min) of the oral glucose tolerance test (OGTT). At 180 min, CD11c expression significantly decreased in intermediate monocytes (IM) and nonclassical monocytes (NCM) of subjects that received 48 mg sucralose as compared to placebo controls. When comparing -15 and 180 min, classical monocytes (CM), IM, and NCM showed decreased CD11c expression in volunteers receiving sucralose. (b) CD206 expression showed no differences in subjects receiving placebo or sucralose at the beginning of the OGTT (-15 min). At 180 min, CD206 expression significantly decreased in the NCM subpopulation of subjects that received sucralose as compared to placebo controls. The placebo group is shown in open bars, whereas the sucralose group can be seen in closed bars. Monocytes were gated on a $CD14^+CD16^+$ dot plot to identify $CD14^{++}CD16^-$ classical monocytes, $CD14^{++}CD16^+$ intermediate monocytes, and $CD14^+CD16^+$ nonclassical monocytes and then measure the mean fluorescence intensity (MFI) of CD11c and CD206 on each monocyte subset. Data are expressed as media ± standard deviation. Significant differences between subjects receiving placebo or sucralose were estimated by performing two-tailed, 2-way ANOVA followed by the Bonferroni multiple comparisons test. Significant differences are indicated by asterisks. Differences were considered significant when $P < 0.05$.

expression in murine macrophages [41]. It is then feasible to speculate that sucralose may alter CD14 and CD16 expression via T1R3, which would lead to unbalance in the percentages of classical and nonclassical monocytes. However, we still need to measure sweet taste receptor expression on human monocyte subpopulations to draw major conclusions regarding this point.

Another possible mechanism by which sucralose may orchestrate dynamic changes in classical and nonclassical monocyte subsets involves the probable role of serum insulin. In our study, increase in serum insulin was importantly correlated with elevation of classical monocytes and reduction of nonclassical monocytes only in volunteers that drank sucralose but not placebo. Devevre and coworkers previously demonstrated that serum insulin is significantly associated with classical, intermediate, and nonclassical monocyte subpopulations of morbidly obese patients with insulin resistance [18]. Moreover, another study showed that insulin is able to

induce protein kinase B (AKT) phosphorylation in both human classical and nonclassical monocyte subsets in a dose-dependent fashion *in vitro* [42]. Furthermore, Bunn and coworkers also reported that insulin boosts the palmitate-induced TNF-alpha and IL-6 expression in human monocytes *in vitro* [43]. Taking into account that (1) sucralose can directly stimulate pancreatic insulin secretion via T1R2 and T1R3 [33] and (2) insulin is able to regulate human monocyte activity [42, 43], it is then reasonable to suppose that serum insulin may directly modify the percentages of classical and nonclassical monocytes in subjects receiving sucralose but not placebo. Although plausible, it is a speculative scenario and further experimental studies should be performed with the aim of determining the exact mechanism by which sucralose affects human monocyte subpopulations *in vivo*.

In humans, monocyte subpopulations have been shown to exert different immune roles that are associated with expression patterns of cell surface molecules [16]. In this sense, classical and intermediate monocytes have been described to express CCR2 and CD11c and thus play pivotal roles in cell adhesion and migration [19, 44]. On the other hand, nonclassical monocytes have been shown to exert inflammatory actions within the circulation and progressive loss of CD206 expression on these immune cells is associated with enhanced proinflammatory capacity [21]. In this sense, our results show that sucralose consumption associates with low CD11c expression in all monocyte subsets and suggest alteration of the migratory capacity of these cells. However, such a hypothesis needs to be experimentally tested before drawing major conclusions regarding the effect of sucralose on the monocyte migratory capacity. To this respect, it has been previously reported that trehalose ingestion reduces CD11c expression in the colonic mucosa of mice treated with 2,4,6-trinitrobenzenesulfonic acid (TNBS), which in turn was associated with less infiltration of immune cells and improvement of intestinal inflammation [45]. However, to the best of our knowledge this is the first study reporting that sucralose consumption is able to decrease CD11c expression in human monocytes, a notion that may open new avenues to investigate the effect of sucralose on immune cells. In parallel, our findings also show that sucralose consumption associates with low expression levels of CD206 in nonclassical monocytes. Since CD206 is a cell surface marker related to the anti-inflammatory ability of mononuclear cells, it is thus feasible to speculate that sucralose ingestion may associate with increased proinflammatory capacity of human monocytes. As mentioned above, Rosales-Gomez and collaborators recently demonstrated that sucralose consumption exerts proinflammatory effects on mouse $CD3^+$ T cells by rising TNF-alpha and IFN-gamma expression and reducing the expression of IL-10 [5]. Similarly, Bian and coworkers found increased expression of the proinflammatory markers TNF-alpha and nitric-oxide synthase 2 (NOS2) in the liver of mice receiving sucralose in the drinking water [46]. Present evidence concurs with our findings and supports the idea that sucralose may exert proinflammatory actions on nonclassical monocytes by decreasing CD206 expression. Nevertheless, we want to state that we still did not conduct any experimental *in vitro* study that firmly supports a direct role of sucralose on the anti-inflammatory activity of monocyte subsets and we are unable to draw solid conclusions regarding this topic at this time. Therefore, further *in vitro* studies are needed to characterize the possible effect of sucralose as a nonprototypic proinflammatory signal able to decrease CD206 expression in human monocytes.

It is worth mentioning that this study has some limitations including a possible participation of the sucralose sweet taste that may modify insulin secretion via the central nervous system as well the limited number of participants in each group. The amendment of these limitations (i.e., by using capsules containing sucralose) will bring more solid data to study the effect of sucralose on human metabolism and immunology.

5. Conclusions

This work demonstrates that a single sip of 48 mg sucralose increases the serum levels of insulin in age- and sex-matched non-insulin-resistant young adults subjected to an OGTT. Sucralose consumption was not only related to elevated levels of insulin but also increased proportion of classical monocytes and reduced percentage of nonclassical monocytes that in turn showed low expression levels of CD11c and CD206. Present results expand on the body of work that links sucralose consumption with unbalance of immune cell populations and alteration of insulin homeostasis. This work is relevant since the amount of sucralose studied here is contained in numerous "light" beverages available in the market and encourages further research focused on exploring the potential long-term impact of noncaloric artificial sweeteners on insulin metabolism and immune response in humans.

Data Availability

The data used to support the findings of this study are available from the corresponding author upon request.

Conflicts of Interest

The authors declare that there is no conflict of interest regarding the publication of this article.

Authors' Contributions

Angélica Y. Gómez-Arauz, and Nallely Bueno-Hernández equally contributed to this work.

Acknowledgments

This work was supported by grant no. 261575 from the Fondo Sectorial de Investigación y Desarrollo en Salud y Seguridad Social SS/IMSS/ISSSTE/CONACYT-México to G Meléndez and grant no. 286209 from the Fondo Sectorial de Investigación para la Educación-CONACYT-México to G Escobedo, and is a component of the M.Sc. requirements of A-Y Gómez-Arauz in the Posgrado en Ciencias Médicas, Odontológicas y de la Salud de la Universidad Nacional

Autónoma de México. Dr. Blair Brown from the Medical School of the University of Minnesota corrected the English version of the manuscript. Authors thank the Flow Cytometry core facility from "Coordinación de Investigación en Salud" at "Centro Médico Nacional, Siglo XXI" of IMSS for instrumentation.

References

[1] E. Palkowska-Gozdzik, A. Bigos, and D. Rosolowska-Huszcz, "Type of sweet flavour carrier affects thyroid axis activity in male rats," *European Journal of Nutrition*, vol. 57, no. 2, pp. 773–782, 2018.

[2] P. J. Rogers, P. S. Hogenkamp, C. de Graaf et al., "Does low-energy sweetener consumption affect energy intake and body weight? A systematic review, including meta-analyses, of the evidence from human and animal studies," *International Journal of Obesity*, vol. 40, no. 3, pp. 381–394, 2016.

[3] S. E. Swithers, "Artificial sweeteners are not the answer to childhood obesity," *Appetite*, vol. 93, pp. 85–90, 2015.

[4] T. Feehley and C. R. Nagler, "Health: the weighty costs of non-caloric sweeteners," *Nature*, vol. 514, no. 7521, pp. 176-177, 2014.

[5] C. A. Rosales-Gomez, B. E. Martinez-Carrillo, A. A. Resendiz-Albor et al., "Chronic consumption of sweeteners and its effect on glycaemia, cytokines, hormones, and lymphocytes of GALT in CD1 mice," *BioMed Research International*, vol. 2018, Article ID 1345282, 15 pages, 2018.

[6] A. Lertrit, S. Srimachai, S. Saetung et al., "Effects of sucralose on insulin and glucagon-like peptide-1 secretion in healthy subjects: a randomized, double-blind, placebo-controlled trial," *Nutrition*, vol. 55-56, pp. 125–130, 2018.

[7] J. Suez, T. Korem, D. Zeevi et al., "Artificial sweeteners induce glucose intolerance by altering the gut microbiota," *Nature*, vol. 514, no. 7521, pp. 181–186, 2014.

[8] K. I. Rother, E. M. Conway, and A. C. Sylvetsky, "How non-nutritive sweeteners influence hormones and health," *Trends in Endocrinology & Metabolism*, vol. 29, no. 7, pp. 455–467, 2018.

[9] M. Y. Pepino, C. D. Tiemann, B. W. Patterson, B. M. Wice, and S. Klein, "Sucralose affects glycemic and hormonal responses to an oral glucose load," *Diabetes Care*, vol. 36, no. 9, pp. 2530–2535, 2013.

[10] A. C. Sylvetsky, R. J. Brown, J. E. Blau, M. Walter, and K. I. Rother, "Hormonal responses to non-nutritive sweeteners in water and diet soda," *Nutrition & Metabolism*, vol. 13, no. 1, p. 71, 2016.

[11] P. Gonzalez-Muniesa, M. A. Martinez-Gonzalez, F. B. Hu et al., "Obesity," *Nature Reviews Disease Primers*, vol. 3, article 17034, 2017.

[12] C. Herder, S. Schneitler, W. Rathmann et al., "Low-grade inflammation, obesity, and insulin resistance in adolescents," *The Journal of Clinical Endocrinology & Metabolism*, vol. 92, no. 12, pp. 4569–4574, 2007.

[13] C. N. Lumeng and A. R. Saltiel, "Inflammatory links between obesity and metabolic disease," *The Journal of Clinical Investigation*, vol. 121, no. 6, pp. 2111–2117, 2011.

[14] R. V. Considine, "Activated monocytes: yet another link between systemic inflammation and obesity," *The Journal of Clinical Endocrinology & Metabolism*, vol. 99, no. 7, pp. 2347–2349, 2014.

[15] R. Mukherjee, P. Kanti Barman, P. Kumar Thatoi, R. Tripathy, B. Kumar Das, and B. Ravindran, "Non-classical monocytes display inflammatory features: validation in sepsis and systemic lupus erythematous," *Scientific Reports*, vol. 5, no. 1, article 13886, 2015.

[16] L. Ziegler-Heitbrock, "Blood monocytes and their subsets: established features and open questions," *Frontiers in Immunology*, vol. 6, p. 423, 2015.

[17] J. L. Grun, A. N. Manjarrez-Reyna, A. Y. Gomez-Arauz et al., "High-density lipoprotein reduction differentially modulates to classical and nonclassical monocyte subpopulations in metabolic syndrome patients and in LPS-stimulated primary human monocytes in vitro," *Journal of Immunology Research*, vol. 2018, Article ID 2737040, 12 pages, 2018.

[18] E. F. Devevre, M. Renovato-Martins, K. Clement, C. Sautes-Fridman, I. Cremer, and C. Poitou, "Profiling of the three circulating monocyte subpopulations in human obesity," *The Journal of Immunology*, vol. 194, no. 8, pp. 3917–3923, 2015.

[19] K. Wouters, K. Gaens, M. Bijnen et al., "Circulating classical monocytes are associated with $CD11c^+$ macrophages in human visceral adipose tissue," *Scientific Reports*, vol. 7, no. 1, article 42665, 2017.

[20] H. Wu, X. D. Perrard, Q. Wang et al., "CD11c expression in adipose tissue and blood and its role in diet-induced obesity," *Arteriosclerosis, Thrombosis, and Vascular Biology*, vol. 30, no. 2, pp. 186–192, 2010.

[21] W. D. Cornwell, V. Kim, X. Fan et al., "Activation and polarization of circulating monocytes in severe chronic obstructive pulmonary disease," *BMC Pulmonary Medicine*, vol. 18, no. 1, p. 101, 2018.

[22] M. D. Kristensen, M. T. Lund, M. Hansen et al., "Macrophage area content and phenotype in hepatic and adipose tissue in patients with obesity undergoing roux-en-Y gastric bypass," *Obesity*, vol. 25, no. 11, pp. 1921–1931, 2017.

[23] D. Liu, F. E. Morales, H. B. IglayReger et al., "Expression of macrophage genes within skeletal muscle correlates inversely with adiposity and insulin resistance in humans," *Applied Physiology, Nutrition, and Metabolism*, vol. 43, no. 2, pp. 187–193, 2018.

[24] J. M. Wentworth, G. Naselli, W. A. Brown et al., "Pro-inflammatory $CD11c^+CD206^+$ adipose tissue macrophages are associated with insulin resistance in human obesity," *Diabetes*, vol. 59, no. 7, pp. 1648–1656, 2010.

[25] H. Q. Qu, Q. Li, A. R. Rentfro, S. P. Fisher-Hoch, and J. B. McCormick, "The definition of insulin resistance using HOMA-IR for Americans of Mexican descent using machine learning," *PLoS One*, vol. 6, no. 6, article e21041, 2011.

[26] V. Purohit and S. Mishra, "The truth about artificial sweeteners – are they good for diabetics?," *Indian Heart Journal*, vol. 70, no. 1, pp. 197–199, 2018.

[27] K. Takahashi, H. Nakamura, H. Sato, H. Matsuda, K. Takada, and T. Tsuji, "Four plasma glucose and insulin responses to a 75 g OGTT in healthy young Japanese women," *Journal Diabetes Research*, vol. 2018, article 5742497, 7 pages, 2018.

[28] D. Young-Hyman, D. G. Schlundt, L. Herman, F. De Luca, and D. Counts, "Evaluation of the insulin resistance syndrome in 5- to 10-year-old overweight/obese African-American children," *Diabetes Care*, vol. 24, no. 8, pp. 1359–1364, 2001.

[29] A. Algoblan, M. Alalfi, and M. Khan, "Mechanism linking diabetes mellitus and obesity," *Diabetes, Metabolic Syndrome and Obesity: Targets and Therapy*, vol. 7, pp. 587–591, 2014.

[30] A. C. Meyer-Gerspach, L. Cajacob, D. Riva et al., "Mechanisms regulating insulin response to intragastric glucose in lean and non-diabetic obese subjects: a randomized, double-blind, parallel-group trial," *PLoS One*, vol. 11, no. 3, article e0150803, 2016.

[31] M. E. Røder, D. Porte Jr., R. S. Schwartz, and S. E. Kahn, "Disproportionately elevated proinsulin levels reflect the degree of impaired B cell secretory capacity in patients with noninsulin-dependent diabetes mellitus," *The Journal of Clinical Endocrinology & Metabolism*, vol. 83, no. 2, pp. 604–608, 1998.

[32] P. A. Velasquez-Mieyer, P. A. Cowan, K. L. Arheart et al., "Suppression of insulin secretion is associated with weight loss and altered macronutrient intake and preference in a subset of obese adults," *International Journal of Obesity*, vol. 27, no. 2, pp. 219–226, 2003.

[33] Y. Nakagawa, M. Nagasawa, S. Yamada et al., "Sweet taste receptor expressed in pancreatic β-cells activates the calcium and cyclic AMP signaling systems and stimulates insulin secretion," *PLoS One*, vol. 4, no. 4, article e5106, 2009.

[34] J. F. Ferguson, R. Y. Shah, R. Shah, N. N. Mehta, M. R. Rickels, and M. P. Reilly, "Activation of innate immunity modulates insulin sensitivity, glucose effectiveness and pancreatic β-cell function in both African ancestry and European ancestry healthy humans," *Metabolism*, vol. 64, no. 4, pp. 513–520, 2015.

[35] K. Moganti, F. Li, C. Schmuttermaier et al., "Hyperglycemia induces mixed M1/M2 cytokine profile in primary human monocyte-derived macrophages," *Immunobiology*, vol. 222, no. 10, pp. 952–959, 2017.

[36] I. Torres-Castro, U. D. Arroyo-Camarena, C. P. Martinez-Reyes et al., "Human monocytes and macrophages undergo M1-type inflammatory polarization in response to high levels of glucose," *Immunology Letters*, vol. 176, pp. 81–89, 2016.

[37] F. Rahiman and E. J. Pool, "The in vitro effects of artificial and natural sweeteners on the immune system using whole blood culture assays," *Journal of Immunoassay and Immunochemistry*, vol. 35, no. 1, pp. 26–36, 2014.

[38] M. O. Welcome, N. E. Mastorakis, and V. A. Pereverzev, "Sweet taste receptor signaling network: possible implication for cognitive functioning," *Neurology Research International*, vol. 2015, Article ID 606479, 13 pages, 2015.

[39] D. Hofer, B. Puschel, and D. Drenckhahn, "Taste receptor-like cells in the rat gut identified by expression of alpha-gustducin," *Proceedings of the National Academy of Sciences of the United States of America*, vol. 93, no. 13, pp. 6631–6634, 1996.

[40] I. Kojima and Y. Nakagawa, "The role of the sweet taste receptor in enteroendocrine cells and pancreatic β-cells," *Diabetes & Metabolism Journal*, vol. 35, no. 5, pp. 451–457, 2011.

[41] K. Taya, K. Hirose, and S. Hamada, "Trehalose inhibits inflammatory cytokine production by protecting IκB-α reduction in mouse peritoneal macrophages," *Archives of Oral Biology*, vol. 54, no. 8, pp. 749–756, 2009.

[42] M. M. Thewissen, J. van de Gaar, A. T. den Boer, M. J. Munsters, E. E. Blaak, and A. Duijvestijn, "Monocytes, but not T cells, respond to insulin with Akt(S473) phosphorylation independent of the donor glucometabolic state," *Diabetes/Metabolism Research and Reviews*, vol. 30, no. 4, pp. 323–332, 2014.

[43] R. C. Bunn, G. E. Cockrell, Y. Ou, K. M. Thrailkill, C. K. Lumpkin, and J. L. Fowlkes, "Palmitate and insulin synergistically induce IL-6 expression in human monocytes," *Cardiovascular Diabetology*, vol. 9, no. 1, p. 73, 2010.

[44] C. Shi and E. G. Pamer, "Monocyte recruitment during infection and inflammation," *Nature Reviews Immunology*, vol. 11, no. 11, pp. 762–774, 2011.

[45] D. C. Macias-Ceja, J. Cosin-Roger, D. Ortiz-Masia et al., "Stimulation of autophagy prevents intestinal mucosal inflammation and ameliorates murine colitis," *British Journal of Pharmacology*, vol. 174, no. 15, pp. 2501–2511, 2017.

[46] X. Bian, L. Chi, B. Gao, P. Tu, H. Ru, and K. Lu, "Gut microbiome response to sucralose and its potential role in inducing liver inflammation in mice," *Frontiers in Physiology*, vol. 8, p. 487, 2017.

Received: 12 June 2018 | Revised: 27 August 2018 | Accepted: 2 September 2018

DOI: 10.1111/sji.12716

EXPERIMENTAL IMMUNOLOGY

WILEY Scandinavian Journal of Immunology

Infliximab ameliorates tumor necrosis factor-alpha-induced insulin resistance by attenuating PTP1B activation in 3T3L1 adipocytes in vitro

Lucia A. Méndez-García[1] | **Fernanda Trejo-Millán**[1] | **Camilo P. Martínez-Reyes**[1] | **Aarón N. Manjarrez-Reyna**[1] | **Marcela Esquivel-Velázquez**[1] | **Guillermo Melendez-Mier**[1] | **Sergio Islas-Andrade**[1] | **Araceli Rojas-Bernabé**[2] | **Julia Kzhyshkowska**[3] | **Galileo Escobedo**[1]

[1]Laboratory for Proteomics and Metabolomics, Research Division, General Hospital of Mexico "Dr. Eduardo Liceaga", Mexico City, Mexico

[2]Research Unit for Experimental Medicine, School of Medicine, National Autonomous University of Mexico, Mexico City, Mexico

[3]Department of Innate Immunity and Tolerance, Institute of Transfusion Medicine and Immunology, Medical Faculty Mannheim, Heidelberg University, Mannheim, Germany

Correspondence
Galileo Escobedo, Laboratory for Proteomics and Metabolomics, Research Division, General Hospital of Mexico "Dr. Eduardo Liceaga", Mexico City, Mexico.
Email: gescobedo@unam.mx; gescobedog@msn.com.

Funding information
Marie Curie International Research Staff Exchange Scheme, Grant/Award Number: 295185-EULAMDIMA; Fondo Sectorial de Investigación para la Educación SEP-CONACYT-México, Grant/Award Number: 286209

Abstract

Insulin resistance is the inability to respond to insulin and is considered a key pathophysiological factor in the development of type 2 diabetes. Tumor necrosis factor-alpha (TNF-alpha) can directly contribute to insulin resistance by disrupting the insulin signalling pathway via protein-tyrosine phosphatase 1B (PTP1B) activation, especially in adipocytes. Infliximab (Remicade®) is a TNF-alpha-neutralizing antibody that has not been fully studied in insulin resistance. We investigated the effect of infliximab on TNF-alpha-induced insulin resistance in 3T3L1 adipocytes in vitro, and examined the possible molecular mechanisms involved. Once differentiated, adipocytes were cultured with 5 mmol L^{-1} 2-deoxy-D-glucose-^{3}H and stimulated twice with 2 μmol L^{-1} insulin, in the presence or absence of 5 ng/mL TNF-alpha and/or 10 ng/mL infliximab. Glucose uptake was measured every 20 minutes for 2 hour, and phosphorylated forms of insulin receptor (IR), insulin receptor substrate-2 (IRS-2), protein kinase B (AKT) and PTP1B were determined by Western blotting. TNF-alpha-treated adipocytes showed a significant 64% decrease in insulin-stimulated glucose uptake as compared with control cells, whereas infliximab reversed TNF-alpha actions by significantly improving glucose incorporation. Although IR phosphorylation remained unaltered, TNF-alpha was able to increase PTP1B activation and decrease phosphorylation of IRS-2 and AKT. Notably, infliximab restored phosphorylation of IRS-2 and AKT by attenuating PTP1B activation. This work demonstrates for the first time that infliximab ameliorates TNF-alpha-induced insulin resistance in 3T3L1 adipocytes in vitro by restoring the insulin signalling pathway via PTP1B inhibition. Further clinical research is needed to determine the potential benefit of using infliximab for treating insulin resistance in patients.

1 | INTRODUCTION

Insulin resistance is the inability of skeletal muscle, liver and adipose tissue to respond to normal levels of insulin that results in alteration of glucose homeostasis.[1] In normal conditions, insulin binds to IR and orchestrates phosphorylation of the IRS protein family.[2] Downstream, IRS activation leads to phosphorylation of PI3-kinase (PI3K) that in turn triggers phosphorylation of AKT.[2] Upon activation, AKT orchestrates translocation of cytoplasmic vesicles

containing glucose transporter proteins (GLUT) into the plasma membrane that facilitates transport of glucose for cell metabolism.[1,2] Glucose uptake via activation of the IRS-PI3K-AKT pathway is able to reduce glucose levels in the extracellular milieu, which in turn contributes to decrease hyperglycaemia.[3] In insulin resistance, activation of the insulin signalling pathway is progressively abrogated resulting in glucose intolerance, hyperglycaemia and hyperinsulinemia.[4] For this reason, insulin resistance is considered a key pathophysiological factor in the development of type 2 diabetes (T2D),[4,5] a chronic disease with increasing morbidity and mortality rates around the globe.[6]

TNF-alpha is a cytokine with prominent actions in cell differentiation and apoptosis, inflammation, autoimmunity and recruitment of other immune cell types toward peripheral tissues.[7-9] TNF-alpha has been also shown to play a pivotal role in glucose homeostasis by promoting insulin resistance in mice and humans, especially in adipose tissue.[10,11] In this sense, mRNA and protein levels of TNF-alpha have been previously reported to elevate in visceral adipose tissue of high-fat diet (HFD)-fed mice and obese subjects that show increased insulin resistance.[12] Moreover, TNF-alpha-deficient mice are protected against insulin resistance development,[13] while also TNF-alpha directly induces insulin resistance in 3T3L1 adipocytes in vitro.[14]

TNF-alpha favours insulin resistance by abrogating phosphorylation of IRS-1 and AKT in a variety of insulin-dependent cells including adipocytes.[15] Besides reducing IRS-1 and AKT activation, TNF-alpha can also attenuate GLUT4 expression in adipocytes,[11,16] which demonstrates that this proinflammatory cytokine is able to disrupt the insulin signalling pathway in adipose tissue. Thus, blockage of TNF-alpha actions is now considered a matter of urgency to improve insulin action in adipose tissue of patients with insulin resistance such as T2D patients.

Infliximab (Remicade®) is a chimeric monoclonal IgG1 antibody that specifically binds to TNF-alpha and prevents the interaction of TNF-alpha with TNF-alpha receptor (TNFR) 1 and TNFR2.[17] For this reason, infliximab has been used to treat a variety of autoimmune and chronic inflammatory diseases such as rheumatoid arthritis, Crohn's disease, ulcerative colitis, psoriatic arthritis and ankylosing spondylitis.[18-23] Interestingly, besides exerting anti-inflammatory actions, infliximab has been also shown to improve insulin resistance. In this sense, rheumatoid arthritis patients receiving infliximab show decreased values of the homeostatic model assessment of insulin resistance (HOMA-IR) as well as increase in the quantitative insulin sensitivity check index (QUICKI).[24] Similarly, non-diabetic patients with ankylosing spondylitis also exhibit reduced HOMA-IR and increased QUICKI after 2 hour of receiving an intravenous infliximab infusion.[25] However, despite the clinical evidence, there are no studies exploring the effect of infliximab on TNF-alpha-induced insulin resistance in target organs of insulin such as adipose tissue. Here, we investigated the effect of infliximab on TNF-alpha-induced insulin resistance in 3T3L1 adipocytes in vitro and examined the possible molecular mechanisms involved.

2 | MATERIAL AND METHODS

2.1 | 3T3L1 cell line differentiation

The murine 3T3L1 cell line (ATCC®, USA) was propagated in Dulbecco's Modified Eagle Medium (DMEM)-High Glucose (Thermo Fisher-Scientific, USA) containing 10% foetal bovine serum (FBS) and 50 μg/mL gentamicin (Sigma-Aldrich, USA) for 4 days at 37°C in humidified 5% CO_2 atmosphere, using 6-well cell-culture plates (Costar, USA) at a density of 50×10^3 cells per well. Once fibroblasts reached about 80% confluence, they were differentiated into adipocytes using DMEM supplemented with 10% FBS, 50 μg/mL gentamicin, 1 μmol L^{-1} dexamethasone, 0.5 mmol L^{-1} IBMX and 1 μmol L^{-1} insulin (Sigma-Aldrich, USA). Culture media were replaced every other day for 6 days. Mature adipocytes were seen after 10 days on the in vitro culture conditions described above.

2.2 | Glucose uptake assay

For glucose uptake assay, 3T3L1 mature adipocytes were in vitro cultured in DMEM containing 10% FBS, 50 μg/mL gentamicin and 5 mmol L^{-1} 2-deoxy-D-glucose-^{3}H (Sigma-Aldrich, USA) for 2 hour at 37°C in humidified 5% CO_2 atmosphere, using 6-well cell-culture plates at a density of 30×10^4 cells per well. Adipocytes were stimulated twice at zero and 60 minutes with 2 μmol L^{-1} insulin. In the infliximab-treated group, adipocytes were stimulated with 10 ng/mL infliximab (Remicade®, Janssen Biotech, USA) at the beginning of the 2-hour in vitro assay. In the TNF-alpha-treated group, adipocytes were stimulated with 5 ng/mL murine TNF-alpha (Peprotech,Mexico) at the beginning of the 2-hour in vitro assay. In the infliximab+TNF-alpha-treated adipocyte group, 10 ng/mL infliximab was added at the beginning of the 2-hour in vitro assay, whereas 5 ng/mL murine TNF-alpha was added five minutes later. Control cells received neither infliximab nor TNF-alpha stimulation. All cultured 3T3L1 adipocytes were collected every 20 minutes for 2 hour for measuring glucose uptake in counts per minute (cpm), using a liquid scintillation counter (Beckman-Coulter, USA).

2.3 | Western blot for pIR, pIRS-2, pAKT and pPTP1B

Two hours after having been incubated with or without TNF-alpha and/or infliximab, 3T3L1 adipocytes were collected

and disrupted in protein extraction buffer containing 500 mmol L^{-1} Tris-HCl (1 mL/50 × 10^4 cells) and protease inhibitor cocktail (Calbiochem, Germany). After 15 minutes of centrifugation at 20 800 g/4°C, the supernatant was recovered for total protein quantification by measuring absorbance at 595 nm using the Bradford Protein Assay (Bio-Rad, USA). Then, 30 mg of total protein extract was boiled in Laemmli sample buffer and separated by SDS-PAGE (10% acrylamide) to transfer into PVDF membranes. Membranes were blocked overnight in PBS 1× buffer (0.2% Tween 20) containing 1% BSA. Immediately after, PVDF membranes were washed five times in PBS 1X-Tween 20 and separately incubated for up to 60 minutes at room temperature with 1:250 rabbit anti-mouse phosphorylated insulin receptor (pIR, 90 KDa), 1:500 rabbit anti-mouse phosphorylated pan-AKT (pAKT, 56 KDa), 1:650 rabbit anti-mouse phosphorylated protein-tyrosine phosphatase 1B (pPTP1B, 50 KDa), 1:1000 goat anti-mouse beta-Actin (42 KDa) (Abcam, USA) or 1:250 rabbit anti-human phosphorylated insulin receptor substrate-2 (pIRS-2, 160 KDa) (Merck-Millipore, Germany). Protein bands for pIR, pIRS-2, pAKT and pPTP1B were visualized using the peroxidase-diaminobenzidine reaction (Sigma-Aldrich, Mexico) and quantified by optical density (OD) analysis using beta-Actin as control.

2.4 | Statistical analysis

The Shapiro-Wilk test was performed to estimate normality in data distribution and then proceed to perform one-way ANOVA followed by a post-hoc Tukey test. Data represent at least five independent experiments and are expressed as media ± SD. Statistical analysis was performed using the GraphPad Prism 6.01 software. Areas under the curve (AUC) were calculated using R statistics and expressed as arbitrary units (a.u). Differences were considered significant when $P < 0.05$.

3 | RESULTS

After 40 minutes of having been in vitro stimulated with insulin, TNF-alpha-treated 3T3L1 adipocytes started to show a significant decrease in glucose uptake with respect to control untreated cells (Figure 1A). Infliximab exhibited no deleterious effects on glucose incorporation when added alone but clearly blocked TNF-alpha actions by improving glucose uptake in 3T3L1 cells in vitro (Figure 1A). At the end of the in vitro culture, 3T3L1 adipocytes treated with TNF-alpha showed a significant 2.6-fold reduction in glucose incorporation as compared to control cells ($P < 0.0001$). In contrast, adipose cells stimulated with infliximab and TNF-alpha exhibited a 2-fold increase in glucose uptake with respect to adipocytes only treated with TNF-alpha ($P < 0.0001$),

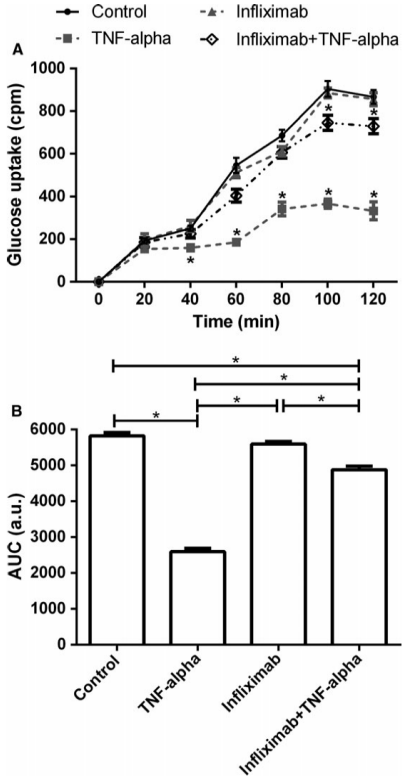

FIGURE 1 Infliximab restores insulin-dependent glucose uptake in TNF-alpha-treated 3T3L1 adipocytes. 3T3L1 adipocytes were in vitro stimulated twice with 2 μmol L^{-1} insulin at zero and 60 minutes in the presence of 2-deoxy-D-glucose-^{3}H as well as infliximab and/or TNF-alpha for 2 hours. Control adipocytes received neither infliximab nor TNF-alpha stimulation. (A) After 40 minutes, TNF-alpha (dotted grey line with solid squares) significantly decreased glucose uptake in 3T3L1 adipocytes as compared to control (black line with solid circles) and infliximab-treated adipocytes (dotted grey line with solid triangles). In contrast, infliximab restored cellular glucose incorporation by inhibiting TNF-alpha (dotted black line with hollow rhombus). Asterisks (*) indicate significant differences with respect to control untreated cells. (B) Glucose uptake kinetics in all groups was quantified as area under the curve (AUC). Overall, TNF-alpha induced 64% decrease in the AUC of glucose uptake as compared with control and infliximab-treated adipocytes. On the contrary, infliximab partially blocked TNF-alpha actions by increasing 50% the AUC of glucose uptake in 3T3L1 adipocytes. Asterisks (*) indicate significant differences among groups. Data are expressed as media ± SD. Significant differences were estimated by means of performing one-way ANOVA followed by a *post-hoc* Tukey test. Differences were considered significant when $P < 0.05$ and can be seen as asterisks (*) on the figure. TNF-alpha, tumor necrosis factor-alpha; cpm, counts per minute; a.u., arbitrary units

although glucose incorporation values were 0.15-fold lower than those found in control cells ($P = 0.0002$) (Figure 1A). Glucose uptake kinetics in 3T3L1 adipocytes was also analyzed as area under the curve (AUC) and can be seen in Figure 1B. Overall, TNF-alpha-treated 3T3L1 adipocytes showed a significant 64% decrease in the AUC of glucose uptake as compared with control cells ($P < 0.0001$) (Figure 1B). On the contrary, infliximab did not alter the AUC of glucose incorporation when added alone but partially reverted TNF-alpha actions by increasing 50% the AUC of glucose uptake in these adipose cells ($P < 0.0001$) (Figure 1B). Although use of infliximab significantly reversed the effect of TNF-alpha on 3T3L1 adipocytes in vitro, the AUC of glucose incorporation was 15% lower than that found in control cells ($P < 0.001$) (Figure 1B).

Neither TNF-alpha nor infliximab, alone or combined, altered the phosphorylation pattern of pIR in 3T3L1 adipocytes when compared to untreated cells (Figure 2A, B). On the contrary, pIRS-2 was significantly decreased by 3.25-fold in 3T3L1 adipocytes treated with TNF-alpha as compared to untreated cells ($P < 0.0001$) (Figure 2A, C). Infliximab showed no effect on pIRS-2 when added alone but significantly reverted TNF-alpha actions by restoring phosphorylation of pIRS-2 at similar levels than those found in control cells ($P < 0.0001$) (Figure 2A, C). When in vitro treated with TNF-alpha, 3T3L1 adipocytes showed a significant 2-fold decrease in pAKT as compared to untreated cells ($P < 0.0001$) (Figure 2A, D). On the other hand, infliximab had no effect on pAKT when added alone but partially reestablished phosphorylation of this protein in TNF-alpha-treated 3T3L1 adipocytes ($P = 0.0021$); however, AKT phosphorylation levels remained nether in comparison to control cells (Figure 2A and D) ($P = 0.0034$).

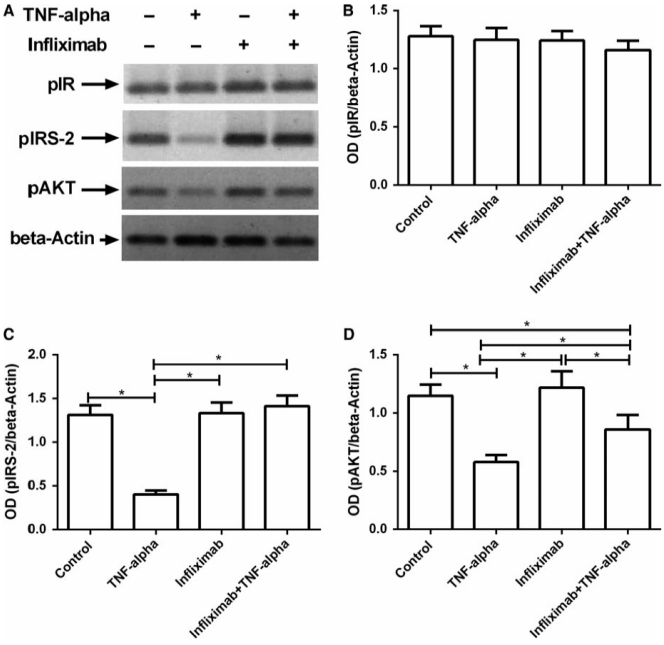

FIGURE 2 Infliximab restores phosphorylation of the insulin signaling pathway in TNF-alpha-treated 3T3L1 adipocytes. (A) Representative Western blot showing phosphorylated forms of IR, IRS-2 and AKT in 3T3L1 adipocytes with and without TNF-alpha or infliximab treatment. The beta-Actin was used as control for optical density (OD) analysis. (B) According to OD analysis, neither TNF-alpha nor infliximab, alone or combined, altered pIR in 3T3L1 adipocytes. (C) TNF-alpha induced 65% decrease in pIRS-2 as compared with control and infliximab-treated adipocytes. On the contrary, infliximab blocked TNF-alpha actions by restoring phosphorylation of IRS-2 in 3T3L1 adipocytes. (D) TNF-alpha induced 50% decrease in pAKT as compared with control and infliximab-treated adipocytes. On the other hand, infliximab blocked TNF-alpha actions by partially restoring phosphorylation of AKT in 3T3L1 adipocytes. Asterisks (*) indicate significant differences among groups. Data are expressed as media ± SD. Significant differences were estimated by means of performing one-way ANOVA followed by a post-hoc Tukey test. Differences were considered significant when $P < 0.05$. TNF-alpha, tumor necrosis factor-alpha; pIR, phosphorylated form of insulin receptor; pIRS-2, phosphorylated form of insulin receptor substrate-2; pAKT, phosphorylated form of protein kinase B; OD, optical density

The effects of TNF-alpha and infliximab on pPTP1B can be seen in the representative Western blotting shown in Figure 3A. TNF-alpha-treated 3T3L1 adipocytes exhibited a significant 4-fold increase in pPTP1B as compared to untreated cells ($P = 0.0055$) (Figure 1B). On the contrary, infliximab showed no effect on pPTP1B when added alone but revoked TNF-alpha actions by partially reducing phosphorylation of PTP1B in 3T3L1 adipocytes ($P = 0.0372$) (Figure 3B).

4 | DISCUSSION

TNF-alpha has been consistently shown to play a causal role in the development of insulin resistance in adipose tissue of HFD-fed mice and humans with obesity. For instance, T2D patients carrying the TNF-alpha 308 G/A polymorphism that has been associated with increased TNF-alpha levels, show higher values of the homeostatic model assessment of insulin resistance (HOMA-IR) than patients with the G/G wild genotype.[26] For this reason, numerous studies are now focused on finding novel therapeutic agents with the ability to abrogate the effects of TNF-alpha on insulin sensitivity, although results are still controversial. In this regard, Sprague-Dawley rats treated with goat anti-murine TNF-alpha IgG antibody showed improvement in insulin-mediated glucose transport in skeletal muscle.[27] In contrast, blockage of TNF-alpha using the recombinant-engineered human TNF-alpha-neutralizing antibody CDP571 did not show improvement in insulin sensitivity of patients with T2D.[28] Our study shows that neutralization of TNF-alpha improves glucose uptake by reversing insulin resistance and provides solid evidence regarding the use of therapeutic agents against TNF-alpha for improving insulin sensitivity in adipose cells. However, these results should be considered with caution as they reflect only the behaviour of an adipocyte cell line on in vitro culture conditions.

Infliximab is a medication used to treat patients with autoimmune and chronic inflammatory diseases.[18-22] Notably, besides improving joint pain, swelling and inflammation, infliximab also reduces the levels of serum insulin, fasting glucose and insulin resistance in patients with ankylosing spondylitis and rheumatoid arthritis.[29,30] It has been also reported that obese people show improvement in insulin resistance when treated with 5 mg/kg infliximab every 2 months, including a T2D patient who did not longer require insulin administration about 5 months after infliximab therapy.[31] Concurring with previous evidence, our data reveal that infliximab directly reverses insulin resistance and restores glucose homeostasis in adipose cells, even under proinflammatory conditions such as those promoted by TNF-alpha.

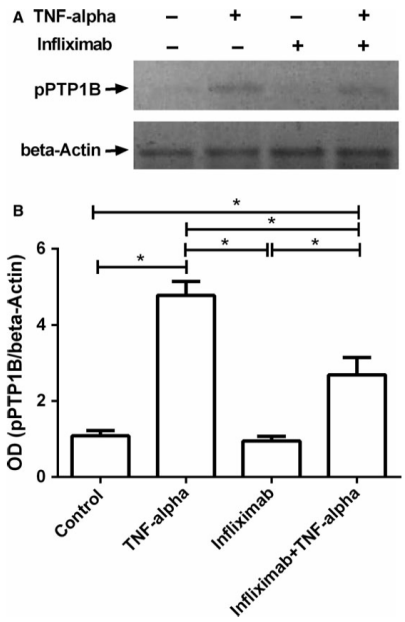

FIGURE 3 Infliximab attenuates TNF-alpha-induced PTP1B activation in 3T3L1 adipocytes. (A) Representative Western blot showing phosphorylated form of PTP1B in 3T3L1 adipocytes with and without TNF-alpha or infliximab treatment. beta-Actin was used as control for optical density (OD) analysis. (B) According to OD analysis, TNF-alpha induced a 4-fold increase in phosphorylation of PTP1B as compared to control and infliximab-treated adipocytes. However, infliximab blocked TNF-alpha actions by decreasing PTP1B activation in 3T3L1 adipocytes. Asterisks (*) indicate significant differences among groups. Data are expressed as media ± standard deviation. Significant differences were estimated by means of performing one-way ANOVA followed by a *post-hoc* Tukey test. Differences were considered significant when $P < 0.05$. TNF-alpha, tumor necrosis factor-alpha; pPTP1B, phosphorylated form of protein-tyrosine phosphatase 1B; OD, optical density

Another phenomenon captured in our study involves the possible molecular mechanism by which infliximab exerts its beneficial effects on TNF-alpha-induced insulin resistance in 3T3L1 adipocytes in vitro. Our data show that TNF-alpha is not able to impair insulin-mediated IR phosphorylation, a finding that has been previously reported in mice and rats.[14,32,33] Thus, it is reasonable to consider that TNF-alpha may promote adipocyte insulin resistance by inducing downstream activation of PTP1B. PTP1B is a negative regulator of the insulin signalling pathway with the ability to dephosphorylate tyrosine residues in numerous activated tyrosine kinase proteins including the IRS protein family.[33,34] A previous work reported that mice

lacking PTP1B expression ($PTP1B^{-/-}$) show enhanced insulin sensitivity and normal body weight, even after having been fed a HFD.[35] Notably, re-expression of PTP1B in the liver of $PTP1B^{-/-}$ mice attenuated whole-body insulin sensitivity and IRS-2 activation in hepatocytes.[35] A similar study showed that PTP1B activity abrogates phosphorylation of IRS-1 in skeletal muscle cells that results in decreased insulin sensitivity and altered glucose homeostasis.[36] Our data expand on this body of work by revealing for the first time that TNF-alpha-induced PTP1B activation can directly decrease phosphorylation of IRS-2 in adipose cells, which in turn might lead to AKT inhibition and increased insulin resistance. Furthermore, our results also demonstrate that infliximab is able to reverse PTP1B activation, which (a) confirms the causative role of TNF-alpha in insulin resistance and (b) might explain the improvement of IRS-2 phosphorylation and glucose uptake in adipocytes exposed to a proinflammatory milieu (Figure 4).

PTP1B has now emerged as a key molecule in mediating TNF-alpha-induced insulin resistance in insulin-dependent cells as is the case of skeletal muscle cells and adipocytes. For this reason, a growing number of studies have examined the effect of PTP1B inhibitors on insulin resistance. In this sense, Yi-ming Ma and coworkers previously showed that CCF06240, a PTP1B inhibitor, restores insulin sensitivity in HFD-fed mice and promotes phosphorylation of IRS-1 in HepG2 cells in vitro.[37] Similarly, a recent study reported a decrease in blood glucose and insulin resistance in ob/ob mice receiving Fudan-Yueyang-Ganoderma-lucidum (FYGL), a proteoglycan with the ability to inhibit PTP1B.[38] Interestingly, FYGL was also shown to improve insulin-stimulated glucose uptake and activation of IRS-1, PI3K and AKT by blocking PTP1B activation in rat myoblast L6 cells.[38] Consistent with previous evidence, we found that infliximab also acts as PTP1B inhibitor by exerting the ability to improve insulin signalling pathway and consequently glucose homeostasis in 3T3L1 adipocytes exposed to TNF-alpha in vitro.

Little is known yet about the activity of PTP1B in other tissues different from adipose tissue. In this sense,

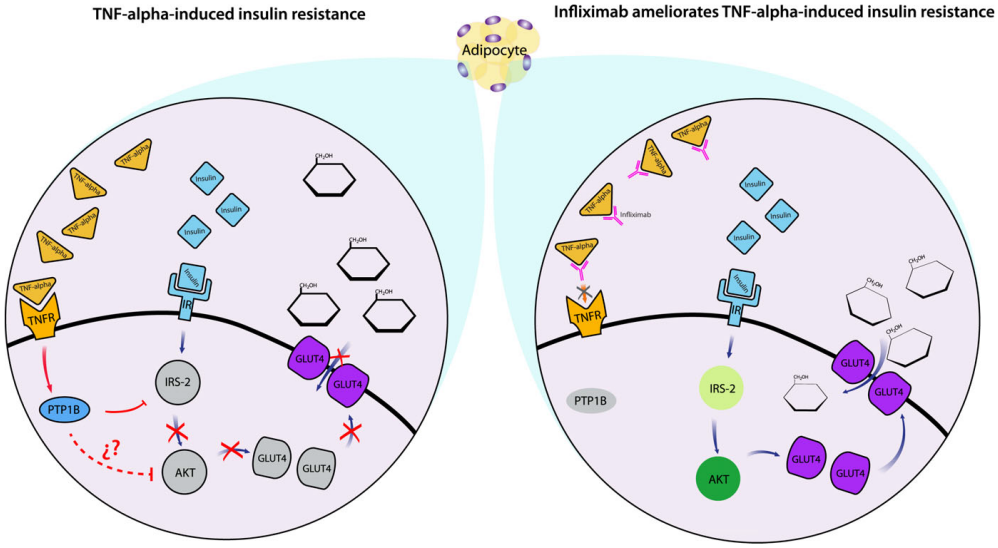

FIGURE 4 Possible molecular mechanism involved in mediating the effect of infliximab on TNF-alpha-induced insulin resistance in adipocytes in vitro. In TNF-alpha-induced insulin resistance (left panel), TNF-alpha binds to TNFR found on the cell surface of adipocytes, which in turn triggers PTP1B activation. Downstream, PTP1B is able to dephosphorylate IRS-2 that in turn leads to AKT arrest, even though insulin is continually binding to IR. Alternatively, AKT phosphorylation may be directly inhibited by PTP1B; however, there are not yet solid evidence supporting this notion. As a consequence of IRS-2 and AKT attenuation, GLUT4 translocation into the plasma membrane is arrested that in turn impedes the intracellular transport of glucose and leads to hyperglycaemia. On the contrary (right panel), infliximab specifically binds to TNF-alpha and neutralizes the interaction of TNF-alpha with TNFR that results in PTP1B attenuation. In consequence, IRS-2 and AKT are normally phosphorylated in response to insulin, which facilitates membrane translocation of GLUT4 and promotes glucose homeostasis, even when TNF-alpha levels are elevated. TNF-alpha, tumor necrosis factor-alpha; TNFR, tumor necrosis factor-alpha receptor; PTP1B, protein-tyrosine phosphatase 1B; IR, insulin receptor; IRS-2, insulin receptor substrate-2; AKT, protein kinase B; GLUT4, glucose transporter protein 4

liver-specific PTP1B$^{-/-}$ mice show improved glucose homeostasis and lipid metabolism, accompanied by reduction in HFD-induced endoplasmic reticulum stress.[39] Interestingly, aging has been shown to increase PTP1B expression and insulin resistance in liver of rats, a phenomenon that can be reversed by workout.[40] It has been also shown that PTP1B contributes to hypothalamic inflammation and leptin resistance in rodents fed a HFD.[41] As a matter of fact, PTP1B$^{-/-}$ mice exhibit decreased TNF-alpha expression, accompanied by increased interleukin-10 mRNA levels in the hypothalamus, even under HFD-feeding.[42] Notably, TNF-alpha has been shown to increase PTP1B expression in hypothalamic organotypic cultures in a dose and time-dependent fashion.[43] Nevertheless, despite PTP1B has been consistently shown to mediate insulin and leptin resistance in response to proinflammatory signals including endoplasmic reticulum stress, aging and TNF-alpha, there is still scant evidence regarding the benefit of using PTP1B and TNF-alpha-specific inhibitors. In this sense, this work brings to light the potential impact of using infliximab as a PTP1B inhibitor for ameliorating TNF-alpha-induced insulin resistance in adipose tissue. For this reason, we encourage exploring the possible effect of infliximab on other signaling cascades stimulated by TNF-alpha that may also disrupt insulin-dependent glucose uptake in adipocytes *in vitro* and in vivo, such as those depending on ceramides and extracellular-signal-regulated kinases (ERK). The implications for understanding the mechanisms through which infliximab improves TNF-alpha-induced insulin resistance are profound, and the idea that further knowledge of these pathways might allow prediction of susceptibility to type 2 diabetes adds a compelling degree of urgency to further study.

In conclusion, this work demonstrates for the first time that infliximab ameliorates TNF-alpha-induced insulin resistance in 3T3L1 adipocytes in vitro by restoring phosphorylation of key mediators of the insulin signaling pathway such as IRS-2 and AKT via PTP1B inhibition that in consequence improves insulin-dependent glucose uptake in these adipose cells (Figure 4).

ACKNOWLEDGMENT

This work was supported by grant no. 286209 from the Fondo Sectorial de Investigación para la Educación SEP-CONACYT-México to GE. The authors thank Ing. Omar Agni García Hernández for his valuable technical assistance with electronic artwork. This project has received funding from the Marie Curie International Research Staff Exchange Scheme with the 7th European Community Framework Program under grant agreement No. 295185-EULAMDIMA.

CONFLICT OF INTEREST

The authors declare that there is no conflict of interests regarding the publication of this manuscript.

ORCID

Galileo Escobedo http://orcid.org/0000-0002-9224-7400

REFERENCES

1. DeFronzo RA, Tripathy D. Skeletal muscle insulin resistance is the primary defect in type 2 diabetes. *Diabetes Care*. 2009;32 (Suppl 2):S157-S163.
2. Boucher J, Kleinridders A, Kahn CR. Insulin receptor signaling in normal and insulin-resistant states. *Cold Spring Harb Perspect Biol*. 2014;6:a009191.
3. Stanford KI, Goodyear LJ. Exercise and type 2 diabetes: molecular mechanisms regulating glucose uptake in skeletal muscle. *Adv Physiol Educ*. 2014;38:308-314.
4. Shanik MH, Xu Y, Skrha J, Dankner R, Zick Y, Roth J. Insulin resistance and hyperinsulinemia: is hyperinsulinemia the cart or the horse? *Diabetes Care*. 2008;31(Suppl 2):S262-S268.
5. Taylor R. Insulin resistance and type 2 diabetes. *Diabetes*. 2012;61:778-779.
6. Zheng Y, Ley SH, Hu FB. Global aetiology and epidemiology of type 2 diabetes mellitus and its complications. *Nat Rev Endocrinol*. 2018;14:88-98.
7. Baregamian N, Song J, Bailey CE, Papaconstantinou J, Evers BM, Chung DH. Tumor necrosis factor-alpha and apoptosis signal-regulating kinase 1 control reactive oxygen species release, mitochondrial autophagy, and c-Jun N-terminal kinase/p38 phosphorylation during necrotizing enterocolitis. *Oxid Med Cell Longev*. 2009;2:297-306.
8. Sade-Feldman M, Kanterman J, Ish-Shalom E, Elnekave M, Horwitz E, Baniyash M. Tumor necrosis factor-alpha blocks differentiation and enhances suppressive activity of immature myeloid cells during chronic inflammation. *Immunity*. 2013;38:541-554.
9. Chyuan IT, Tsai HF, Liao HJ, Wu CS, Hsu PN. An apoptosis-independent role of TRAIL in suppressing joint inflammation and inhibiting T-cell activation in inflammatory arthritis. *Cell Mol Immunol*. 2017; https://doi.org/10.1038/cmi.2017.2.
10. Tse MCL, Herlea-Pana O, Brobst D, et al. Tumor necrosis factor-alpha promotes phosphoinositide 3-kinase enhancer A and AMP-activated protein kinase interaction to suppress lipid oxidation in skeletal muscle. *Diabetes*. 2017;66:1858-1870.
11. Akash MSH, Rehman K, Liaqat A. Tumor necrosis factor-alpha: role in development of insulin resistance and pathogenesis of type 2 diabetes mellitus. *J Cell Biochem*. 2018;119:105-110.
12. Hotamisligil GS. The role of TNFalpha and TNF receptors in obesity and insulin resistance. *J Intern Med*. 1999;245:621-625.
13. Hotamisligil GS. Inflammatory pathways and insulin action. *Int J Obes Relat Metab Disord*. 2003;27(Suppl 3):S53-S55.
14. Stephens JM, Lee J, Pilch PF. Tumor necrosis factor-alpha-induced insulin resistance in 3T3-L1 adipocytes is accompanied by a loss of insulin receptor substrate-1 and GLUT4 expression without a loss of insulin receptor-mediated signal transduction. *J Biol Chem*. 1997;272:971-976.

15. Hotamisligil GS, Peraldi P, Budavari A, Ellis R, White MF, Spiegelman BM. IRS-1-mediated inhibition of insulin receptor tyrosine kinase activity in TNF-alpha- and obesity-induced insulin resistance. *Science*. 1996;271:665-668.
16. Guilherme A, Virbasius JV, Puri V, Czech MP. Adipocyte dysfunctions linking obesity to insulin resistance and type 2 diabetes. *Nat Rev Mol Cell Biol*. 2008;9:367-377.
17. Lis K, Kuzawinska O, Balkowiec-Iskra E. Tumor necrosis factor inhibitors - state of knowledge. *Arch Med Sci*. 2014;10:1175-1185.
18. Alten R, van den Bosch F. Dose optimization of infliximab in patients with rheumatoid arthritis. *Int J Rheum Dis*. 2014;17:5-18.
19. Colombel JF, Loftus EV Jr, Tremaine WJ, et al. The safety profile of infliximab in patients with Crohn's disease: the Mayo clinic experience in 500 patients. *Gastroenterology*. 2004;126:19-31.
20. Fiorino G, Cortes PN, Ellul P, et al. Discontinuation of infliximab in patients with ulcerative colitis is associated with increased risk of relapse: a multinational retrospective cohort study. *Clin Gastroenterol Hepatol*. 2016;14:1426-1432 e1.
21. Antoni C, Krueger GG, de Vlam K, et al. Infliximab improves signs and symptoms of psoriatic arthritis: results of the IMPACT 2 trial. *Ann Rheum Dis*. 2005;64:1150-1157.
22. Braun J, Deodhar A, Dijkmans B, et al. Efficacy and safety of infliximab in patients with ankylosing spondylitis over a two-year period. *Arthritis Rheum*. 2008;59:1270-1278.
23. Dahlen R, Strid H, Lundgren A, et al. Infliximab inhibits activation and effector functions of peripheral blood T cells in vitro from patients with clinically active ulcerative colitis. *Scand J Immunol*. 2013;78:275-284.
24. Burska AN, Sakthiswary R, Sattar N. Effects of tumour necrosis factor antagonists on insulin sensitivity/resistance in rheumatoid arthritis: a systematic review and meta-analysis. *PLoS ONE*. 2015;10:e0128889.
25. Miranda-Filloy JA, Llorca J, Carnero-Lopez B, Gonzalez-Juanatey C, Blanco R, Gonzalez-Gay MA. TNF-alpha antagonist therapy improves insulin sensitivity in non-diabetic ankylosing spondylitis patients. *Clin Exp Rheumatol*. 2012;30:850-855.
26. Golshani H, Haghani K, Dousti M, Bakhtiyari S. Association of TNF-alpha 308 G/A polymorphism with type 2 diabetes: a case-control study in the Iranian Kurdish Ethnic Group. *Osong Public Health Res Perspect*. 2015;6:94-99.
27. Borst SE, Lee Y, Conover CF, Shek EW, Bagby GJ. Neutralization of tumor necrosis factor-alpha reverses insulin resistance in skeletal muscle but not adipose tissue. *Am J Physiol Endocrinol Metab*. 2004;287:E934-E938.
28. Ofei F, Hurel S, Newkirk J, Sopwith M, Taylor R. Effects of an engineered human anti-TNF-alpha antibody (CDP571) on insulin sensitivity and glycemic control in patients with NIDDM. *Diabetes*. 1996;45:881-885.
29. Kiortsis DN, Mavridis AK, Vasakos S, Nikas SN, Drosos AA. Effects of infliximab treatment on insulin resistance in patients with rheumatoid arthritis and ankylosing spondylitis. *Ann Rheum Dis*. 2005;64:765-766.
30. Stagakis I, Bertsias G, Karvounaris S, et al. Anti-tumor necrosis factor therapy improves insulin resistance, beta cell function and insulin signaling in active rheumatoid arthritis patients with high insulin resistance. *Arthritis Res Ther*. 2012;14:R141.
31. Yazdani-Biuki B, Stelzl H, Brezinschek HP, et al. Improvement of insulin sensitivity in insulin resistant subjects during prolonged treatment with the anti-TNF-alpha antibody infliximab. *Eur J Clin Invest*. 2004;34:641-642.
32. Zinker BA, Rondinone CM, Trevillyan JM, et al. PTP1B antisense oligonucleotide lowers PTP1B protein, normalizes blood glucose, and improves insulin sensitivity in diabetic mice. *Proc Natl Acad Sci USA*. 2002;99:11357-11362.
33. Picardi PK, Caricilli AM, de Abreu LL, Carvalheira JB, Velloso LA, Saad MJ. Modulation of hypothalamic PTP1B in the TNF-alpha-induced insulin and leptin resistance. *FEBS Lett*. 2010;584:3179-3184.
34. Nieto-Vazquez I, Fernandez-Veledo S, Kramer DK, Vila-Bedmar R, Garcia-Guerra L, Lorenzo M. Insulin resistance associated to obesity: the link TNF-alpha. *Arch Physiol Biochem*. 2008;114:183-194.
35. Haj FG, Zabolotny JM, Kim YB, Kahn BB, Neel BG. Liver-specific protein-tyrosine phosphatase 1B (PTP1B) re-expression alters glucose homeostasis of PTP1B-/-mice. *J Biol Chem*. 2005;280:15038-15046.
36. Tiganis T. PTP1B and TCPTP–nonredundant phosphatases in insulin signaling and glucose homeostasis. *FEBS J*. 2013;280:445-458.
37. Ma YM, Tao RY, Liu Q, et al. PTP1B inhibitor improves both insulin resistance and lipid abnormalities in vivo and in vitro. *Mol Cell Biochem*. 2011;357:65-72.
38. Yang Z, Wu F, He Y, et al. A novel PTP1B inhibitor extracted from Ganoderma lucidum ameliorates insulin resistance by regulating IRS1-GLUT4 cascades in the insulin signaling pathway. *Food Funct*. 2018;9:397-406.
39. Delibegovic M, Zimmer D, Kauffman C, et al. Liver-specific deletion of protein-tyrosine phosphatase 1B (PTP1B) improves metabolic syndrome and attenuates diet-induced endoplasmic reticulum stress. *Diabetes*. 2009;58:590-599.
40. de Moura LP, Souza Pauli LS, Cintra DE, et al. Acute exercise decreases PTP-1B protein level and improves insulin signaling in the liver of old rats. *Immun Ageing*. 2013;10:8.
41. White CL, Whittington A, Barnes MJ, Wang Z, Bray GA, Morrison CD. HF diets increase hypothalamic PTP1B and induce leptin resistance through both leptin-dependent and -independent mechanisms. *Am J Physiol Endocrinol Metab*. 2009;296:E291-E299.
42. Tsunekawa T, Banno R, Mizoguchi A, et al. Deficiency of PTP1B attenuates hypothalamic inflammation via activation of the JAK2-STAT3 pathway in microglia. *EBioMedicine*. 2017;16:172-183.
43. Ito Y, Banno R, Hagimoto S, Ozawa Y, Arima H, Oiso Y. TNFalpha increases hypothalamic PTP1B activity via the NFkappaB pathway in rat hypothalamic organotypic cultures. *Regul Pept*. 2012;174:58-64.

How to cite this article: Méndez-García LA, Trejo-Millán F, Martínez-Reyes CP, et al. Infliximab ameliorates tumor necrosis factor-alpha-induced insulin resistance by attenuating PTP1B activation in 3T3L1 adipocytes in vitro. *Scand J Immunol*. 2018;88:e12716. https://doi.org/10.1111/sji.12716

Immunology Letters 176 (2016) 81–89

Contents lists available at ScienceDirect

Immunology Letters

journal homepage: www.elsevier.com/locate/immlet

Human monocytes and macrophages undergo M1-type inflammatory polarization in response to high levels of glucose

Israel Torres-Castro[a], Úrsula D. Arroyo-Camarena[a], Camilo P. Martínez-Reyes[a], Angélica Y. Gómez-Arauz[a], Yareth Dueñas-Andrade[a], Joselín Hernández-Ruiz[a], Yadira L. Béjar[b], Verónica Zaga-Clavellina[c], Jorge Morales-Montor[d], Luis I. Terrazas[e], Julia Kzhyshkowska[f,g,h], Galileo Escobedo[a,*]

[a] Laboratory of Liver, Pancreas and Motility, Unit of Experimental Medicine, School of Medicine, National Autonomous University of Mexico, General Hospital of Mexico, 06726, Mexico City, Mexico
[b] Blood Bank Service, General Hospital of Mexico, 06726, Mexico City, Mexico
[c] Department of Cellular Biology, National Institute of Perinatology, 11000, Mexico City, Mexico
[d] Department of Immunology, Biomedical Research Institute, National Autonomous University of Mexico, 04510, Mexico City, Mexico
[e] Unit of Biomedicine, School of Superior Studies (FES)-Iztacala, National Autonomous University of Mexico, 54090, State of Mexico, Mexico
[f] Department of Innate Immunity and Tolerance, Institute of Transfusion Medicine and Immunology, Medical Faculty Mannheim, Heidelberg University, D-68167, Mannheim, Germany
[g] Red Cross Blood Service Baden-Württemberg–Hessen, Friedrich-Ebert Str. 107 D-68167 Mannheim, Germany
[h] Laboratory for Translational Cellular and Molecular Biomedicine, Tomsk State University, 36 Lenin Prospekt, Tomsk, 634050, Russia

ARTICLE INFO

Article history:
Received 12 January 2016
Received in revised form 27 May 2016
Accepted 3 June 2016
Available online 4 June 2016

Keywords:
Monocytes
Inflammatory
Hyperglycemia
Glucose
M1 macrophages
Diabetes

ABSTRACT

Emerging data suggest that elevated glucose may promote inflammatory activation of monocytic lineage cells with the ability to injure vascular endothelial tissue of diabetic patients, however evidence in primary human monocytes and macrophages is still insufficient. We investigated the effect of high glucose concentration on the inflammatory capacity of human macrophages *in vitro* and examined whether similar responses were detectable in circulating monocytes from prediabetic patients. Primary monocytes were isolated from healthy blood donors and differentiated into macrophages. Differentiated macrophages were exposed to normal levels of glucose (NG), high glucose (HG) or high mannitol as osmotic pressure control (OP) for three days. Using PCR, ELISA and flow cytometry, we found that HG macrophages showed overexpression of CD11c and inducible nitric oxide synthase as well as down-regulation of arginase-1 and interleukin (IL)-10 with respect to NG and OP macrophages. Consistent with *in vitro* results, circulating monocytes from hyperglycemic patients exhibited higher levels of CD11c and lower expression of CD206 than monocytes from normoglycemic controls. In subjects with hyperglycemia, elevation in $CD11c^+$ monocytes was associated with increased obesity, insulin resistance, and triglyceridemia as well as low serum IL-10. Our data suggest that human monocytes and macrophages undergo M1-like inflammatory polarization when exposed to high levels of glucose on *in vitro* culture conditions and in patients with hyperglycemia. These results demonstrate that excess glucose has direct effects on macrophage activation though the molecular mechanisms mediating such a response remain to be elucidated.

1. Introduction

Hyperglycemia is a metabolic alteration characterized by abnormally high levels of blood glucose (blood glucose ≥ 5.5 mM or 100 mg/dl) [1]. Hyperglycemia is considered a key component of the metabolic syndrome and hallmark of *Diabetes Mellitus*, a chronic disease with high prevalence and mortality rates worldwide [2–4]. In diabetic patients, hyperglycemia has been shown to adversely affect both large and small blood vessels, leading to macro- and microvascular complications that include coronary artery disease as well as diabetic nephropathy, neuropathy, and retinopathy [5–7].

Abbreviations: AGEs, advanced glycation end products; PKC, protein kinase C; ROS, reactive oxygen species; CD, cluster of differentiation; iNOS, inducible nitric oxide synthase; TNF-α, tumor necrosis factor alpha; IL, interleukin; Arg-1, arginase 1; LPS, lipopolysaccharide; PBMCs, peripheral blood mononuclear cells; PCR, polymerase chain reaction; ELISA, enzyme-linked ImmunoSorbent Assay; WBCs, white blood cells; BMI, body mass index; HOMA-IR, homeostatic model assessment for insulin resistance; M, male; F, female; NG, normal glucose levels; HG, high glucose levels; OP, osmotic pressure control; MDM, monocyte-derived macrophages; M-CSF, macrophage-colony stimulating factor; M1, classically activated macrophage; M2, alternatively activated macrophage.

* Corresponding author.
E-mail addresses: gescobedog@msn.com, gescobedo@unam.mx (G. Escobedo).

http://dx.doi.org/10.1016/j.imlet.2016.06.001
0165-2478/

Numerous studies have proposed three main mechanisms through which high levels of glucose may damage vascular endothelial tissue: intracellular glucose toxicity, production of advanced glycation end products (AGEs), and protein kinase C (PKC) activation [8–10]. Intracellular glucose toxicity (also referred to as the polyol pathway) is able to elicit endothelial release of reactive oxygen species (ROS), while AGEs and PKC activation are involved in promoting leukocyte adhesion to vascular endothelial tissue and subsequent blood vessel injury [10–12]. Interestingly, emerging data have now pointed to macrophage inflammatory activation as a possible additional mechanism through which high levels of glucose may also damage vascular endothelium.

Macrophages are white blood cells that originate from monocytes [13]. In the bone marrow, hematopoietic stem cells are capable of differentiating into monocytes. Monocytes are believed to persist in blood circulation for 4–7 days and afterward migrate into tissues where they will differentiate into tissue resident macrophages [13,14]. Depending on the extracellular milieu, macrophages are capable of carrying out inflammatory or anti-inflammatory actions [15–17]. Macrophages displaying a pro-inflammatory phenotype of activation (also referred to as M1, or classically activated) are characterized by expression of specific cell surface markers such as the cluster of differentiation (CD) 11c [18,19]. Functionally, M1 macrophages are characterized by production of inflammatory mediators including inducible nitric oxide synthase (iNOS), tumor necrosis factor alpha (TNF-α), and interleukin (IL)-1β [20]. In contrast, macrophages exhibiting anti-inflammatory activation (also referred to as M2, or alternatively activated) typically show expression of CD206 and arginase 1 (Arg-1) as well as increased production of IL-10, a cytokine with potent immunoregulatory actions [20–22]. A growing body of experimental evidence has recently suggested that excessive amounts of glucose may be capable of acting directly on monocyte-macrophage cell lines by shifting the polarization of these immune cells toward a pro-inflammatory state that resembles an M1 phenotype [17,23–25]. Indeed, RAW264.7 cells (a monocyte-macrophage cell line derived from murine leukemia) significantly increase TNF-α production after being exposed to high levels of glucose [23]. Similarly, exposure to high glucose levels results in stimulation of IL-6 and IL-8 secretion in lipopolysaccharide (LPS)-stimulated U937 monocytes [17]. Furthermore, murine peritoneal macrophages show increased mRNA levels of TNF-α, IL-1β, IL-6, and IL-12 in response to elevated concentrations of glucose [24]. Human peripheral blood mononuclear cells (PBMCs) have been demonstrated to exhibit decreased production of IL-10 when exposed to high glucose conditions [25]. These findings suggest that excess glucose may be associated with an M1/M2 imbalance; however, such a phenomenon has not been explored in primary human monocytes and macrophages to date. To this end, we chose to investigate the effect of high levels of glucose on the inflammatory and anti-inflammatory capacity of human macrophages *in vitro*, while also examining whether a similar response could be seen in circulating monocytes from patients with hyperglycemia.

2. Materials and methods

2.1. Subjects

For *in vitro* studies, ten healthy male volunteers with no metabolic disease were included. For *in vivo* studies, 101 women and men attending the Blood Bank or the Internal Medicine Department of the General Hospital of Mexico were included and divided into normoglycemic or hyperglycemic groups. All of the participants provided written informed consent, previously approved by the institutional ethical committee of the General Hospital of Mexico, which guaranteed that the study was conducted in accordance with the principles described at the Helsinki Declaration. For both *in vitro* and *in vivo* studies, subjects were excluded if they had previous diagnosis of non-communicable or infectious diseases. We also excluded pregnant or lactating women as well as subjects taking any kind of anti-inflammatory, anti-aggregant, or anti-hypertensive medication.

2.2. Monocyte isolation and cell culture

For *in vitro* studies, buffy coat samples were collected from each donor (n = 10) and separately diluted 1:2 with phosphate saline buffer 1X (PBS 1X, Sigma-Aldrich, Mexico) for posterior isolation of PBMC by density gradient centrifugation using histopaque-1077 (Sigma-Aldrich, Mexico). Monocyte cells were then isolated from PBMC by CD14-negative selection using magnetic columns (Miltenyi Biotec, Germany). Purified monocytes were placed in glucose-free RPMI-1640 medium containing 10% fetal bovine serum (FBS), 2 mM L-glutamine, 50 μg/ml gentamicin, 5.5 mM D-glucose, and 10 μg/ml macrophage-colony stimulating factor (M-CSF) in 6-well cell-culture plates (Costar, USA), at a density of 3×10^6 monocytes per well. Culture media and M-CSF were replaced every other day for six days.

2.3. High glucose stimulation

After six days of *in vitro* culture differentiation, monocyte-derived macrophages (MDM) were exposed to a high glucose environment. Control MDM (NG) were incubated in glucose-free RPMI-1640 medium containing 10% FBS, 2 mM L-glutamine, 50 μg/ml gentamicin, and 5.5 mM D-glucose for three days designed to resemble normal glucose levels observed in healthy subjects. High glucose MDM (HG) were incubated in glucose-free RPMI-1640 medium containing 10% FBS, 2 mM L-glutamine, 50 μg/ml gentamicin, and 15 mM D-glucose for three days designed to resemble sugar levels seen in diabetic patients with uncontrolled hyperglycemia. Control for osmotic pressure (OP) was achieved by incubating MDM in glucose-free RPMI-1640 medium containing 10% FBS, 2 mM L-glutamine, 50 μg/ml gentamicin, 5.5 mM D-glucose, and 9.5 mM D-manitol for three days. After three days in culture, MDM were harvested using sterile cell scrapers (Corning, USA) and supernatant was collected from each culture well. Collected MDM were equally divided into 1 ml of PBS 1X (Sigma-Aldrich, Mexico) or 500 μl of TRIzol Reagent (Life Technologies, USA) for being used in flow cytometry and RT-PCR assays, respectively.

2.4. Characterization of cell surface markers by flow cytometry

After collecting MDM, 1×10^6 cells were resuspended in 50 μl of sterile PBS 1X (Sigma-Aldrich, Mexico). Immediately after, 3 μl of Human TruStrain (BioLegend, Inc., USA) was added and incubated for 5 min on ice. Then, MDM were simultaneously incubated with anti-CD45 FITC, anti-CD14 PE/Cy7, anti-CD11c PE/Cy5, and anti-CD206/Cy7 APC (BioLegend, Inc., USA) for 20 min for posterior analysis on a FACSCanto II flow cytometer (BD Biosciences, Mexico) by means of BD FACSDiva™ software 6.0, acquiring 50,000 events per test in triplicate. FITC mouse IgG1, PE/Cy7 mouse IgG2, APC/Cy7 mouse IgG1, and PE/Cy5 mouse IgG1 (BioLegend, Inc., USA) were used as isotype control antibodies for cell surface staining of CD45, CD14, CD206, and CD11c, respectively.

2.5. Cytokine production by ELISA

In vitro production of TNF-α and IL-10 were measured in MDM culture supernatants by the Enzyme-Linked ImmunoSorbent Assay

(ELISA) (Peprotech, Mexico), using 100 μl of undiluted supernatant per test. All cytokine measurements were performed in triplicate according to manufacturer's instructions.

2.6. Gene expression profile by RT-PCR

After collecting MDM, 1×10^6 cells were resuspended in 500 μl of TRIzol Reagent (Life Technologies, USA) for posterior RNA isolation following manufacturer's instructions. Then, total RNA samples were reverse-transcribed by means of the M-MLV Retrotranscriptase system using dT primer (Invitrogen, USA). Resulting cDNA samples were specifically amplified by polymerase chain reaction (PCR) using TaqDNA polymerase (Biotecnologías Universitarias, UNAM, Mexico) and human-specific primers to detect mRNA levels of iNOS, and Arg-1. 18S-ribosomal RNA was used to control for constitutive expression. Relative expression of each amplified gene was obtained by optical density analysis (OD) using the 18S-ribosomal RNA as the control for constitutive expression.

2.7. Anthropometric, metabolic, and immunological measurements in normoglycemic and hyperglycemic subjects

For *in vivo* studies, body mass index (BMI), waist circumference, and body fat percentage were individually recorded in 101 subjects. Serum glucose levels were measured in triplicate by the glucose oxidase assay, following the manufacturer's instructions (Megazyme International, Ireland). Serum insulin levels were measured in triplicate by ELISA, following the manufacturer's instructions (Abnova Corporation, Taiwan). The estimate of insulin resistance was individually calculated by means of the homeostasis model assessment of insulin resistance (HOMA-IR). Total cholesterol and triglyceride levels were individually measured in triplicate by enzymatic assays according to manufacturer's instructions (Roche Diagnostics, Mannheim, Germany). Serum levels of TNF-α and IL-10 were measured in triplicate by ELISA kits (Peprotech, Mexico) using serum samples diluted 1:250 in PBS 1X (Sigma-Aldrich, Mexico). All of the metabolic and immunological measurements were performed at the same time in order to avoid procedural variations.

2.8. White blood cell isolation and characterization of monocyte surface markers

Twenty milliliters of venous blood were obtained from each subject and collected into tubes containing EDTA (Vacutainer™, BD Diagnostics, NJ, USA). Collection tubes were then centrifuged at 1800*g* for 10 min and white blood cells (WBCs) separated using a micropipette. Total WBCs were separately placed into 1.6 ml pyrogen-free eppendorf tubes containing 1 ml of ACK Lysing Buffer (Life Technologies, USA) and incubated at 4 °C for 8 min. Each sample was then centrifuged at 1800*g*/4 °C for 4 min and cell pellets washed twice with PBS 1X (Sigma-Aldrich, Mexico). After an additional centrifugation step and removal of the supernatant, each cell pellet was resuspended in 50 μl of PBS 1X (Sigma-Aldrich, Mexico). On each test, 3 μl of Human TruStrain Reagent (BioLegend, Inc., USA) was added to 2×10^5 WBCs and then incubated for 5 min on ice. Immediately after, WBCs were incubated with anti-CD45 FITC, anti-CD14 PE/Cy7, anti-CD11c PE/Cy5, and anti-CD206/Cy7 APC following the same experimental procedure described above. Assessment of the levels of CD11c and CD206 was performed on $CD45^+CD14^+$ double positive cells, which correspond to circulating monocytes.

2.9. Statistical analysis

For *in vitro* studies, Friedman test was used to compare control, HG, and OP MDM groups in terms of CD11c and CD206 expression, as well as TNF-α and IL-10 *in vitro* production. One-way ANOVA, followed by a post-hoc Tukey test, was used to compare the expression of iNOS and Arg-1 in HG, NG, and OP macrophages. For *in vivo* studies, *t*-test was used to compare normoglycemic and hyperglycemic subjects in terms of BMI, waist circumference, body fat percentage, fasting glucose, fasting insulin, HOMA-IR, total cholesterol, and triglycerides. Mann-Whitney test was used to compare normoglycemic and hyperglycemic subjects in terms of CD11c and CD206 expression as well as TNF-α and IL-10 serum levels. All statistical analyses were performed using the GraphPad Prism 5 software. Differences were considered significant when $P < 0.05$.

3. Results

With regard to M1 macrophage cell-surface markers, all cultured macrophages showed expression of CD11c, irrespective of having been exposed to normal (NG) or high (HG) glucose concentrations (Fig. 1A). In contrast, a 2-fold increase in the intensity of CD11c expression was observed in MDM exposed to high glucose concentrations as compared with MDM exposed to normal glucose concentrations or hyperosmotic (OP) conditions (Fig. 1B). With regard to M2 macrophage cell-surface markers, neither the percentage of MDM producing CD206 nor the intensity of CD206 expression significantly differed in response to high glucose levels or hyperosmolar conditions (Fig. 1C and D, respectively).

In terms of the cytokine production profile associated with macrophage polarization, no significant differences were observed in the secretion level of TNF-α in MDM exposed to high glucose concentrations with respect to NG and OP human macrophages (Fig. 2A). In contrast, a 3-fold reduction in the average secretion of IL-10 was seen in MDM cultured in high glucose concentrations as compared with cells exposed to normal levels of glucose or hyperosmolar conditions (Fig. 2B). With respect to gene expression markers for M1 macrophages, a significant 3-fold increase in the expression of iNOS was observed when MDM were cultured under elevated concentrations of glucose as compared with NG and OP human macrophages (Fig. 2C). In terms of gene expression markers for M2 macrophages, expression of Arg-1 exhibited a clear 3.5-fold decrease in MDM treated with high glucose concentrations in comparison with macrophages exposed to normal levels of glucose or hyperosmolar conditions (Fig. 2D).

After evaluating the effect of high levels of glucose upon human macrophages *in vitro*, we attempted to corroborate our main findings in circulating monocytes of patients with hyperglycemia. No significant differences were observed in the average age and woman/man ratio between hyperglycemic and normoglycemic individuals (Table 1). However, subjects with hyperglycemia showed higher values of BMI (30.77 ± 3.21 *versus* $23.76 \pm 2.56\ kg/m^2$), waist circumference (99.42 ± 10.63 *versus* 82.17 ± 7.46 cm), and body fat percentage (33.17 ± 7.34 *versus* 26.33 ± 8.07) than normoglycemic controls (Table 1). Insulin resistance and triglycerides were also prominently elevated in hyperglycemic subjects when compared to normoglycemic individuals (for HOMA-IR, 4.09 ± 1.62 *versus* 2.51 ± 0.67, and for triglycerides, 219.2 ± 42.56 mg/dl *versus* 147.5 ± 18.75 mg/dl, respectively) (Table 1). Serum insulin and total cholesterol were slightly higher in hyperglycemic subjects than in normoglycemic individuals (for insulin, 15.43 ± 6.05 *versus* 12.67 ± 3.19 mU/l, and for cholesterol, 196.9 ± 9.10 *versus* 192.3 ± 10.47 mg/dl, respectively) (Table 1).

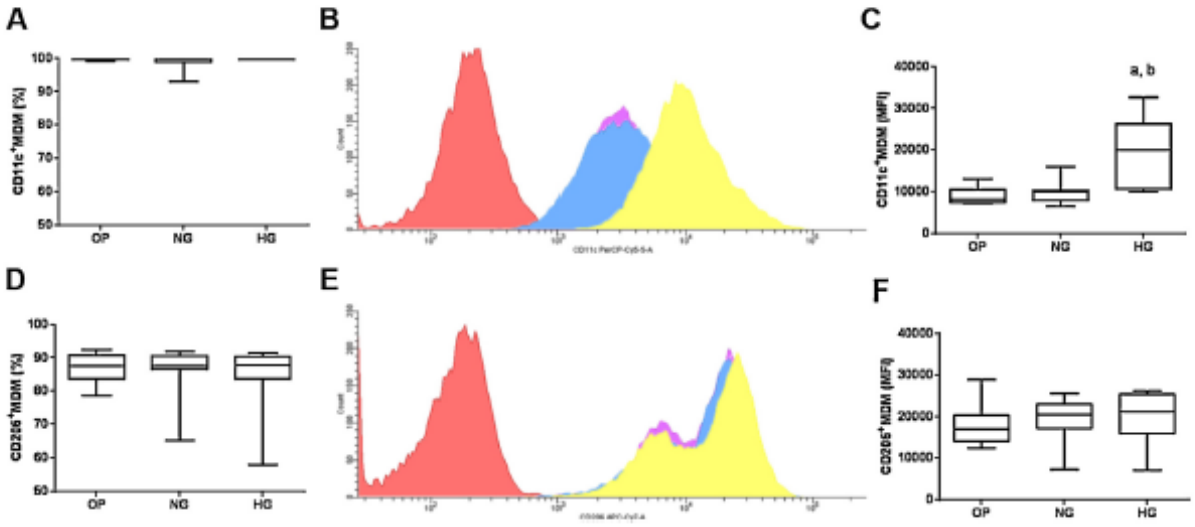

Fig. 1. Cell-surface CD11c and CD206 expression in human macrophages exposed to high levels of glucose. After three days of *in vitro* culture, all cultured monocyte-derived macrophages (MDM) showed expression of CD11c (A). Panel B illustrates representative FACS histograms showing a significant increase in the intensity of CD11c expression in MDM treated with high levels of glucose (yellow) with respect to MDM exposed to normal glucose concentrations (blue) or hyperosmolar conditions (purple). Average values for the intensity of CD11c expression are shown in C. Neither the percentage of MDM expressing CD206 (panel D) nor the intensity of CD206 expression (E and F) significantly differed in response to high levels of glucose or hyperosmolar conditions. Panel E illustrates representative FACS histograms for the intensity of CD206 expression. Panel F shows average values for the intensity of CD206 expression. PE/Cy5 mouse IgG1 and APC/Cy7 mouse IgG1 were used as isotype control antibodies for staining of CD11c and CD206, respectively, and are illustrated in red color. Data are expressed as median and inter-quartile range in a box plot analysis. Significant differences were estimated by means of the Friedman test. Differences were considered significant when $P < 0.05$, as follows: [a]significant difference *versus* the OP group; [b]significant difference *versus* the NG group; [c]significant difference *versus* the HG group. NG, normal glucose levels (5.5 mM D-glucose); HG, high glucose levels (15 mM D-glucose); OP, control of osmotic pressure (5.5 mM D-glucose + 9.5 mM mannitol); MFI, mean fluorescence intensity (for interpretation of the references to color in this figure legend, the reader is referred to the web version of this article.)

Table 1
Anthropometric and metabolic characteristics of the study subjects. Subjects were divided into normoglycemic or hyperglycemic individuals depending on the levels of fasting blood glucose. Data are presented as median ± standard deviation. n = 101. Significant differences were estimated by means of the Student's T-test. Differences were considered significant when $P < 0.05$.

	Normoglycemic	Hyperglycemic	*P*-value
	n = 51	n = 50	
Gender (M/F)	20/31	29/21	0.0739
Age (years)	31.08 ± 11.41	35.72 ± 10.40	0.0801
BMI (kg/m^2)	23.76 ± 2.56	30.77 ± 3.21	<0.0001
Waist circumference (cm)	82.17 ± 7.46	99.42 ± 10.63	<0.0001
Body fat (%)	26.33 ± 8.07	33.17 ± 7.34	<0.0001
Fasting blood glucose (mg/dl)	80.34 ± 4.14	107.2 ± 3.28	<0.0001
Serum insulin (mU/l)	12.67 ± 3.19	15.43 ± 6.05	0.0046
HOMA-IR	2.51 ± 0.67	4.09 ± 1.62	<0.0001
Total cholesterol (mg/dl)	192.3 ± 10.47	196.9 ± 9.10	0.0692
Triglycerides (mg/dl)	147.5 ± 18.75	219.2 ± 42.56	<0.0001

Abbreviations: M, male; F, female; BMI, body mass index; HOMA-IR, homeostatic model assessment of insulin resistance.

The percentage of circulating monocytes expressing CD11c was 1.8 times higher in hyperglycemic subjects than in normoglycemic individuals, although no differences were observed in the intensity of CD11c expression between groups (Fig. 3A and B, respectively). Concomitantly, a 3-fold decrease was found in the percentage of circulating CD206$^+$ monocytes in hyperglycemic subjects with respect to normoglycemic controls (Fig. 3C). The intensity of CD206 expression in the total percentage of circulating monocytes from normoglycemic and hyperglycemic individuals did not show any significant difference (Fig. 3D).

The percentage of CD11c$^+$ monocytes showed a significant inverse relationship with the number of circulating monocytes expressing CD206 in our study population ($r = -0.6624$, $P < 0.0001$) (Fig. 4). Ninety four percent of hyperglycemic subjects had a high percentage of circulating CD11c$^+$ monocytes, frequently accompanied by low numbers of CD206$^+$ monocytes. In contrast, sixty three percent of individuals with normal levels of blood glucose exhibited high values of circulating CD206$^+$ monocytes, accompanied by a low percentage of CD11c$^+$ monocytes (Fig. 4).

Consistent with *in vitro* results, systemic levels of TNF-α did not significantly differ between normoglycemic and hyperglycemic subjects (Fig. 5A). However, patients with hyperglycemia exhibited a 1.5-fold decrease in the serum levels of IL-10 as compared with individuals showing normal glycemia (Fig. 5B).

4. Discussion

CD11c is a heterodimeric integrin expressed in monocytes and macrophages exhibiting an inflammatory response [26–28]. CD11c has been shown to mediate monocyte recruitment to the inner lining of arteries, where these cells are able to differentiate into macrophages and foam cells contributing to the formation of atherosclerotic lesions and acute coronary arteritis [29–32]. It is well known that several immunological stimuli can induce CD11c expression in M1 macrophages including interferon gamma (IFN-γ), LPS, lipocalin, and galectin-3 [33–36]. However, little is understood about the role of non-immunological stimuli, such as glucose, in promoting CD11c expression in macrophages [37]. Our data show that elevated levels of glucose have an effect on CD11c expression in human monocytes and macrophages. *In vitro*, CD11c was expressed by all cultured macrophages, regardless of glucose exposure, which is consistent with previous reports demonstrating that adherence to a plastic surface is capable of inducing CD11c expression on macrophages [38,39]. However, the expression of CD11c on each macrophage was considerably increased in response to excess glucose suggesting that the production rate of this integrin may be susceptible to modulation by glucose concentrations

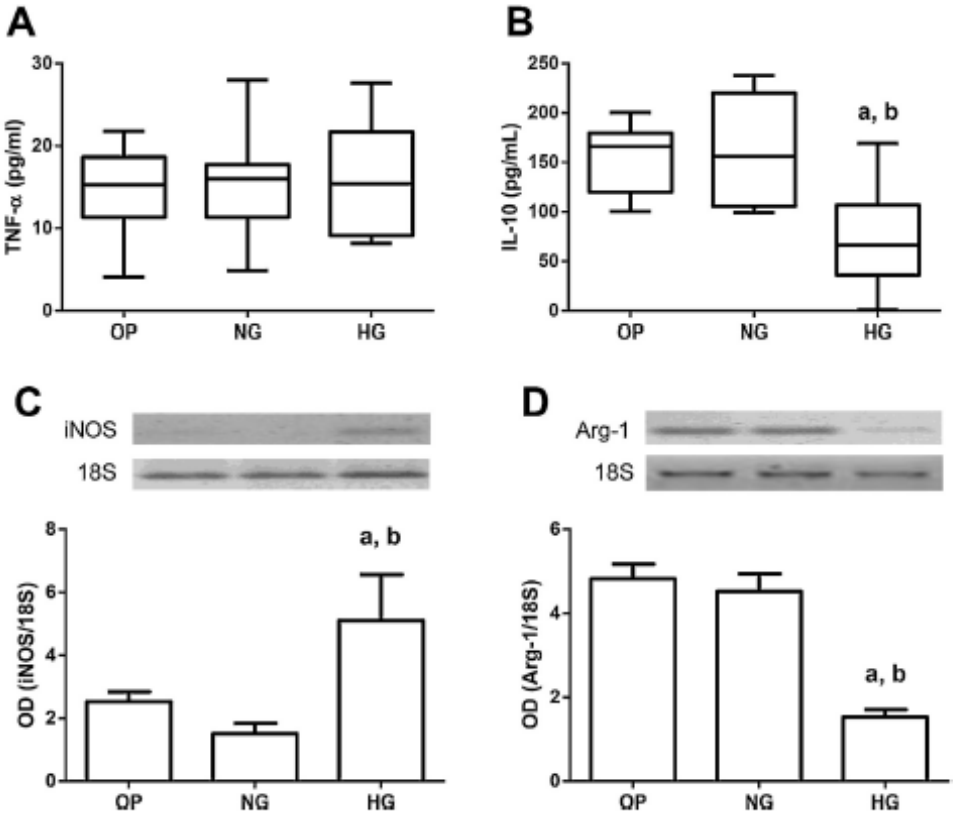

Fig. 2. Cytokine production and gene expression profile of human macrophages exposed to high levels of glucose. After three days of *in vitro* culture, no significant differences were observed in the secretion level of TNF-α (A) in human monocyte-derived macrophages exposed to high levels of glucose with respect to NG and OP macrophages. In contrast, secretion of IL-10 showed a significant reduction in HG macrophages as compared with NG and OP macrophages (B). A significant increase in the expression of iNOS was observed in HG macrophages as compared with NG and OP macrophages (C). In contrast, expression of Arg-1 exhibited a clear decrease in HG macrophages as compared with NG and OP macrophages (D). Representative agarose gels showing differential expression of iNOS and Arg-1 are shown. In A and B, data are expressed as median and inter-quartile range in a box plot analysis. In C and D, data are expressed as mean ± standard deviation. Differences were considered significant when $P<0.05$, as follows: [a]significant difference *versus* the OP group; [b]significant difference *versus* the NG group; [c]significant difference *versus* the HG group. NG, normal glucose levels (5.5 mM D-glucose); HG, high glucose levels (15 mM D-glucose); OP, control of osmotic pressure (5.5 mM D-glucose + 9.5 mM mannitol.)

independent of the *in vitro* adherence effect. Our *in vivo* findings support the idea that there is a relationship between high levels of glucose and CD11c expression as the number of circulating monocytes expressing CD11c increased in hyperglycemic subjects when compared to euglycemic individuals. These data support the idea that non-immunological stimuli, specifically metabolism-related stimuli such as glucose, have the ability to alter the inflammatory profile of monocytes and macrophages [40]. This notion is consistent with prior studies demonstrating that elevated levels of plasma triglycerides also seem to be capable of stimulating CD11c expression in circulating monocytes from healthy individuals after eating a standardized high-fat meal [41]. Our data show that $CD11c^+$ monocytes are most strongly associated with hyperglycemia, but also exhibit a positive correlation with high triglyceride levels in our study population, which would support the aforementioned findings (data not shown). The implications for understanding the mechanisms through which glucose concentrations and other metabolism-related stimuli are able to induce CD11c expression on human monocytes and macrophages are profound and the idea that further knowledge of these pathways might allow prediction of cardiovascular disease susceptibility adds a compelling degree of urgency to further study.

As described above, increased production of CD11c is strongly indicative of inflammatory polarization in both monocytes and macrophages [26–28]. This possible M1-like phenotype in macrophages exposed to high glucose was also supported by increased mRNA levels of iNOS, a marker consistently expressed by proinflammatory macrophages both *in vivo* and *in vitro* [42,43]. iNOS is known to play a major role in the production of nitric oxide, a free radical that can in turn stimulate NF-κB-dependent inflammatory pathways in M1 macrophages [44–47]. In contrast, M2 macrophages are characterized by high levels of Arg-1, a key marker of alternative activation in these immune cells [48]. Our data demonstrate a relationship between elevated glucose concentration and increased iNOS expression as well as Arg-1 reduction in human macrophages. This relationship suggests a role for excess glucose in biasing macrophages toward an M1-like phenotype. As mRNA expression is not always correlated with protein synthesis and enzymatic activity, it is important to note that iNOS and Arg-1 were assessed by means of mRNA analysis only and the discussion of these results makes no attempt to conjecture beyond that. Further research is needed to draw conclusions regarding the role of high concentrations of glucose on the protein levels and enzymatic activity of iNOS and Arg-1 in human macrophages.

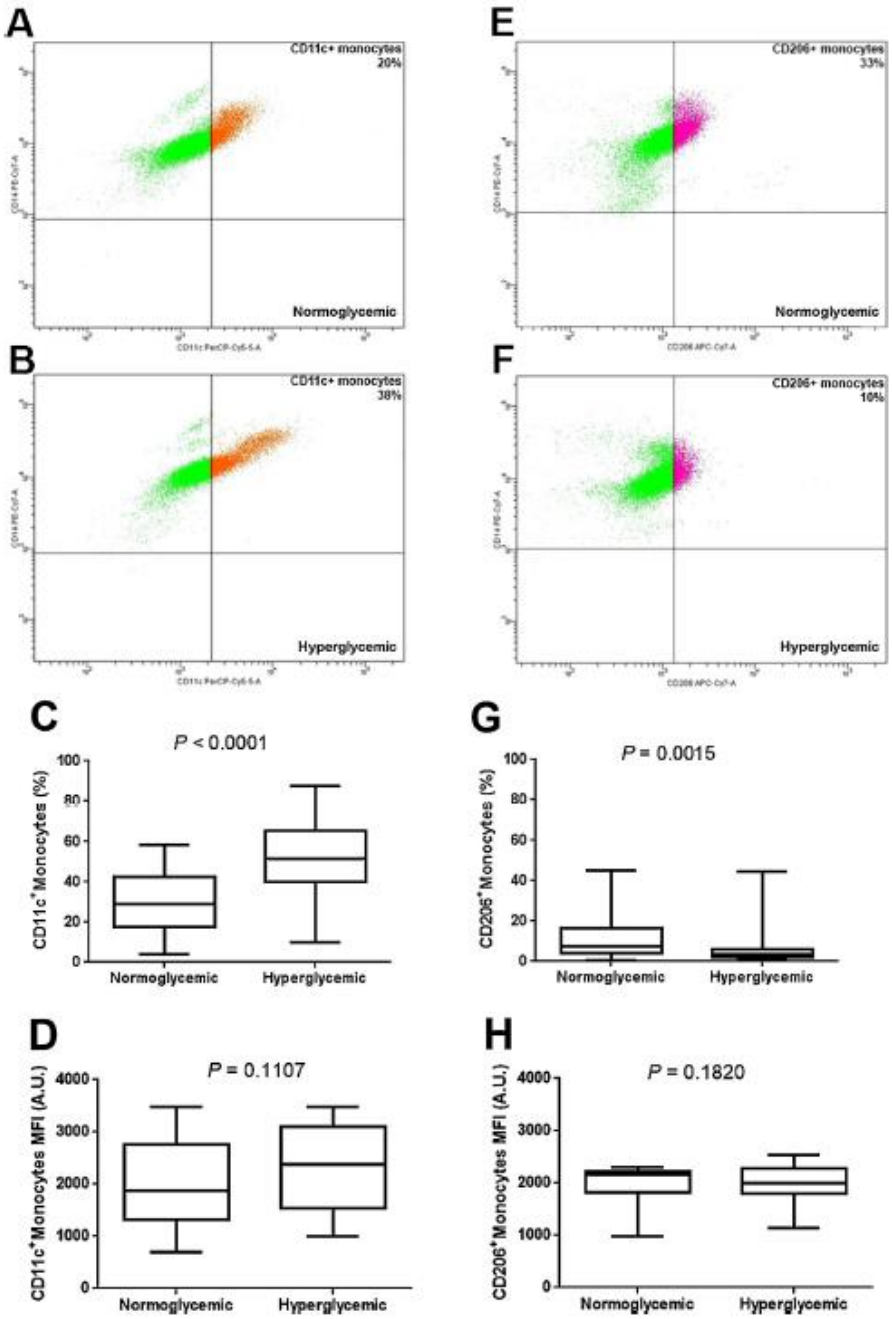

Fig. 3. Cell-surface CD11c and CD206 expression in circulating monocytes of patients with hyperglycemia. Panel A and B illustrate representative dot plots showing CD11c$^+$ monocytes percentage in normoglycemic subjects and hyperglycemic patients, respectively (orange). Patients with hyperglycemia showed higher levels of circulating CD11c$^+$ monocytes than normoglycemic controls (C). The intensity of CD11c expression in circulating monocytes was not significantly different between hyperglycemic patients and controls (D). Panel E and F illustrate representative dot plots showing CD206$^+$ monocytes percentage in normoglycemic subjects and hyperglycemic patients, respectively (pink). Patients with hyperglycemia showed lower levels of circulating CD206$^+$ monocytes than normoglycemic controls (G). The intensity of CD206 expression in circulating monocytes was not significantly different between hyperglycemic patients and controls (H). Average data are expressed as median and inter-quartile range in a box plot analysis. Differences were considered significant when $P < 0.05$ and calculated using the Mann-Whitney test. MFI, mean fluorescence intensity; AU, arbitrary units (for interpretation of the references to color in this figure legend, the reader is referred to the web version of this article.)

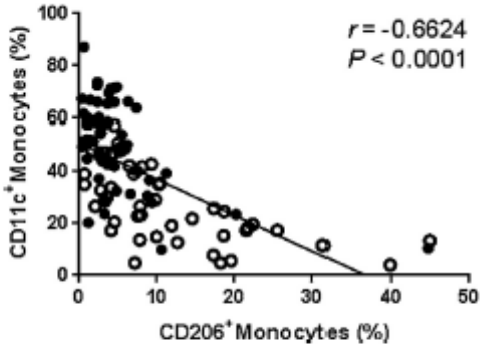

Fig. 4. Relationship between circulating CD11c$^+$ monocytes and CD206$^+$ monocytes in the study population. The percentage of CD11c$^+$ monocytes showed a significant inverse relationship with the number of circulating monocytes expressing CD206 in our study population. Ninety-four percent of hyperglycemic subjects showed a high percentage of CD11c$^+$ monocytes in circulation, frequently accompanied by low numbers of CD206$^+$ monocytes. In contrast, sixty-three percent of individuals with normal blood glucose levels exhibited a high percentage of CD206$^+$ monocytes in the circulation, accompanied by low numbers of CD11c$^+$ monocytes. Assessment of CD11c- and CD206-positive cells was exclusively performed on CD45$^+$CD14$^+$ double positive cells, which correspond to a monocyte cell population. PE/Cy5 mouse IgG1 and APC/Cy7 mouse IgG1 were used as isotype control antibodies for cell surface staining of CD11c and CD206, respectively. Solid dots= hyperglycemic patients; open dots= normoglycemic controls. Coefficients (r) and P values were calculated by the Spearman's correlation model. The correlation level was considered significant when $P< 0.05$.

Consistent with an apparent inclination toward an M1-like phenotype, we found that human macrophages exposed to excess glucose have a reduction in IL-10 secretion. It has been proposed that IL-10-producing macrophages may play a pivotal role in preventing vascular endothelial damage during hyperglycemia as it occurs in atherosclerosis. Sato et al. recently demonstrated that the number of IL-10-producing macrophages decreases in the hemorrhagic atheromatous plaques of patients with acute coronary syndrome (ACS) and hyperglycemia when compared to ACS patients without hyperglycemia who have more stable plaques [49]. Additionally, Chung et al. have shown that adipose tissue macrophages from hyperglycemic mice have less capacity for expressing IL-10 than macrophages derived from adipose tissue of mice exhibiting normal levels of plasma glucose [40]. Our data expand on this body of work by revealing that increased levels of glucose are associated with diminished IL-10 secretion in human macrophages, which may negatively affect their capacity to regulate inflammatory events. These *in vitro* data are congruent with *in vivo* results showing that patients with hyperglycemia exhibit high percentages of circulating CD11c$^+$ monocytes and low systemic values of IL-10. However, further clinical studies are needed to clarify the relationship between CD11c$^+$ monocytes and decreasing serum levels of IL-10 in hyperglycemic patients.

Another phenomenon captured in our study is that macrophages exposed to high glucose concentrations exhibit low production of IL-10 without a concomitant increase in the synthesis of TNF-α. In the presence of prototypic activating stimuli such as IFN-γ/LPS or IL-4/IL-13, macrophages are capable of polarizing toward M1 or M2 phenotypes, which in turn are characterized by increased production of TNF-α and IL-10, respectively [50–52]. However, numerous studies have also reported non-prototypic activating stimuli with the capacity to prime macrophages to assume an M2-like phenotype, as is the case of M-CSF [52–55]. M-CSF has been shown to induce a state in which macrophages appear to be primed for a M2-like profile denoted by high production of IL-10, whereas macrophages exposed to granulocyte-macrophage colony stimulating factor seem to be capable of overproducing TNF-α [56]. M-CSF is produced by a variety of epithelial and stromal cells which drive macrophages to adopt an M2-like phenotype under normal homeostatic conditions [16,57–59]. Our *in vitro* culture system used M-CSF to differentiate human monocytes into MDM and this exposure may largely explain that the resulting macrophages showed improved IL-10 secretion but negligible capacity to produce TNF-α. In this scenario, it is reasonable to consider that prolonged exposure of macrophages to elevated levels of glucose may not only reduce IL-10 secretion, but also favor the production of pro-inflammatory cytokines, which would support the body of work that suggests M2 macrophages initially lose anti-inflammatory capacity prior to adopting an M1 inflammatory profile [60–63].

Consistent with evidence of possible M2 to M1 repolarization, we found that the monocyte subpopulation primed to an inflammatory phenotype (CD11c$^+$ monocytes) is inversely correlated with the subpopulation of monocytes exhibiting an M2 phenotype (CD206$^+$ monocytes) in the circulation of hyperglycemic patients. Despite having been firstly described in obese mice (high-fat diet), CD11c and CD206 are also now recognized as cell surface markers for M1 and M2 macrophages in human beings, respectively [64–66]. In this sense, our results suggest that CD206$^+$ monocytes may be converted into CD11c$^+$ monocytes in response to high glu-

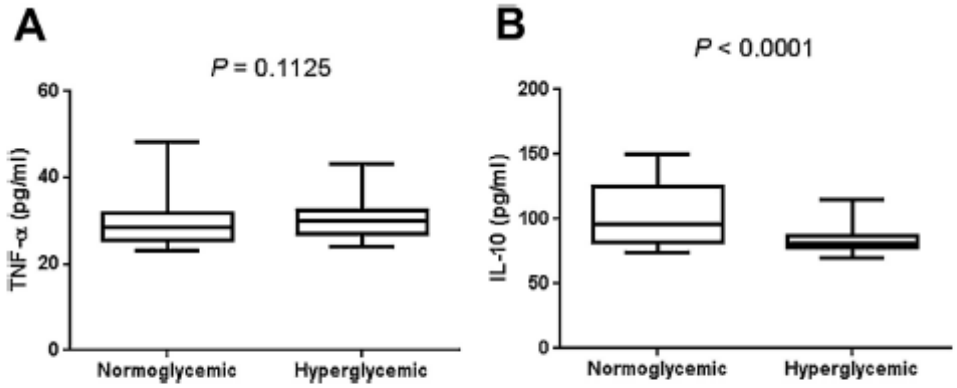

Fig. 5. Serum levels of TNF-α and IL-10 in patients with hyperglycemia. Consistent with *in vitro* results, systemic levels of TNF-α did not show significant differences between hyperglycemic subjects and normoglycemic subjects (A). In contrast, patients with hyperglycemia exhibited a significant decrease in systemic levels of IL-10 with respect to normoglycemic individuals (B). Data are expressed as median and inter-quartile range in a box plot analysis. Differences were considered significant when $P< 0.05$ and calculated using the Mann-Whitney test.

cose concentrations, which supports the idea that macrophages may be primed toward an inflammatory phenotype in the first stages of monocyte differentiation. Interestingly, the imbalance between both monocyte subpopulations was not only associated with hyperglycemia but also with increased insulin resistance, triglycerides, BMI and central obesity. This could suggest that the phenotype of monocytes is influenced by numerous parameters of metabolic dysfunction, which should be taken into account in designing therapeutic interventions focused on monocyte repolarization in prediabetic and diabetic patients.

With regard to the possible cell mechanisms involved in the inflammatory polarization of human macrophages, it has been demonstrated that high levels of glucose are associated with elevation of the glucose efflux into the intracellular space [8]. In endothelial and smooth muscle cells, the increase of the intracellular glucose concentration induces activation of the polyol pathway that results in overproduction of sorbitol and fructose by aldose reductase and sorbitol dehydrogenase, respectively. The excessive activity of both enzymes has been associated with imbalance in the Redox cell mechanisms that in turn leads to free radical overproduction [8,11]. In macrophages, production of free radicals has been shown to activate NFκB-dependent signaling pathways resulting in inflammatory cytokine release [46,47]. Thereby, it is reasonable to consider that high levels of glucose may trigger the polyol pathway in macrophages, which could lead to free radical production, NFκB-dependent signaling pathway activation, and finally macrophage inflammatory polarization. However, to the best of our knowledge there is not yet solid evidence demonstrating the role of the polyol pathway upon free radical production and NFκB activation during macrophage polarization and these speculations should be carefully considered in further studies.

5. Conclusions

Our data demonstrate for the first time that high glucose concentrations have direct effects on the polarization of primary human macrophages toward an M1-like phenotype, characterized by up-regulation of CD11c and iNOS as well as down-regulation of Arg-1 and IL-10. The apparent inclination to M1-like activity was also observed in circulating monocytes in the setting of hyperglycemia, in which we found increased values of $CD11c^{+}$ monocytes accompanied by decreased levels of $CD206^{+}$ monocytes and IL-10. Furthermore, this study included an osmotic pressure control in all of the *in vitro* experiments in order to ensure that the results attributed to elevated glucose concentrations were not due to hyperosmolarity caused by the elevated levels of glucose. The molecular mechanisms through which high glucose concentrations and other non-prototypical metabolic stimuli are able to promote the expression of pro-inflammatory markers in monocytes and macrophages remain unclear and will require further study. In patients with elevated risk of developing vascular endothelial damage, including the vast number of people living with diabetes across the world, the potential impact of such work stands to be profound.

Conflict of interest

The authors have declared that no conflict of interest exists.

Acknowledgments

This work was supported by grant no. CB-129316-M from Consejo Nacional de Ciencia y Tecnologia (CONACYT-México) to GE as well as EU FP7 Program EULAMDIMA to GE and JK, and is a component of the Ph.D. requirements of Israel Torres-Castro in the Programa de Doctorado en Ciencias Biomédicas de la Universidad Nacional Autónoma de México. Israel Torres-Castro thanks financial support from CONACYT by granting the scholarship number 269684. We sincerely thank Dr. Blair Brown, who corrected the English version of the manuscript.

References

[1] V. Woo, M.V. Shestakova, C. Orskov, A. Ceriello, Targets and tactics: the relative importance of HbA, fasting and postprandial plasma glucose levels to glycaemic control in type 2 diabetes, Int. J. Clin. Pract. 62 (2008) 1935–1942.
[2] E. Ginter, V. Simko, Type 2 diabetes mellitus, pandemic in 21st century, Adv. Exp. Med. Biol. 771 (2012) 42–50.
[3] N. Babio, E. Toledo, R. Estruch, E. Ros, M.A. Martinez-Gonzalez, O. Castaner, et al., Mediterranean diets and metabolic syndrome status in the PREDIMED randomized trial, CMAJ 186 (2014) E649–657.
[4] P.M. Siu, Q.S. Yuen, Supplementary use of HbA1c as hyperglycemic criterion to detect metabolic syndrome, Diabetol. Metab. Syndr. 6 (2014) 119.
[5] R. Nielsen, H. Norrelund, U. Kampmann, H.E. Botker, N. Moller, H. Wiggers, Effect of acute hyperglycemia on left ventricular contractile function in diabetic patients with and without heart failure: two randomized cross-over studies, PLoS One 8 (2013) e53247.
[6] A. Piwkowska, D. Rogacka, M. Jankowski, S. Angielski, Metformin reduces NAD(P)H oxidase activity in mouse cultured podocytes through purinergic dependent mechanism by increasing extracellular ATP concentration, Acta Biochim. Pol. 60 (2013) 607–612.
[7] R. Shenoy, R. Khandekar, A. Bialasiewicz, A. Al Muniri, Corneal endothelium in patients with diabetes mellitus: a historical cohort study, Eur. J. Ophthalmol. 19 (2009) 369–375.
[8] M. Lorenzi, The polyol pathway as a mechanism for diabetic retinopathy: attractive, elusive, and resilient, Exp. Diab. Res. 2007 (2007) 61038.
[9] Y. Ishibashi, T. Matsui, S. Maeda, Y. Higashimoto, S. Yamagishi, Advanced glycation end products evoke endothelial cell damage by stimulating soluble dipeptidyl peptidase-4 production and its interaction with mannose 6-phosphate/insulin-like growth factor II receptor, Cardiovasc. Diabetol. 12 (2013) 125.
[10] P. Geraldes, G.L. King, Activation of protein kinase C isoforms and its impact on diabetic complications, Circ. Res. 106 (2010) 1319–1331.
[11] M. Mittal, M.R. Siddiqui, K. Tran, S.P. Reddy, A.B. Malik, Reactive oxygen species in inflammation and tissue injury, Antioxid. Redox Signal. 20 (2014) 1126–1167.
[12] D.L. Michell, K.L. Andrews, K.J. Woollard, J.P. Chin-Dusting, Imaging leukocyte adhesion to the vascular endothelium at high intraluminal pressure, J. Vis. Exp. 23 (2011) 54.
[13] S. Wallner, M. Grandl, T. Konovalova, A. Sigruner, T. Kopf, M. Peer, et al., Monocyte to macrophage differentiation goes along with modulation of the plasmalogen pattern through transcriptional regulation, PLoS One 9 (2014) e94102.
[14] N. Lachmann, M. Ackermann, E. Frenzel, S. Liebhaber, S. Brennig, C. Happle, et al., Large-scale hematopoietic differentiation of human induced pluripotent stem cells provides granulocytes or macrophages for cell replacement therapies, Stem Cell Rep. 4 (2015) 282–296.
[15] P.J. Murray, J.E. Allen, S.K. Biswas, E.A. Fisher, D.W. Gilroy, S. Goerdt, et al., Macrophage activation and polarization: nomenclature and experimental guidelines, Immunity 41 (2014) 14–20.
[16] P. Italiani, D. Boraschi, From monocytes to M1/M2 macrophages: phenotypical vs. functional differentiation, Front. Immunol. 5 (2014) 514.
[17] J. Haidet, V. Cifarelli, M. Trucco, P. Luppi, C-peptide reduces pro-inflammatory cytokine secretion in LPS-stimulated U937 monocytes in condition of hyperglycemia, Inflamm. Res. 61 (2012) 27–35.
[18] H. Cucak, L. Nielsen Fink, M. Hojgaard Pedersen, A. Rosendahl, Enalapril treatment increases T cell number and promotes polarization towards M1-like macrophages locally in diabetic nephropathy, Int. Immunopharmacol. 25 (2015) 30–42.
[19] R.K. Rai, N.K. Vishvakarma, T.M. Mohapatra, S.M. Singh, Augmented macrophage differentiation and polarization of tumor-associated macrophages towards M1 subtype in listeria-administered tumor-bearing host, J. Immunother. 35 (2012) 544–554.
[20] N. Wang, H. Liang, K. Zen, Molecular mechanisms that influence the macrophage m1–m2 polarization balance, Front. Immunol. 5 (2014) 614.
[21] J. Svensson-Arvelund, R.B. Mehta, R. Lindau, E. Mirrasekhian, H. Rodriguez-Martinez, G. Berg, et al., The human fetal placenta promotes tolerance against the semiallogeneic fetus by inducing regulatory t cells and homeostatic M2 macrophages, J. Immunol. 194 (2015) 1534–1544.
[22] L. Xie, Q. Fu, T.M. Ortega, L. Zhou, D. Rasmussen, J. O'Keefe, et al., Overexpression of IL-10 in C2D macrophages promotes a macrophage phenotypic switch in adipose tissue environments, PLoS One 9 (2014) e86541.
[23] C.I. Cheng, P.H. Chen, Y.C. Lin, Y.H. Kao, High glucose activates Raw264.7 macrophages through RhoA kinase-mediated signaling pathway, Cell. Signal. 27 (2015) 283–292.
[24] Y. Pan, Y. Wang, L. Cai, Y. Cai, J. Hu, C. Yu, et al., Inhibition of high glucose-induced inflammatory response and macrophage infiltration by a novel curcumin derivative prevents renal injury in diabetic rats, Br. J. Pharmacol. 166 (2012) 1169–1182.

[25] D. Reinhold, S. Ansorge, E.D. Schleicher, Elevated glucose levels stimulate transforming growth factor-beta 1 (TGF-beta 1), suppress interleukin IL-2, IL-6 and IL-10 production and DNA synthesis in peripheral blood mononuclear cells, Horm. Metab. Res. 28 (1996) 267–270.
[26] R. Pujari, N. Kumar, S. Ballal, S.M. Eligar, S. Anupama, G. Bhat, et al., Rhizoctonia bataticola lectin (RBL) induces phenotypic and functional characteristics of macrophages in THP-1 cells and human monocytes, Immunol. Lett. 163 (2015) 163–172.
[27] H. Zhang, X. Wang, Z. Shen, J. Xu, J. Qin, Y. Sun, Infiltration of diametrically polarized macrophages predicts overall survival of patients with gastric cancer after surgical resection, Gastric Cancer (2014).
[28] M.R. Boon, L.E. Bakker, M.C. Haks, E. Quinten, G. Schaart, L. Van Beek, et al., Short-term high-fat diet increases macrophage markers in skeletal muscle accompanied by impaired insulin signalling in healthy male subjects, Clin. Sci. (Lond.) 128 (2015) 143–151.
[29] G.A. Foster, R.M. Gower, K.L. Stanhope, P.J. Havel, S.I. Simon, E.J. Armstrong, On-chip phenotypic analysis of inflammatory monocytes in atherogenesis and myocardial infarction, Proc. Natl. Acad. Sci. U. S. A. 110 (2013) 13944–13949.
[30] K.Y. Cho, H. Miyoshi, S. Kuroda, H. Yasuda, K. Kamiyama, J. Nakagawara, et al., The phenotype of infiltrating macrophages influences arteriosclerotic plaque vulnerability in the carotid artery, J. Stroke Cerebrovasc. Dis. 22 (2013) 910–918.
[31] Y. Hirata, M. Tabata, H. Kurobe, T. Motoki, M. Akaike, C. Nishio, et al., Coronary atherosclerosis is associated with macrophage polarization in epicardial adipose tissue, J. Am. Coll. Cardiol. 58 (2011) 248–255.
[32] Y. Motomura, S. Kanno, K. Asano, M. Tanaka, Y. Hasegawa, H. Katagiri, et al., Identification of pathogenic cardiac CD11c+ macrophages in nod1-mediated acute coronary arteritis, Arterioscler. Thromb. Vasc. Biol. (2015).
[33] C.A. Sergio, T.B. Bertolini, A.F. Gembre, R.Q. Prado, V.L. Bonato, CD11c(+) CD103(+) cells of mycobacterium tuberculosis-infected C57BL/6 but not of BALB/c mice induce a high frequency of interferon-gamma- or interleukin-17-producing CD4(+) cells, Immunology 144 (2015) 574–586.
[34] Y. Miyata, A. Fukuhara, M. Otsuki, I. Shimomura, Expression of activating transcription factor 2 in inflammatory macrophages in obese adipose tissue, Obesity (Silver Spring) 21 (2013) 731–736.
[35] H. Guo, D. Jin, X. Chen, Lipocalin 2 is a regulator of macrophage polarization and NF-kappaB/STAT3 pathway activation, Mol. Endocrinol. 28 (2014) 1616–1628.
[36] V.R. Sunil, M. Francis, K.N. Vayas, J.A. Cervelli, H. Choi, J.D. Laskin, et al., Regulation of ozone-induced lung inflammation and injury by the beta-galactoside-binding lectin galectin-3, Toxicol. Appl. Pharmacol. 284 (2015) 236–245.
[37] F.O. Martinez, S. Gordon, The M1 and M2 paradigm of macrophage activation: time for reassessment, F1000Prime Rep. 6 (2014) 13.
[38] C. Ammon, S.P. Meyer, L. Schwarzfischer, S.W. Krause, R. Andreesen, M. Kreutz, Comparative analysis of integrin expression on monocyte-derived macrophages and monocyte-derived dendritic cells, Immunology 100 (2000) 364–369.
[39] T. Georgakopoulos, S.T. Moss, V. Kanagasundaram, Integrin CD11c contributes to monocyte adhesion with CD11b in a differential manner and requires Src family kinase activity, Mol. Immunol. 45 (2008) 3671–3681.
[40] S. Chung, R. Ranjan, Y.G. Lee, G.Y. Park, M. Karpurapu, J. Deng, et al., Distinct role of FoxO1 in M-CSF- and GM-CSF-differentiated macrophages contributes LPS-mediated IL-10: implication in hyperglycemia, J. Leukoc. Biol. 97 (2015) 327–339.
[41] R.M. Gower, H. Wu, G.A. Foster, S. Devaraj, I. Jialal, C.M. Ballantyne, et al., CD11c/CD18 expression is upregulated on blood monocytes during hypertriglyceridemia and enhances adhesion to vascular cell adhesion molecule-1, Arterioscler. Thromb. Vasc. Biol. 31 (2011) 160–166.
[42] D. Zheng, Y. Wang, Q. Cao, V.W. Lee, G. Zheng, Y. Sun, et al., Transfused macrophages ameliorate pancreatic and renal injury in murine diabetes mellitus, Nephron Exp. Nephrol. 118 (2011) e87–99.
[43] G.P. Christophi, M. Panos, C.A. Hudson, R.L. Christophi, R.C. Gruber, A.T. Mersich, et al., Macrophages of multiple sclerosis patients display deficient SHP-1 expression and enhanced inflammatory phenotype, Lab. Invest. 89 (2009) 742–759.
[44] J.A. Moreno, C. Sastre, J. Madrigal-Matute, B. Munoz-Garcia, L. Ortega, L.C. Burkly, et al., HMGB1 expression and secretion are increased via TWEAK-Fn14 interaction in atherosclerotic plaques and cultured monocytes, Arterioscler. Thromb. Vasc. Biol. 33 (2013) 612–620.
[45] W. Ni, Q. Zhang, G. Liu, F. Wang, H. Yuan, Y. Guo, et al., Escherichia coli maltose-binding protein activates mouse peritoneal macrophages and induces M1 polarization via TLR2/4 in vivo and in vitro, Int. Immunopharmacol. 21 (2014) 171–180.
[46] D. Tugal, X. Liao, M.K. Jain, Transcriptional control of macrophage polarization, Arterioscler. Thromb. Vasc. Biol. 33 (2013) 1135–1144.
[47] J.L. Kang, K. Lee, V. Castranova, Nitric oxide up-regulates DNA-binding activity of nuclear factor-kappaB in macrophages stimulated with silica and inflammatory stimulants, Mol. Cell. Biochem. 215 (2000) 1–9.
[48] B. Pourcet, I. Pineda-Torra, Transcriptional regulation of macrophage arginase 1 expression and its role in atherosclerosis, Trends Cardiovasc. Med. 23 (2013) 143–152.
[49] T. Sato, T. Kameyama, T. Noto, H. Inoue, Impaired macrophage production of anti-atherosclerotic interleukin-10 induced by coronary intraplaque hemorrhage in patients with acute coronary syndrome and hyperglycemia, J. Diab. Complications 28 (2014) 196–202.
[50] F.O. Martinez, A. Sica, A. Mantovani, M. Locati, Macrophage activation and polarization, Front. Biosci. 13 (2008) 453–461.
[51] R. Susarla, L. Liu, E.A. Walker, I.J. Bujalska, J. Alsalem, G.P. Williams, et al., Cortisol biosynthesis in the human ocular surface innate immune response, PLoS One 9 (2014) e94913.
[52] T.A. Hamilton, C. Zhao, P.G. Pavicic Jr., S. Datta, Myeloid colony-stimulating factors as regulators of macrophage polarization, Front. Immunol. 5 (2014) 554.
[53] C.I. Caescu, X. Guo, L. Tesfa, T.D. Bhagat, A. Verma, D. Zheng, et al., Colony stimulating factor-1 receptor signaling networks inhibit mouse macrophage inflammatory responses by induction of microRNA-21, Blood 125 (2015) e1–13.
[54] D.Y. Vogel, J.E. Glim, A.W. Stavenuiter, M. Breur, P. Heijnen, S. Amor, et al., Human macrophage polarization in vitro: maturation and activation methods compared, Immunobiology 219 (2014) 695–703.
[55] I. Brocheriou, S. Maouche, H. Durand, V. Braunersreuther, G. Le Naour, A. Gratchev, et al., Antagonistic regulation of macrophage phenotype by M-CSF and GM-CSF: implication in atherosclerosis, Atherosclerosis 214 (2011) 316–324.
[56] A.J. Fleetwood, T. Lawrence, J.A. Hamilton, A.D. Cook, Granulocyte-macrophage colony-stimulating factor (CSF) and macrophage CSF-dependent macrophage phenotypes display differences in cytokine profiles and transcription factor activities: implications for CSF blockade in inflammation, J. Immunol. 178 (2007) 5245–5252.
[57] D.C. Lacey, A. Achuthan, A.J. Fleetwood, H. Dinh, J. Roiniotis, G.M. Scholz, et al., Defining GM-CSF- and macrophage-CSF-dependent macrophage responses by in vitro models, J. Immunol. 188 (2012) 5752–5765.
[58] P.J. Wermuth, S.A. Jimenez, The significance of macrophage polarization subtypes for animal models of tissue fibrosis and human fibrotic diseases, Clin. Transl. Med. 4 (2015) 2.
[59] E. Tagliani, C. Shi, P. Nancy, C.S. Tay, E.G. Pamer, A. Erlebacher, Coordinate regulation of tissue macrophage and dendritic cell population dynamics by CSF-1, J. Exp. Med. 208 (2011) 1901–1916.
[60] D. Sag, C. Cekic, R. Wu, J. Linden, C.C. Hedrick, The cholesterol transporter ABCG1 links cholesterol homeostasis and tumour immunity, Nat. Commun. 6 (2015) 6354.
[61] K.A. Kigerl, J.C. Gensel, D.P. Ankeny, J.K. Alexander, D.J. Donnelly, P.G. Popovich, Identification of two distinct macrophage subsets with divergent effects causing either neurotoxicity or regeneration in the injured mouse spinal cord, J. Neurosci. 29 (2009) 13435–13444.
[62] M.J. Davis, T.M. Tsang, Y. Qiu, J.K. Dayrit, J.B. Freij, G.B. Huffnagle, et al., Macrophage M1/M2 polarization dynamically adapts to changes in cytokine microenvironments in *Cryptococcus neoformans* infection, MBio 4 (2013) e00264–00213.
[63] G. Chinetti-Gbaguidi, B. Staels, Macrophage polarization in metabolic disorders: functions and regulation, Curr. Opin. Lipidol. 22 (2011) 365–372.
[64] J.M. Wentworth, G. Naselli, W.A. Brown, L. Doyle, B. Phipson, G.K. Smyth, et al., Pro-inflammatory CD11c+ CD206+ adipose tissue macrophages are associated with insulin resistance in human obesity, Diabetes 59 (2010) 1648–1656.
[65] M. Zeyda, D. Farmer, J. Todoric, O. Aszmann, M. Speiser, G. Gyori, et al., Human adipose tissue macrophages are of an anti-inflammatory phenotype but capable of excessive pro-inflammatory mediator production, Int. J. Obes. (Lond.) 31 (2007) 1420–1428.
[66] V. Bourlier, A. Zakaroff-Girard, A. Miranville, S. De Barros, M. Maumus, C. Sengenes, et al., Remodeling phenotype of human subcutaneous adipose tissue macrophages, Circulation 117 (2008) 806–815.